The structure and function of human soluble CD23

Grundy, Gabrielle Jane

THE STRUCTURE AND FUNCTION OF HUMAN SOLUBLE CD23

Gabrielle Grundy

A thesis submitted in partial fulfilment of the requirements for the degree of Doctor of Philosophy in the University of London

The Randall Centre for Molecular Mechanism of Cell Function,
Division of Biomedical Sciences,
King's College London,
New Hunt's House,
Guy's Campus,
St Thomas Street,
London. SE1 1UL

July 2001

ABSTRACT

CD23, the low affinity IgE receptor, is a trimeric C-type lectin (45 kDa) expressed on the surface of several haematopoetic cells. Several soluble CD23 fragments, monomeric and trimeric, are produced by endogenous proteases and by the dust mite allergenic protease, Der p 1. These fragments have many ligands resulting in a variety of functions; including the regulation of IgE production by B-cells (*via* CD21) and triggering the release of pro-inflammatory mediators from monocytes (by binding CD11b/c integrins). A recombinant version of the monomeric CD23 fragment produced by *Der p* 1 (Der-CD23) was expressed in *E.coli* and was able to bind an IgE-Fc mutant (K_A = 9.0 x 10^6 M^{-1}). Two chimeric proteins were assessed for their ability to form stable, trimeric CD23. A fusion protein comprising the neck region of surfactant protein-D and CD23 formed trimers, but was unstable and had low affinity for IgE. When extracellular CD23 sequence was fused with an isoleucine zipper (LZ-CD23), dimeric or trimeric CD23 formed, which did not degrade as readily and had wild type affinity for an IgE-Fc mutant (K_A = 5.3 x 10^7 M^{-1}). LZ-CD23 was shown to be more effective at binding IgE and CD21 than Der-CD23 by ELISA, presumably because of its ability to form trimers. An attempt at expressing recombinant soluble integrin, CD11b/CD18, in insect cells lead to both subunits being sequestered within the cell. Using soluble integrins expressed by mammalian cells, specific interactions between Der-CD23 and CD11b/CD18 and the vitronectin receptor ($\alpha v\beta 5$) were demonstrated. Preliminary experiments indicated a suppressive effect of Der-CD23 and LZ-CD23 upon *in vitro* IgE synthesis. Thus, Der-CD23 and LZ-CD23 are useful molecular tools to study the biological roles of monomeric and trimeric sCD23. Furthermore, NMR techniques are currently being employed to elucidate the 3D structure of the lectin domain and identification of ligand binding sites.

ACKNOWLEDGEMENTS

I am grateful to Professor Hannah Gould and Dr Ray Owens for giving me the opportunity to work on this project. My studentship was supported by the Medical Research Council in collaboration with Celltech. My thanks goes to Ray Owens, Carl Doyle, Paul Stevens, Bernie Sweeney, Viv Perkins, Tony Shock, Marion Dorning and all at Celltech, who have generously guided me, shared their skills and materials, and made the months spent in Slough a rewarding experience. I acknowledge Byran Smith (N-terminal sequencing), Lloyd King (mass spectrometry), Alan Lyons (sequencing) for their expertise and especially Carl Doyle who selflessly supervised my time in Slough. I have been lucky to be involved in many collaborations. Jim McDonnell at the University of Oxford is currently working on the structure of CD23 and I'd like to thank him for several enlightening discussions and to Dan Conrad and his laboratory at the Commonwealth University of Virginia for kindly donating LZ-CD23.

I am indebted to members of the Randall Centre, past and present, who have assisted me with my studies; particularly, Hannah Gould, Brian Sutton, Rebecca Beavil, Andrew Beavil, Jianguo Shi, Check Ma; and to Natalie McCloskey who has gone beyond the call of duty for any post-doc by providing me with a home. I am very grateful to Rebecca for direction, advice, proof reading, and the professional looking diagrams in Chapter 1. I would also like to thank all my friends at the Randall Centre for making it an enjoyable place to work.

Finally, appreciation for the love and support of my family: Jack, Betty, Charles, Amanda, Gilda, Randall and Margret, to whom this thesis is dedicated.

TABLE OF CONTENTS

LIST OF FIGURES

LIST OF TABLES

ABBREVIATIONS

APS	ammonium persulphate
bp	base pair
BSA	Bovine Serum Albumin
CD	Cluster of Differentiation
cDNA	complementary DNA
CHO	Chinese Hamster Ovary cells
CR	Complement receptor
CRD	Carbohydrate Recognition Domain
d.H_2O	distilled, deionised water
Der p	*Dermatophagoides pteronyssinus*
DFDNB	di-fluoro, di-nitrobenzene
DMSO	Dimethylsulphoxide
DNA	deoxyribonucleic acid
dNTP	deoxynucleoside triphosphate
DTT	Dithioreitol
E. coli	*Escherichia coli*
EBV	Epstein Barr Virus
ECL	Enzyme Chemo-luminescence
EDC	1-Ethyl-3-(3-dimethylaminopropyl)carbodiimide Hydrochloride
EDTA	Ethylene Diamine Tetra-acetic Acid
ELISA	Enzyme Linked Immunosorbent Assay
HBS	HEPES buffered saline
HEPES	N-(2-Hydroxyethyl)piperazine-N'-(2-ethanesulfonic acid)
HIC	Hydrophobic Interaction Chromatography
HPLC	High Pressure Liquid Chromatography
HRP	Horse radish Peroxidase
ICAM	Intercellular Adhesion Molecule
IFN	Interferon
IgE	Immunoglobulin E
IL	Interleukin
IPTG	Isopropyl-D-thiogalactopyranoside
kb	kilobases

kDa	kilo-Daltons
LB	Luria-Bertani
LZ	Leucine zipper
MHC	Major Histocompatability Complex
MMP	Matrix metalloproteinase
MOI	Multiplicity of infection
Mw	Molecular weight
NMR	Nuclear Magnetic Resonance
OPD	o-Phenylenediamine
PBS	Phosphate Buffered Saline
PCR	Polymerase Chain Reaction
pfu	plaque forming units
PMSF	phenylmethylsulphonyl fluoride
rpm	revolutions per minute
sCD23	Soluble CD23
SCR	Short Consensus Repeat
SD	Standard Deviation
SDS-PAGE	sodium dodecyl sulphate-polyacrylamide gel electrophoresis
SPD	Surfactant Protein D
SPR	Surface Plasmon Resonance
TAE	Tris-Acetate-EDTA
Taq	*Thermus aquaticus*
TBE	Tris-Borate-EDTA
TBS	Tris-Buffered Saline
TCA	Trichloroactetic acid
TE	Tris-EDTA
TEMED	N,N,N',N' Tetramethylethylenediamine
T_H	T helper lymphocyte
TLCK	Tosyl L Lysyl chloromethanhydrochloride
TNF	Tumour Necrosis factor
UV	Ultra-violet
X-Gal	5-bromo-4 chloro-3-indoly-β-D-galactopyranoside

CHAPTER 1: INTRODUCTION

1.1 Introduction to IgE and its Receptors

IgE is one of five classes of antibody (IgM, IgG, IgE, IgA and IgD), distinguished by its heavy chain (Cε). When a foreign antigen is recognised by the variable regions of the antibody, it is the constant region of the antibody (Fc) that determines its 'effector' response through ligation to Fc receptors (FcεRI and FcεRII) on a variety of cells (Figure 1.1). IgE is present in the serum at very low concentrations (50-300 ng/ml) and has a short half life (2 days) when compared to other antibody classes (IgG1 at 10 mg/ml, 3 week half life) but is effective in providing protection from parasites. Aberrant production of IgE is characteristic of allergic diseases affecting 20% of Western populations. Thus, there is much interest to understand the mechanisms of IgE production and the interactions with its receptors.

The high affinity IgE receptor is expressed on the surface of mast cells and basophils. IgE binds to FcεRI with a very high affinity ($K_A = 10^{10}\ M^{-1}$) through residues in the Cε2 and Cε3 domains (reviewed by Sutton and Gould, 1993). The receptor is a complex of four transmembrane subunits, αβγ2. The α chain belongs to the immunoglobulin (Ig) superfamily, consisting of two Ig-like domains α1 and α2 which form the IgE binding site (Figure 1.1). The β and γ chains are not involved directly in IgE binding but mediate a transmembrane signal on allergen binding.

IgE can bind to FcεRI on mast cells even in the absence of antigen, thus 'sensitising' the cell. On re-introduction of antigen/allergen the receptors are cross-linked, which signals the release of mediators. This process is very rapid as the antigen-specific antibody is already bound to the effector cell (hence, the immediate hypersensitivity response). The

a)

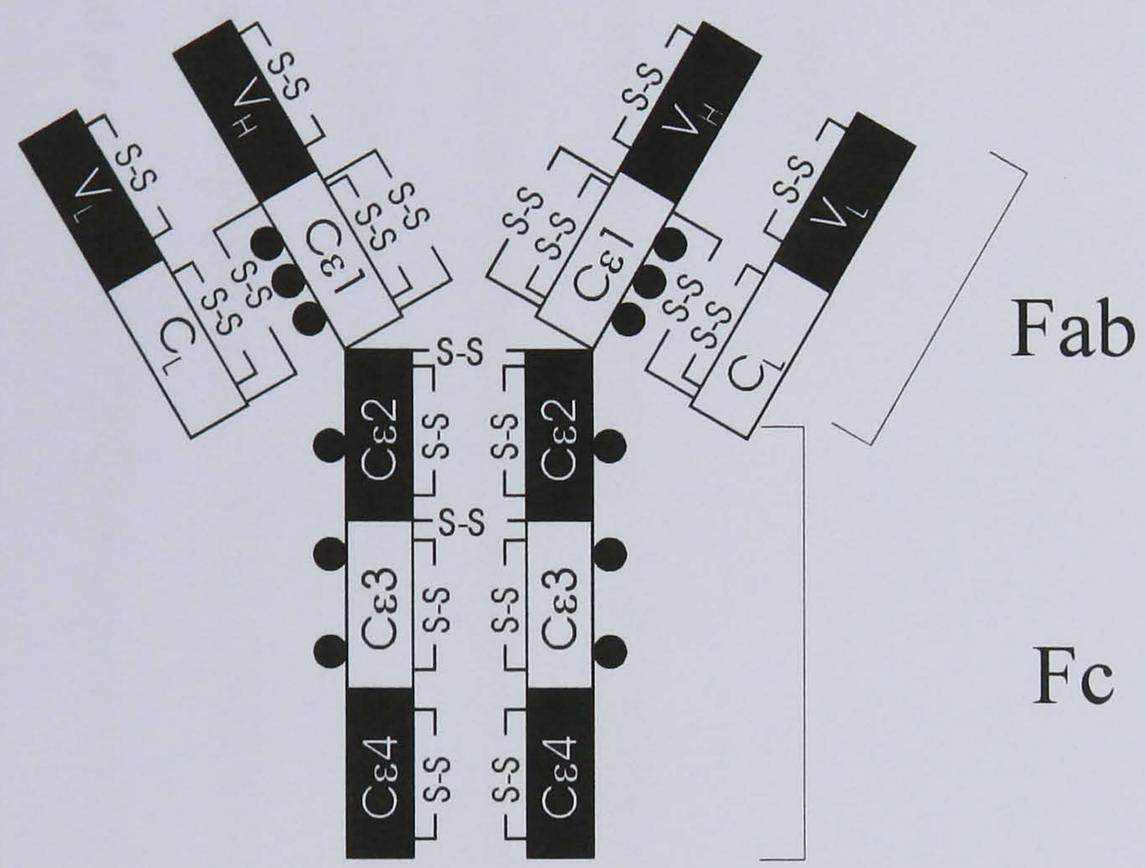

b)

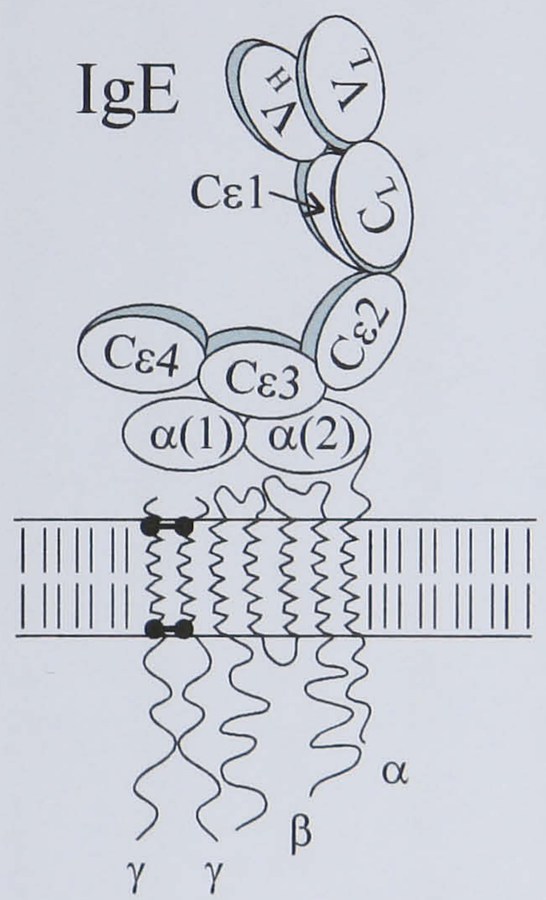

FcεRI

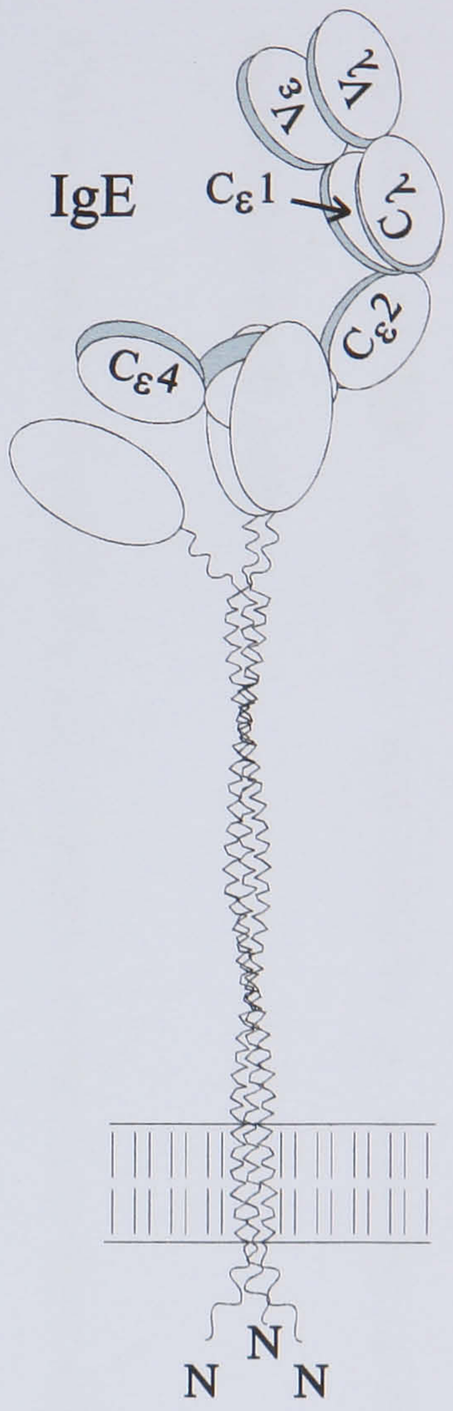

$Fc_{\varepsilon}RII$
(CD23)

Figure 1.1: Schematic Diagram of IgE Structure and Its Interaction with FcεRI and FcεRII (CD23)

signal transduction pathway leads to the degranulation of the effector cell, releasing histamine and a number of lymphokines, including IL-4, to recruit and activate inflammatory cells. IL-4 is an important multifunctional cytokine involved in the up-regulation of IgE synthesis, and notably is a potent stimulator of FcεRII (CD23) expression on B cells.

Cross-linking of FcεRII by IgE-allergen complexes also triggers effector functions of inflammatory cells e.g. facilitating phagocytosis or cytotoxicity by macrophages, eosinophils, monocytes and platelets. Cross-linking membrane CD23 induces activation of a tyrosine kinase, leading to a cascade through IKK and IkBa leading to NF-κB activation and gene transcription (Ten *et al.*, 1999). FcεRII exists as a membrane protein, from which a soluble form is released. Both have several other biological functions, IgE dependent and independent (section 1.5), mediated by other counter structures (CD21, CD11b/CD18). To clarify its role in functions distinct from effector mechanisms, it will be referred to as CD23.

1.2 CD23

1.2.1 Expression

CD23, is present on populations of B-lymphocytes and a variety of haematopoietic cells. These include macrophages, monocytes, eosinophils, platelets, follicular dendritic cells in the light zone of the lymph node, Langerhans cells and T lymphocytes (reviewed by Delespesse *et al.*, 1991). CD23 has also been detected on some epithelial cells (Billaud *et al.*, 1989). CD23 is expressed on a subset of resting B cells, and can be induced following antigen activation, and lost on differentiation into plasma cells. In addition to the expression on cell surfaces, it has been detected in bodily fluids as a

soluble form (sCD23). Pathologically, a high level of sCD23 is regarded as a disease marker in conditions such as chronic lymphocytic leukaemia, allergy and in chronic inflammatory diseases such as rheumatoid arthritis.

1.2.2 Structure of CD23

The gene encoding CD23 was identified on Chromosome 19p13, adjacent to the recently discovered DC-SIGN and DC-SIGNR (Trask *et al.,* 1993; Soilleux *et al.,* 2000). CD23 cDNA was cloned by 3 different groups (Kikutani *et al.,* 1986; Ludin *et al.,* 1987; Ikuta *et al.,* 1987) from human lymphocytes and B-cell lines. The nucleotide sequence predicted a protein of 321 amino acids, with residues Cys161 to Cys288 showing homology with the carbohydrate recognition domain (CRD) of animal calcium-dependent (C-type) lectins, e.g. human and rat asialoglycoprotein receptor, chicken hepatic lectin and CD72. This makes CD23 an unusual Fc receptor, as all other known Fc receptors belong to the Ig superfamily (Figure 1.2). To date, a high resolution structure of CD23 has not been obtained; instead much is inferred from modelling based on the crystal structures of Mannose Binding Protein (Weis *et al.,* 1991) and E-selectin (Graves *et al.,* 1994). The atomic structure of several (>9) C-type lectins have been solved by crystallography and show that the CRD to contains equal proportions of alpha helices and beta sheet but contain a significant amount of 'random coil'. One or two calcium binding sites are co-ordinated by this backbone. Stable coordination of the calcium ion is provided by the ligand (hydroxyl groups of terminal sugar groups). The sugar specificity of CD23 was defined as galactose, particularly glycoproteins terminating in Gal-GalNac (Kijimoto *et al.,* 1994). As will be described in section 1.4, additional, or accessory, protein binding sites in the CRD are important for CD23 ligand binding. Indeed, interaction with IgE is not through carbohydrate recognition (Richards and Katz, 1990), therefore, it will be simply referred to as the lectin domain.

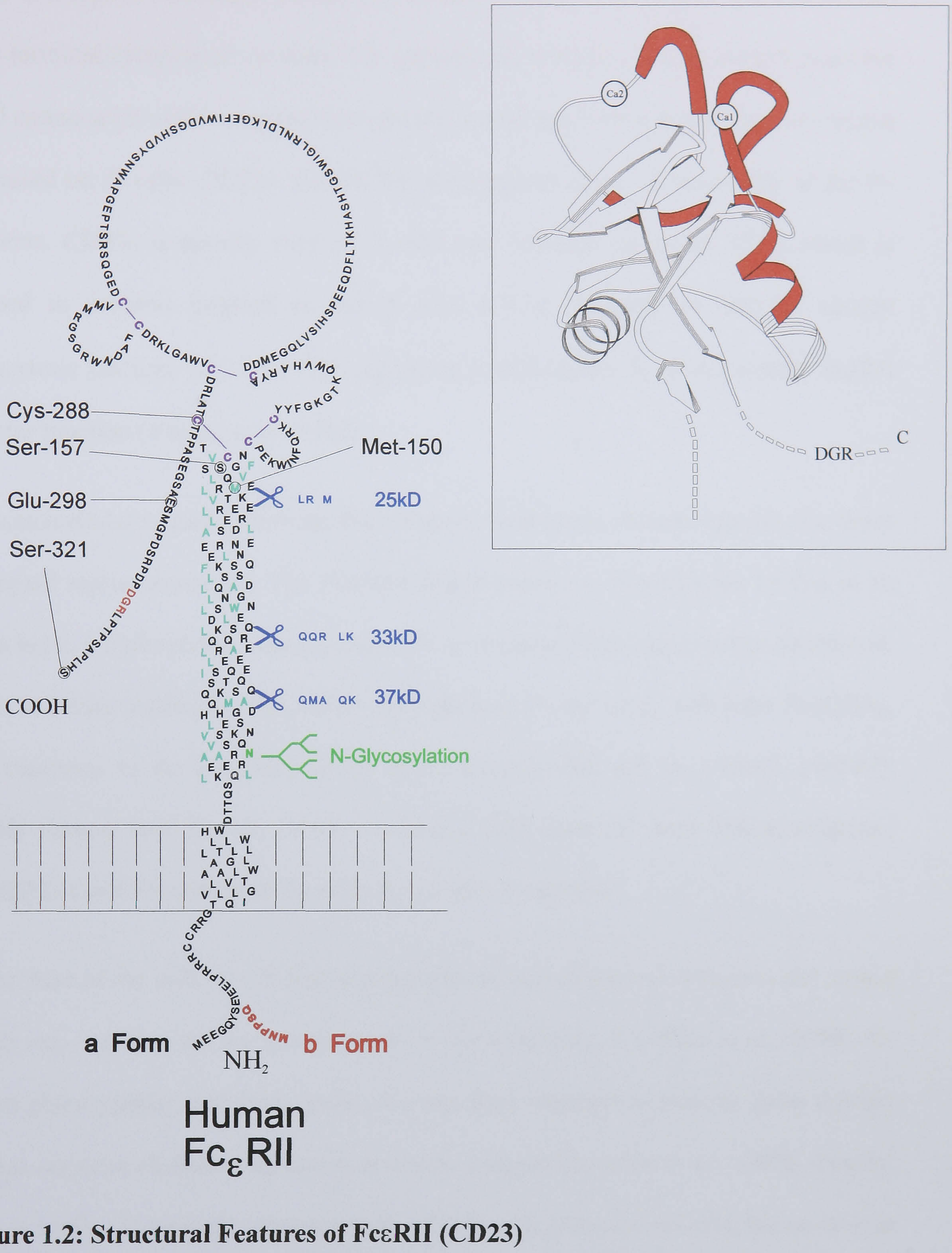

Figure 1.2: Structural Features of FcεRII (CD23)

CD23 is a type II membrane protein with 2 isoforms, a and b, differing in N-terminal residues. The 'stalk' region contains leucine rich heptad repeat sequences that are predicted to form alpha helical coiled coil associations. Hydrophobic residues are coloured cyan. Along the stalk are several sites of proteolysis and a N-linked glycosylation site (green). Sequence in the 'head' region has homology to animal C-type lectins and is modeled on the crystal structure of rat mannose binding protein A (inset). Highlighted regions have been identified to form interactions with IgE (Bettler *et al.,* 1992). The C-terminal 'tail' is of unknown structure but contains an inverse RGD motif (red). Circled residues indicate the start and end points of the recombinant proteins described in this thesis (Chapters 3 and 4).

CD23 is a type II membrane protein that contains a single transmembrane domain and an N-terminal cytoplasmic domain. The cytoplasmic domain contains a short sequence of 20 amino acids rich in arginine and glutamate residues. There are two splice variants expressed on B cells, CD23a and CD23b differing by 6 or 7 amino acids at the N-terminus. CD23a is present only on B cells and contains the motif YSEI, which is utilized in proteins targeted to coated pits, and so supports its role in antigen endocytosis (section 1.5.2). CD23b expression is induced by IL-4 and confers FcεRII effector function (Yokota *et al.,* 1992).

The extracellular sequence between the membrane and lectin domain consists of a series of heptad repeat sequences. The first and fourth residue is hydrophobic so that in an alpha helix, a hydrophobic side promotes the association of an alpha helical coiled-coil. From structure prediction, this coiled coil region is 10 nm long, with little flexibility, and continues to the boundary of the lectin domains that are, as a result, probably closely packed. Beavil *et al.* (1995) confirmed, with chemical cross-linking evidence, that CD23 can form trimers at the cell surface and in solution.

At the base of the stalk is a N-linked glycosylation site conserved in human and mouse which may stabilise the associated trimer in the membrane (Letellier *et al.,* 1990). O-linked glycosylation containing sialic acid has been reported to exist in lectin domain but has not been characterised or any function assigned (Letellier *et al.,* 1988). Finally, there is a short C-terminal sequence (tail) of unknown structure but contains an inverse RGD motif, a common requirement in the binding sites of several ligands of integrins. The C-terminal tail may be important in association with MHC-II (HLA-DR) in the membrane (Kijimoto-Ochiai and Noguchi, 2000).

CD23 cDNA has also been cloned from mouse (Kondo *et al.,* 1994) rat, horse and partially from cattle (Watson *et al.,* 2000). Although the key structural features are present in these species, i.e. lectin domain and stalk region, some vital differences are apparent, notably the length of stalk region and the sequence and length of the C-terminal tail. These structural contrasts could account for the differences in CD23 ligand binding and function, particularly evident between the better characterised human and mouse systems, for instance, the murine CD23-CD21 interaction has yet to demonstrated.

1.3 Production of Soluble CD23

Fragments of extracellular CD23 (37 kDa, 33 kDa, 29 kDa, 25 kDa and 16 kDa) can be detected in B cell cultures and body fluids (Figure 1.3) and were previously referred to as IgE Binding Factors (Delepesse *et al.,* 1989). The 29-37 kDa fragments are short lived and contain varying lengths of the alpha helical stalk region and have been shown to exist as trimers in solution (Beavil *et al.,* 1995). The serine/cysteine protease inhibitor, tosyl-L-lysyl chloromethanhydrochloride ketone (TLCK) appears to prevent degradation along the stalk region and release of CD23 from membranes (Cairns *et al.,* 1990). The stable 25 kDa fragment contains only lectin domain and C-terminal tail and is monomeric. Its production can be inhibited by iodoacetamide (Letellier *et al.,* 1990). A further cleavage site is present in the tail resulting in a monomeric 16 kDa fragment that Sarfati *et al.,* (1984) were able to purify from human colostrum. Production of 16 kDa CD23 can not be inhibited by iodoacetamide thus, a different protease again is acting on CD23.

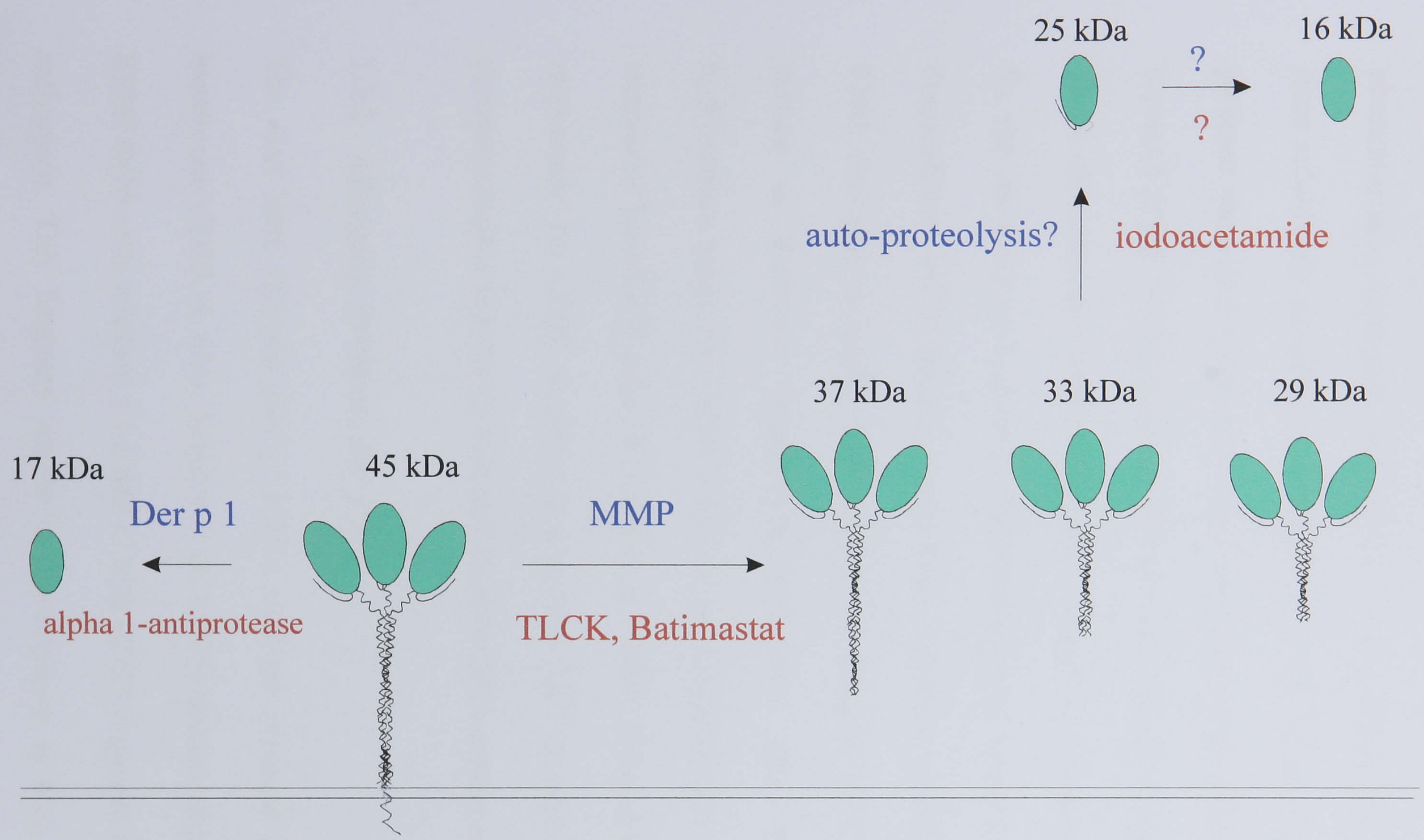

Figure 1.3: Production and Inhibition of CD23 Fragments

Membrane bound CD23 (45 kDa) sheds 37 kDa, 33 kDa and 29 kDa soluble fragments. Processing can be inhibited by matrix metalloproteinase (MMP) inhibitors, e.g. Batimastat (Marolewski *et al.,* 1998). TLCK (serine/cysteine protease inhibitor also prevents shedding (Cairns and Gordon, 1990). Proteolysis to the stable 25 kDa fragment may be an autoproteolytic mechanism, which is inhibited by the cysteine protease inhibitor, iodoacetamide (Letellier *et al.,* 1990). 16 kDa CD23 has can be detected but is produced by an unknown mechanism. The house dust mite allergen Der p 1 is a cysteine protease (inhibited by α1-antiprotease) that also cleaves membrane bound CD23 to a 17 kDa fragment.

1.3.1 Endogenous Proteases

Initially it was thought CD23 was being cleaved by an auto-proteolytic activity, as it was being specifically degraded by a factor present in CD23+ cells and recombinant CD23 preparations (Letellier *et al.,* 1990). Recently, metalloproteinase inhibitors 1,10, phenanthroline, imidazole and batimastat were found to inhibit 33 kDa sCD23 release from solubilised membranes (Marolewski *et al.,* 1998). Further characterisation of the protease showed it to be membrane anchored (approximately 63 kDa), pH dependent (optimal at pH 7) with a Km of 220 nM and present in most cell lines except T-cells. These characteristics were similar to the matrix metalloproteinases (MMP) responsible for the shedding of L-selectin. This finding was supported by Gu *et al.,* 1998, who demonstrated the hydroxamic acid based inhibitor of zinc dependent MMPs, Ro31-9790, was able to inhibit ATP-induced shedding of CD23 (and L-selectin) from the surface of B-chronic lymphocytic leukaemia cells. Also, GI 129471, another hydroxamate based Zn^{2+} MMP inhibitor, prevented sCD23 production by IL-4, CD40L stimulated tonsillar B-cells (Wheeler *et al.,* 1998). Thus, evidence suggests the protease responsible for CD23 shedding is a neutral Zn^{2+} dependent MMP. The endogenous proteases responsible for 25 kDa and 16 kDa CD23 remain unknown.

1.3.2 Allergenic Protease, *Der p* 1

The dust mite allergen *Der p* 1 is a cysteine protease that was shown to cleave membrane CD23 *in vitro*. Schultz *et al.* (1995) demonstrated *Der p* 1 incubated with RPMI 8866 cells released a soluble 17 kDa CD23 fragment and can be inhibited by α-1 antitrypsin. This fragment has been characterised at both termini and identified as Ser156-Glu298, encompassing the lectin domain. Shakib *et al.* (1998) hypothesise that *Der p* 1 is able to cross the mucosal barrier and remain active suggesting CD23

proteolysis may occur *in vivo*. In addition to CD23 proteolysis Schultz *et al.* (1998) also showed *Der p* 1 was able to cleave the alpha subunit of the IL-2R (CD25) on T_H1 cells. Inactivation of these receptors is speculated to bias immune response toward T_H2 cells, typical of an allergic response.

1.4 CD23 Ligand Interactions

1.4.1 CD23-IgE Interaction

Consistent with other classes of Immunoglobulin, IgE comprises of two heavy and two light chains (Figure 1.1). Unlike IgG, the heavy chain contains an extra immunoglobulin domain (Cε2) where the hinge region would be. A number of biophysical experiments suggest the IgE molecule assumes a bent conformation (Zheng *et al.,* 1991; Beavil *et al.,* 1995). A high resolution structure has been obtained for IgE Fc (Cε3-Cε4) and in a complex with its high affinity receptor (Garman *et al.,* 2000; Wurzburg *et al.,* 2000). However, no crystallography data describes the IgE-CD23 interaction.

Despite being referred to as the low affinity IgE receptor, CD23 has a fairly high affinity for IgE, K_A = 3-7 x 10^{-7} M^{-1} (Anderson and Spielgelberg, 1981, Bettler *et al.,* 1992; Sato *et al.,* 1997). Ultracentrifugation data suggests that the stoichiometry of the interaction is 2 lectin domains binding one IgE Fc molecule (Shi *et al.,* 1997) Figure 1.1b). It is believed that 2 sites on IgE interact with the CD23 trimer, one being on the Cε3 domain close to the N371 glycosylation site. Despite this proximity, CD23 does not require carbohydrate for binding. Indeed, the absence of exposed carbohydrate allows IgE Fc to bind FceRII with a 10 fold higher affinity than the wild type IgE-Fc (Young *et al.,* 1995). Thus, CD23 is not utilising its lectin activity in the IgE interaction. The interaction sites are contained within the lectin domain alone. Homologue scanning

mutagenesis (Bettler *et al.*, 1992) identified discontinuous regions of lectin domain that potentially interact with IgE (Figure 1.2) that are located around the calcium ion binding sites. This would account for the calcium dependent binding observed.

1.4.2 CD21, Complement Receptor 2 (CR2)

CD21 (CR2) binds inactivated forms of C3b that opsonise pathogenic surfaces and is important in B cell activation and the alternative pathway of activation of the complement system (reviewed by Fearon and Carroll, 2000). CR2 was identified as the ligand for CD23 on B-cells (Aubry *et al.*, 1992) that participates in the IL-4 induced IgE up-regulation, and B-cell growth and differentiation (section 1.5). CD21 is present on mature B cells (IgM+/IgD+), until activated, and follicular dendritic cells (FDC) in germinal centres. CD21 has also been found at low levels on epithelial cells and some T lymphocytes (Timens *et al.*, 1991).

The structure of CD21 (approximately 145 kDa) is composed of 15 or 16 short consensus repeat (SCR) domains found in several complement proteins e.g. CR1, C2, Factor B and Factor H. These domains of 60-75 amino acids are arranged like a 'string of beads'. Monoclonal antibodies have helped to identify the SCR domains involved in CD21 ligand binding to C3d (SCR 1-2), CD23 (SCR 1-2 and 5-8), EBV (SCR 1-2) and interferon-α (SCR 3-4; Figure 1.4). There are 11 N-linked glycosylation sites but no apparent O-linked glycosylation. Unlike C3d binding, carbohydrate is required for the interaction with CD23 (Aubry *et al.*, 1994). The sugar specificity of the CD23-CD21 interaction is unknown; galactose was unable to inhibit the interaction, and reports of fucose 1 phosphate inhibition are contradictory (Pochon *et al.*, 1992, Sato *et al.*, 1997).

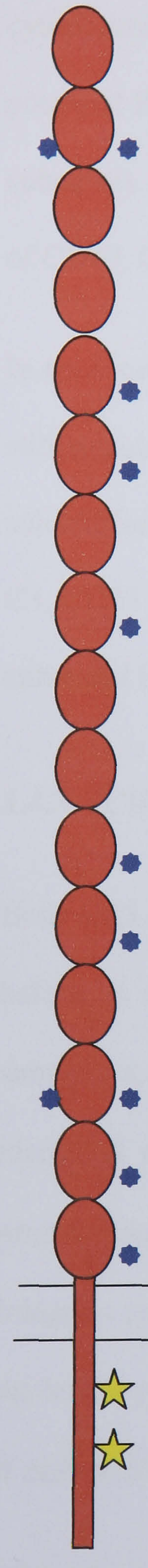

SCR	Anti-CD21 mAb (% inhibition CD23 binding)	CD23 interaction	Other Ligands
1	OKB7 (10-20)	Protein-protein	EBV
2	BE-5 (0-10)		C3d
3	NZ1 (30-40)		IFNα
4	HB5 (10-20)		p120RNP
5	BU33 (80-90)	Carbohydrate N370 (N295)	
6			
7			
8			
9	BL13 (10-20)		
10			
11	BU32 (40-50)		
12	IF8 (0-10)		
13			
14			
15			
16			
TM			
p53			
p68			

Short concensus repeat domain

N-Glycosylation

Intracellular protein binding

Figure 1.4: Schematic diagram of CD21 Structure and Ligand Binding Sites

This diagram shows the results of epitope mapping anti-CD21 monoclonal antibodies and ligands (Aubry *et al.,* 1994). This data has lead to the partial identification of CD23 binding sites.

A single transmembrane domain anchors the receptor to the cell surface, and a cytoplasmic domain of 34 amino acids is responsible for signal transduction via a potential Protein Kinase C motif (TSQK) and/or a sequence common to tyrosine kinase substrates. CD21 is part of a large signal transduction complex involving the association of CD19, CD81 and Leu 13.

In addition to the membrane bound form CD21 is shed from the surface of B-cells and still retains iC3b and CD23 binding capabilities (Fremeaux-Bacchi *et al.*, 1996). The soluble form of CD21 (135 kDa and 90 kDa) was shown to circulate in complexes with C3, CD23 and IgE. Biological relevance of sCD21 is unknown but could inhibit sCD23 enhanced IgE synthesis (Fremeaux-Bacchi *et al.*, 1998; section 1.5.1).

1.4.3 CD11b/CD18 and CD11c/CD18 (CR3 and CR4)

Both CR3 (Mac-1, CD11b/CD18, αMβ2) and CR4 (p150, p95, CD11c/CD18 αXβ2) belong to the integrin superfamily. Integrins comprise two non-covalently associated subunits α (~150 kDa) and β (~ 90 kDa). To date, 14 alpha and 8 beta chains have been identified which are able to form up to 21 distinct heterodimers. Some subunits are promiscuous (e.g. αV) whereas some pair exclusively with one other subunit, e.g. αM. Integrins can be grouped according to their beta subunit. Both CR3 and CR4 belong to the leukocyte β2 family expressed on monocytes, granulocytes, NK cells and a subset of B cells and T cells.

CD11b and CD11c are type I transmembrane proteins with a short cytoplasmic domain of 19 and 26 residues, respectively. The structure of the extracellular region is only partially understood. Structure predictions suggest seven repeating sequences assume a

β-propeller fold similar to that found in the trimeric G protein β subunit (Springer, 1997) .

In between the second and third repeat is a domain homologous to the von Willebrand A domain called the I (inserted) domain. Crystallography studies of CD11b I domain shows this domain resembles a dinucleotide binding 'Rossman' fold of a beta sheet surrounded by 7 alpha helices (Lee *et al.,* 1995). Many of the receptor's ligands have been mapped to this domain, which contains a Metal Ion Dependent Adhesion Site (MIDAS). Divalent cations in particular, Mn^{2+}, Mg^{2+}, and Ca^{2+} regulate the binding at this site. The β2 integrins have many ligands: cell surface, matrix and soluble proteins, endogenous and foreign (Table 1.1).

Ligand binding requires the presence of both subunits. The beta subunit (CD18) has an 'I'-like domain and a cytoplasmic domain that contains an actin-binding site, thereby linking cellular and extracellular adhesions to the cytoskeleton. Through the cytoplasmic domains an 'inside-out' signal can be transmitted to alter the adhesive states of the extracellular domains. Resting cells are in a low adhesive state until an intracellular signal can rapidly activate the cell to a high adhesive state, e.g. during transmigration of leukocyte through endothelium. β2 integrins also serve as classic signal transduction receptors for several soluble ligands, e.g. Factor X, C3 and CD23.

The interaction of CD23 with CD11b/CD18 and CD11c/CD18 was partly characterised by Lecoanet-Henchoz *et al.* (1995). The CD23 binding site on the integrin was mapped to the alpha subunit by blocking monoclonal antibodies. Factor X was the most potent inhibitor of CD23 binding of the β2 ligands tested, suggesting their binding sites are in close proximity. If this was the case, it is likely that CD23 form contacts with regions outside of the I domain as well (Zhou *et al.,* 1994). The interaction was calcium

dependent as it was inhibited by EDTA and was also sensitive to deglycosylation by tunicamycin. This would be indicative of C-type lectin activity, however, EDTA could be disrupting metal ion dependent binding of either CD23 or the integrin. Activation of monocytes via CD11b and CD11c was achieved using monomeric 25 kDa sCD23 (Aubry *et al.*, 1995). Therefore, this putative lectin-carbohydrate interaction does not rely on avidity effects to improve affinity.

A common motif found in some integrin ligands is Arg-Gly-Asp (RGD) found in fibronectin, vitronectin, von Willebrand factor and the foot and mouth virus, and is used in the integrin interaction. Human CD23 contains an inverse RGD sequence in its C-terminal tail. However, RGD peptide and antibodies failed to inhibit CD23 binding to CD11b and CD11c. Furthermore, the absence of such a motif in murine CD23 (which also exhibits monocyte activation via CD11b) suggests the integrin binding site is elsewhere on CD23.

Table 1.1: Ligands of the β2 Integrins and Vitronectin Receptors

Integrin	Other names	Ligands	CD23 Binding
αLβ2	LFA-1, CD11a/CD18	ICAM-1,2,3,4	No
αMβ2	CR3, Mac-1, CD11b/CD18	ICAM-1,2, iC3b, LPS, Fibronectin, Factor X, sCD16, sCD23	Lecoanet-Henchoz *et al.*, 1995
αXβ2	CR4, p150,p95, CD11c/CD18	Fibronectin, iC3b, LPS, sCD16, sCD23	Lecoanet-Henchoz *et al.*, 1995
αDβ2		ICAM-3	Not determined
αvβ1	Vitronectin receptor	Vitronectin, fibronectin, von Willebrand factor, fibrinogen	Not determined
αvβ3	Vitronectin receptor, CD51/CD61	Vitronectin, PECAM-1, Laminin, Fibrinogen, Fibronectin, Von Willebrand Factor, Collagen, osteopontin, Thrombospondin	Hermann *et al.*, 1999
αvβ5	Vitronectin receptor	Vitronectin, Fibrinogen, Fibronectin	Matheson *et al.*, 1999

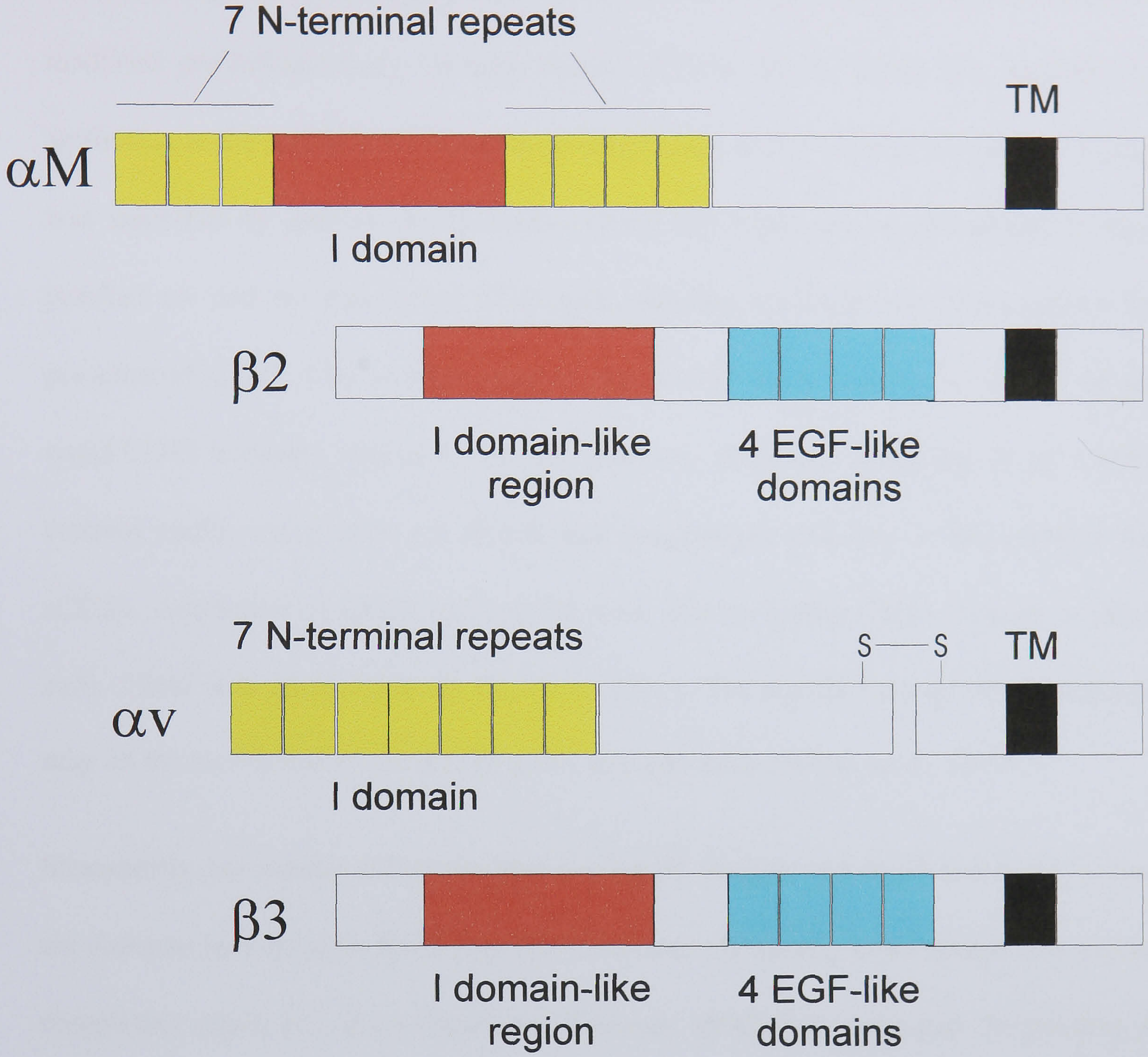

Figure 1.5: Structure of Integrin Subunits

The alpha subunits of integrin superfamily are type I glycoproteins with a short cytoplasmic domain. There are seven N-terminal repeat sequences believed to fold into a β propeller domain (Springer, 1997). Some alpha subunits (α1, α2 αL αM αX αD αE α9) have a conserved I domain between the 3rd and 4th repeat, where most ligands bind. Other alpha subunits are proteolytically processed in the extracellular domain which remains attached by disulphide bridge (α3, α5, α6, α7, α8 αIIb and αv). The beta subunits form intracellular protein contacts. An I-like domain and 4 EGF-like cysteine rich domains are present in the extracellular domain but are of unknown structure and function.

1.4.4 Vitronectin Receptors, αvβ3 and αvβ5

Hermann *et al.* (1999) provided evidence for another CD23-integrin interaction. CD23 mediated pro-inflammatory cytokine release (TNFα, IL-12, IFNγ) was inhibited by antibodies to the αvβ3/CD47 complex on monocytes. CD23 binding to αvβ3+ cell lines was inhibited by anti-αv. Furthermore, CD23 (25 kDa) was demonstrated to bind purified αv and αv transfected CHO cells. Binding to αvβ3 was improved by the presence of CD47. The authors propose that sCD23 binds directly to the αv of the αvβ3/CD47 complex mediating an inflammatory response. Matheson *et al.* (1999) isolated αvβ5 chains from pre B cell like lymphocytic cell line as the receptor for sCD23. Antibodies to CD23, αv and β5 were able to inhibit CD23 binding to these cells. CD47 was present but not β3, β2 or CD21. The significance of this interaction may be the prevention of pre B cells going into apoptosis (White *et al.*, 1997).

Structurally, the notable difference between the β2 integrin and αvβ3 and αvβ5, is that αv contains no I domain. RGD peptides have been chemically cross-linked to a region comprising repeat 2-7 of αv (Smith and Cheresh, 1990) that forms part the putative β propeller structure (Springer, 1997). In this model, a Mg^{2+} ion binds to the upper cavity of the propeller, providing a binding site similar to the MIDAS in the I domain.

Functionally, αv integrins which are widely expressed also have a large repertoire of ligands in addition to vitronectin and fibronection (Table 1.1). αvβ3 and αvβ5 and are implicated in, tumour invasion, bone resorption and transendothelial migration. The interaction of αvβ3 and αvβ5 with CD23 has yet to be confirmed and the biological significance remains unclear.

1.5 Biological Functions of CD23

1.5.1 Regulation of IgE Synthesis

Several lines of *in vitro* evidence have implicated CD23 in the up-regulation and down-regulation of IgE synthesis, using recombinant CD23, B-cell line cultures, anti-CD23 monoclonal antibodies and CD23 processing inhibitors (summarised in Table 1.2). Furthermore, inhibition of CD23 processing *in vivo* also resulted in IgE suppression (Mayer *et al.,* 2000). CD23 regulation of IgE occurs in IgE committed (i.e. IL-4 dependent) B cells (Saxon *et al.,* 1990). Furthermore, CD21 was identified as a ligand for CD23, also involved in the enhancement of IgE production (Aubry *et al.,* 1992).

Figure 1.6 illustrates a hypothetical model of a molecular mechanism for IgE regulation proposed by Sutton and Gould (1993). Down regulation or up regulation of IgE production is attributed to whether CD23 is in its membrane or soluble form, respectively. CD23 on the surface of B cells binding IgE or IgE-immune complexes transduces an inhibitory signal that prevents further IgE synthesis. This is supported by observations that IgE-CD23 blocking antibodies stimulate IgE synthesis (Sherr *et al.,* 1989) and that CD23 knockout mice have constantly increased IgE levels (Yu *et al.,* 1994). IgE binding appears to prevent CD23 being shed from the surface, presumably by stabilising the trimer (Munoz *et al.,* 1998). In the absence of IgE, the CD23 is cleaved terminating the negative feedback and allows the B cell to increase IgE synthesis.

In the human system, sCD23 is thought to up-regulate IgE synthesis either through ligation to membrane expressed CD21 or possibly by trapping IgE in the medium preventing it binding to membrane CD23 and triggering the negative signal, or both. The hypothetical cross-linking of IgE-CD23-CD21 to trigger IgE up-regulation (Figure

1.6) attempts to consolidate the wealth of *in vitro* results (Table 1.2). Certain evidence, e.g. enhancement by monomeric 25 kDa CD23 (Mayer *et al.*, 2000) and the contradictory effects of anti-CD23 Fab, IgG1 and IgG4 molecules (Sarfati *et al.*, 1988, Natamura *et al.*, 2000), suggest other mechanisms or receptors are responsible in these *in vitro* systems. Thus, the role of CD23 in IgE regulation is still uncertain.

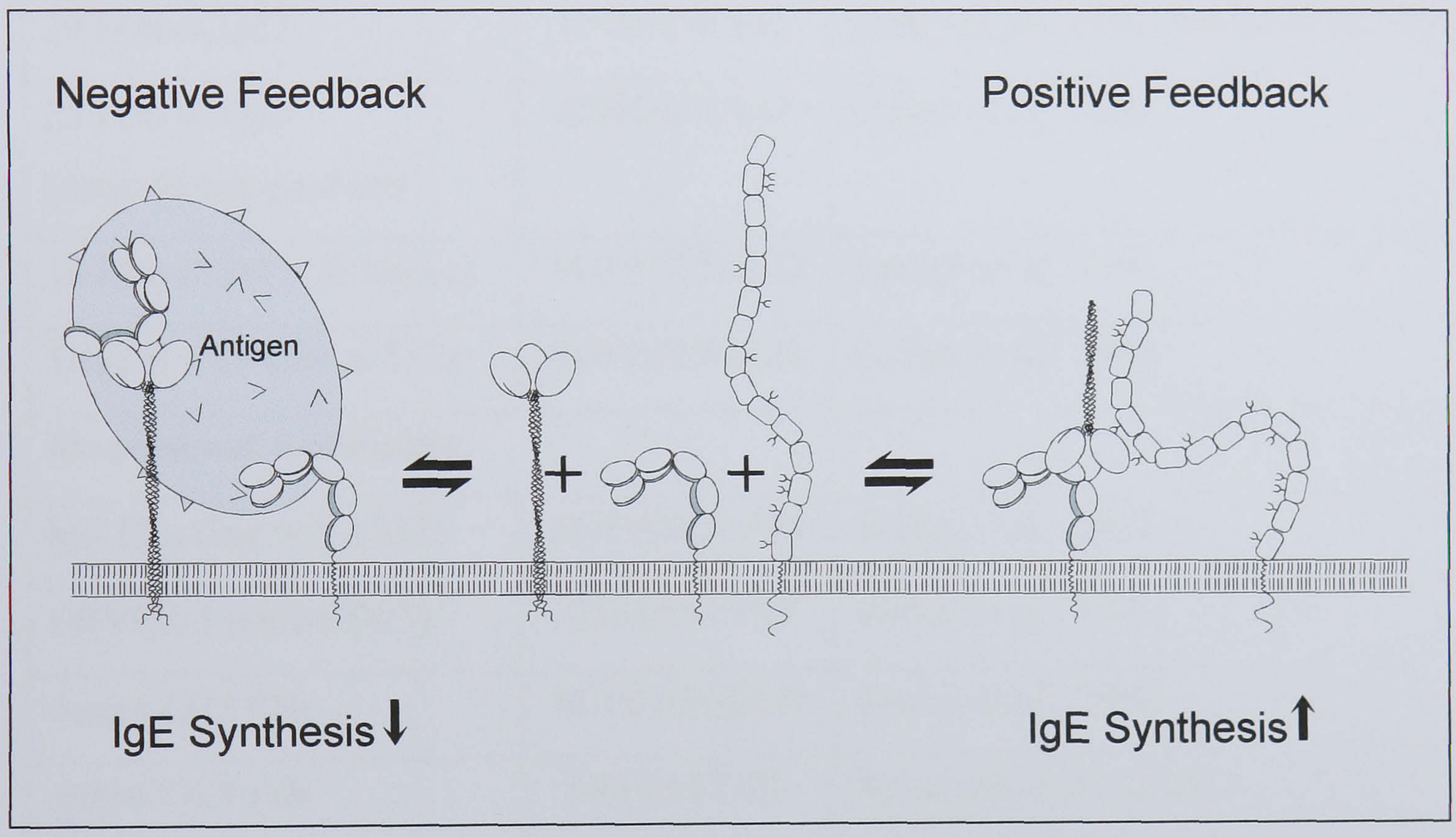

Figure 1.6: Hypothetical Molecular Mechanism For IgE regulation by CD23.

IgE, CD23 and CD21 are expressed on the surface of antigen activated B cells. In the presence of antigen and soluble IgE, a negative feedback signal is transduced on binding IgE. In a situation where membrane CD23 remains unligated, sCD23 is released and triggers a stimulatory signal possibly through the cross-linking of surface IgE and CD21 (Sutton and Gould, 1993).

Table 1.2: Evidence for role of CD23 in IgE Regulation

Culture Additive	Effect on IgE Production	Reference
Cell line supernatants		
RPMI 8866 (sCD23)	ENHANCED	Sarfati *et al.*, 1984
EBV (sCD23)	ENHANCED	Sarfati *et al.*, 1984
Recombinant sCD23		
33 kDa sCD23	ENHANCED	Chretien *et al.*, 1990
29 kDa sCD23	ENHANCED	Aubry *et al.*, 1992, Sarfati *et al.*, 1992
25 kDa sCD23 (degradation product)	ENHANCED	Mayer *et al.*, 2000
16 kDa sCD23 (& native)	SUPPRESSED	Sarfati *et al.*, 1992
16 kDa + 29 kDa sCD23	SUPPRESSED	Sarfati *et al.*, 1992
Monoclonal Antibodies		
IgE blocking anti-CD23	SUPPRESSED	Wakai *et al.*, 1993
EBVCS-1 (anti-CD23)	ENHANCED	Wakai *et al.*, 1993
Anti-CD23 Fab	SUPPRESSED	Sarfati *et al.*, 1988
Anti-CD23 Fab	NO EFFECT	Natamura *et al.*, 2000
Anti-CD23-chimeras	SUPPRESSED (IgG1 > IgG4)	Natamura *et al.*, 2000
Others		
EBV peptide	SUPPRESSED	Henchoz *et al.*, 1996
Anti-CD21	ENHANCED	Aubry *et al.*, 1992
Soluble CD21	SUPPRESSED	Fremeaux-Bacchi *et al.*, 1996
MMP Inhibitors	SUPPRESSED	Mayer *et al.*, 2000, Christie *et al.*, 1998, Wheeler *et al.*, 1998

1.5.2 IgE-CD23 Facilitated Antigen Presentation

Antibodies IgM, IgG and IgE have the ability to enhance or suppress an immunological response to their specific antigen. IgE is able to upregulate specific IgM, IgG1, IgG2 and IgE. Mice immunised with haptenated protein plus a monoclonal IgE specific for the hapten group gave a 100 fold increase in serum levels of specific IgG than with haptenated protein alone (Heyman *et al.,* 1993). Through the use of blocking antibodies and knockout mice, CD23 was identified as the receptor for this IgE mediated enhancement of specific antibody production. Furthermore, CD23 expressed on B cells, not follicular dendritic cells, is responsible in the murine system and requires the presence of T cells (reviewed by Heyman, 2000). In humans CD21 is also implicated in CD23 facilitated antigen presentation (Grosjean *et al.,* 1994).

A plausible mechanism is an increase in antigen binding, processing and presentation. CD23a expressed on the surface of B cells has been shown to be effective at internalising IgE-antigen complexes for processing and presentation of peptides by MHC II to antigen specific CD4+ T helper cells *in vitro*. CD23 has been shown to be spatially associated with MHC II (HLA-DR) in human B cell membranes (Bonnefoy *et al.,* 1988), which could be a result of antigen processing but also CD23 may be acting as a co-stimulatory or cell-cell adhesion molecule with CD21 at the immunological synapse. Alternatively, the binding of IgE-antigen complexes by CD23 may focus antigen on B-cells. Bound antigen could readily activate the B-cell through surface immunoglobulin and complement receptor.

1.5.3 Growth and Differentiation Factor

CD23 acts as a growth factor for antigen activated (or phorbol ester treated) B cells in culture. Soluble CD23 (25 kDa) in conjunction with IL-1 is able to rescue germinal

centre B cells (centrocytes) from apoptosis *in vitro (*Liu *et al.,* 1991). *In vivo* CD23 would allow those centrocytes primed with antigen to survive, presumably because sCD23 upregulates Bcl-2. This mechanism is thought to occur through IgE and CD21 cross-linking (Sutton and Gould, 1993; Reljic *et al.,* 1997). In this way expression of CD23 (induced by IL-4) might promote the survival of IgE switched centrocytes. CD23 and IL-1 (also *in vitro*) promotes the differentiation of centrocytes to antibody synthesising plasma cells, pro-thymocytes into T-cells (Bertho *et al.,* 1991) and myeloid precursors into basophils (Arock *et al.,* 1991).

1.5.4 Monocyte Activation.

Armant *et al.* (1994) demonstrated that sCD23 alone was able to stimulate the release of inflammatory cytokines TNF-α, IL-6, IL-1α and IL-1β from PBMC, typical of activated monocytic cells. Armant *et al.,* 1995 went further to show that sCD23 plus IL-2 co-stimulation of monocytes upregulates accessory molecules (CD40, B7) which induces the release of IFNγ by resting T-cells (in the absence of TCR occupancy).

This activity of sCD23 could not be attributed to binding to IgE or CD21. Lecoanet-Henchoz *et al.* (1995) identified the β2 integrins CD11b/CD18 (CR3) and CD11c/CD18 (CR4) as the monocyte receptors for recombinant CD23 in fluorescent liposomes. Interaction of recombinant soluble CD23 (25 kDa) with CD11b or CD11c triggers a transient calcium ion influx that activates a membrane bound, constitutively expressed, nitric oxide synthase (NOS). Nitric oxide is produced; cGMP accumulates ultimately leading to the production of TNF-α and other pro-inflammatory mediators (Aubry *et al.,* 1997). Two mitogen activated protein kinase pathways were identified as essential for the induction and control of IL-1β synthesis triggered by the sCD23-CD11b/CD18 and CD11c/CD18 interaction (Rezzonico *et al.,* 2000). CD11b, CD11c ligation with sCD23

was also shown to activate NF-κB leading to the expression of macrophage inflammatory protein, MIP 1α and MIP 1β (Rezzonico *et al.,* 2001). Activation of monocytes through β2 integrins is likely to influence adherence to endothelial cells in transmigration, monocyte-T-cell interactions, chemotaxis of other immune cells to site of inflammation, phagocytosis and cytotoxicity.

1.5.5 Other Possible Roles for CD23

Homotypic B-cell adhesion as observed with EBV transformed cells has been attributed to CD23 interactions with galactose glycoproteins (Kijimoto-Ochaia *et al.,* 1994) suggests CD23 could act as a cell adhesion molecule. CD23 may even play a role in cell migration. Stimulating anti-CD23 monoclonal antibodies have been reported to enhance eosinophil migration towards the chemokine, C5a (Lantero *et al.,* 2000). In studies with a monocytic cell line, U937, purified soluble CD23 was a potent inhibitor of monocyte migration which could be reversed by anti-CD23 monoclonal antibodies (Flores-Romo *et al.,* 1989). With the discovery of CD11b and CD11c as the receptor for sCD23 on monocytes, it remains to be seen whether inhibition of spontaneous migration was a result of blocking these adhesion molecules.

1.6 Implications of Soluble CD23 in Disease

It is established that overproduction of IgE is a hallmark of allergic disease. Serum sCD23 is also significantly increased in atopic patients as compared to normal controls. With the mounting *in vitro* evidence that sCD23 (in addition to IL-4) is capable of enhancing IgE synthesis, and that anti-CD23 monoclonal antibodies, and CD23 processing inhibitors can suppress IgE production, makes CD23 a potential target for therapeutics (Sutton *et al.,* 2000; Riffo-Vasquez *et al.,* 2000).

High levels of sCD23 are found in the serum of patients with B-chronic lymphocytic leukaemia. Levels indicate the extent of tumour load and clinic stage of the disease and are therefore used as a prognostic marker. CD21 is also upregulated and it is speculated that the CD21-sCD23 interaction underlies the B cell proliferation aspect of this disease (Lopez-Matas *et al.*, 2000). CD23 levels are also elevated in other diseases characterised by aberrantly proliferating B-cells: in certain immunocytomas and low-grade non-Hodgkin's lymphomas and EBV infections.

Elevated sCD23 levels are reported in a variety of chronic inflammatory diseases (reviewed by Bonnefoy *et al.*, 1996) e.g. systemic lupus erythematosus, inflammatory bowel, Sjogren's syndrome glomerulonephritis and rheumatoid arthritis (RA). In RA patients, sCD23 levels are high in serum but even greater in the synovial fluid of the joint. Within the synovial compartment there are very few B-cells (CD21+ or IgE+), quiescent T-cells but macrophages (CD11b+ CD11c+) are plentiful and are considered responsible for joint damage (Huissoon *et al.*, 2000). The importance of CD23 in the pathology of joint disease was shown by the suppression of collagen-induced arthritis in mice by anti-CD23 monoclonal antibodies (Plater Zyberk *et al.*, 1995). Thus, it is tempting to speculate that increased sCD23 contributes to the on-going inflammatory damage through continued activation of synovial macrophages. Prevention of sCD23 binding to CD11b and CD11c would be a valid target for anti-inflammatory therapies and justifies further investigation of the interaction.

1.7 Objectives of the Thesis

This thesis describes the expression and characterisation of two recombinant sCD23 fragments. The first, Der-CD23 comprises the sequence of the lectin domain produced by proteolysis by the house dust mite protease, *Der p* 1. This recombinant 16 kDa CD23 was used for NMR structural determination of the CD23 C-type lectin domain. The second CD23 fragment produced was a chimeric recombinant protein designed to stabilise the trimeric association of CD23. Two motifs for chimeric CD23 were compared; the surfactant protein D neck region and an isoleucine rich leucine zipper.

Both the CD23 lectin domain and trimeric sCD23 were included in ligand binding assays with recombinant IgE, CD21 and its integrin ligands in order to characterise their interactions in a cell free system. Kinetic data was obtained by surface plasmon resonance for the interactions between the novel proteins and IgE-Fc. Finally, the recombinant 16 kDa CD23 and trimeric CD23 were included in preliminary *in vitro* IgE synthesis assays utilising human peripheral blood mononuclear cells so that the mechanism of IgE suppression and enhancement could be investigated.

Thus, by the use of recombinant components, the structure and function of the 16kDa and trimeric soluble CD23 can be understood in more detail.

CHAPTER 2: MATERIALS AND METHODS

2.1 Materials

2.1.1 Buffers, Solutions and Media

Carbonate-Bicarbonate Buffer (pH 9.8): 22 ml 0.2 M anhydrous sodium carbonate, 28 ml 0.2 M sodium hydrogen carbonate, d.H_2O to 200 ml.

Coomassie Blue Stain: 0.25% Coomassie Brilliant Blue, 7.5% acetic acid, 5% methanol

Coomassie De-stain: 10% Acetic Acid, 40% methanol in d.H_2O

DNA loading Buffer: 0.25% Bromophenol Blue, 0.25% xylene cyanol, 30% glycerol

Extraction Solution 1: 10 mM Tris-Cl pH 7.9, 25% sucrose, 0.1 M KCl, 10 mM DTT, 2 mM PMSF (in isopropanol)

Extraction Solution 2: 0.3 M Tris-Cl pH 7.9, 100 mM EDTA, 0.1 g Lysozyme

Extraction Solution 3: 20 mM EDTA, 1 M LiCl, 0.5% Igepal

Extraction Solution 4: 10 mM Tris-Cl pH 7.9, 2.5 mM EDTA, 1 M LiCl, 0.5% Igepal, 10 mM DTT, 1 mM PMSF

Extraction Solution 5: 10 mM Tris-Cl pH 7.9, 2.5 mM EDTA, 2% Igepal, 10 mM DTT, 2 mM PMSF

Extraction Solution 6: 10 mM Tris-Cl pH 7.9, 2.5 mM EDTA, 0.5% Igepal, 10 mM DTT, 2 mM PMSF

HBS-Ca: 10 mM HEPES, 150 mM NaCl, 2 mM $CaCl_2$, 0.05% NaN_3, 0.002% SP20

Luria-Bertani media (1 l): 10 g Bactotryptone, 5 g Yeast extract, 10 g NaCl pH 7.5 (with NaOH)

M9 salts (10X): 10 g NH_4Cl, 30 g KH_2PO_4, 60 g $Na_2HPO_4 \cdot 7H_2O$

M9 minimal media (500 ml): 50 ml 10X M9 salts, 450 ml d.H_2O autoclave.

12.5 ml 20% casamino acids, 25 ml 20% glucose, 0.5 ml 0.1 M $CaCl_2$, 0.5 ml 1 M $MgSO_4$, 0.5 ml 10 mg/ml thiamine (all additives are filter sterilised)

PBS: 0.14 M NaCl, 2.7 mM KCl, 1.5 mM KH_2PO_4, 8.1 mM Na_2HPO_4, pH 7.4

Plasmid Preparation Solution 1 (P1): 50 mM Tris-Cl pH 8.0, 10 mM EDTA, 0.1 mg/ml RNase I

Plasmid Preparation Solution (P2): 1% SDS, 0.2 M NaOH

Plasmid Preparation Solution 3 (P3): 5 M Potassium Acetate pH 5.5

SDS Loading Buffer (4X): 0.25 M Tris-Cl pH 6.8, 0.01% Bromophenol Blue, 40% glycerol, 8% SDS (plus 10% β-mercaptoethanol for reducing buffer)

SDS Running Buffer (10X): 30.2 g Tris, 114 g Glycine, 10 g SDS up to 1 l with d.H_2O

SDS Tris Glycine Separation Gel Buffer*:* 1.5 M Tris-Cl, 0.4% SDS, pH 8.8

SDS Tris Glycine Stacking Gel Buffer*:* 0.5 M Tris-Cl, 0.4% SDS, pH 6.8

Semi-Dry Western Blot: Cathode Buffer*:* 25 mM Tris-Cl, pH 9.4, 40 mM ε-aminocaproic acid, 20% methanol

Semi-Dry Western Blot: Anode Buffer*:* 0.3 M Tris-Cl, pH 10.4, 20% methanol

Silver Diamine Solution: 21 ml 0.36% NaOH, 1.4 ml ammonia, 4 ml 20% silver nitrate, d.H_2O to 100 ml

Silver Stain Reducing Solution: 2.5 ml 1% citric acid, 0.26 ml formaldehyde, d.H_2O to 500 ml

Silver Stain Stop Solution*:* 10% Acetic Acid, 45% methanol

Silver Stain Farmer's Reducer: 0.3% (w/v) potassium ferricyanide, 0.6% (v/v) sodium thiosulphate, 0.1% (w/v) sodium carbonate

SOC: 2 g bactotryptone, 0.55 g yeast extract, 10 mM NaCl, 10 mM KCl autoclave in 97 ml d.H_2O. Add 10 mM $MgSO_4$, 10 mM $MgCl_2$ and 20 mM glucose, filter sterilise.

TAE (10X): 48.4 g Tris, 11.4 ml glacial acetic acid, 20 ml 0.5 M EDTA, d.H_2O up to1l

TBE: 90 mM Tris, 90 mM orthoboric acid, 2 mM EDTA

TBS-Ca: 25 mM Tris-Cl pH 7.5, 137 mM NaCl, 2 mM $CaCl_2$

TE: 10 mM Tris-Cl, pH 8.0, 1 mM EDTA

Wet transfer Western Blot Buffer: 3 g Tris, 14 g glycine, 20% methanol, d.H_2O to 1 l

2.1.2 Antibodies, Recombinant Proteins and Peptides

Anti-CD23 Antibodies: rb55, rabbit polyclonal (Glaxo) was used in Western blotting. A variety of monoclonal antibodies recognising epitopes on the lectin domain were used in ELISA (Table 2.1), EBV-CS1 being the exception as it binds to residues in the stalk domain (epitope mapping by Wakai *et al.*, 1993). MHM6 used in Western Blotting only recognises CD23 under non-reducing conditions.

Table 2.1: Details of Monoclonal anti-CD23 Antibodies.

Monoclonal Antibody	Source	CD23 epitope	Isotype
B6	Coulter Immunotech	Lectin Domain	IgG2b
BU38	Hybridoma (also Binding Site)	Lectin Domain	IgG1
EBV-CS1	W. Sugdon, WI, USA	Stalk	IgG1
EBV-CS2	W. Sugdon, WI, USA	Lectin Domain	IgG1
EBV-CS4	W. Sugdon, WI, USA	Lectin Domain	IgM
EBV-CS5	W.Sugdon (also BD)	Lectin Domain	IgG1
IOB8	Coulter Immunotech	Lectin Domain	IgG1
mAb 25	Coulter Immunotech, Glaxo	Lectin Domain	IgG1
MHM6	Hybridoma (also Dako)	Lectin Domain	IgG1

Anti-CD21 Antibodies*:* HB5 (hybridoma culture); BU33 (Binding Site, Birmingham, UK); IF8 (DAKO)

Anti-Integrin Antibodies: KIM87 (CD18), KIM127 (CD18), 6.E (CD18) mapped by Stephens *et al.,* 1995; Ab44 was obtained from Serotec; L230 (αvβ5), Ab1961 (αvβ5), Ab1980 (αvβ5), were all obtained from Celltech (Slough, UK).

Other Antibodies: M2 anti-FLAG (Kodak), donkey anti-rabbit immunoglobulin-HRP (DAKO); rabbit anti-mouse immunoglobulin-HRP (DAKO); G anti-CD40; goat anti-IgE (DAKO); goat anti-IgE-HRP (DAKO).

Recombinant proteins: rCD23 (31kDa) *E.coli* expression and purification described by R. Reljic (1996); sCD21 recombinant baculovirus (gift of VM Holers, Colorado, USA); anti-NIP IgE (JW8 hybridoma culture), IgE-Fc bIIgII (NS0 culture, Young *et al.*, 1995) recombinant soluble integrin (Fc fusions) αMβ2, αvβ1, αvβ3 and αvβ5 were produced at Celltech (Stephens *et al.,* 2000); iC3b (Calbiochem); IL-4 (R&D), Fibronectin, Fibronectin RGD peptide and Vitronectin RGD peptide (Sigma).

2.2 DNA Manipulation Techniques

2.2.1 Plasmid Vectors

The cloning of PCR products and engineering of DNA constructs were carried out in either pBluescript KS II (Stratagene) or in pSP73 (Promega). Both shuttle vectors are high copy and can be selected through their resistance to Ampicillin. Plasmid vectors for expression in *E.coli* and insect cells by baculovirus: pET5a (Novagen), pFastBac and pFastBacDUAL (GibcoBRL).

2.2.2 PCR

1 pmol of each primer was used in 50 µl PCR using 1 ng of cDNA template. 1-3 mM magnesium chloride, 20 µM dNTP and 1 U of *Taq* polymerase (all Promega) or *Pwo* polymerase (Expand, Boehringer Mannheim, for longer PCR products) were included in the reaction. The annealing temperatures of the primers were estimated by (4n[G/C] + 2n[A/T]) from Suggs *et al.* (1981) and was used in a 25 cycles of: 95 °C, 1 minute; annealing temperature 4 °C, 1 min; 72 °C, 1-1.5 minutes on a Biometra Trio-thermoblock PCR machine. 5 µl of PCR products were analysed on a TBE-agarose gel. Pooled PCR products were precipitated by adding sodium acetate, pH 3.5 to 0.1 M and then 3 volumes of 100% ethanol, incubating on ice for 30 minutes and spun down at 13,000 rpm for 10 minutes. The DNA pellet was washed with 70% ethanol, dried in air for 10 minutes and resuspended in 50 µl of the appropriate restriction digest buffer.

2.2.3 Agarose Gel Electrophoresis of DNA

0.5-1.5% agarose was melted in TBE or TAE buffer, cooled, 0.5 µg/ml ethidium bromide added and set in a gel tray with plastic comb. Once set, the gel was placed into electrophoresis apparatus and covered in buffer. 5 µl samples in DNA Loading Buffer were placed in the wells alongside appropriate DNA Molecular weight markers (λ-HindIII, pBS-HpaII) and a voltage of 100 V was applied across the gel until the fragments were separated, viewed by UV radiation.

2.2.4 Restriction Digest

1-5 U of restriction enzyme (or Promega or NEB recommendation) was used per microgram of DNA (PCR product or plasmid vector) and incubated at 37 °C for 1-2

hours in manufacturers' recommended reaction buffer. The reaction was stopped by heating to 60 ºC for 15 minutes. DNA loading buffer was added and the digested PCR fragment and vector were separated on an agarose-TAE gel. The band was excised and the DNA purified by QIAGEN gel extraction kit. Concentration of insert and vector were estimated by comparison of similar sized DNA of known concentration on a TBE-agarose gel.

2.2.5 Ligation

Relative quantities of vector to insert were calculated by the following equation using 100 ng of vector per ligation:

$$\text{Mass of insert (ng)} = \frac{100 \times \text{size of insert (kb)}}{\text{size of vector (kb)}} \times \text{molar ratio of insert:vector}$$

Ligation in 10 µl was carried out with 10 U T4 ligase and buffer (New England Biolabs) for 24 hours at 16 ºC. Reactions containing a molar ratio of insert:vector of 1 and 3 were performed alongside a negative control containing no insert to give an indication of the effectiveness of the vector digestion.

2.2.6 Transformation

100 ng plasmid or 5 µl of ligation product was used to transform chemically competent *E.coli* cells (Xli Blue) prepared by P.Marsh. 50 µl cells were added on ice and incubated for 15 minutes; heat shock at 42 ºC for 2 minutes was followed by addition of 200 µl SOC and 30 minutes at 37 ºC. 100 µl was spread onto LB-agar plate containing 100 µg/ml ampicillin (and also 40 µg/ml IPTG and 100 µg/ml X-gal for blue/white colony selection of pBluescript) and incubated overnight at 37 ºC

2.2.7 Plasmid purification

Single colonies (white if selected on IPTG/X-gal plates) were picked and cultured in 2 ml LB (plus 100 μg/ml Ampicillin) overnight at 37 ℃. 1.5 ml of the culture was spun at 10,000 rpm for 2 minutes and the plasmid DNA from the bacterial pellet was extracted by the method of Birnboim, 1983. Cultures of positive colonies were used to produce larger, purer quantities of plasmid DNA using the QIAGEN plasmid purification MIDI-kit following the manufacturers instructions. Concentrations of purified plasmid were estimated by spectrophotometry, where A_{260} of 1 is the equivalent of 50 μg/ml double stranded DNA.

2.2.8 Colony Screening

Identification of colonies containing the insert of interest was carried out by either restriction digest or a PCR screen. Restriction digest was performed using 3 μl of purified plasmid in a 10 μl reaction. For the PCR screen, 20 μl reactions were spiked with cells picked from a single colony with NUNC inoculating needles. Clones were also spotted onto a fresh agar plate labelled with colony numbers. Up to 94 colonies could be analysed by PCR using a 96 well plate in a Hybaid PCR machine. DNA loading dye was added to the digests or PCR reactions and analysed by TBE-agarose gel electrophoresis. Colonies screened as positives were confirmed by sequencing

2.2.9 Sequencing

Oligonucleotides of 20 bases, of 50/50 AT/GC content, were designed along both strands of the insert at 350-400 bp staggered intervals. Primers outside the cloning site were also designed or provided by the vector's supplier. The insert was sequenced by a

dideoxy termination method using the Big Dye Terminator cycle Sequencing kit (PE biosystems). Following a 7.5 µl cycling reaction (including 0.5-1.0 µg DNA, 3.2 pmol primer) the products were analysed using ABI Prism Technology (PE biosystems) by A. Lyons (Celltech). Clones with the no sequence errors were used in further construct assembly rounds or the insert was excised and transferred to the expression vector.

2.2.10 Sequence Analysis

Sequencing data from each primer were overlapped and edited by the Autoassembler software (Perkin Elmer). The sequence obtained was then compared to the original sequence using Mac Vector 6.5 software (Oxford Molecular). The sequence of the cDNAs were obtained from Genbank databank available on the internet (listed in Table 2.2). Any point mutations found were checked to see whether they were silent (and therefore acceptable) by translating the sequence data by Mac Vector and comparing it to the correct protein sequence.

Table 2.2: Genbank Names and Numbers of Construct Sequences

DNA	Genbank Name	Accession Number	Author reference
Human CD23	HUMFCERA	M14766	Kikutani,H. 1986
Human CD11b	HUMLAPA	M18044	Arnaout,M.A. 1988
Human CD18	HUMLAP	M15395	Kishimoto,T. 1987
Human SPD	HUMSPD02	L05484	Rust,K. 1991

2.3 Protein Expression Systems

2.3.1 *Escherichia.coli*

2.3.1.1 Expression Conditions

100 ng of recombinant expression plasmid was used to transform either BL21 (DE3) or BL21 (DE3) (pLysS) supplied by P.Marsh, KCL, or Invitrogen.

Genotypes:

BL21 (DE3): F^- *ompT hsdS*$_B$ ($r_B^- m_B^-$) *gal dcm* (DE3)

BL21 (DE3) pLysS: F^- *ompT hsdS*$_B$ ($r_B^- m_B^-$) *gal dcm* (DE3) pLysS (Cam^R)

Transformation into these cells differs from the standard protocol as heat shock stage at 42 ºC only needed 40 seconds. Cells containing the target plasmid (pET5a) were selected by 50 μg/ml ampicillin (or 50 μg/ml carbenicillin). When using the *E.coli* host strain containing pLysS, 34 μg/ml chloramphenicol was also required.

A single colony was picked and grown in 2 ml M9 media containing antibiotics for 8 hours. An overnight culture of 100 ml was inoculated with 1 ml. The following day, 500 ml M9 media containing antibiotics was inoculated with 10 ml of overnight culture in a 2 l conical flask. The culture was incubated at 37 ºC, with orbital agitation at 200 rpm until the A_{600} reached 0.6-1.0. Expression of the target was induced with 0.4 mM IPTG. The cells were harvested after further incubation at 3 hours by centrifugation at 5000 rpm for 10 minutes in a GSA rotor (Sorvall). The pellets were stored frozen at –20 ºC.

2.3.1.2 Purification of Der-CD23 from Inclusion Bodies

Inclusion bodies from at least 1 litre of culture were extracted and purified by the method of Bohmann and Tjian (1989) using the extraction solutions listed in 2.1. The pellet was resuspended in 72 ml of Solution 1 with DNase I (Sigma) to break up viscous

cellular DNA. The cells lyse on thawing if using BL21 (DE3) (pLysS) strain, even so, 18 ml Solution 2 was added containing lysozyme and incubated on ice for 10 minutes. 90 ml solution 3 was added, vortexed and sonicated on ice for up to 10 minutes to disperse clumps of material, then centrifuged for 10 minutes at 10,000 rpm in a GSA rotor at 4 °C. The inclusion body pellet was resuspended in 200 ml Solution 4, sonicated and pelleted as before. This washing step was repeated using Solutions 5 and 6. The final purified preparation of inclusion bodies was resuspended in 5 ml 6 M Guanidine and incubated at room temperature for 1 hour. Soluble proteins are separated from insoluble material by centrifugation at 10,000 rpm, 4 °C for 5 minutes. The protein concentration was measured by A_{280} adjusted to 10 mg/ml and stored at 4 °C.

2.3.1.3 Refolding

This was the method used by Taylor *et al.,* 1992, involving the reduction of cysteine residues with glutathione to facilitate refolding by dilution into cysteine buffer. 20 mg of protein in 6 M Guanidine was reduced by 10 mM DTT, 100 mM Tris-Acetate, pH 8.6, and left standing at room temperature for 1 hour. The reduced protein was diluted ten-fold in 6 M Guanidine, 0.5 M Tris-Acetate pH 8.6 and 100 mM glutathione (oxidised form, Sigma). The glutathione intermediate was formed at 4 °C for 24 hours. The protein was further diluted 100-fold into a refolding buffer containing 100 mM Tris-Acetate pH 8.6, 3 mM cysteine and 2 mM $CaCl_2$. This addition was made slowly to avoid precipitation. The protein was allowed to refold at 4 °C, in the dark for 48 hours.

2.3.2 Baculovirus Expression System

Expression in insect cells was carried out with the pFastBac baculovirus expression system. Methods for virus production were adapted from the manufacturers handbook (GibcoBRL) and virus handling methods taken from O'Reilly *et al.* (1994).

2.3.2.1 Transposition

10 ng of pFastBac containing the cloned construct was placed in sterile 15 ml polypropylene tubes and 100 µl of D_{H10}Bac competent cells were added. After 30 minutes incubation on ice, the cells were heat shocked at 42 °C for 45 seconds then chilled on ice for 2 minutes. 900 µl SOC medium was added and the mixture placed at 37 °C with medium agitation for 4 hours. 100 µl and a dilution of 1 in 1000 of the transposed cells were plated on agar plates (containing 50 µg/ml Kanamycin, 7 µg/ml Gentamycin, 10 µg/ml Tetracyclin, plus 100 µg/ml Bluo-gal and 40 µg/ml IPTG for blue/white colony selection). The plates were left to incubate at 37 °C for at least 24 hours. 10 white colonies were picked, streaked onto fresh plates and incubated at 37 °C for another 24 hours.

2.3.2.2 Isolation of Recombinant Bacmid DNA.

3 colonies were picked and grown at 37 °C for 24 hours in 2 ml LB (containing antibiotics). 1.5 ml of the culture was used to produce a preparation of the bacmid DNA by standard plasmid purification: resuspension in 250 µl Buffer P1; lysis 3-4 minutes with the addition of 250 µl Buffer P2; and neutralisation at room temperature on gentle mixing with 250 µl Buffer P3. The suspension was centrifuged for 10 minutes at 13,000 rpm and the supernatant carefully transferred to an equal volume of isopropanol. The DNA was precipitated by incubation on ice for 10 minutes. After centrifugation 13,000 rpm, 10 minutes, the pellet was washed with 0.5 ml 70% ethanol, dried, resuspended in 50 µl TE and stored at –20 °C. The samples of the DNA preparation were run on a 0.5% agarose gel in TAE buffer to confirm the presence of the bacmid DNA by its characteristic pattern.

2.3.2.3 Transfection of Sf9 Cells with Recombinant Bacmid DNA.

9×10^5 Sf9 cells in mid-log phase were seeded in a 6 well plate in 2 ml sf-900 II serum free media (JRH) or excell 420 (JRH). After the cells had been left to attach for an hour at 27 °C, the media removed and washed with fresh media. A mixture of 5 µl bacmid DNA in 100 µl media and 6 µl of the lipid suspension CELLFECTIN in 100 µl media were gently mixed and incubated at room temperature for 30 minutes and then diluted to 1 ml with media. The lipid-DNA complexes was used to overlay the cells and incubated for 5 hours or overnight. The transfection mixture was removed and 2 ml of media added and incubated at 27 °C for 48 hours. Between 48-72 hours the virus infected cells had died and the cells and media were assayed for protein by Western blot.

2.3.2.4 Estimating Virus Titre by Plaque Assay.

The culture was centrifuged at 4000 rpm for 5 minutes and the supernatant (viral fraction) was stored in the dark at 4 °C. 1.2×10^6 Sf9 cells in 1.8 ml media were seeded in 6 well trays and left to attach for 1 hour. A serial dilution of the virus (10^{-1},10^{-2}…10^{-9}) were made in the wells and left to adsorb onto the cells by incubating at 28 °C. After 2 hours the media was removed and to the wells 2 ml of a 1:1 mixture of media and 3.2% low gelling temperature agarose in PBS was added. Once set, 1 ml of media was placed on top of the agarose overlay. The trays were incubated at 28 °C for 7 days. To detect the plaques, the live cells were stained by the addition of 1 ml of a 1 in 20 dilution of Neutral Red (Sigma) in PBS for 1 hour. The stain was removed and the wells left in the dark for a couple of hours or overnight before estimating the virus titre by the number of clear plaques (dead, infected, cells from a single virus).

2.3.2.5 Amplifying the viral titre.

To amplify the viral titre a monolayer or suspension of Sf9 cells of density 0.8 x 10^6 per ml were infected with the stock virus. 400 ml and 800 ml suspensions could be produced in flat bottomed round flasks with agitation by a magnetic bar stirrer at 180 rpm at 28 °C. The following formula was applied where the multiplicity of infection (MOI) for viral amplification was 0.1 (i.e. the ratio of plaque forming units of virus to host cell number). Higher densities of cells could be used with excell 420 as this richer media could support growth to 4 x 10^6 cells/ml therefore could be infected at 2 x 10^6 cells/ml.

$$\text{Inoculum required (ml)} = \frac{\text{MOI (pfu/ml)} \times \text{(total number of cells)}}{\text{titre of Inoculum (pfu/ml)}}$$

2.3.2.6 Infection of Sf9 Insect Cells for Protein Expression

The MOI for protein expression was between 5 and 10. Up to 800 ml culture could be infected in a suspension, or a large scale (5 l) fermenter was used to produced large quantites of protein conditions described in Chapter 4. The culture was harvested after 3 days when expressing a secreted recombinant protein.

2.4 Protein Purification Methods

All chromatography steps were carried out using either an HPLC system (Gilson) for size exclusion chromatography or peristaltic pump apparatus (Gilson) for other methods.

2.4.1 Affinity Chromatography

Antibody was coupled to Affiprep-10 through primary amines (Biorad). 5 ml matrix was washed with 30-50 volumes 10 mM sodium acetate pH 4.5 in a Buchner funnel. 10

mg of purified antibody dialysed into acetate buffer was added to the matrix, transferred to a 50 ml tube and incubated at 4 °C for 4 hours on a rotating wheel. Free active esters were blocked with 0.1 M ethanolamine, washed with 4 volumes 0.5 M NaCl. The coupled matrix was packed into an Econo-column (Biorad) and washed with PBS until no more uncoupled protein was eluted. A mock-elution step with 5 volumes 0.1 M glycine pH 2.5 was also performed on the newly made column.

For purification, the column was equilibrated with TBS-Ca (+ 0.05% NaN_3) at 1 ml/min at 4 °C using a peristaltic pump, the sample loaded then washed with at least 10 column volumes (CV) of TBS-Ca. The protein was eluted with 3-5 CV 0.1 M glycine, pH 2.5, into tubes containing 1/10 volume 1M Tris-Cl, pH 8.0. The column was immediately re-equilibrated with 5 CV TBS-Ca

2.4.2 Hydrophobic Interaction Chromatography

25 ml phenyl sepharose 6 (high substituted) HIC matrix was packed into a 16 x 30 cm column (both Amersham Pharmacia Biotech) and equilibrated with 25 mM Tris-Cl pH 7.5, 1.5 M ammonium sulphate. The sample was adjusted to 1.5 M ammonium sulphate and filtered through a 43 mm cellulose acetate filter (0.8 µm pore; Sattorius). The sample was loaded at 5 ml/min at 4 °C using a peristaltic pump, then washed with 5 CV equilibration buffer. The bound proteins were eluted by a gradient to low salt (25 mM Tris-Cl, pH 7.5) over 10 CV and separated according to increasing hydrophobicity. Tightly bound proteins were removed by 3 CV 30% isopropanol, followed by 10 CV d.H_2O. Further sanitization was carried out with 3 CV 0.1 M NaOH.

2.4.3 Size Exclusion Chromatography

Superdex 75 or Superdex 200 column (Amersham Pharmacia Biotech) were equilibrated with 0.5 M Tris-Cl, 0.25 M NaCl, pH 7.2, 0.05% NaN_3 at a flow rate of 0.75 ml/min. 200 µl samples were injected onto the column and was separated according to size. Higher molecular weight components elute first, not being impeded by diffusion into the pores in the beads. The columns were calibrated by injecting proteins of known molecular weight obtained from the Molecular Weight Standards Kit (Sigma). By plotting log(Mw) against time of elution, the Mw of the sample protein can be estimated from the linear section of the plot.

2.4.4 Concentration Techniques

Proteins in solution were concentrated using ultrafiltration through 10 kDa cut off YM10 cellulose membranes (Millipore) in Amicon Stirred cells (300 ml, 50 ml or 10 ml sizes). Ultrafiltration was carried out at 4 °C under pressure provided by compressed air. Smaller volumes for analysis were concentrated by microcon-10 (Millipore) spun in a cooled micro-centrifuge at 8 000 rpm for 20 minutes at 4°C.

2.4.5 Buffer Exchange

The buffer of the protein sample was changed either during concentration or by dialysis. Dialysis membrane (MW cut off 8 kDa, Medicell) was prepared by boiling with EDTA for 10 minutes. The sample inside the dialysis tubing was placed into at least 200 volumes of the desired buffer and stirred at 4 °C. The dialysis buffer was changed twice in the course of 24 hours. Buffer exchange was also performed using PD10 ion

exchange columns (Amersham Pharmacia Biotech) using the manufacturer's instructions.

2.5 Protein Characterisation

2.5.1 Estimating Protein Concentration

Total protein in a supernatant was approximated using the Biorad protein assay (based on the Bradford protein test) using BSA for a standard curve as instructed in the manual. The concentration of a specific protein in a heterogeneous solution was crudely estimated by comparing the signal density in a Western blot against a titration of the same protein of known concentration. A quantitative ELISA for CD23 was designed (see 2.5.8.2) for the same purpose.

Pure protein was more accurately calculated by UV spectrophotometry. A spectrum measuring wavelengths between 240 nm and 340 nm was recorded on a Cary Varian UV-visible spectrophotometer using an appropriate buffer blank as baseline. A concentration of the protein sample was calculated from Beer's Law:

$$A = c\varepsilon l$$

Where A is the absorbance at a specified wavelength, c is the molar concentration, ε is the molar extinction coefficient and l is the path length of the cell (1cm for quartz spectrometer cuvette manufactured by Hellmann). Concentrations in mg/ml can be calculated multiplying the molar concentration with the molecular weight. The molar extinction coefficient and the Mw of protein from *E.coli* can be estimated from the sequence by the peptidesort programme in the GCG Wisconsin package (Table 2.3).

Table 2.3: Data of commonly used recombinant proteins.

Peptide	Expression System	Molecular weight (Da)	Extinction Coefficient ($M^{-1}cm^{-1}$)
Der-CD23	*E.coli*	16145	45430
H-CD23	NS0 / *E.coli*	15774	45430
LZ-CD23	*E.coli*	37638	63300
rCD23	*E.coli*	30991	51120
sCD21	Baculovirus	120000	84730
SPD-CD23	Baculovirus	22325	46710

2.5.2 SDS-PAGE

SDS-PAGE was employed to judge the presence, purity and molecular weight of a protein in a sample. The methods are based on Laemmli (1970) and carried out in Atta or Novex mini gel apparatus. Gels were either purchased from Novex or created using the solutions listed in Table 2.4, where Acylamide refers to 30% w/v acrylamide bis-acrylamide 37.5:1, and APS, ammonium persulphate. Gradient gels were also made using a gradient maker attached to a peristalic pump.

The gel was placed in the tank and filled with running buffer, the samples were loaded after boiling in reducing or non-reducing sample buffer for 6 minutes alongside molecular weight markers: See-Blue, Mark-12 (both Novex) or full range Rainbow markers (Amersham Life Sciences). A voltage of 150 mV was applied and the proteins separated until the dye reached the bottom of the plate.

Table 2.4: Preparation of Solutions for SDS Mini-Gel

	Stacking	5% Separation	10% Separation	12% Separation	15% Separation	20% Separation
Acyrlamide	1.00	1.68	3.33	4.18	5.00	6.65
Gel Buffer	1.25	2.50	2.50	2.5	2.50	2.50
d.H_2O	3.18	5.68	4.03	3.18	2.36	0.70
10% APS	0.05	0.05	0.05	0.05	0.05	0.05
TEMED	0.025	0.0075	0.0075	0.0075	0.0075	0.0075

2.5.3 Staining Protein on SDS Gels

The choice of stain depended on the amount of protein loaded onto the gel. Coomassie was used for samples containing 5-10 μg and silver staining for less than 0.5 μg. Gels were removed from the plates and covered with Coomassie stain and incubated at room temperature overnight on an orbital shaking platform. Background staining was removed with De-stain Solution for several hours until protein bands were visible.

The silver stain protocol was adapted from Wray *et al.* (1981). After electrophoresis, the gel was fixed in 20% TCA for at least 1 hour. The gel was then washed twice in 50% methanol for 30 minutes then in d.H_2O twice for 20 minutes. The Silver Diamine Solution was added for 15 minutes (neutralised with HCl before disposal) then washed in d.H_2O twice for 5 minutes. Protein bands appear after 5-10 minutes in Reducing Solution, the solution was poured away, rinsed and Stop Solution added. Partial de-staining could be achieved in Farmer's Reducer and returned to Stop Solution.

2.5.4 Western Blotting

Following electrophoresis, the protein on the gel were transferred to either nitrocellulose (0.4 μM pore, Schleicher and Schuell) or 0.45 μm pore Immobilon-P (Millipore) which requires activation in methanol for 30 seconds. Protein could be transferred by a semi-dry or a wet method.

For semi-dry transfer, 2 pieces of thick Whatman blotting paper adsorbed with Anode and Cathode Buffer and was used to sandwich the gel and dry nitrocellulose between graphite electrode plates. The nitrocellulose, free of air bubbles, was placed at the anode side of the assembled blot. Transfer was usually complete after 20 minutes at 20 V.

Wet transfer involved all components of the blot being soaked in cold Wet Transfer Blotting Buffer and assembled as above in a Novex Western Blot apparatus. The tank was completely filled with buffer and a current of 220 mA was applied for 1 hour.

Following transfer, the immunoblot was blocked 1 hour (or overnight) in 5% BSA in TBS-Ca. CD23 was detected by the polyclonal antibody rb55 in 1% BSA TBS-0.05% azide (which was reused) and incubated for 1 hour at room temperature with gentle agitation. The blot was washed 3 times for 10 minutes with TBS-Ca 0.05% Tween 20. Goat anti rabbit immunoglobulin HRP (Dako) was added as a 1 in 2000 dilution in 1% BSA TBS-Ca-T and incubated for one hour. The blot was washed again, and developed with SuperSignal (Pierce) chemoluminescence reagents. The blot was wrapped in cling film and used to expose autoradiography film (Kodak) initially for 1 minute. The film was developed by an X-omat machine.

Alternatively, following blocking with 10% Marvel PBS, monoclonal antibodies were used at 1 μg/ml in 2% Marvel PBS-Tween and revealed with rabbit anti-mouse immunoglobulin HRP conjugate (Dako).

2.5.5 Chemical Crosslinking

2.5.5.1 1-Ethyl-3-(3-dimethylaminopropyl)carbodiimide Hydrochloride (EDC)

1-Ethyl-3-(3-dimethylaminopropyl)carbodiimide Hydrochloride (EDAC or EDC) is a water soluble condensing reagent. The method employed was that described by Beavil *et al.*, 1995. Cross-linking was performed in a 15 minute reaction at room temperature with 1 μg of protein in 20 μl 25 mM acetate buffer pH 5 and 25 mM EDC. Non-reducing SDS loading buffer was added to stop the reaction. The cross-linking reactions were loaded onto a 5-15% Tris-glycine gel alongside non-cross linked protein and visualised by silver staining or western blot (using rb55 polyclonal antibody).

2.5.5.2 Di-fluoro di-nitrobenzene (DFDNB)

50 mM stock solution of DFDNB was made in ethanol. 1 μg/ml protein was incubated with 1 mM DFDNB (or a titration of concentrations) in 100 mM carbonate buffer, pH 10 for 2 hours at room temperature. The reaction was stopped on addition of reducing SDS loading buffer and resulting crosslinked products were analysed by western blot.

2.5.6 Mass Spectrometry

50 μg of sample was run by positive ion electrospray, scanning 1000 - 2000 amu performed by L. King (Celltech). The sample was injected onto a 5 cm C18 column at 5:95 MeCN:H_2O, 0.1% formic acid, at 0.1 ml/min. After 1 min, the solvent was ramped quickly up to 70:30, and the eluting protein was acquired, after approximately 10 minutes.

2.5.7 N-terminal Protein sequencing

30 pmol of pure protein was prepared using Prosorb Sample Preparation Cartridge and analysed in a Procise 492 Protein Sequencer (PE biosystems) by B.Smith (Celltech).

2.5.8 Enzyme-Linked Immunosorbent Assay (ELISA)

2.5.8.1 Preparation of Biotinylated Proteins for ELISA

Protein at 1 mg/ml in PBS was incubated for 1 hour at room temperature in the dark with a 1:20 molar ratio of protein to 6-(Biotinamidocaproylamido) caproic acid succinamide ester (Biotin-X-X-NHS, Sigma) dissolved in DMSO. Free biotin was dialysed away in PBS. For purposes such as preparing ligand for streptavidin coated SPR sensorchips, a ratio of 1:5 was employed.

2.5.8.2 Quantitative sCD23 ELISA

The quantification of soluble CD23 was carried out using Nunc maxi-sorb 96 well flat bottomed plates (GibcoBRL). 100 µl EBVCS-4 anti-CD23 capture antibody at 2 µg/ml was coated in bicarbonate-carbonate buffer, pH 9, overnight at 4 °C. The coating solution was discarded and free binding sites on the plate were blocked with 2% Marvel in PBS for 1 hour at room temperature. The plate was washed 4 times with 200 µl PBS 0.05% Tween 20.

A standard CD23 protein (e.g. H-CD23 from NS0 cell cultures) of known concentration was serially diluted (x2) in triplicate across the plate (from 0.5 µg/ml). Proteins of unknown concentration were added in triplicate at a couple of dilutions as were an appropriate negative control and an internal control of known concentration. These 100 µl samples in assay buffer (1% Marvel, PBS, 0.02% Tween 20) were incubated at room temperature for 1-2 hours. The plate was washed as before.

The next step involved incubation of 1 μg/ml biotinylated BU38 in assay buffer for 1-2 hours as before. Following washing, a 1 in 2000 dilution of streptavidin-horse radish peroxidase conjugate (Amersham Life Sciences) in assay buffer was added and incubated for one hour at room temperature.

After a final washing procedure, the ELISA was developed using 5 mg/ml OPD in phosphate-citrate buffer plus 0.8 μl/ml hydrogen peroxide. 50 μl of OPD solution was added to each well and allowed to develop in the dark for 10 minutes. The enzyme reaction producing colour development was terminated on addition of 50 ml of 3 M HCl. The A_{492} of the wells were recorded by a Titertek micro-plate reader. The A_{492} readings of the standards were plotted against log concentration. A sigmoidal curve was fitted to the data points using Ascent software. The concentration of the sample triplicates were estimated from the linear part of the curve.

EBVCS-2 and biotinylated MHM6 was another combination of anti-CD23 monoclonal antibodies, that could be reliably used in this ELISA.

2.5.8.3 Quantitative IgE ELISA

Microtitre plates were coated with a 1 in 7000 dilution of anti-IgE (Dako, A0094) in carbonate buffer, overnight at 4 °C. 2% Marvel PBS-T was used to block the wells for one hour at room temperature. The wash buffer (PBS-T) used 5 x 400 μl between each step. Anti-NIP IgE was serially diluted by two (from 200 ng/ml) to produce 11 triplicates on the standard curve. Samples were also applied in triplicate and incubated overnight at 4 °C. A 1 in 500 dilution of anti-IgE-HRP (Dako, P0295) was applied for 4 hours at room temperature. OPD was used to develop the enzyme reaction and quantification calculated as above.

2.5.8.4 CD23 - IgE ELISA

Plates were coated with 3 μg/ml CD23 in TBS containing 2 mM $CaCl_2$, overnight at 4 °C. 5% BSA in TBS-Ca was used as blocking buffer and TBS-Ca O.05% Tween 20 used as a wash buffer between each step (4 x 200 μl). 1 μg/ml biotinylated IgE or IgE-Fc (or a serial dilution) in 0.5% BSA-TBS-Ca-T was incubated for 3 hours at room temperature. Interactions were revealed by 1 in 2000 dilution of streptavidin-HRP (Life Technologies) for 1 hour at room temperature. OPD was used to develop the enzyme reaction.

2.5.8.5 Sandwich CD23-IgE ELISA

Microtitre plates were coated in 2 μg/ml mAb25 (Immunotech) overnight at 4 °C in carbonate buffer. The blocking buffer, wash buffer and assay buffer were the same as used in the direct ELISA. CD23 samples were applied for 2 hours at room temperature. 1 μg/ml biotinylated NIP IgE or IgE Fc were added for a 3 hour incubation at room temperature. The interaction was detected by streptavidin-HRP (1 in 2000) as before and visualised with OPD.

2.5.8.6 CD23 - CD21 ELISA

Based on the ELISA described by Fremeaux-Bacchi *et al.*, 1996, 10 μg/ml CD23 was coated in TBS-Ca (using iC3b as a positive control). 1% BSA in hypotonic phosphate buffer (10 mM sodium phosphate, 25 mM NaCl) was used as a blocking buffer and hypotonic phosphate buffer with 0.1% Tween as a wash buffer. Serial dilutions of sCD21 (baculovirus) from 10 μg/ml in 0.1% BSA hypotonic phosphate–T were incubated for 3 hours at room temperature. 1.5 μg/ml anti-CD21 antibody HB5 was added for 2 hours at room temperature. A rabbit anti-mouse immunoglobulin –HRP conjugate (1 in 2000) was added for 1 hour, then developed with OPD.

2.5.8.7 CD23 – recombinant soluble integrin ELISA

5 μg/ml Der-CD23 in TBS-Ca and positive controls were coated (unless otherwise stated) overnight at 4 °C. 5% BSA in TBS-Ca was used as a blocking buffer (1 hour room temperature) and TBS-Ca-T plus 1 mM $MnCl_2$ as a wash buffer. Dilutions of culture supernatants containing integrin-Fc chimeras in wash buffer were to used establish optimum concentration (detailed in Chapter 6). Following incubation for 2 hours at room temperature the plates were washed and a 1 in 5000 dilution of anti mouse (or human) IgG Fc-HRP in 1% BSA in wash buffer added for 1 hour. TMB substrate was added and absorbance at 630 nm measured after 15-20 minutes.

2.5.9 Surface Plasmon Resonance

Surface Plasmon Resonance (SPR) was performed using a Biacore Biosensor apparatus (Pharmacia Biosensor) at 25 °C using HBS-Ca buffer. The ligand was lightly biotinylated (2.5.9.1) at molar ratio 1:5 protein:biotin reagent so that it would bind the streptavidin coated SA sensor chip. The ligand, IgE-Fc bIIgII (diluted in HBS-Ca) was passed over the conditioned flow cell at 5 μg/min until approximately 450 response units (RU) and 900 RU were obtained. A control protein (rCD23) was used to select the optimum regeneration conditions (3 x 2 minute injections of HBS, 50 mM EDTA). To obtain data for kinetic analysis, the analyte (soluble CD23) was injected at various concentrations at a flow rate of 10 μl/min. The association phase and dissociation phases were measured for 6 minutes, then the ligand was regenerated. A conditioned flow cell with no ligand bound to the streptavidin was used as a negative control. The data obtained was analysed using BiaEvaluation 3.0 (Pharmacia Biosensor) using the 1:1 Langmuir association/dissociation model.

2.5.10 Culturing Human Peripheral Blood Mononuclear Cells (PBMC)

PBMC preparations were performed by N. McCloskey and D. Fear. 60 ml of blood containing anti-coagulant were diluted 1:1 in PBS. 20 ml of the diluted blood was layered onto 15 ml of Ficoll-paque (apb) and centrifuged for 2000 rpm for 20 minutes (brake off). The interface was pipetted off and washed in PBS by a further centrifugation at 200 rpm for 10 minutes at room temperature. Pelleted cells were resuspended in 10 ml culture media: RPMI 1640, 10 μg/ml penicillin, 100 μg/ml streptomycin, 2 mM glutamine (all GibcoBRL) and 10% FCS (HI clone). 10 μl cells, 40 μl culture media and 50 μl 0.4% trypan blue (Sigma) were mixed to count the cells which were then adjusted to $3 \times 10^6\ ml^{-1}$.

A 4x stock of anti-CD40 (G28.5) at 4 μg/ml and IL-4 at 800 IU/ml were made in culture media. 4x stocks of filter sterilised recombinant CD23 in PBS and batimastat (donated by Ruth Mayer, SKB, MA, USA) were also made. Thus, 0.5 ml of cells and additives were placed in sterile 24 well Nunclon plates (Nunc) and made upto 2 ml with culture media. Each additive (CD23 and Batimastat) was cultured with IL-4/anti-CD40 or culture media alone. Duplicates or triplicates of each condition were made depending on the yield of cells. PBMC cultures were incubated for 12 days at 37 °C with 5% enriched CO_2 atmosphere. Cells and supernatants were harvested on day 12 or 13 by centrifugation and stored at –20 °C.

CHAPTER 3: PRODUCTION OF A RECOMBINANT CD23 C-TYPE LECTIN DOMAIN

3.1 Introduction

At the time of writing, the molecular structure of CD23 is undefined. The CD23 lectin domain has been modelled through homology to the carbohydrate recognition domain (CRD) of rat mannose binding protein and E-selectin (Bajorath and Aruffo, 1996; Padlan and Helm, 1993) whose structures have been solved by x-ray crystallography. Models are informative, but are insufficient to provide insights at the atomic level of ligand binding sites. Indeed, all known ligands to CD23 (IgE, CD21, certain integrins) interact with residues in the lectin domain. Clearly, structural information would benefit biochemical understanding of relevant biological interactions and, long term, could aid design of potential therapies for diseases in which CD23 may be a factor, e.g. rheumatoid arthritis (Plater-Zyberk and Bonnefoy, 1995).

The lack of diffracting CD23 crystals in this laboratory has lead to the investigation of nuclear magnetic resonance (NMR) as a method to determine the structure of the CD23 lectin domain (reviewed by Bax, 1989 and Wuthrich, 1989). In addition, NMR experiments are able to determine the atoms involved in ligand binding sites and any conformational changes occurring during binding.

The mass of the CD23 lectin domain (approximately 16 kDa) made it a good candidate for NMR structure determination, as it is within the size limits of these techniques. Two possible versions of the lectin domain were investigated, differing in start and end positions but each containing the complete lectin domain (Table 3.1). A characterised recombinant CD23 lectin domain H-CD23, 16 kDa, has been previously expressed in

mammalian cells (Shi *et al.*, 1997). Furthermore, H-CD23 gave well resolved, 1D ^{1}H-NMR spectra. The second candidate, denoted Der-CD23, is the recombinant equivalent of the CD23 fragment formed by the allergenic protease Der p 1 (Schultz *et al.*, 1995). Little is known about the activity of this fragment, so in addition to NMR studies Der-CD23 could be included in biological assays (Chapter 5).

The intention was to produce H-CD23 and Der-CD23 using a bacterial expression system and refold and purify them using techniques established for the full length CD23 (R. Reljic, 1996). Expression in bacteria would allow the recombinant proteins to be easily labelled with ^{15}N and ^{13}C isotopes using minimal media. This strategy would satisfy the criteria for NMR experiments assuming large enough yields could be obtained.

Table 3.1: Proposed recombinant CD23 constructs for expression in *E.coli*.

H-CD23	Der-CD23
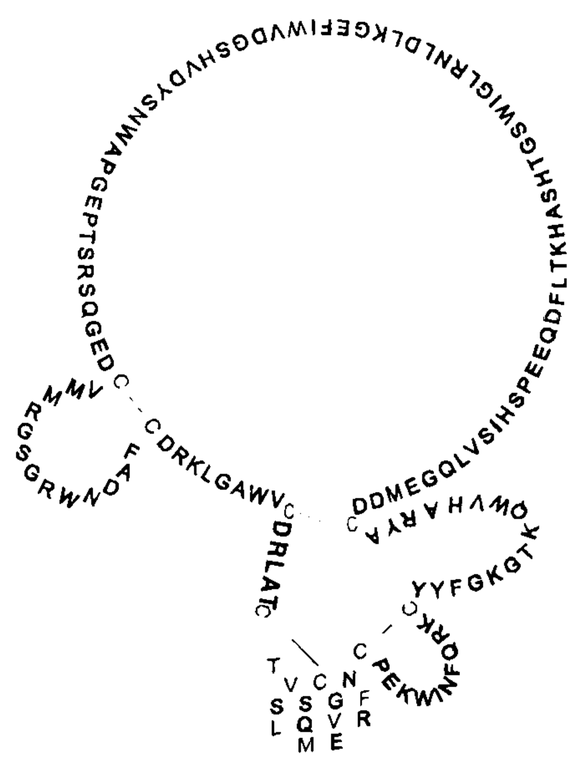	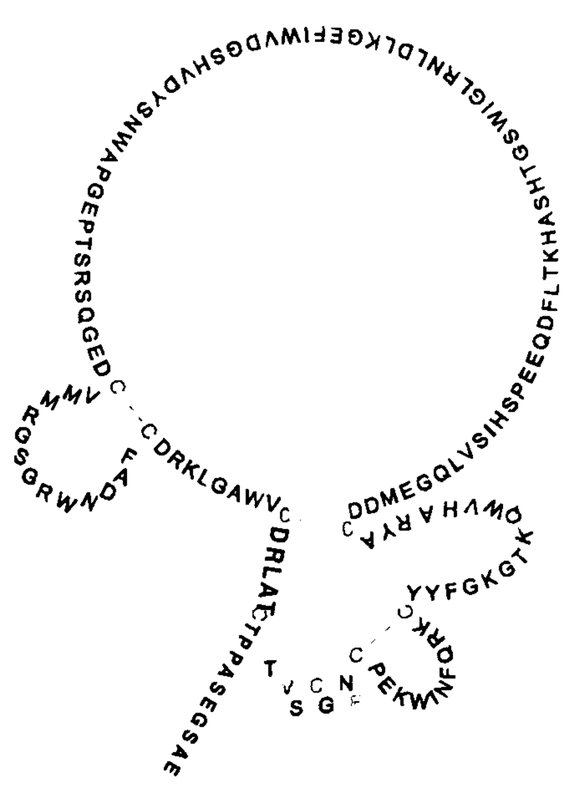
Met 150 - Cys 288 Mw = 15,774	Ser 157 - Glu 298 Mw = 16,145

3.2 Cloning

The lectin domain constructs were sub-cloned from CD23 cDNA by PCR. The primers HF, HR and DF, DR (Appendix I) were used to produce H-CD23 and DerCD23 DNA, respectively, using the following cycle conditions: 95 °C, 1 min; 52 °C, 1 min; 72 °C, 1 min; 25 cycles, and were of the correct size ~450 bp when analysed by gel electrophoresis. The PCR products were digested and ligated into the HindIII and BamHI sites of the shuttle vector, pBluescript KS. In this vector, positive colonies were blue/white colony selected, analysed by restriction digest of plamid DNA and sequenced using T3 and T7 primers. The constructs were excised using NdeI and BamHI and ligated into the multiple cloning site of the *E.coli* expression vector pET5a (Figure 3.1).

NdeI has a palindromic cleavage site (CATATG) which provides the recombinant construct an initiation codon when inserted in phase. The resulting methionine is either preserved or cleaved in expression in *E.coli,* depending on the following residue as outlined by Ben-Bassat, 1990. The initiation methionine of H-CD23 remains uncleaved, whereas in the Der-CD23 peptide it is cleaved. Therefore, this vector is able to produce recombinant peptides with no unnatural residues.

3.3 Expression

3.3.1 Expression of H-CD23 in Bacteria.

The target gene cloned into the pET vector is under the control of a strong T7 bacteriophage promoter. Expression of a T7 RNA polymerase, coded in the chromosomal DNA of the *E.coli* host cell, is induced by IPTG (controlled by a lacUV5 region). T7 RNA polymerase is able to selectively transcribe the target gene. During

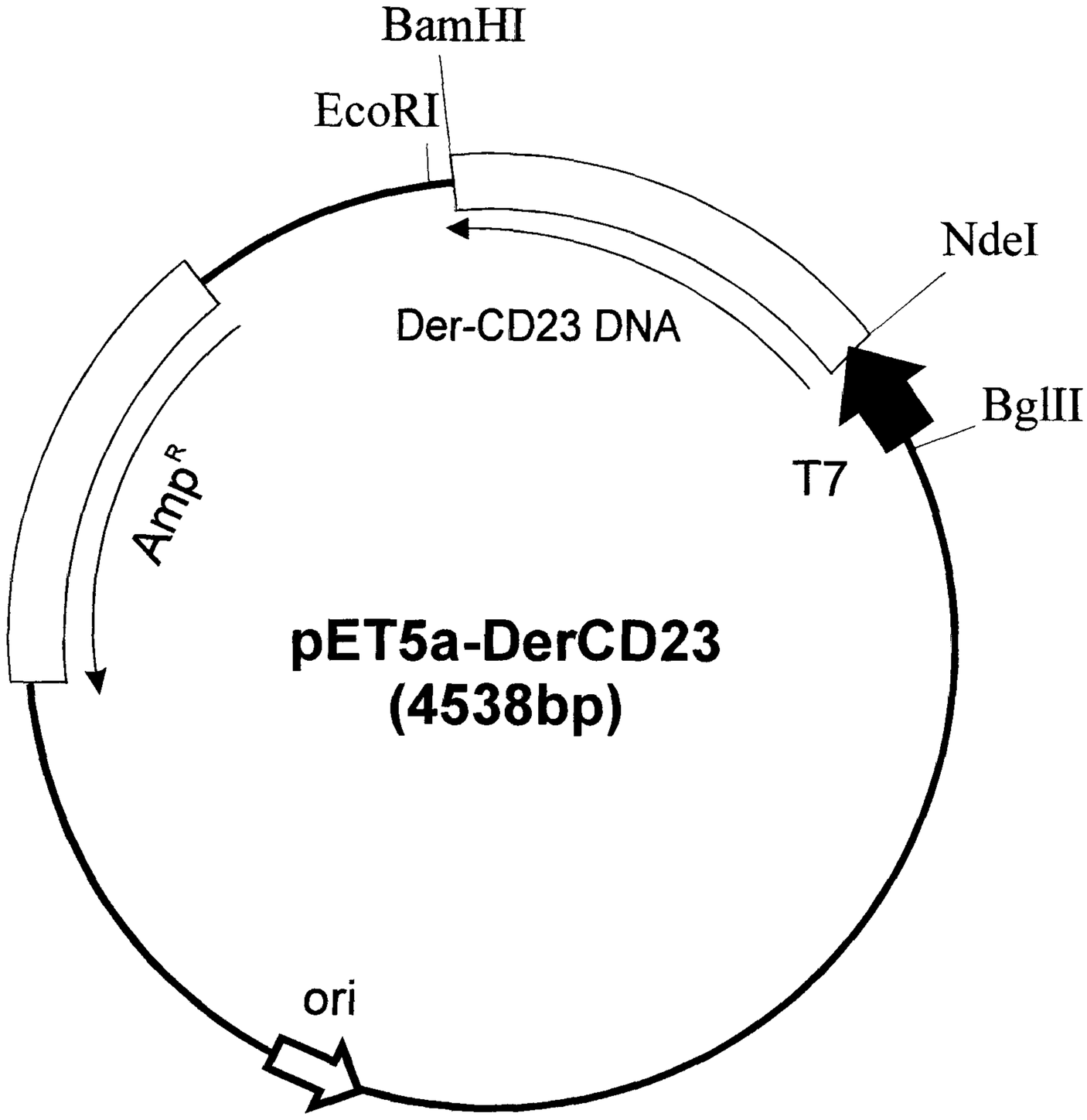

Figure 3.1: Vector map of the Der-CD23 Expression Vector.

Both H-CD23 and Der-CD23 (shown) DNA constructs were ligated into the NdeI/BamHI cloning sites of the bacterial expression vector pET5a (Novagen). The plasmid contains a T7 promoter from which transcription is induced on addition of IPTG. The plasmid also contains an ampicillin resistance gene (Amp^R).

expression of the recombinant protein, the majority of the cells' resources are used and large amounts of product can accumulate in a few hours.

Initial expression was carried out in the BL21 (DE3) *E.coli* strain. A time course of expression following induction with 0.4 mM ITPG was analysed by Western blot (Figure 3.2a). 100 µl aliquots at time 1, 4, 6 hours were taken, spun down and resuspended in 10 µl SDS-loading buffer. The presence of H-CD23 in total protein of the extract was detected by Western blot using the polyclonal antibody Rb55.

It was apparent that the recombinant protein was being degraded within the cells after 1 hour of culture (Figure 3.2a). The background signal was particularly bad because so much protein needed to be loaded to obtain signal, suggesting yields were very low. Comparison with 1 µg H-CD23 (obtained from NS0 cell line) on a western blot showed expression levels approximated 1 mg/l at 1 hour.

There was a possibility that the construct was toxic to the cells. To minimise any toxicity effects, the expression plasmid was transferred to another host strain, BL21 (DE3) (pLysS). The pLysS plasmid expresses low levels of T7 lysozyme that binds any T7 RNA polymerase before induction and therefore prevents 'leaky' transcription of toxic product. However, the peptide was still being lost with time and was undetectable at 5 hours (Figure 3.2b). H-CD23 must be unstable and being degraded, because if soluble it would still be detected in the total protein extract.

It was decided that the poor yields made H-CD23 from *E.coli* an unsuitable candidate for NMR isotopic labelling because large volumes of culture would require too much expensive glucose isotope. No further work was done with H-CD23 in *E.coli* because the equivalent recombinant protein was established in NS0 cell and was well characterised.

a) BL21(DE3)

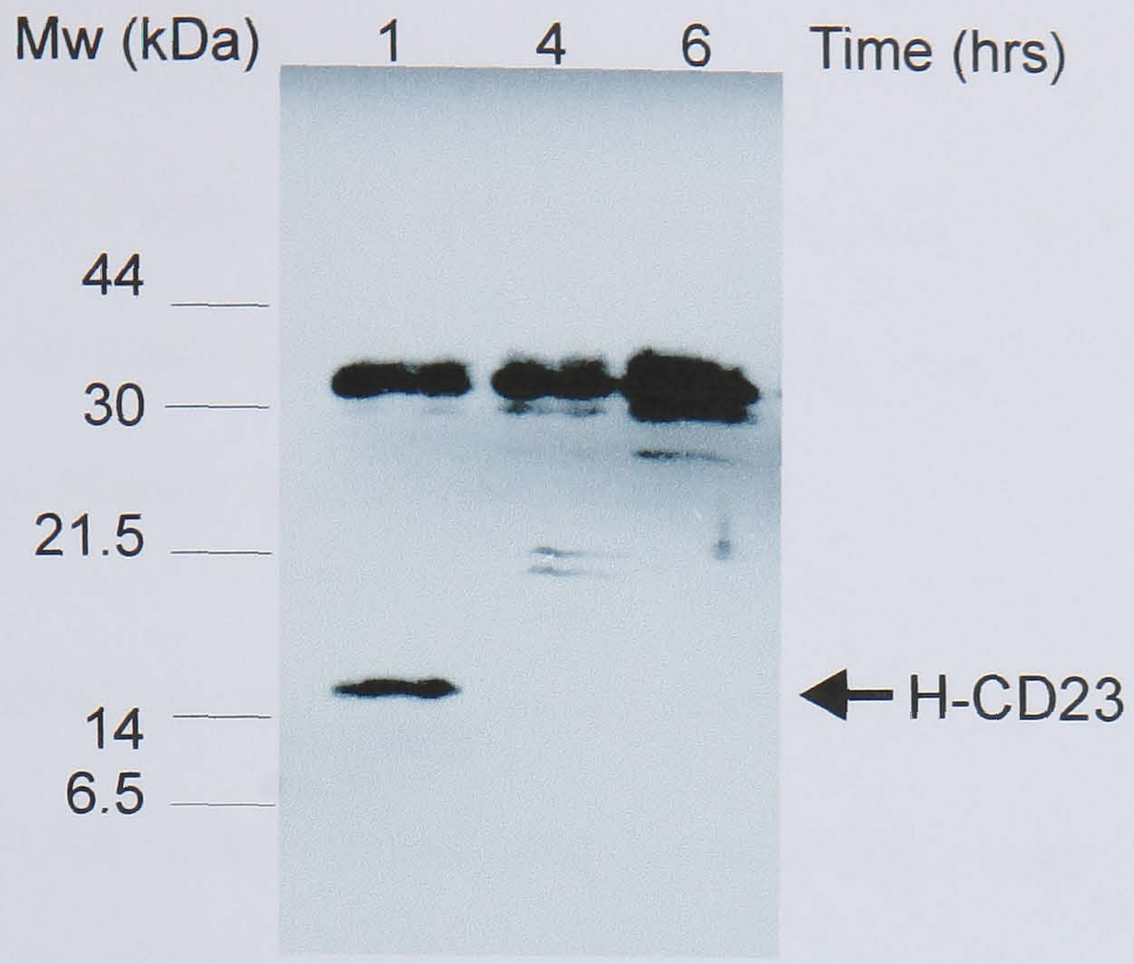

b) BL21 (DE3) (pLysS)

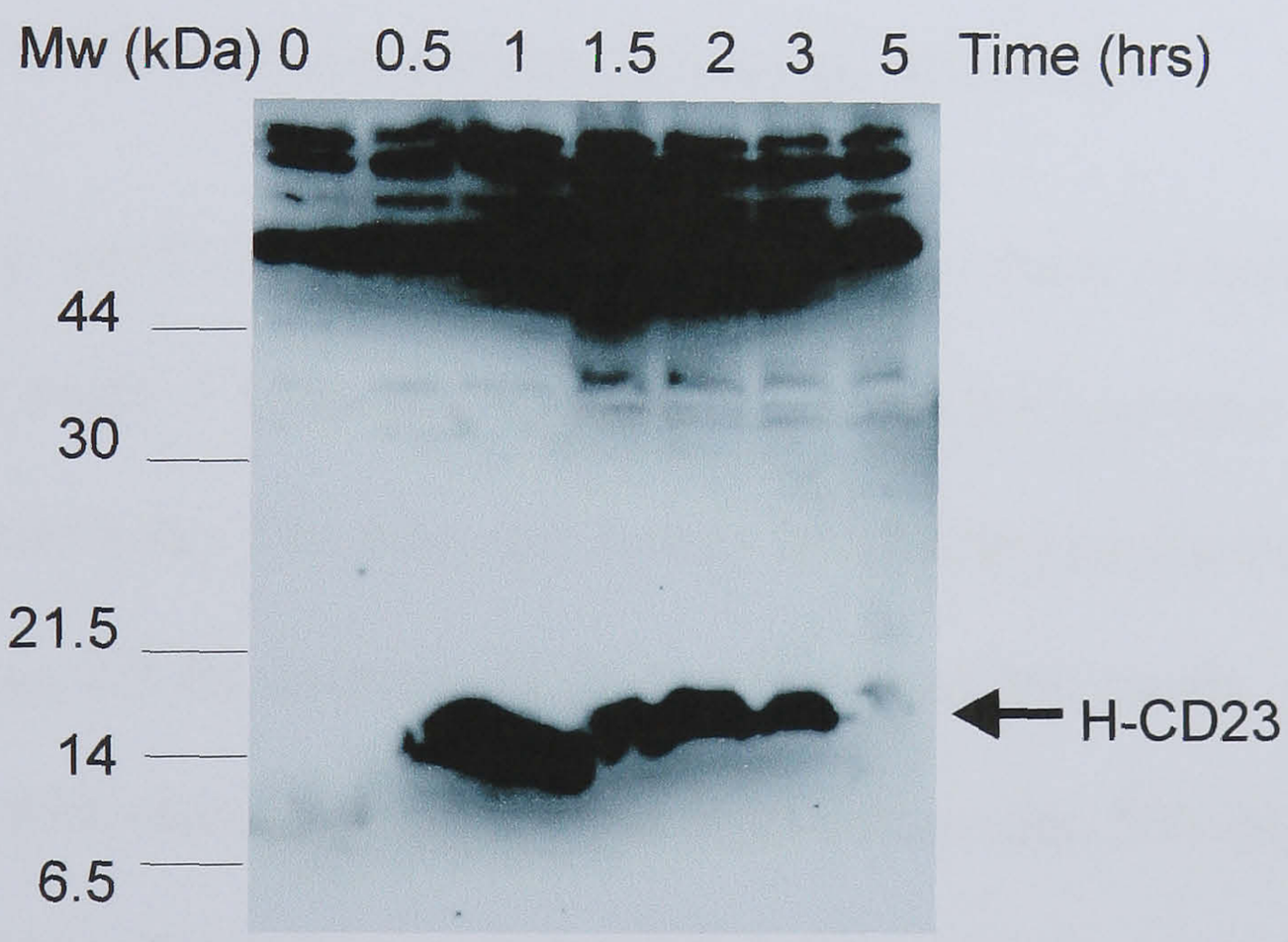

Figure 3.2: Western Blot Analysis of H-CD23 Expression in *E.coli*

a) 50µl of BL21 (DE3) culture and b) 100µl sample of BL21(DE3)(pLysS) culture was analysed by Western blot using rb55. Expression was induced by 0.4mM IPTG, aliquots taken at intervals(hours). Total cell protein (soluble and insoluble fractions was loaded under non reducing conditions. H-CD23 (16 kDa) was detected in the first hour but was undetectable after 4 hours.

3.3.2 Expression of Der-CD23 in Bacteria

A time course of expression after induction showed the Der-CD23 to be stable three hours after induction (Figure 3.3). The amount of peptide expressed was estimated to be about 50 mg/l on an immunoblot. At this yield, less than 5 l of culture would provide enough material for NMR experiments at 2 mM.

Mock labelling conditions were carried out on a large scale i.e. 500 ml. ^{15}N labelling was carried out in M9 media containing no casamino acids. The media for $^{15}N/^{13}C$ labelling also has a reduction of glucose from 10 g/l to 2 g/l. Care was taken to remove traces of complete M9 media from the overnight culture by pelleting the cells and re-suspending in labelling media. Rate of growth, final cell density and amounts of expressed Der-CD23 were compared to the normal M9 media.

Under labelling conditions, cultures took longer to reach optimum cell density for induction (A_{600} >0.6), 7 hours as compared to 3 hours for casamino acid complemented M9 media (Figure 3.4a). The final cell density in labelling media was lower, A_{600} of 1.0 compared to A_{600} 2.3 for casamino acid supplemented M9 media. By inoculating pre-warmed media with more cells (10 ml overnight culture into 500 ml) the time needed to reach an inducible cell density was reduced to 6 hours in label media and reached a final A_{600} of 1.3.

The amount of expressed recombinant protein was similar in all media taking into account cell numbers (Figure 3.4b). Therefore, with cell densities being approximately half of that under normal media conditions, the total protein yielded would also be halved. This was taken into consideration when determining the volume of culture to use for isotopic labelling.

Labelling was carried out once the whole purification procedure had been optimised, activity assessed and preliminary 1D NMR experiments on unlabelled Der-CD23 were satisfactory. 5 l of labelled culture were prepared, which would cover subsequent losses during extraction and purification. Final yields in bacterial cells were 200 mg of ^{15}N labelled protein and also for $^{15}N/^{13}C$ labelled material from 5 l cultures. For a 300 µl NMR experiment at 2 mM (32 mg/ml) approximately 10 mg of protein is required. Accounting for losses during purification (expecting yields of around 10%) this culture volume is sufficient. Expression results are summarised in Table 3.2.

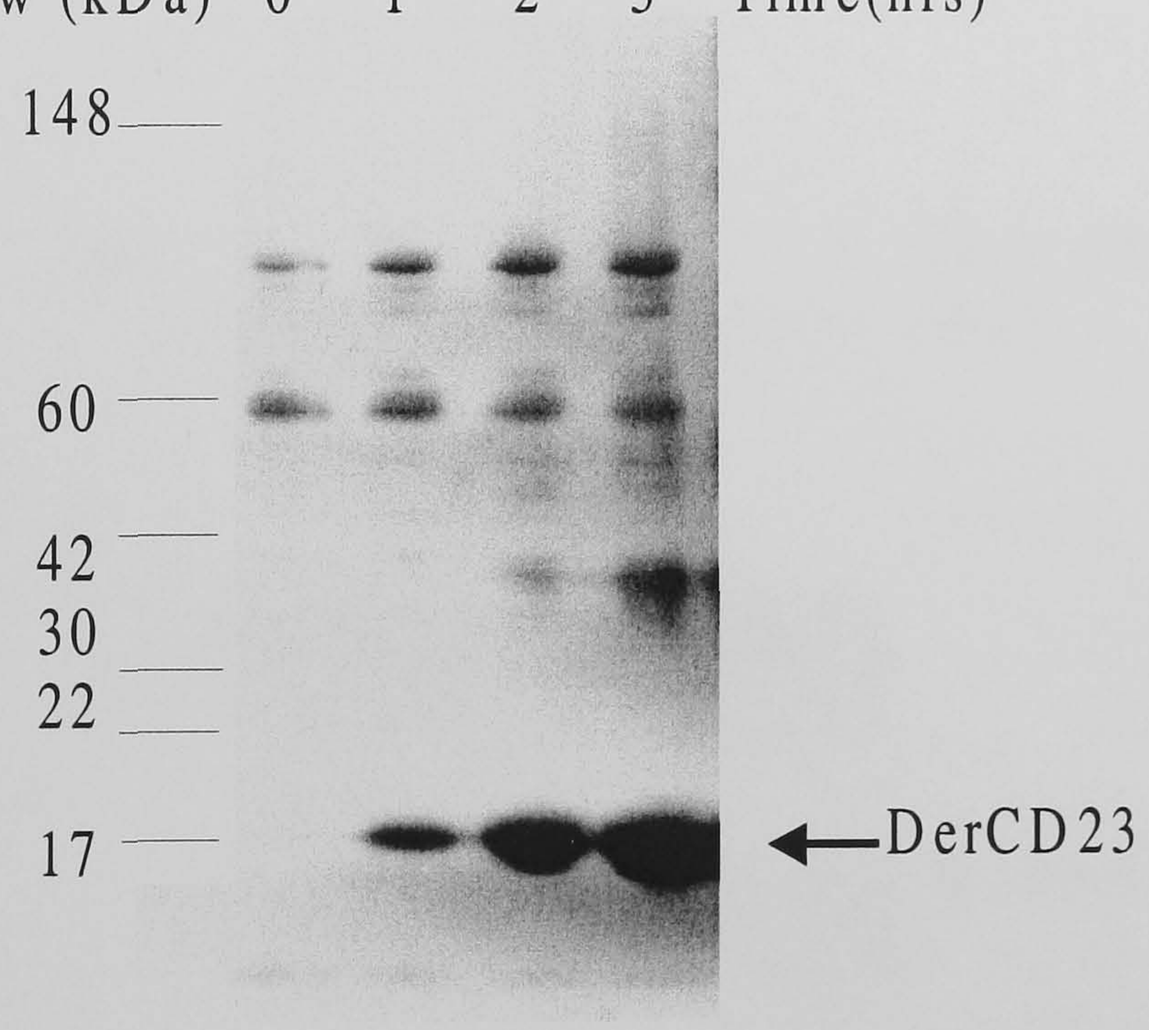

Figure 3.3: Expression of Der-CD23 in the *E.coli* host strain BL21 (DE3) (pLysS)

Western blot analysis of Der-CD23 expression at hourly intervals after induction with 0.4 mM IPTG. 17 kDa CD23 was detected in 50 µl cell lysates by a polyclonal antibody (Rb55). Der-CD23 expression was stable at three hours.

a)

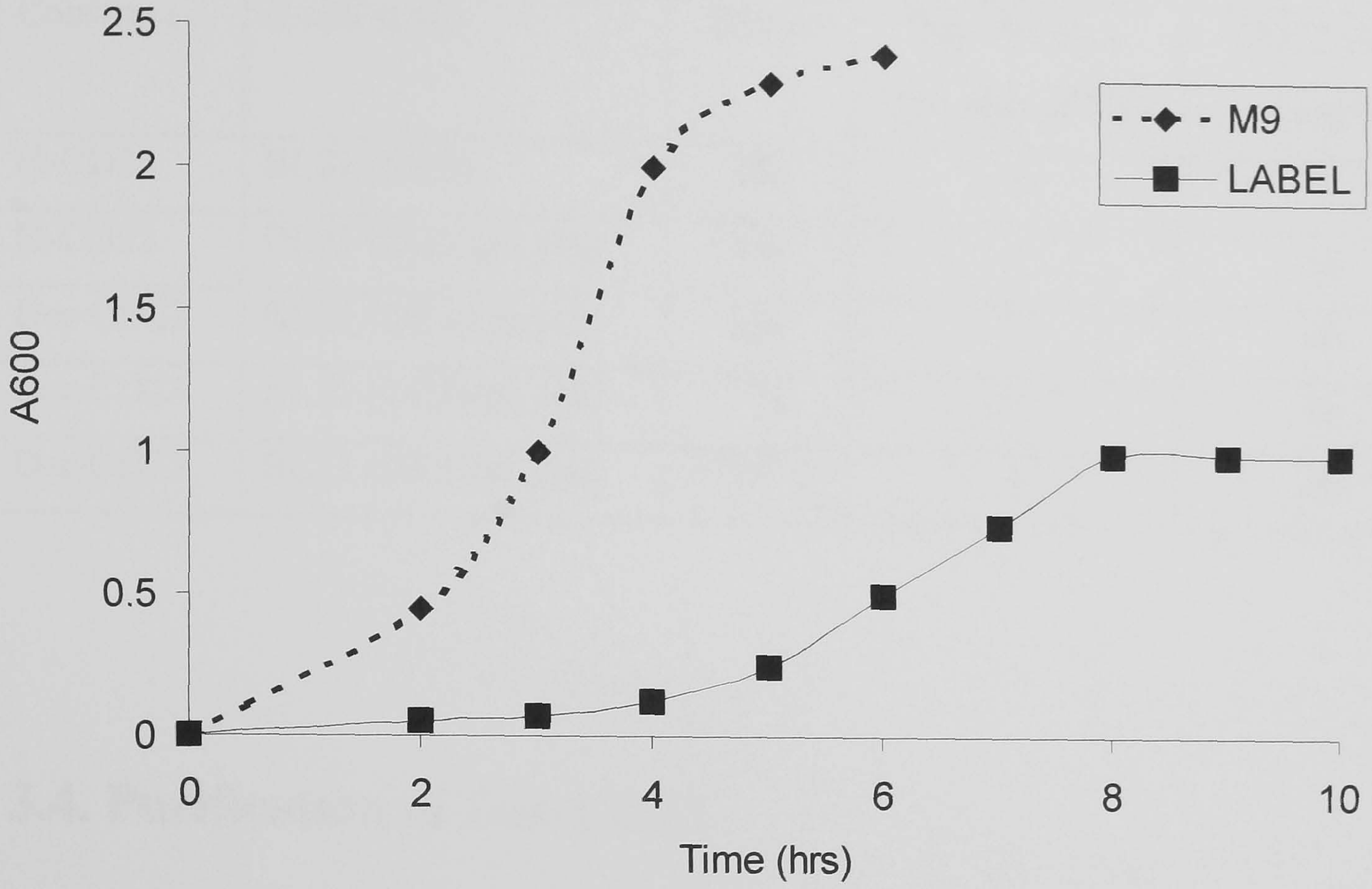

b)

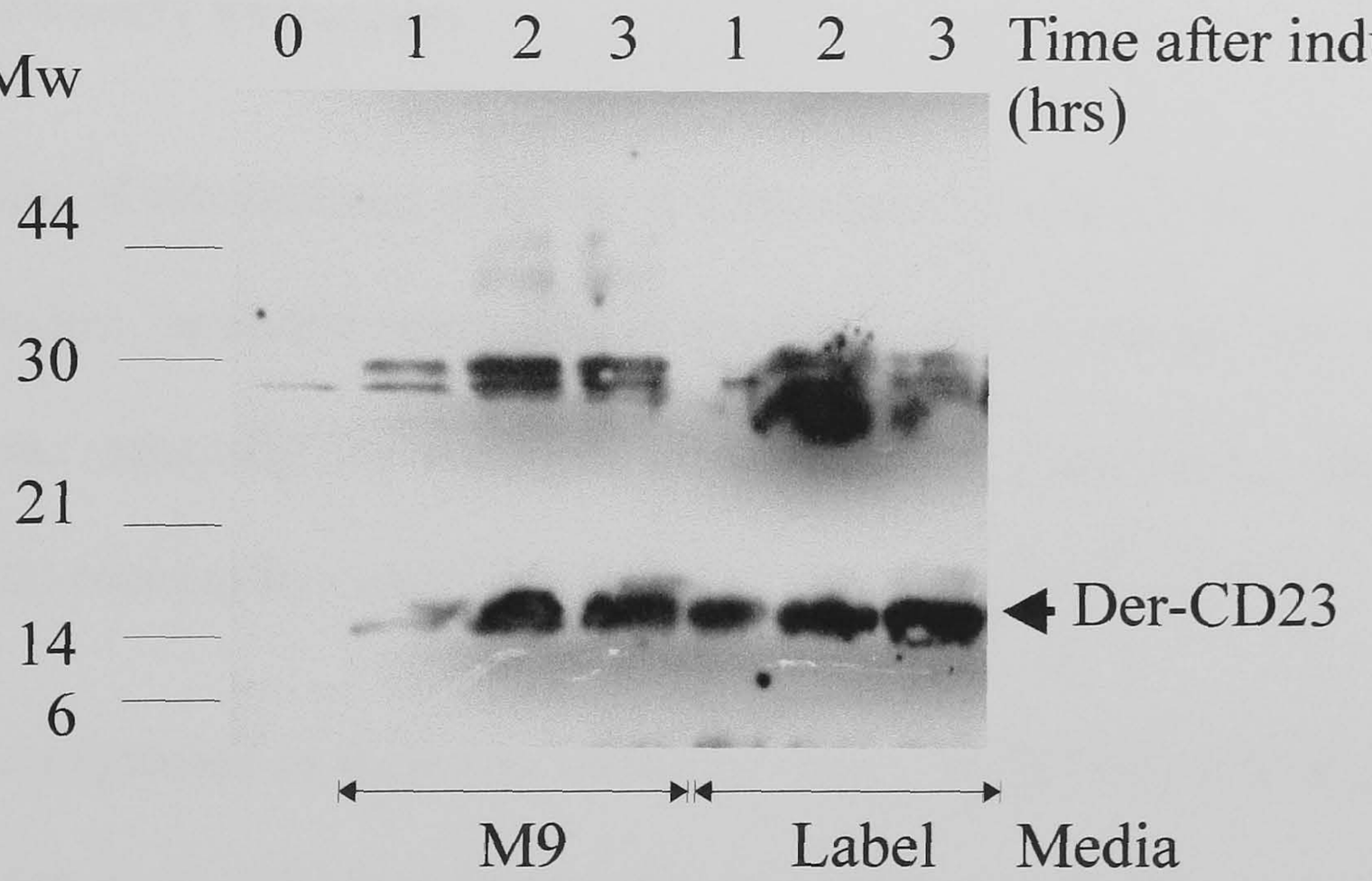

Figure 3.4: Expression of Der-CD23 with Labelling Conditions

500ml cultures of BL21 (DE3) (pLysS) transformed with pET5a-Der-CD23 were grown in M9 (supplemented) media or mock label media (no additional casamino acids and reduced glucose). **a)** The growth curve of the cultures were compared by assessing cell density (A_{600}). Cells grown in label media (bold line) took 6 hours to reach optimal density for induction (A_{600}>0.6) as compared to 3 hours for cells grown in supplemented M9 media (dashed line). Labelled cultures reached a lower maximum density (equivalent to 10^8 cells/ml). **b)** Western blot analysis using Rb55 showed no difference in yields of recombinant protein after induction when samples were corrected for cell number.

Table 3.2: Summary of Expression in *E.coli*.

Construct	*E.coli* strain	Media	Harvest Time (hrs after IPTG)	CD23 yield (mg/l)
H-CD23	BL21 (DE3)	M9	1	1
H-CD23	BL21 (DE3)(pLysS)	M9	1	10
Der-CD23	BL21 (DE3)(pLysS)	M9	3	80
Der-CD23	BL21 (DE3)(pLysS)	^{15}N	3	40
Der-CD23	BL21 (DE3)(pLysS)	$^{15}N/^{13}C$	3	40

3.4. Purification of Der-CD23

3.4.1 Inclusion Body Extraction

Over-expression of recombinant proteins in bacterial cells often leads to the formation of inclusion bodies, insoluble aggregates of protein. Inclusion bodies are advantageous for purification, especially for untagged proteins, as they are easily separated from soluble bacterial proteins by centrifugation.

Der-CD23 was expressed as inclusion bodies as shown by SDS-PAGE of total, soluble and insoluble fractions of protein from cell lysate (Figure 3.5). The extraction method (from Bohnmann and Tjian, 1989, see Chapter 2) yielded moderately pure recombinant protein from inclusion bodies due to the multiple washing steps. The yield was estimated by A_{280} once the final product was solublised in 6 M Guanidine-HCl. Approximately 200 mg extracted protein was recovered routinely from 5 l cultures in M9 media.

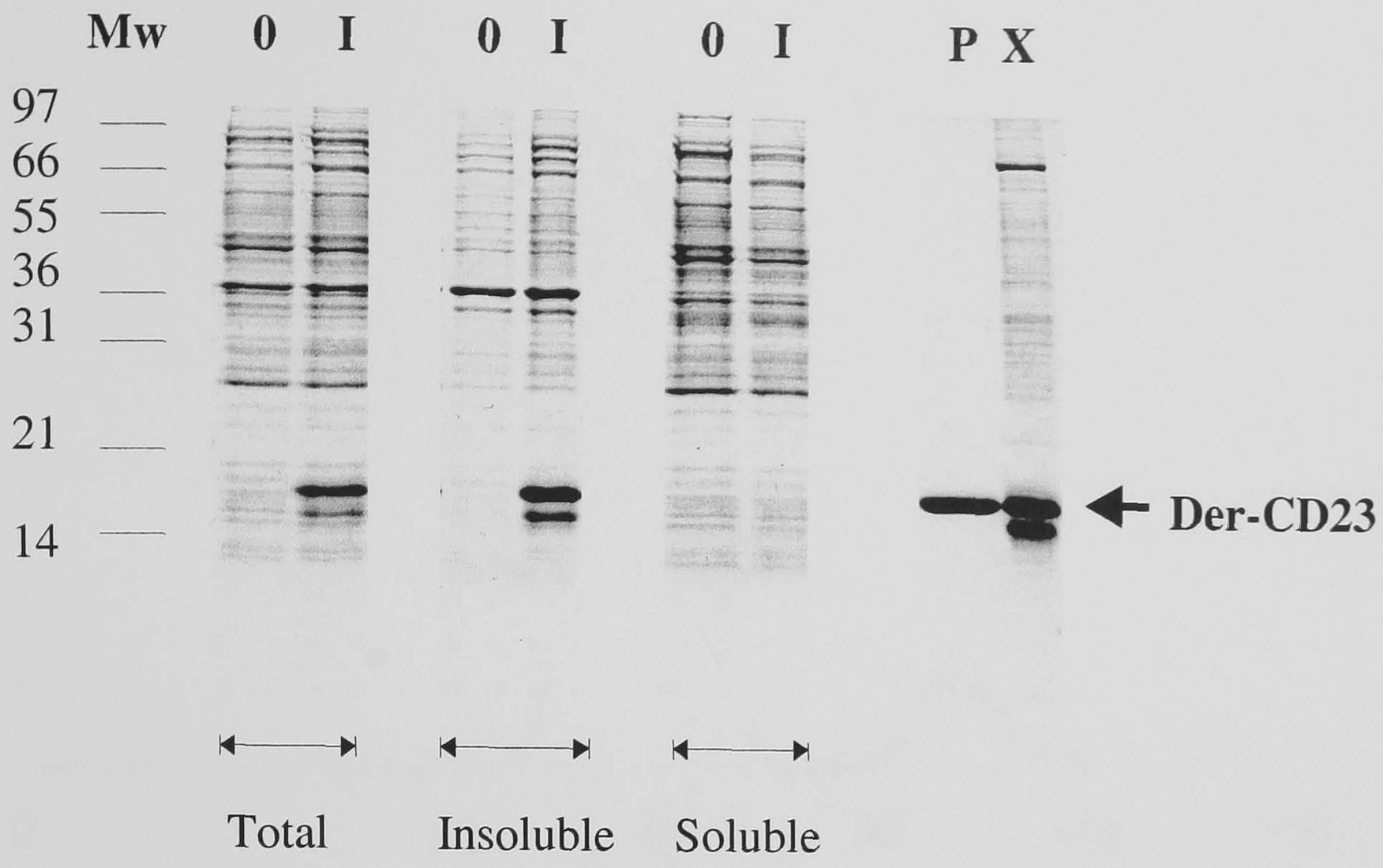

Figure 3.5: Extraction of Der-CD23 from Inclusion Bodies

Total insoluble and soluble protein fractions of bacterial cell lysates loaded onto a 4-20% SDS gel stained by Coomassie. 'O' represents protein before induction with 0.4 mM IPTG, protein samples taken 3 hours after induction are labelled 'I'. 'X' is the final inclusion body extract, prepared from 6 M Guanidine by TCA precipitation (Methods and Materials 2). 'P' is 2 μg final purified Der-CD23. Der-CD23 is present in the insoluble fraction.

3.4.2 Gel Filtration Chromatography under Denaturing Conditions

A denatured gel filtration step on an Sephacryl S100 column (3 cm x 90 cm dimensions) in 6 M Guanidine was used to further purify the protein according to size. The step appeared unnecessary because there was only one major peak resolved (Figure 3.6a) whose fractions were still contaminated by higher molecular weight *E.coli* proteins (Figure 3.6b). Omitting this procedure saved on time for the column run, fraction analysis, fraction concentration, protein losses and the use of several hundred millilitres of 6 M Guanidine. Instead, the extracted protein was adjusted to 10 mg/ml in preparation for refolding.

a)

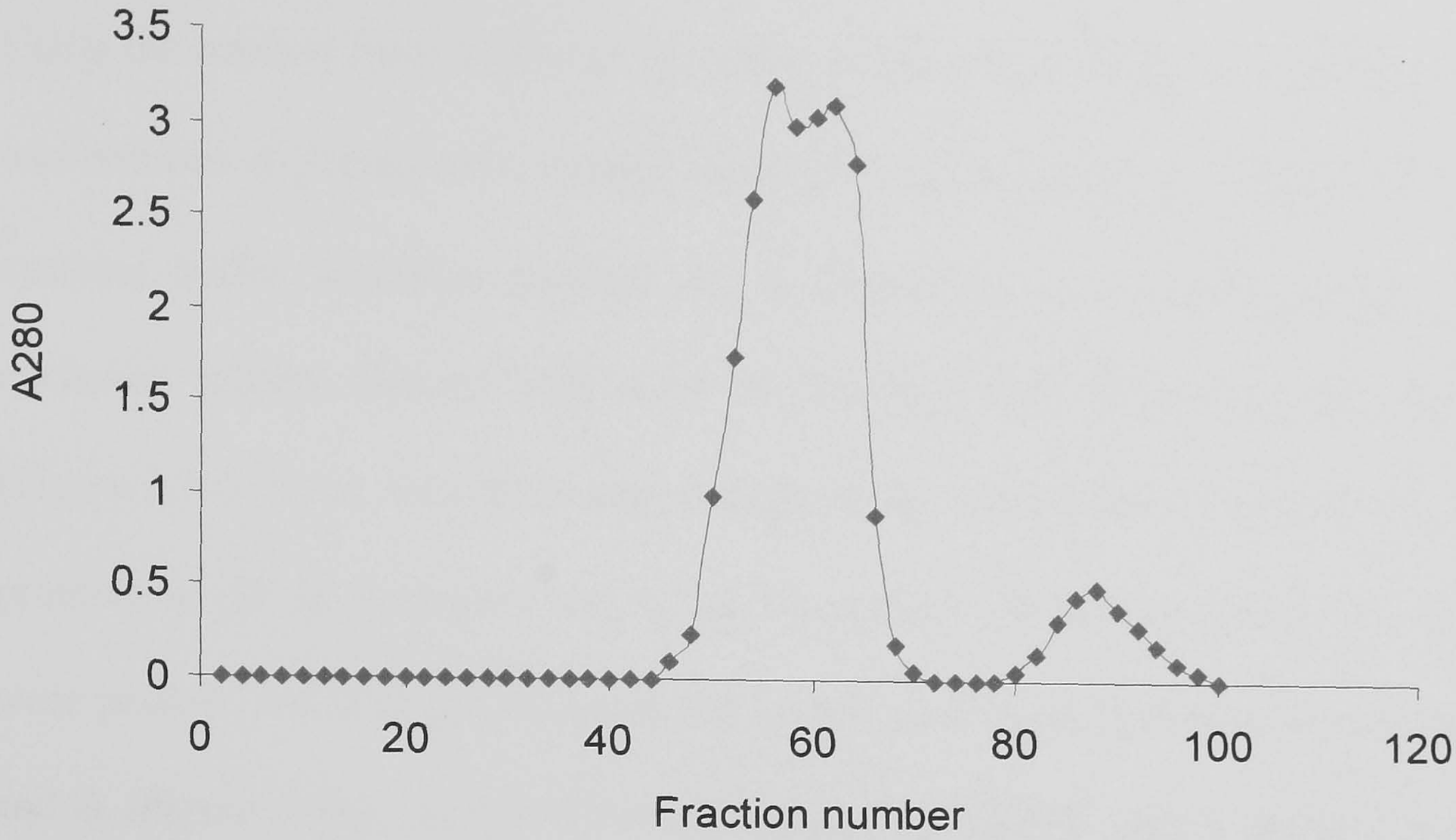

b)

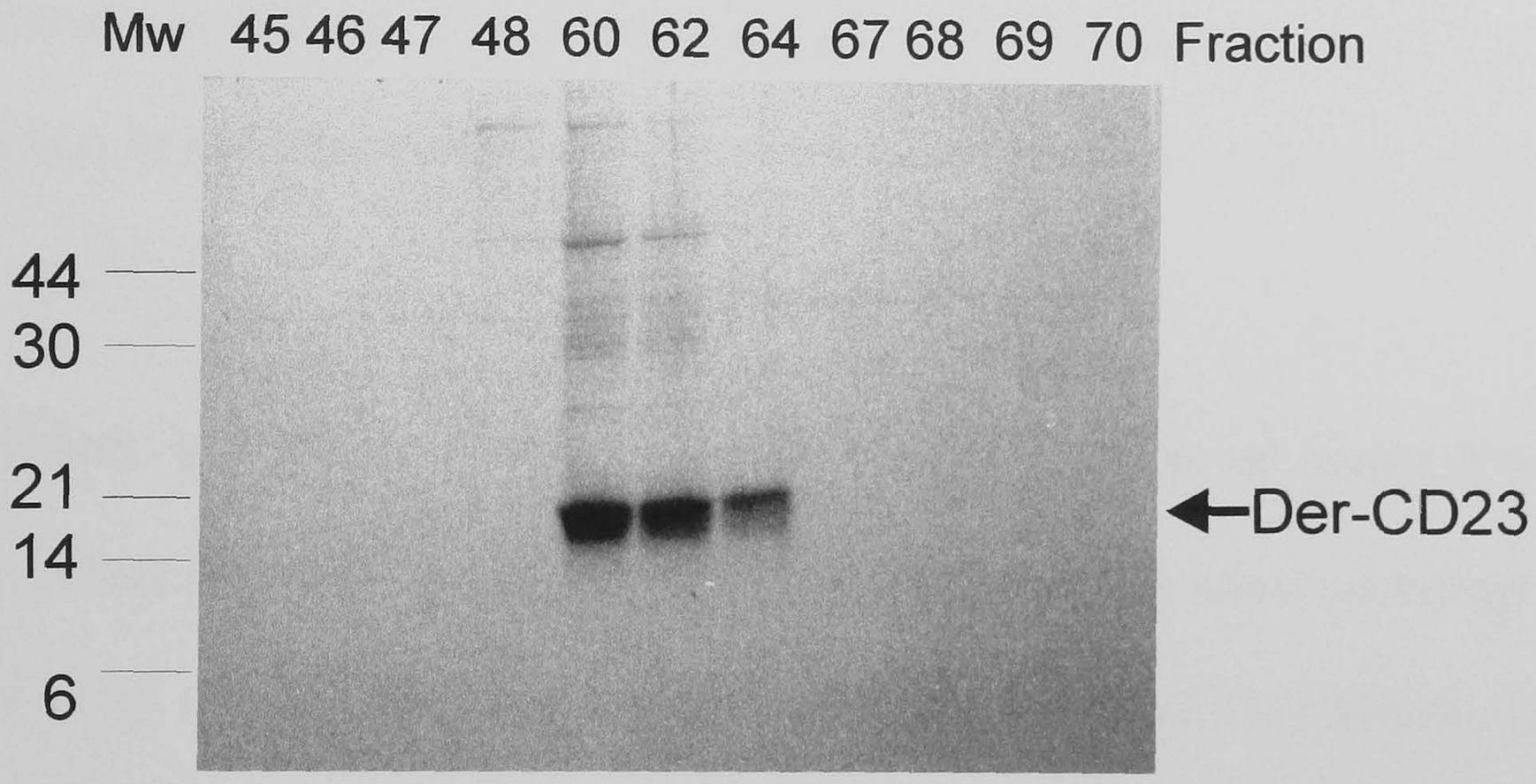

Figure 3.6: Purification of Extracted Der-CD23 by Gel Filtration

Solubilised Der-CD23 in 6 M Guanidine from inclusion bodies was loaded onto a Sephacryl S100 column and run at 1ml/ml at room temperature using 6 M Guanidine running buffer. **a)** The A_{280} profile of the fractions shows the eluted protein to be poorly resolved, a second peak (fractions 80-100) contained other small molecules with absorbance at 280 nm. **b)** A 15% SDS gel stained with coomassie shows fractions 60-64 contains 16 kDa Der-CD23, but are still contaminated by higher molecular weight *E.coli* proteins.

3.4.3 Refolding

Using the method from Taylor *et al.,* 1992, (Chapter 2), 10 mg of extracted Der-CD23 was reduced, a glutathione intermediate formed and renatured by dilution to 10 μg/ml in cysteine buffer. Refolded product was concentrated to 1 mg/ml and run on a size exclusion column, Biosep 2000 in 0.5 M Tris-HCl, 0.25 M NaCl, 0.05% NaN_3 buffer (Figure 3.7a). There were three peaks assigned 'A' at 6 minutes (presumably aggregated protein), at 'B' at 8 minutes and 'C' at 11 minutes. Fractions containing these peaks were pooled. An SDS gel indicated the majority of Der-CD23 was present in pools A and B (Figure 3.7b). An IgE Fc binding assay by ELISA clearly showed pool B was active. Pool C was likely to be small molecules, e.g. glutathione and cysteine which absorb strongly at 280 nm. The amount of aggregate formed was reduced by careful, slow, dilution in refolding buffer and therefore, better yields of refolded product were obtained.

Size exclusion was initially used as means for purification of active Der-CD23. However, it was observed during the procedure, huge losses were occurring; during concentration by ultrafiltration and during the column run itself. In addition, there was no evidence that all of the mis-folded protein would aggregate or what proportion of the purified CD23 is correctly renatured. An alternative method for isolating active refolded protein was investigated.

a)

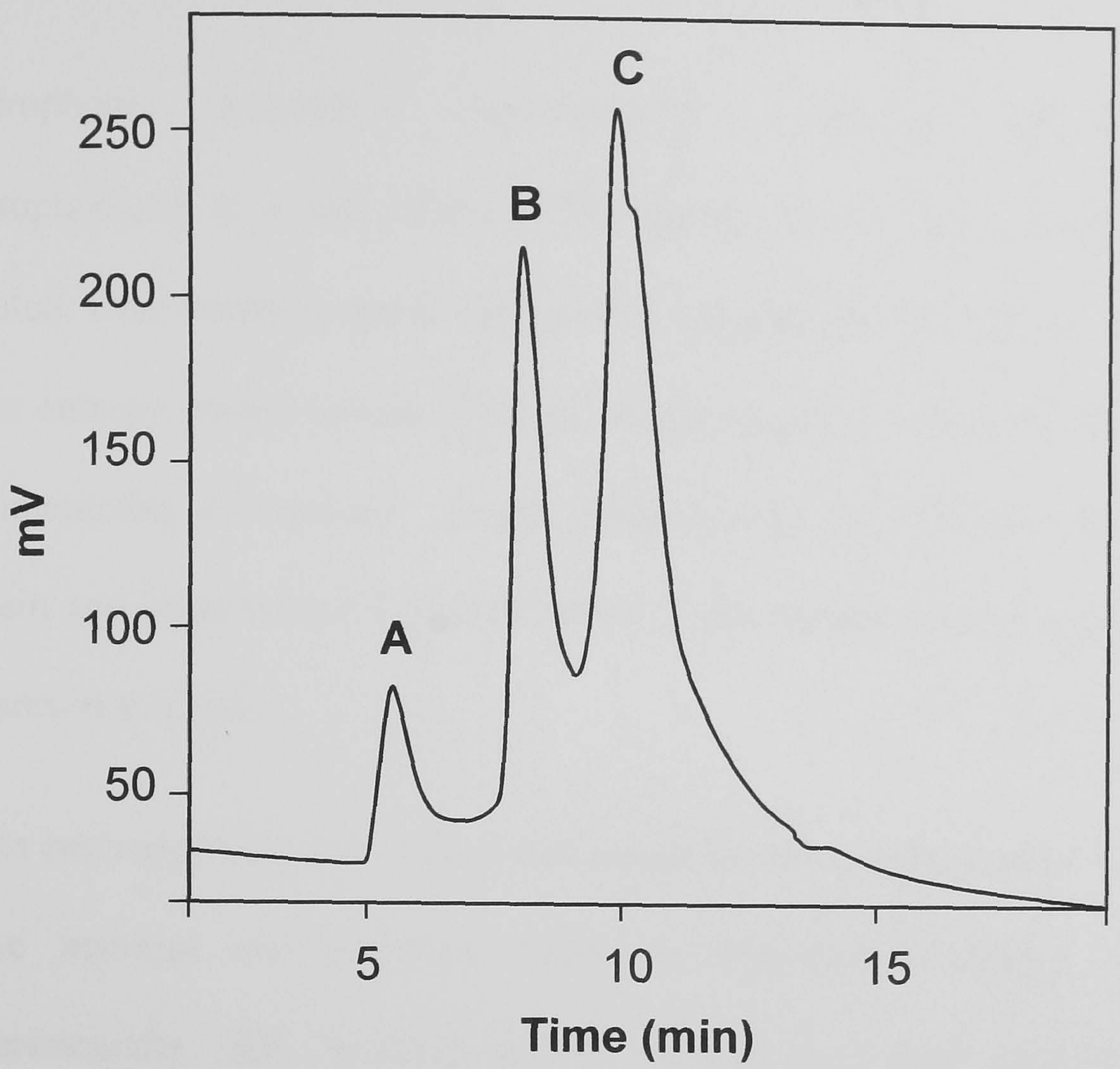

b)

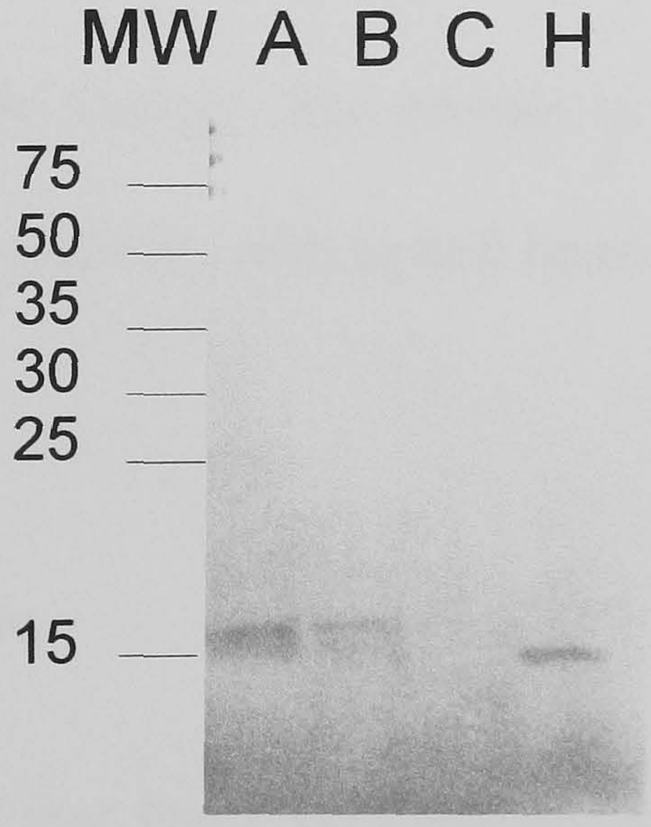

Figure 3.7: Gel Filtration analysis of Refolded Der-CD23.

(a) Refolded, concentrated Der-CD23 was applied to a Biosep 2000 size exclusion column in 0.5 M Tris pH 7.2, 0.25 M NaCl, 0.05% NaN_3. The fractions collected were pooled according to the peaks A, B and C observed in the elution profile. **(b)** The pools A, B and C were loaded onto a 15% SDS gel, under reducing conditions and stained with Coomassie Blue. 16kDa CD23 is present in the high molecular weight pool, **A,** (aggregated Der-CD23) and in pool **B** (monomeric Der-CD23). Pool **C** contains low molecular weight molecules e.g. cysteine and glutathione that absorb at 280 nm. Lane **H** a control sample of H-CD23 (derived from mammalian cells).

3.4.4 Hydrophobic Interaction Chromatography (HIC)

Hydrophobic interaction chromatography separates proteins according to hydrophobicity in a salt solution. The theory behind this chromatography has been debated. One thermodynamic explanation suggests that the driving force of adsorption is the entropy gained arising from the displacement of ordered water molecules around the interacting hydrophobic groups. Alternatively, the Van der Waals forces between protein and immobilised ligand increase as the ordered structure of water increases in the presence of salt.

It was envisaged that unfolded protein would be more hydrophobic than correctly folded active material and therefore could be separated according to hydrophobicity. Experimentally, HIC involves protein sample in a high concentration of a non-chaotropic salt (usually 1M ammonium sulphate) binding to a hydrophobic matrix (with aliphatic or phenyl side chains). The protein is eluted with a decreasing ammonium sulphate concentration gradient, with tightly bound hydrophobic proteins being eluted in a water wash.

3.4.4.1 Matrix Selection

First it was established that Der-CD23 remained soluble in 1 M ammonium sulphate. The proportion of aggregate in the sample was reduced on addition of 1 M ammonium sulphate as shown by analytical size exclusion on Superdex 75 (results not shown) presumably because it has precipitated and been removed on filtering.

There are several different HIC media available each varying in hydrophobicity of the aromatic or alkyl substitutions on Sepharose matrix. The surface of a protein can be up to 50% non-polar that can bind hydrophobic adsorbents, although it is difficult to

predict which matrix is optimal. Interactions between protein and HIC matrices must be screened, in this experiment with a HIC test kit (Amersham Pharmacia Biotech). 300 μg of concentrated refolded Der-CD23 was made up to 1 M ammonium sulphate, filtered, and loaded onto the HIC columns (listed in Table 3.3). The column was eluted with a decreasing ammonium sulphate gradient and any eluted protein was detected by a A_{280} trace. The percentage eluted was estimated the integration of 'flow through' maxima and that observed during the gradient (Table 3.3).

Only Phenyl Sepharose 6 (high substituted) bound Der-CD23 which could be removed upon a decrease in ammonuim sulphate concentration. The experiment was repeated with this matrix with 10 mg refolded protein on 25 ml of matrix but only 0.1 mg was eluted. To improve binding to hydrophobic surfaces, the initial salt concentration can be increased which is believed to increase the 'salting out' effect that promotes interaction.

Table 3.3: HIC Matrix Selection for Der-CD23 Purification

Hydrophobic Interaction Column Matrix	% Total Der-CD23 Eluted
Phenyl Sepharose 6 (low substituted)	0
Phenyl Sepharose 6 (high substituted)	40
High Performance Phenyl Sepharose	0
Butyl Sepharose	0
Octyl Sepharose	0

3.4.4.2 Optimising Ammonium Sulphate Concentration

Further tests were carried out with the Phenyl Sepharose 6 (high substitution) matrix at 1 M, 1.25 M, 1.5 M and 2 M ammonium sulphate. 10 mg of refolded protein at varying salt concentration were loaded onto 25 ml matrix and eluted by decreasing salt

concentration gradient. The amount of recovered protein was estimated by A_{280} readings. A marked increase in binding occurs when ammonium sulphate concentration is increased from 1 M to 1.25 M. No further increase in Der-CD23 yield was observed with 1.5 M ammonium sulphate. 1.25 M was selected to have maximum yields using least salt (Table 3.4).

Only ~25% of the total refolded protein bound. When the flow through was loaded onto the regenerated column, no further protein eluted suggesting that the binding capacity of the column was not exceeded and that this proportion represented the folded Der-CD23 in solution. Moreover, the eluted protein was non-aggregated, pure, the correct size and bound IgE-Fc as described in the characterisation section of this chapter (3.5). The rest of the protein is likely to be contaminants (unbound), mis-folded protein (tightly bound, removed with H_2O or isopropanol) and protein that precipitated on the addition of ammonium sulphate.

Table 3.4: Optimisation of Ammonium Sulphate Concentration for Purification of Der-CD23 by Hydrophobic Interaction Chromatography

Ammonium Sulphate Concentration (M)	CD23 Eluted from 10mg Sample (mg)
1.00	0.1
1.25	2.8
1.50	2.8
2.00	2.5

3.4.6 Final Protein Preparation

HIC fractions were concentrated to 1 mg/ml using stirred cell ultrafiltration using a regenerated cellulose membrane (10 kDa low molecular weight cut off). It was noted that the recovery of CD23 from concentration was improved in the presence of ammonium sulphate in the elution due to decreased interaction with the cellulose membrane. The protein was dialysed into the final buffer of TBS, 2 mM $CaCl_2$ and 0.05% sodium azide. To remove ammonium sulphate the dialysis buffer was changed several times over 2 days.

Table 3.5: Summary of Der-CD23 Purification

STEP	ORIGINAL METHOD	YIELD	MODIFIED METHOD	YIELD
1	EXTRACTION	100mg	EXTRACTION	100mg
2	S100 GEL FILTRATION, FRACTION CONCENTRATION	63mg	RENATURATION & HIC SAMPLE PREPARATION	68mg
3	RENATURATION & CONCENTRATION	36mg	HYDRPHOBIC INTERACTION CHROMATOGRAPHY	28mg
4	SIZE EXCLUSION FRACTIONS	9mg	CONCENTRATION & DIALYSIS	20mg
5	CONCENTRATION & DIALYSIS	5.4mg		

3.5 Characterisation

3.5.1 SDS-PAGE

A silver-stained reducing SDS gel gave an indication of the purity of Der-CD23. 50 ng of contaminant can be detected with this method and no apparent bands were detected when 1μg was loaded, therefore this preparation of Der-CD23 was particularly pure >95%. The gel shows Der-CD23 running above the 14 kDa marker.

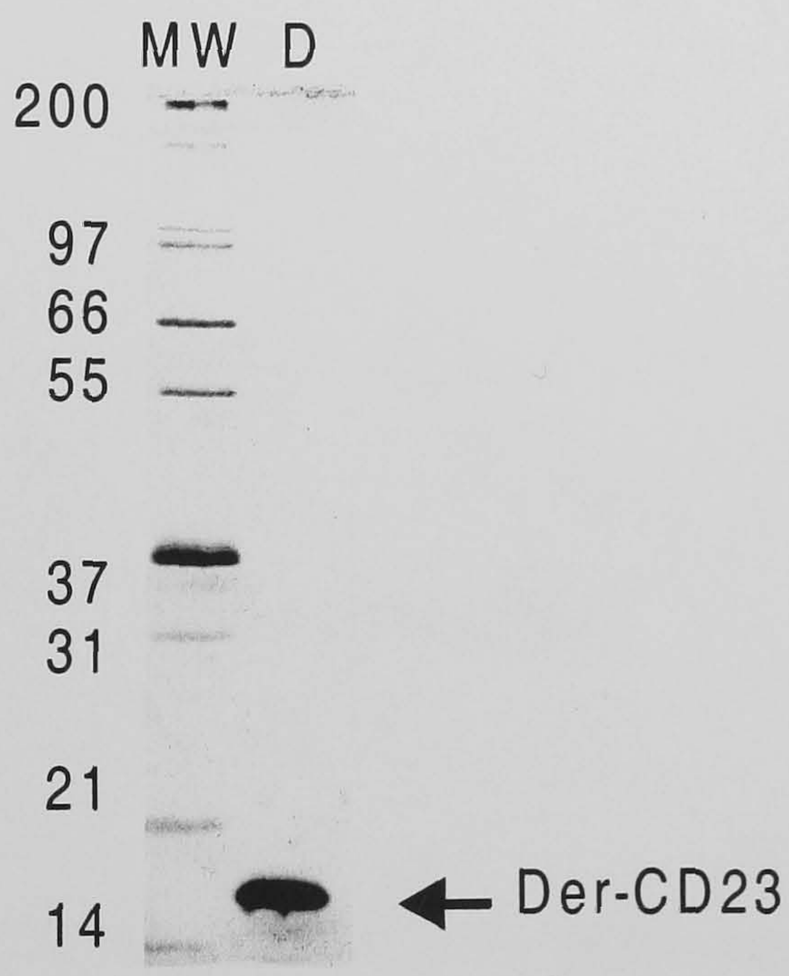

Figure 3.8: Silver Stained SDS gel of refolded Der-CD23 Purified by Hydrophobic Interaction Chromatography

1 μg of purified Der-CD23 was loaded onto a 12% SDS gel under reducing conditions. A single band at approximately 17 kDa was visualised by silver staining.

3.5.2 Analytical Gel Filtration HPLC

Analytical gel filtration HPLC was carried out in order to assess whether the sample contained aggregate or oligomers which would be detrimental to NMR data collection.

The final protein sample derived from HIC was run analytically on a calibrated Superdex G75 (Appendix III). Figure 3.9 shows the resulting A_{280} trace which gave a single peak. When extrapolated on the standard curve (log Mw *vs* elution volume) to be approximately 16 kDa (theoretically 16,145 Da). The experiment was unable to detect a significant amount of higher molecular weight contaminants or aggregate.

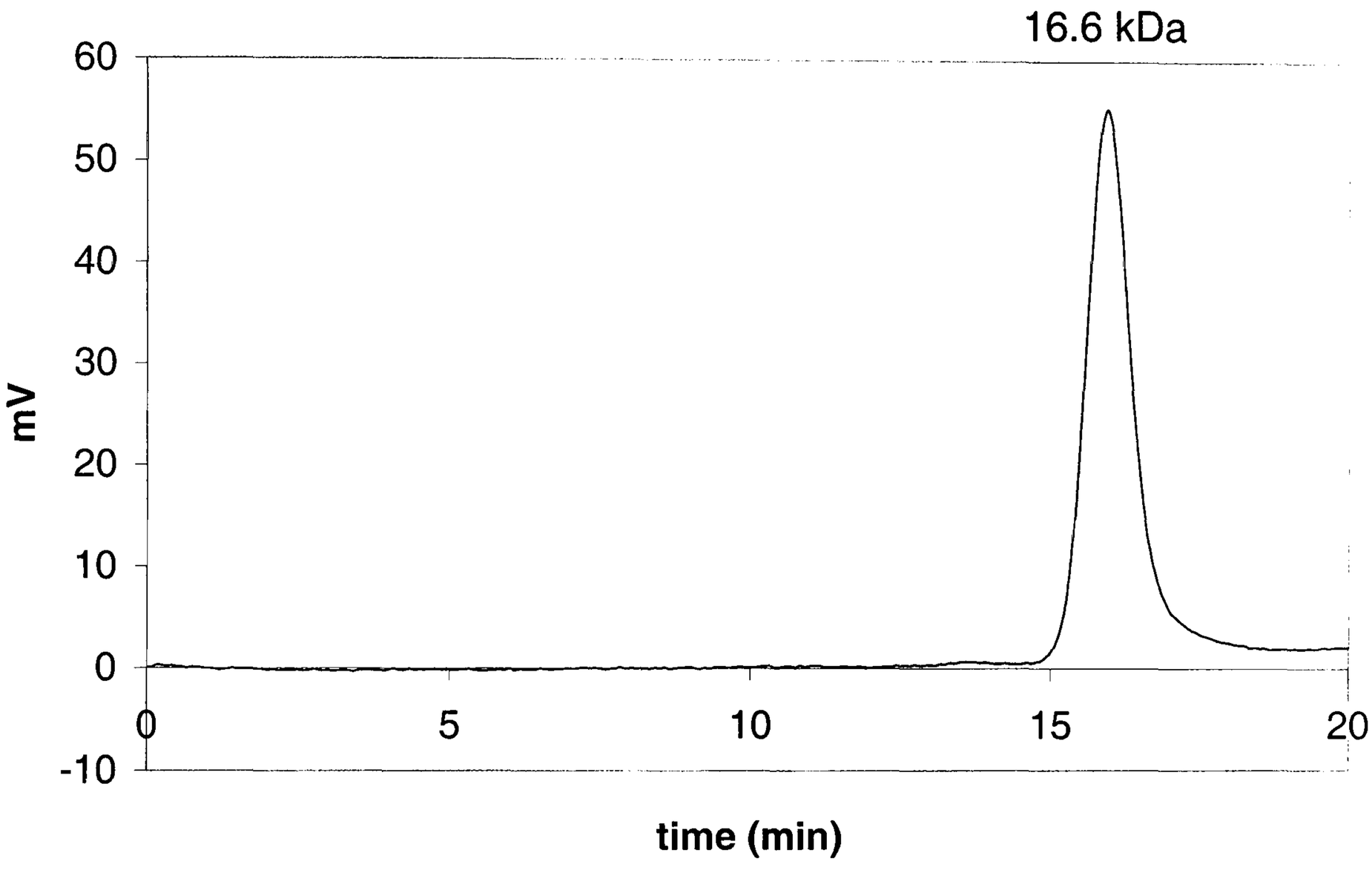

Figure 3.9: Analytical Gel Filtration HPLC of Purified Der-CD23.

Approximately 10 μg of purified Der-CD23 was loaded onto a Superdex G75 size exclusion column and run at 0.75 ml/min in 0.5 M Tris-HCl, pH7.2, 0.25 M NaCl, 0.05% NaN_3. Der-CD23 eluted as a single peak at 15.7 minutes (~16.6 kDa, Appendix IIIa) and there was little evidence of higher molecular weight oligomers or aggregate.

3.5.3 Mass Spectrometry

Positive ion electrospray spectrometry was performed by L.King, Celltech, on unlabelled Der-CD23 (Figure 3.10). One major peak at 16137 amu (referring to the calculated masses listed in the top right hand corner) was identified representing the processed fragment (minus the first Methionine) with 4 disulphide bridges. Another

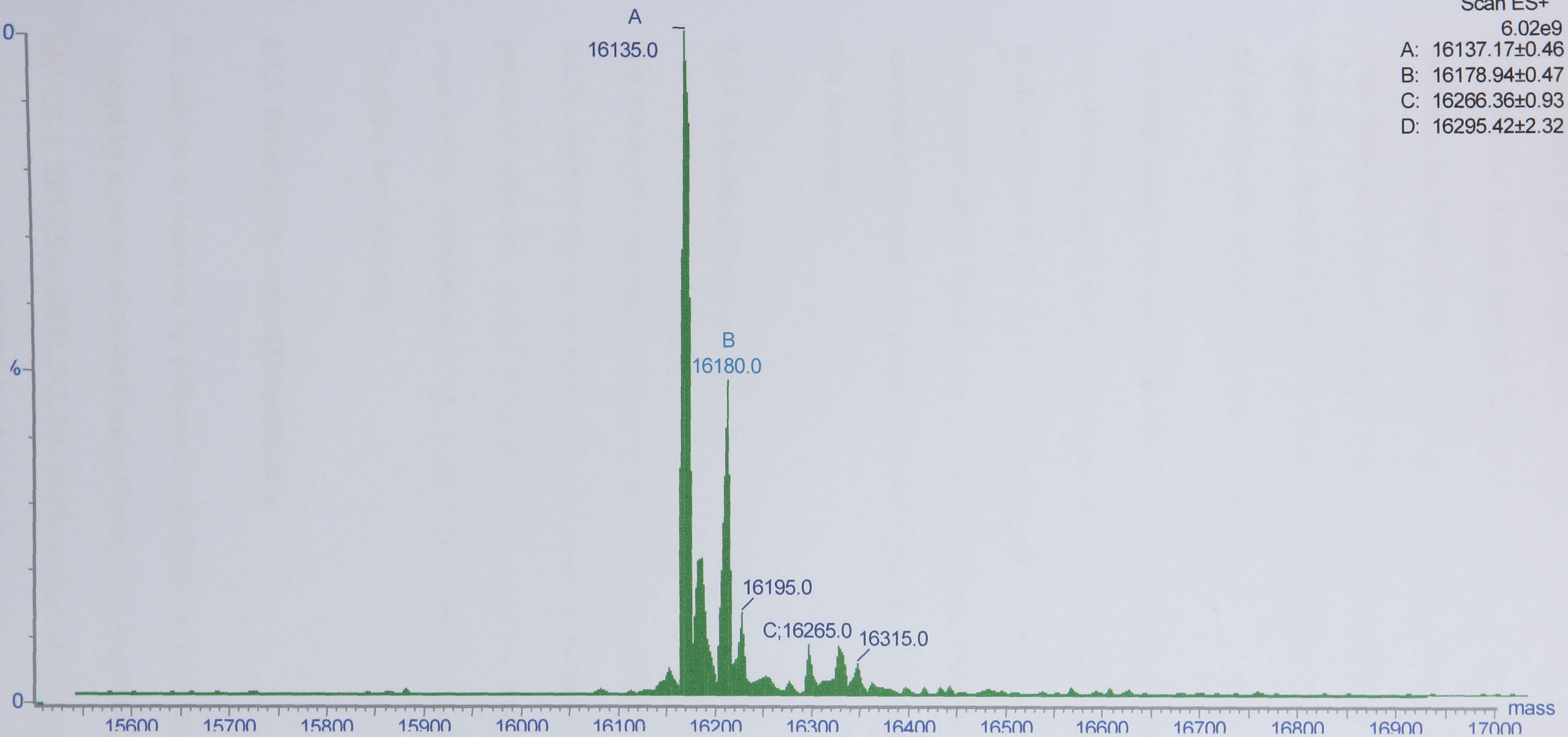

Figure 3.10: Mass Spectrometry of Purified Der-CD23

50μg sample analysed by positive electrospray spectometry (L.King, Celltech) injected onto a C18 column. The major peak A, is full length fully processed peptide. The larger species detected, B, is possibly a calcium ion adduct (+40).

peak occurs 16,179, ~40 mu greater than the desired construct and is most likely to be a Calcium ion bound product. The motif C-X-C, which is present in the Der-CD23 sequence, has been known to chelate positive ions (usually sodium) observed in electron spray mass spectrometry. A small proportion of the protein is 16,266 and 16,295 which represents the full length polypeptide (+ Methionine) with and without the putative calcium ion. No degradation product is apparent.

An NMR sample that had been at 25 °C for 2 days and stored at 4 °C for several months was also analysed by mass spectrometry (by J. McDonnell, Rockefeller University). The products found in this experiment were all smaller than expected, the largest having a mass equivalent to having the 3 carboxyl-terminal residues cleaved. With time and moderate temperatures, degradation of Der-CD23 sequence exterior to the lectin domain was occurring.

3.5.4 N-terminal Sequencing

The results of N terminal sequencing from B.Smith, Celltech (Materials and Methods 2.5.7), showed the major peptide in the final preparation of Der-CD233 had the predicted sequence: SGFV_NT_PEKWINF. A minor fraction of the protein was sequenced as TPPASEGSAE, this represents C-terminal sequence following the final Cys of the lectin domain.

3.5.5 Detection by anti-CD23 antibodies

In addition to detection by polyclonal anti-CD23 in immunoblotting, Der-CD23 was detected by a variety of monoclonal antibodies in a sandwich ELISA format (2.5.8.2). EBVCS-2, EBVCS-4, EBVCS-5, B6, IOB8, mAb25, BU38 and MHM6 which all map to the lectin domain. EBVCS-1, which binds an epitope in the neck region, was also

tested and, predictably, showed no binding to Der-CD23. These results (not shown) suggest the domain was folded into the correct conformation.

3.5.6 Ligand Binding Assay by ELISA

In an IgE binding assay, Der-CD23 bound IgE-Fc albeit at a lower affinity to that of a molar equivalent of full length rCD23 (Chapter 5). Design and further description of this assay is included in Chapter 5. This result has also been demonstrated by Shi *et al.*, 1990, with the mammalian expressed lectin domain (H-CD23).

3.5.7 Chemical Cross-linking with EDC

1-Ethyl-3-(3-dimethylaminopropyl)carbodiimide Hydrochloride (EDAC or EDC) is a water soluble condensing reagent that can assess the oligomeric state of proteins in solution by linking amide and carboxyl groups of adjacent protein molecules with a zero length spacer. The method employed is described in Materials and Methods (2.5.5.1) was used to demonstrate CD23 oligomerisation by Beavil *et al.*, 1995.

1 μg of purified Der-CD23 was cross-linked alongside a full length recombinant CD23 positive control and visualised by non reducing SDS PAGE. Figure 3.11 shows a broad band around 20 kDa (monomeric), some evidence of a dimeric and very small amounts of trimeric protein. The control full length CD23 gave the expected trimeric result, showing the conditions of the cross-linking were similar to those observed by Beavil *et al.*, 1995. They observed that the lectin domains can associate, but the cross-linking sites are found mainly in the stalk. Thus, the stalk region forms the trimeric α-helical coiled coil which is stabilised by weaker interactions in the lectin domain.

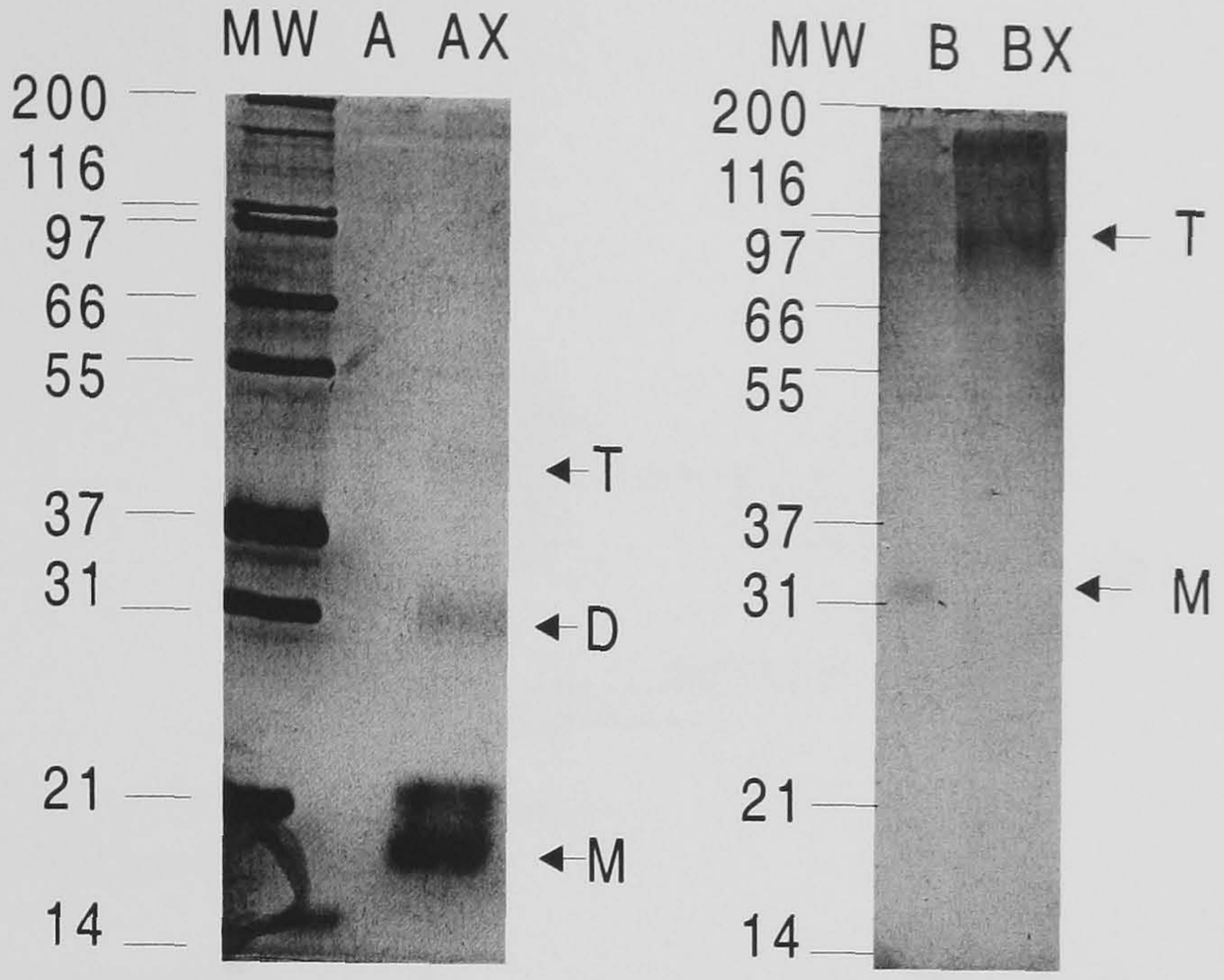

Figure 3.11: EDC cross-linking of Purified Der-CD23

Silver stained non-reducing, 12% SDS gel of 1 μg protein cross-linked with 25 mM EDC for 15 minutes at room temperature. Full length CD23 (**B**) runs as a trimer (T) whereas the lectin domain (**A**, Der-CD23) exists predominantly as a monomer (M) when cross-linked (**X**). Some dimeric (D) and trimeric (T) cross-linked Der-CD23 is also observed.

3.6 NMR

J. McDonnell (Oxford Univerisity) carried out all NMR experiments with the unlabelled, ^{15}N-labelled and ^{15}N-^{13}C-labelled material provided.

3.6.1 One dimensional ^{1}H-NMR Spectra

Comparison of the ^{1}H spectra of H-CD23 (expressed by a mammalian cell line, spectra not shown) and the *E.coli* derived Der-CD23 (Figure 3.12) showed the two lectin domain constructs gave similar spectra. This result indicated that the purified Der-CD23 was folded in a similar way to native CD23. The up-field chemical shifts observed at 0 to -1 ppm results from residues within the folded core of the domain also suggest the peptide is folded correctly. The spectra was well resolved which facilitates peak assignments.

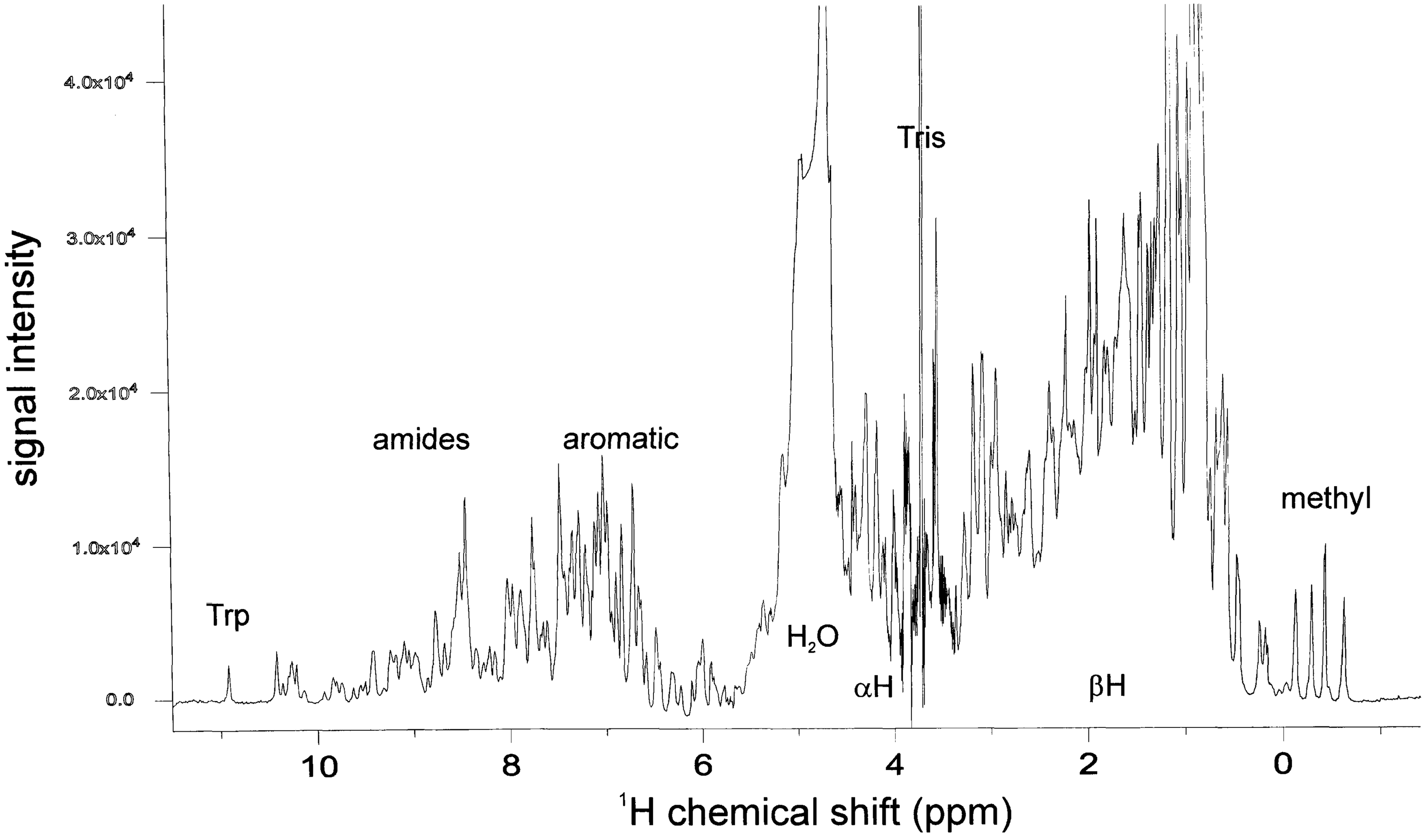

Figure 3.12: One Dimensional ^{1}H NMR Spectra of DerCD23

3.6.2 NMR studies using the ^{15}N Der-CD23 Sample

The proportion of label incorporation of the ^{15}N sample was assessed by electrospray mass spectroscopy (spectra not shown). The heavier nitrogen isotope results in a protein with higher mass than the unlabelled sample (^{14}N). Der-CD23 contains 201 nitrogen atoms, the ^{15}N sample was +202 mu therefore approximately 100% isotope incorporation was achieved.

A number of different experiments can be performed on the single labelled sample, providing a range of structural and ligand binding information, e.g. coupling constant experiments, hydrogen-deuterium exchange and relaxation studies, and eventually the ligand mapping experiments. For instance, the ^{1}H ^{15}N HSQC (heteronuclear single quantum-coherence) spectra (Figure 3.13) shows the protons attached to nitrogen atoms thus representing the backbone of the protein. At the sample concentrations used, the 2D spectra was well resolved allowing accurate data to be extracted. The most important information will require full assignment, which requires the double labelled sample.

3.6.3 $^{15}N/^{13}C$ labelled DerCD23

Evidence of aggregation was observed during the data collection of the double labelled sample. The high concentration of sample needed for the 3D experiment was promoting the dimerisation of the lectin domains and therefore producing poorly resolved spectra. Improvements were made at higher temperatures as the low affinity interaction were reduced and the tumbling time was increased. Experiments and assignments are on-going in the laboratory of J. McDonnell at Oxford University.

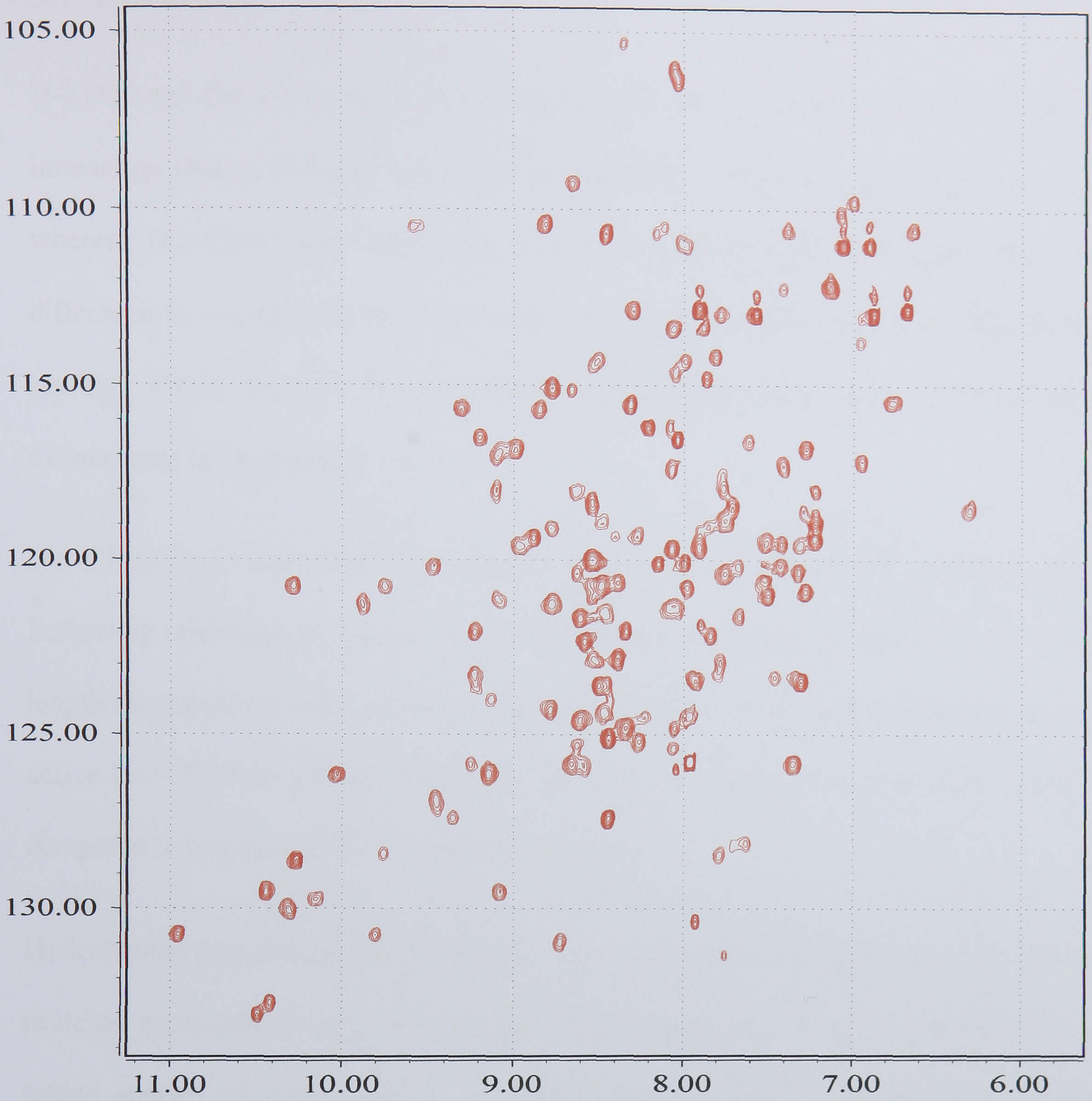

Figure 3.13: ^{1}H-^{15}N HSQC Fingerprint of Der-CD23

1.2 mM Der-CD23 labeled with ^{15}N. Each residue represents protons attached to ^{15}N atoms, thus giving details of the protein backbone. Virtually all of the peaks are well resolved and the difference in intensity indicates a varying amount of flexibility within the molecule.

3.7 Discussion

H-CD23 and Der-CD23 were expressed in *E.coli* for use NMR structural analysis and interaction studies. H-CD23 was found to be unstable in the bacterial expression system whereas Der-CD23 was stable and expressed in high yields (80 mg/l). The slight difference in sequence of the two similar constructs may account for the difference in stability within the cell. H-CD23 RNA or polypetide ends may be susceptible to exonuclease or exoprotease activity.

Der-CD23 was expressed as inclusion bodies and extracted to moderate purity. Following refolding, the purification procedure was improved on methods used for full length recombinant CD23. Hydrophobic interaction chromatography was used to purify active Der-CD23 in a single step. Final recovery of protein was optimised to 20% (as compared to less than 10% in a previous method).

Hydrophobic interaction chromatography greatly benefits the purification of refolded proteins expressed as inclusion bodies. This procedure is able to separate different folded species of the protein on account of the exposure of hydrophobic surfaces. Purification methods such as gel filtration that separate according to size of the molecules are sufficient to separate grossly mis-folded aggregates but are poor at discriminating the numerous folds a domain like the CD23 lectin domain may assume.

The CD23 lectin domain contains 8 cysteine residues, which is relatively high for an extracellular domain of that size. Assuming all cysteine pairings are possible, there would be 24 combinations of disulphide bridges and this does not include any folds with free sulphide groups. The refolding method used assumes the disulphide bonding occurs after the formation of secondary structures and favours folds of least energy, so certain folded species will be less likely because cysteine residues are in the wrong

orientation, too far apart, sterically hindered or the pairing may create an unfavourable torsion. Realistically, eight cysteines may stablise only a few different folded species if the domain contains a high percentage secondary structure. The CD23 lectin domain is approximately 26% alpha helix, 34% beta sheet, and the large remainder being 'other' (although coordinate bonding of the metal ion will account for some of this random coil). With this in mind, to be able to remove wrongly folded recombinant protein during purification is necessary to obtain accurate structural and binding data.

Data from antibody binding, and more convincingly, ligand binding assays and ^{1}H NMR spectra comparisons to H-CD23 (from NS0) suggest the Der-CD23 purified was correctly folded and assumed a conformation able to bind IgE, albeit at a lower affinity to full length CD23, as previously reported (Sarfati *et al.*, 1992).

Analysis of purified Der-CD23 showed that it was more than 95% pure. The majority was the correct sequence and predicted molecular weight. Some degradation was occurring over time, with evidence of the C-terminal 3, 6 and 10 residues being cleaved, but with the lectin domain remaining intact.

Der-CD23 satisfied the requirements for NMR experiments in that millimolar quantities could be purified and were soluble, consequently ^{15}N and $^{15}N/^{13}C$ labelled preparations were produced. Incorporation of isotope was complete and initial NMR 1D and 2D spectra were well resolved which will aid resonance assignment and ultimately structure determination. Unfavourable dimerisation of the lectin domain during 3D NMR experiments (at 1.5 mM) was perhaps foreseen with chemical cross-linking experiments but overcome with an increased experimental temperature. This interaction could stabilise the trimeric form of CD23 and, in addition to the CD23 ligands binding sites, can be identified in future experiments using NMR techniques.

CHAPTER 4: PRODUCTION OF STABLE, TRIMERIC sCD23

4.1 Introduction

CD23 expressed in the membrane forms trimers, through non covalent association of the alpha helical stalk region (Beavil *et al.,* 1995). However, much of the biophysical and *in vitro* biological assays previously carried out with soluble CD23 have used either monomeric (16 kDa or 25 kDa) or readily degradable, unstable trimeric fragments (29-37 kDa). Thus, a recombinant, stable trimeric CD23 would a very useful tool to investigate the properties and function of soluble CD23 as a trimer.

Recombinant, soluble CD23 tends to form unstable trimers for several reasons. Firstly, without the two dimensional constraint of the membrane the long helical stalk is less likely to associate in the correct orientation in solution. Secondly, proteolysis along the stalk region would releases monomeric 25 kDa fragments which, in turn, could interfere with the formation of other trimers. The design of a stable, trimeric CD23 chimera must therefore contain a structural motif that will form a stronger association in solution and omit proteolytic sites.

This criteria could be achieved by fusion with oligomerisation sequences of other stable, soluble trimers, e.g. those with alpha helical coiled coils, particularly the collectin family of C-type animal lectins that includes mannose binding protein, surfactant proteins A and D (Hakansson and Reid, 2000). A heptad repeat sequence in the neck region of SPD was chosen because it forms tightly associated trimers in solution and has been well characterised (Hoppe *et al.,* 1995). Thus the strategy was to produce a chimeric protein comprising of the lectin domain and C-terminal tail of CD23 with the heptad sequence of the SPD. Thus, the ligand binding sites are retained and the CD23 stalk that easily degrades is omitted.

Some success has been achieved in creating recombinant trimeric versions of murine CD23 (Kelly *et al.,* 1998) and CD40L (Morris *et al.,* 1999). The extracellular sequence of murine CD23 (with a point mutation at the site of proteolysis) was fused to a modified leucine zipper motif (lz) that forms trimers when leucines are replaced by isoleucines (Harbury *et al.,* 1993 and 1994). This chimera was less labile and had a greater affinity for IgE than any other recombinant form of murine CD23. Indeed, it was able to inhibit IgE binding to the high affinity IgE receptor. In a collaboration with the laboratory of D. Conrad, a human version of this chimera has been provided for folding, oligomerisation and activity studies.

Consequently, the two human CD23 fusion constructs have been investigated and compared: one with the neck region of surfactant protein D (SPD-CD23); and the other with an engineered isoleucine zipper region (LZ-CD23). Production of a stable trimeric CD23 was hoped to enhance the affinity of recombinant CD23 for its ligands (IgE and CD21). Previous recombinant extracellular CD23 had a tenfold lower affinity for IgE than membrane bound oligomeric CD23 ($K_A = 10^6\ M^{-1}$ and $10^7\ M^{-1}$, respectively; Reljic, 1996).

4.2 Cloning of Chimeric SPD-CD23

The fusion of SPD and CD23 DNA (coding for M150 to S321, as indicated in Figure 1.2) was achieved by a two-stage strategy, as illustrated in Figure 4.1. The polymerase chain reactions were implemented using the primers and oligonucleotides listed in Appendix I. The fusion junction was designed so the hydrophobic residues a and d of the heptad repeats of SPD and the substituted and remaining CD23 stalk were in phase.

```
i.e.                                                    CD23 head
          SPD neck
       .. VAS LRQQ VEA LQGQ VQH LQAA FSQ YKME LQV ...
          a   d    a   d    a   d    a   d    a
```

4.2.1 Construction of Leader-SPD DNA for Chimera Production

Four long, overlapping oligonucleotides (O1-O4) were synthesised to contain the sequence of Vκ light chain leader sequence (M1 to I22; Whittle *et al.,* 1997) and the neck region of surfactant protein D (coding P222 to K249; numbering by Rust *et al.,* 1991). Overhang primers (PF1 and PR1) with BamHI and XhoI restriction sites were included with the oligonucleotides (0.02 μM of each) in a PCR using an annealing temperature of 56 °C (Figure 4.1a). The resulting leader-SPD PCR product (162 bp) was digested, purified by electrophoresis and ligated into BamHI/XhoI sites of pBluescript KS.

Xli Blue cells were transformed and positive colonies identified, amplified and sequenced using T3 and T7 vector primers (full sequence data in Appendix II). This pBluescript Vk-SPD vector could then be used for any trimeric chimeras that may be designed in the future. The XmaI site was included in the 5' end of the construct for potential ligation of SPD chimeras into the mammalian expression vector, pEE12.

4.2.2 Fusion of Leader-SPD and CD23 Sequences by PCR

Two primers were designed to contain the sequence encompassing the fusion junction, one on each strand (CD23FF and SPDFR). Together with PF2 and PR2 the PCR produces intermediate fragments that in turn act as overhang primers to produce the completed fusion product (Figure 4.1b). A 700 bp product was obtained using an annealing temperature of 51 °C. The fusion product was purified, digested and ligated into pBluescript (BamHI and EcoRI sites). Positive clones were identified by analytical restriction digestion of purified plasmid DNA. One positive clone was sequenced using T3, T7 primers and a couple of insert specific primers (Appendix I). No coding errors were found (sequence detailed in Appendix II).

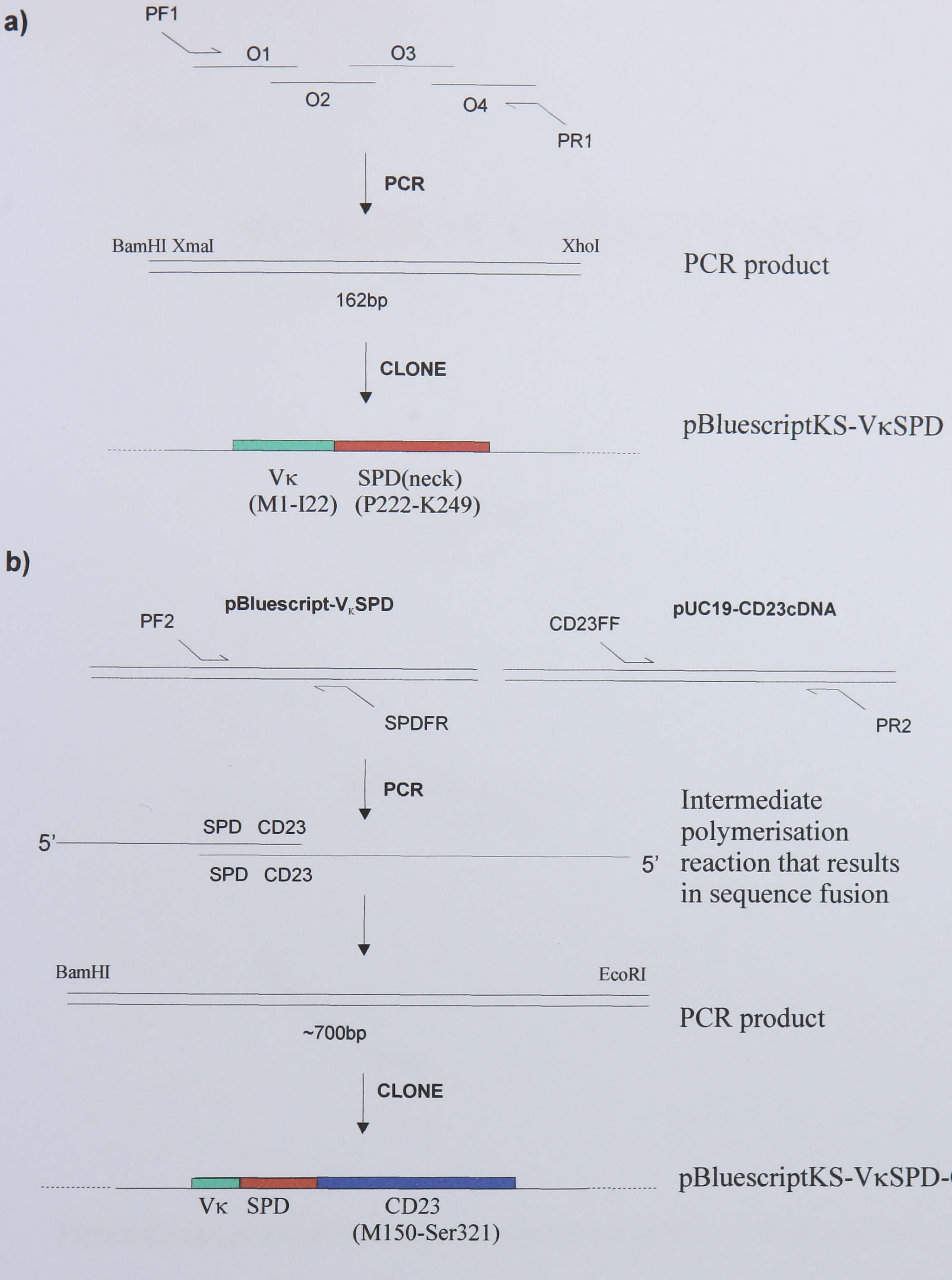

Figure 4.1: Schematic Diagram of the Cloning Strategy for the Construction of SPD-CD23

a) The leader of Immumoglobulin V kappa light chain (encoding M1-I22, Whittle *et al.*, 1997) and the neck region of surfactant protein D (encoding P222-K249, Rust *et al.*, 1991) were synthesised from 4 long oligomers (O1-O4). This sequence was ligated into the shuttle vector pBluescript KS. **b)** Fusion of the leader-SPD and CD23 sequence (encoding M150-S321, i.e. 25 kDa fragment illustrated in Figure 1.2) was achieved using primers that overlap the 3' SPD and 5' CD23 sequence, so that the heptad repeats were in phase The PCR product was ligated into the BamHI and EcoRI restriction sites of pBluescriptKS.

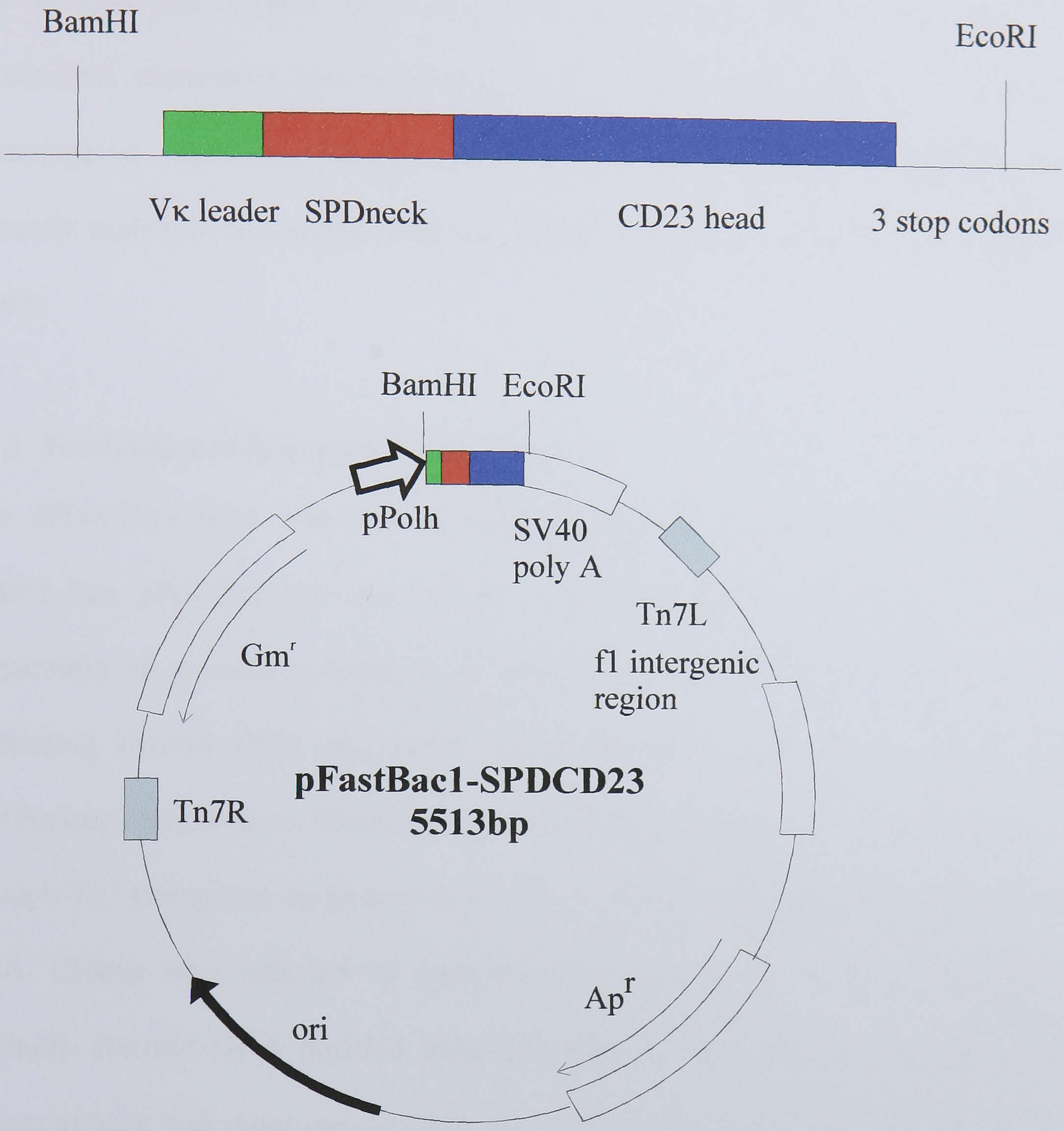

Figure 4.2: Expression Vector for the Production of SPD-CD23 Baculovirus

a) The completed SPD-CD23 construct, including the Vκ leader sequence, SPD-CD23 fusion and stop codons, was inserted into the BamHI and EcoRI sites of pFastBac. **b)** The insert was downstream of a polyhedron promoter (pPolh) which, in addition to gentamycin resistance (Gm^r) was transferred to the bacmid DNA by homologous recombination of the Tn7 elements. The plasmid was also selected by ampicillin resistance (Ap^r)

4.3 Production of SPD-CD23 by the Baculovirus Expression System

The 37 kDa and 25 kDa CD23 fragments have been expressed previously by the baculovirus expression system (Graber *et al.,* 1992 and Rose *et al.,* 1992). The advantage of expression in insect cells is that the recombinant molecule will be correctly folded by the cellular machinery and secreted into a relatively pure, serum free media.

4.3.1 Production of Recombinant Baculovirus

The SPD-CD23 DNA was excised using the BamHI and EcoRI sites, purified and ligated into pFastBac, the baculovirus expression vector (Figure 4.2). A plasmid preparation of a positive colony was used to transform D_H10BAC, an *E.coli* strain containing bacmid DNA and helper DNA (plasmids encoding only the essential baculovirus components). Within the bacterial cell, a homologous recombination event through Tn7 transposon sequences inserts the construct from pFastBac into the bacmid DNA. Clones were selected by antibiotic resistance as described in Materials and Methods. Bacmid DNA purified from the selected clones showed the characteristic pattern of high molecular weight DNA on a 0.5% agarose gel (results not shown). 5 µl of bacmid DNA was used to transfect Sf9 insect cells using DNA-liposome complexes (Material and Methods).

4.3.2 Expression of SPD-CD23 In Insect Cells.

4.3.2.1 Expression

Three days after transfection, the cells were harvested and the supernatant retained. Samples of supernatant were analysed by Western Blot. A band of the correct

approximate molecular weight was detected in a four fold concentrated sample of supernatant showing that SPD-CD23 was expressed and secreted by Sf9 cells. Some evidence of a dimer species was seen, possibly due to insufficient denaturing conditions or intermolecular disulphide bonding.

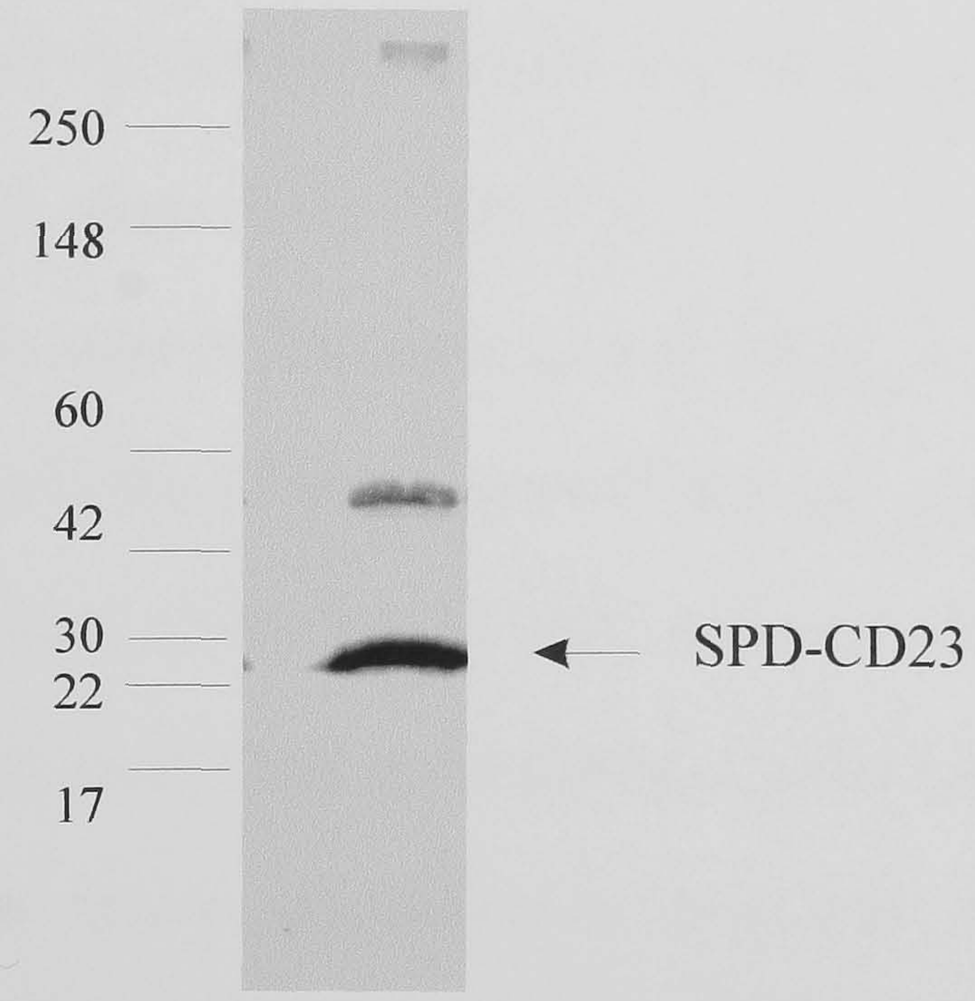

Figure 4.3: Western Blot of Secreted SPD-CD23 from Sf9 Transfected Cells.

CD23 expression in culture supernatants was analysed on a non-reducing, 4-20% SDS gel by Western blot using MHM6 (monoclonal anti-CD23). Lane 1 contained negative control supernatant and lane 2 contained a four fold concentrated sample of SPD-CD23 supernatant from Sf9 cells. The major band was the correct approximate weight (22 kDa). The minor band ran at about the dimeric weight of SPD-CD23.

4.3.2.2 Selection Of Baculovirus Host Cell.

The titre, plaque forming units (pfu) per ml, of the resulting baculovirus was estimated using a plaque assay (Materials and Methods). The titre of the primary infection was 10^5 pfu/ml. This titre was amplified and the volume increased through sequential rounds of infection until 1 l of virus at 5 x 10^7 pfu/ml was obtained. This baculovirus stock was

used to infect 1 l Sf9 and Hi5 cells for expression of SPD-CD23 at a multiplicity of infection (MOI) of 10 i.e. 10 pfu/cell.

The yield of 'active' SPD-CD23 (i.e. that able to bind MHM6 and EBVCS-2 monoclonal antibodies used in the sandwich ELISA) was quantified (Materials and Methods, 2.5.8.2). The active yields were quantified in triplicate by comparison to purified rCD23. Comparatively, Sf9 cells secreted twice as much SPD-CD23 as the Hi5 culture (11 mg/l and 5 mg/l, respectively; Table 4.1).

Hi5 cells, derived from the eggs of *Trichoplusia ni* (Cabbage lopper) are reputed to be better protein expressing cells due to their larger cell size and superior post-translational modification machinery than either Sf9 or Sf21 cells from *Spodoptera fruiperda.* Differences in passage number and sub-optimal culture conditions or MOI would have an effect on recombinant protein expression in these host cells. For the culture conditions employed, Sf9 cells were selected for use in further expression cultures. The estimated yield suggests that a 5 l fermenter culture would provide enough protein for purification and characterisation purposes (around 50 mg).

Table 4.1: Expression Of SPD-CD23 In The Supernatant Of Insect Cell Cultures

Host Insect Cell	Estimated Active yield in 3 day culture supernatant (mg/l)
Hi5	5.0 (+/- 0.2)
Sf9	11.4 (+/- 1.3)

4.3.2.3 Expression of SPD-CD23 in 5l cultures.

A 5 l bio-fermenter (Braun) was equilibrated overnight with 4 l of Excell 420 serum free media at pH 6.2 (regulated by CO_2 addition); O_2 levels set to 70% and incubated at

28 °C with stirring motor speed of 150 rpm. The addition of drops of 10% antifoam solution were added to improve gas exchange in the system. Sf9 cells were added at 0.8 x 10^6 cells/ml. The following day the cells were counted and recombinant baculovirus was added at a MOI of 10. On the third day of infection the culture was harvested.

4.3.3 Purification of SPD-CD23 From Insect Cell Media.

4.3.3.1 Supernatant Treatments

Following centrifugation for 20 minutes at 4000 rpm, the supernatant was filtered through 0.45 μm pore membrane (Millipore). The supernatant was concentrated using a minicassette ultrafiltration system to 1 l. The western blot analysis of these stages estimate the yield of SPD-CD23 in the concentrated supernatant was roughly 20 mg. 0.05% azide and protease inhibitors (benzamidine, iodoacetamide, TLCK, PMSF and aminocaproic acid) were also added.

4.3.3.2 Purification by Affinity Chromatography.

Affinity Chromatography relies on the specific binding of an antibody or ligand to the target molecule. It is good method for the first step of purification because of its specificity and large volumes of protein solution that can be applied, especially advantageous for crude baculovirus or mammalian cell cultures. 10 mg MHM6 was coupled to Affiprep10 via primary amines forming amide bonds with N-hydroxysuccinimide ester groups on a methacylate bead support. Concentrated SPD-CD23 supernatant was loaded at 1 ml/min, then washed with TBS-Ca buffer and eluted with 0.1 M glycine pH 2.5. The column had a low binding capacity (approximately 250 μg) so the supernatant was reapplied several times.

Western blotting of the neutralised eluate showed a band of the correct size for SPD-CD23 (22 kDa). However, the presence of higher molecular weight complexes and aggregates of CD23 were also seen under non reducing conditions (Figure 4.4a). These bands disappear under reducing conditions (Figure 4.4b) suggesting they are mis-folded disulphide-linked CD23 multimers. SDS-PAGE analysis also showed that the eluted SPD-CD23 was contaminated with what appeared to be the 14 kDa breakdown product at a ratio approaching 1:1.

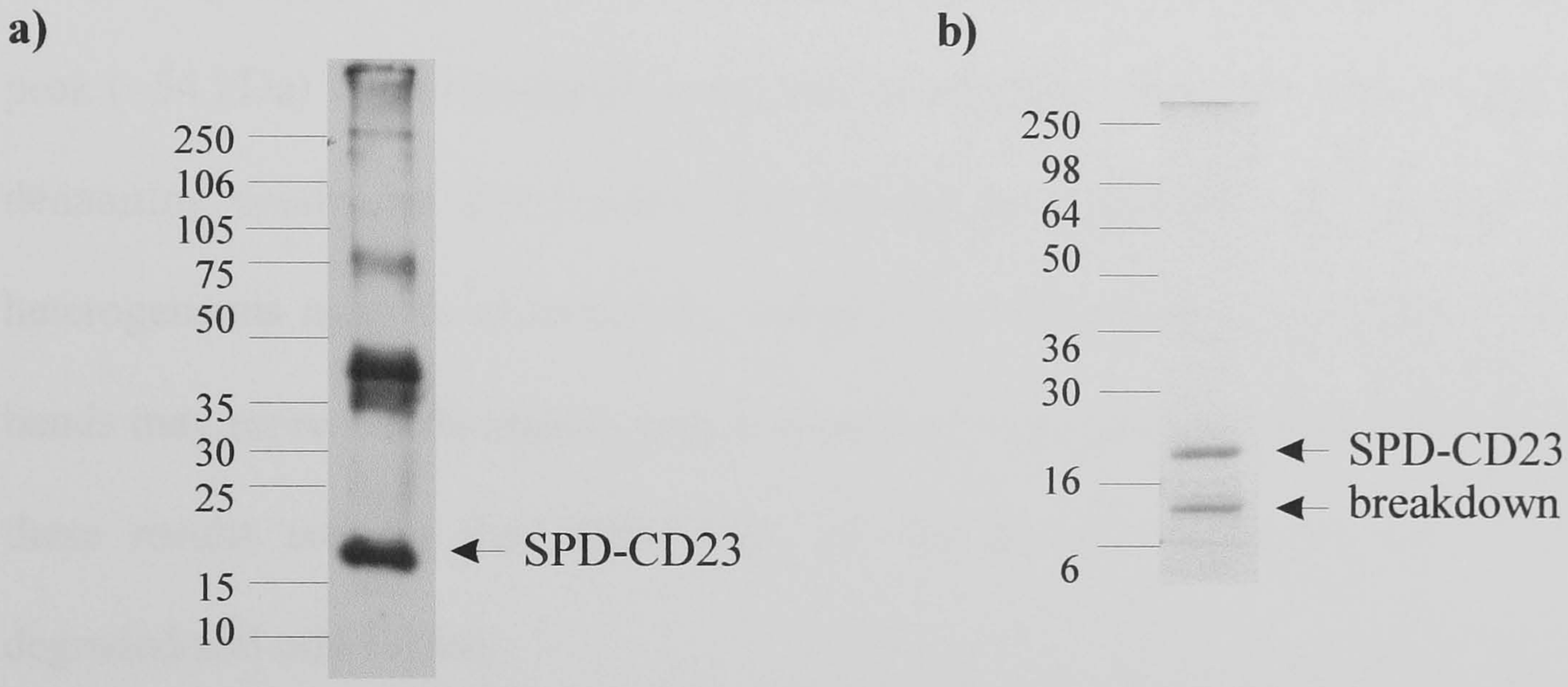

Figure 4.4: Elution of SPD-CD23 from MHM6-Affiprep-10 Affinity Column

a) SPD-CD23 eluted from MHM6-Affiprep10 was analysed under non-reducing, denaturing conditions by Western blot (using MHM6). Although SPD-CD23 was being eluted higher molecular weight complexes were also being detected. **b)** SDS-PAGE of reduced sample shows SPD-CD23 was degrading to smaller fragment (<16 kDa) and showed no higher molecular weight contaminants.

Although no proteolysis of SPD-CD23 had been detected in the supernatant, this column was preferentially binding monomeric lectin domain. This is possible if trimerisation masks the MHM6 epitope or alternatively, MHM6 which has a very high affinity for CD23 disrupts the trimers making them susceptible to dissociation and degradation.

To investigate the oligomeric nature of SPD-CD23 purified by affinity chromatography it was run in its native form on a calibrated gel filtration column (Materials and Methods 2.4.3). The eluate was concentrated to approximately 1 mg/ml by ultrafiltration and applied to a Superdex 75 column. SPD-CD23 eluted as one major peak unresolved from a lower molecular weight peak and a smaller higher molecular weight maximum (Figure 4.5a). Fractions containing these maxima were reinjected and molecular weights estimated from a standard curve. A peak (~24 kDa = monomer) was still contaminated by the major product (~14 kDa = breakdown product). The higher molecular weight peak (~54 kDa) was presumably some sort of oligomer. However, under non-reducing, denaturing conditions this fraction did not run as a monomer as expected but as a heterogeneous mixture of molecular weights between 30-40 kDa (Figure 4.5b). These bands may represent disulphide linked dimers of degradation products. Taken together, these results suggest that SPD-CD23 derived by this procedure was monomeric, degraded and mis-folded.

The limitations of the MHM6 affinity column were similar to those experienced by Dierks *et al.,* 1993. They observed murine CD23 purified by anti-CD23 affinity chromatography resulted in low levels of trimerisation, and subsequently, a reduced avidity to IgE adsorbent. To overcome the problem of binding monomeric CD23 the possibility of using IgE as an affinity ligand was investigated. It was hoped that an IgE column would only bind 'active' CD23 and that it would preferentially bind trimers.

a)

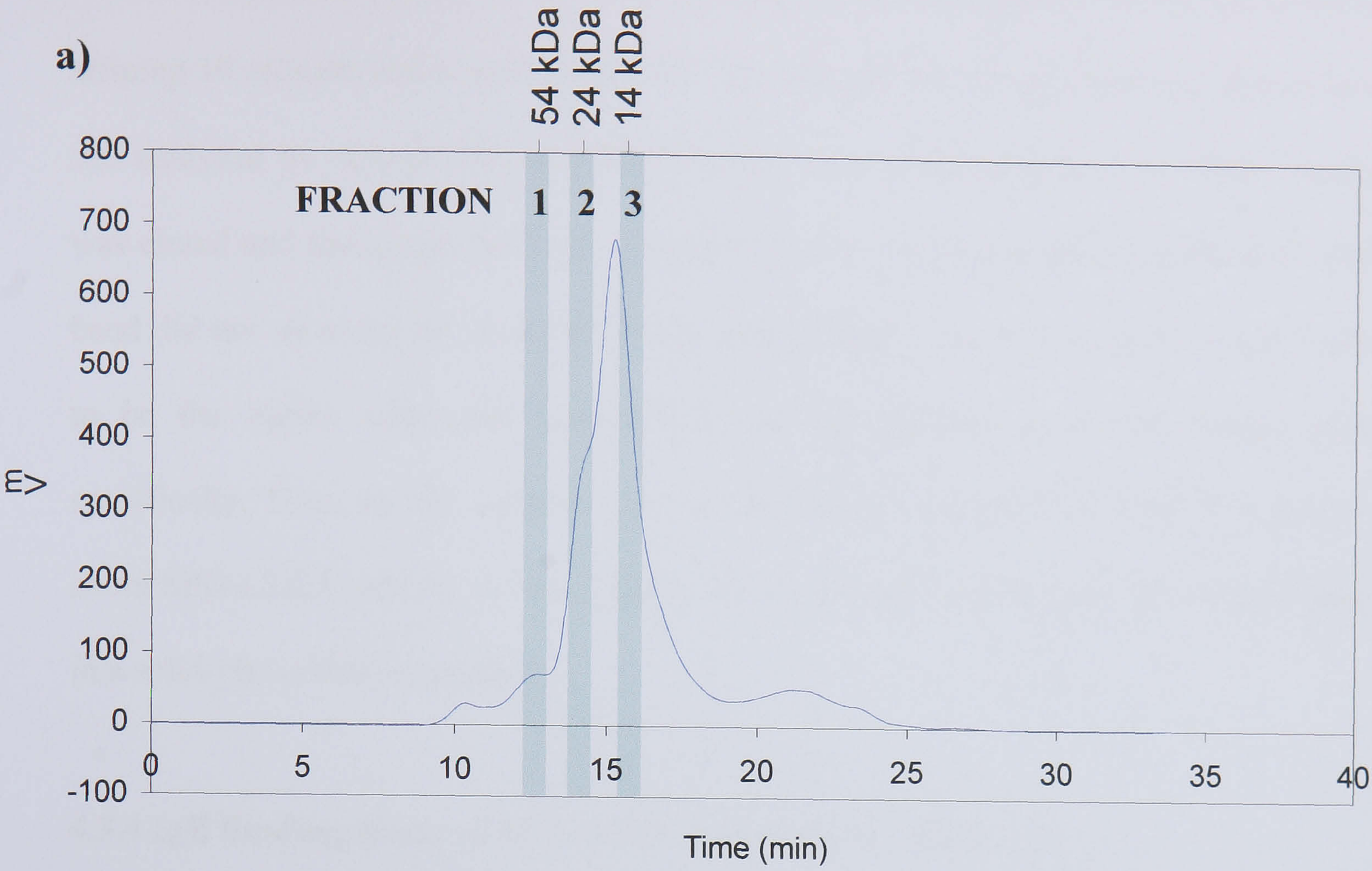

b)

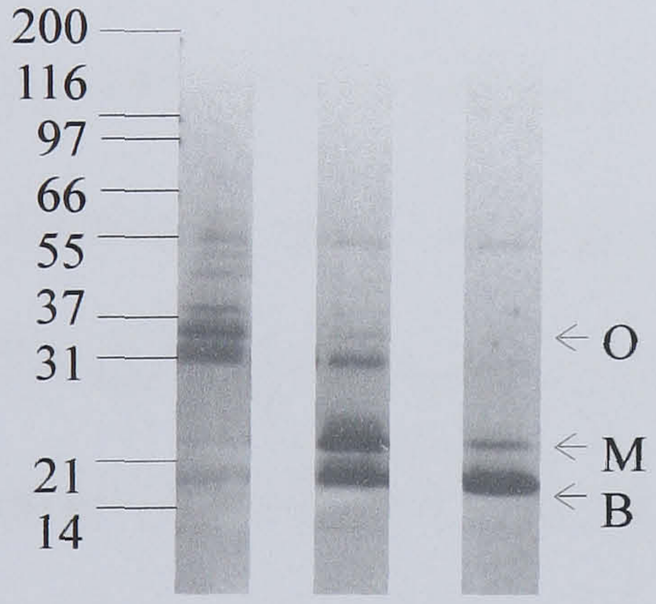

Figure 4.5: Analysis of MHM6 Affinity Purified SPD-CD23 by Size Exclusion Chromatography

a) 0.25 mg SPD-CD23 was loaded onto a calibrated Superdex 75 (Appendix III) and run at 0.75 ml/min in 0.25 M Tris-Cl, 0.125 M NaCl, 1 mM $CaCl_2$ **b)** Fractions 1, 2 and 3 were run under non-reducing conditions on a SDS gel and silver stained. Fraction 1 contained a mixture of mis-folded complexes (**O**), fraction 2 contained mainly monomeric SPD-CD23 (**M**), and fraction 3 was largely breakdown product (**B**).

250 ml of SPD-CD23 infected Sf9 culture supernatant was loaded onto an IgE coupled affiprep 10 column and eluted with 0.1 M glycine pH 2.5. The elution was neutralised and analysed by SDS-PAGE and Western blot (results not shown). Very little protein was eluted and the major band ran at approximately 60 kDa (results not shown). This band did not show up by immunoblotting with MHM6. The 60 kDa protein was likely to be the highly expressed baculovirus coat glycoprotein gp64 that bound non-specifically. Thus, an IgE column was also unsuitable to purify SPD-CD23. Suspicion about SPD-CD23 inability to bind ligands was raised and consequently was investigated in a solid-phase binding assay.

4.3.4 IgE Binding Assay of SPD-CD23 Expressed in Insect Cells.

The IgE binding ability of SPD-CD23 present in the insect culture supernatant was investigated by sandwich ELISA. A monoclonal antibody (mAb25) previously identified to only partially inhibit IgE binding (Wakai *et al.,* 1993; section 5.2.2) was coated on to a microtitre plate to capture CD23 in the supernatant. A CD23 quantification ELISA (2.5.8.2) was used to normalise the concentrations of SPD-CD23 and a positive control (recombinant extracellular CD23 in blank supernatant). Both CD23 were added in serial dilutions to the mAb25 coated plate. A biotinylated form of IgE-Fc, followed by streptavidin-HRP was used to detect ligand binding.

Figure 4.6 shows that full length CD23 was able to bind IgE-Fc (10 nM) at concentrations between 20 nM and 50 nM, whereas no binding to SPD-CD23 was detected within this range. Indeed, SPD-CD23 was not at a high enough concentration within the supernatant to obtain a complete sigmoidal curve. Thus, instead of having a higher affinity for IgE than rCD23, as predicted, unpurified SPD-CD23 either has a

significantly lower affinity or that only a small proportion of SPD-CD23 was able to bind IgE.

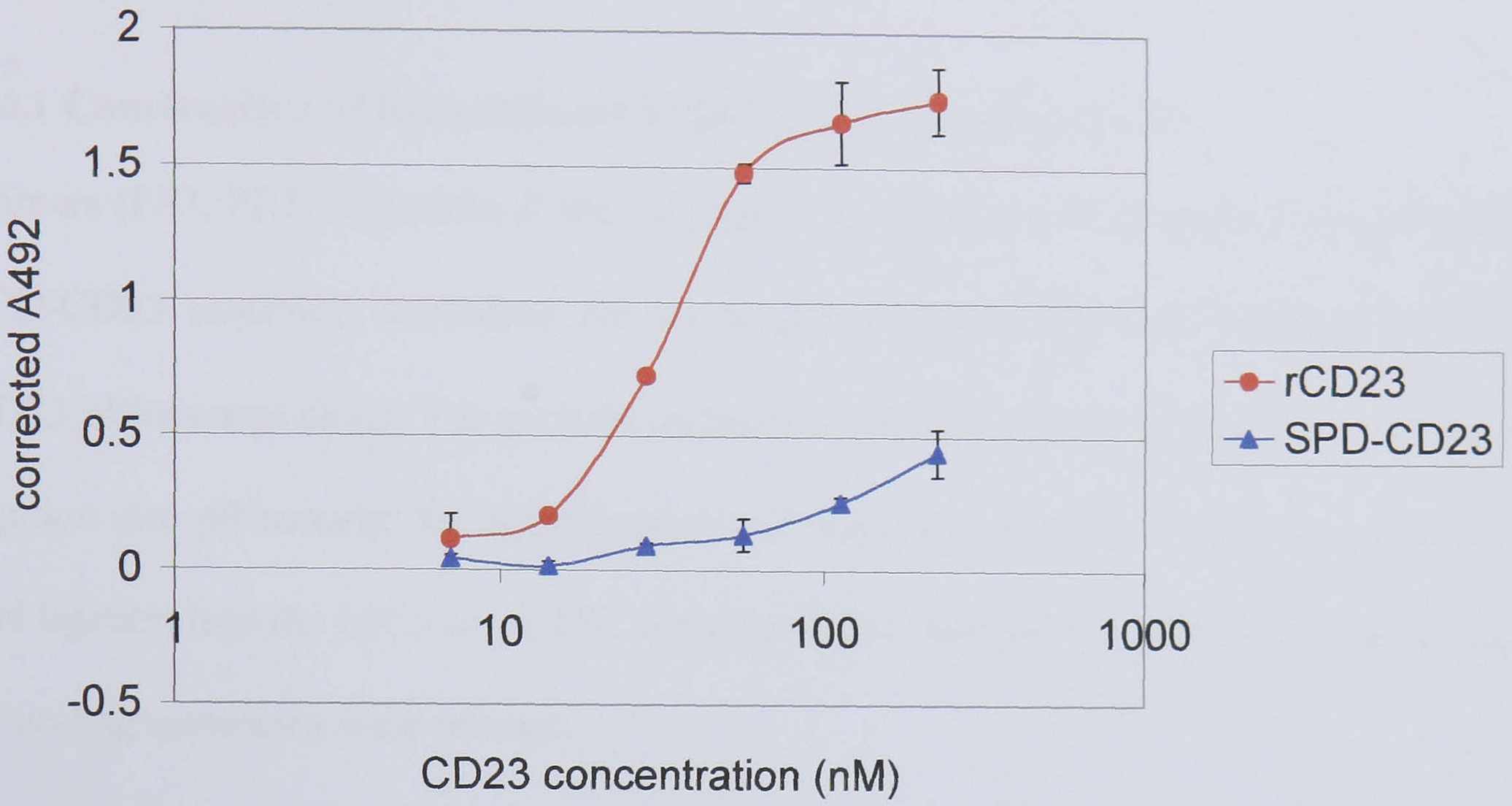

Figure 4.6: Relative IgE binding activities of SPD-CD23 and rCD23 by ELISA

Equivalent concentrations of recombinant rCD23 and SPD-CD23 in insect cell culture supernatants were captured by 2 μg/ml mAb25 coated onto a microtitre plate. 1 μg/ml IgE-Fc was added and interaction revealed by streptavidin-HRP. The curves suggest that rCD23 has a greater affinity for IgE-Fc than SPD-CD23 or that the proportion of 'active' SPD-CD23 was much lower.

4.4 Production of Chimeric CD23 Expressed by Bacteria

It was established that SPD-CD23 from insect cells did not bind IgE with a high affinity as expected. It was not clear whether this was due to the fact that the chimera was not forming trimers or whether the chimera did form trimers that were not capable of ligand binding. Due to the difficulties of obtaining sufficient amounts of intact purified SPD-CD23 for accurate oligomerisation assessment, the construct was transferred to a bacterial expression system where large amounts of relatively pure protein can be made.

Through a collaboration with D. Conrad, a human CD23 fusion protein with an N-terminal isoleucine zipper and T7 tag (LZ-CD23) was available as solubilised inclusion bodies from *E.coli* expression. Thus, the CD23 chimeric designs could be compared.

4.4.1 Construction of Recombinant SPD-CD23 Expression Vector

Primers (PF3, PR3, Appendix I) were designed to produce a PCR product including the SPD-CD23 sequence, excluding the Vκ leader sequence from the original Vκ-SPD-CD23 pBluescript clone. The primers included a HindIII and BamHI restriction sites for ligation into pBluescript for amplification and sequencing, and a NdeI site for excision and ligation into the MCS of pET5a. Sequencing of the insert in pBluescript confirmed no coding mutations were present.

4.4.2 Expression of SPD-CD23 In *E.Coli.*

The BL21 (DE3) (pLysS) host strain was transformed using the SPD-CD23 pET5a vector, as described in methods (2.3.1). Expression in 1 l culture using M9 media was induced by 0.4 mM IPTG at an A_{600}>0.6. A time course of expression following induction was analysed by Western Blot, and the cells were harvested after 3 hours (Figure 4.7a). SPD-CD23 appeared to by expressed at high levels in the insoluble fraction of the cells. Extraction of inclusion bodies resulted in the solubilisation of 100 mg protein from 1 l of culture. SDS-PAGE analysis shows this extract to be of moderate purity similar to that of LZ-CD23 (Figure 4.7b).

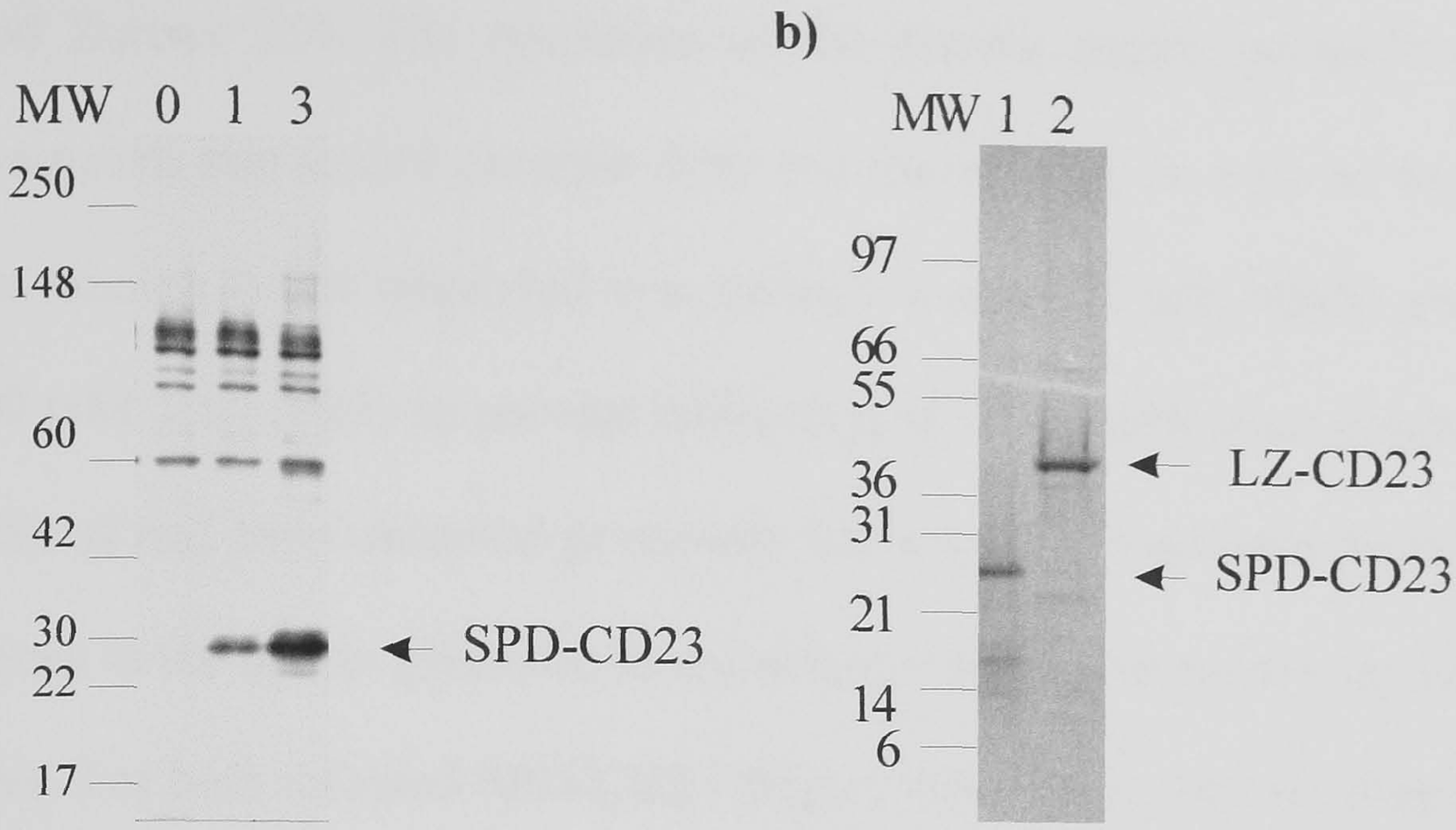

Figure 4.7: Denatured SPD-CD23 and LZ-CD23 from Expression in *E.coli*.

a) SPD-CD23 expression in total cell protein was monitored after induction at time 0, 1 and 3 hours by Western blot using rb55 polyclonal antibody. **b)** SDS-PAGE analysis of SPD-CD23 (1) and LZ-CD23 (2) solubilised inclusion bodies, prepared for loading by TCA precipitation and stained by Coomassie Blue.

4.4.3 Refolding of Chimeras from Solubilised Inclusion Bodies.

10 mg batches were refolded using the optimised refolding method used to refold rCD23 (Reljic, 1996). This involved reduction, formation of a glutathione intermediate and dilution into cysteine buffer. Both refolded chimeras were concentrated to less than 3 ml for purification by gel filtration. The recovery of protein from concentration by ultrafiltration was in the region of 60-70% for SPD-CD23 and 40-50% for LZ-CD23. Large amounts of aggregate and precipitate were occurring that may be attributed to the formation of the associated coiled coil before the stabilisation of the disulphide bonds in the lectin domain, thus, leading to intermolecular disulphide bonds.

4.4.4 Purification of SPD-CD23 and LZ-CD23.

In order to establish the most appropriate column for separation of oligomeric chimeras a series of column matrices were tested: Superdex 75, Superdex 200, Biosep 3000,

TSK4000 and Zorbax 250. The resolution of the desired matrix would be able to separate aggregated, mis-folded proteins from the correct size as well as breakdown material. The running buffer employed was strongly ionic (250 mM NaCl) and highly buffered (500 mM Tris) solely to prevent interaction of CD23 with ionic groups on the column matrix as had been observed previously for several recombinant proteins. The size of the pores in the matrix gives rise to the range of molecular masses the column is able to resolve. For both refolded SPD-CD23 (Figure 4.8a) and LZ-CD23 (Figure 4.9a) Biosep 3000 was selected for its ability to remove aggregate from the refolded material in the preparation. Superdex 200 also gave similar resolution and could also be used for purification. The columns were calibrated with protein molecular weight markers to form a standard curve (log MW against time) but the estimated molecular weights of the maxima did not correspond to the predicted molecular weights of the SPD-CD23 or LZ-CD23 oligomeric species. The fractions obtained had to be analysed by alternative methods in order to select the correctly folded protein.

4.4.5 Characterisation of Fractions

4.4.4.1 Western Blot Analysis

Western blot analysis of fractions run on a SDS-gel under non-reducing conditions was able to show which fractions were mis-folded i.e. contained intermolecular disulphide bonds. The SPD-CD23 showed a large proportion of the refolded material contained high molecular weight aggregate (fractions 4-8, Figure 4.8b). Some protein of the correct size was identified in later fractions (fractions 11-12) which appeared to be well resolved from the mis-folded material. SDS-PAGE analysis confirmed this (results not shown) but also showed some evidence of contamination and degradation in these fractions.

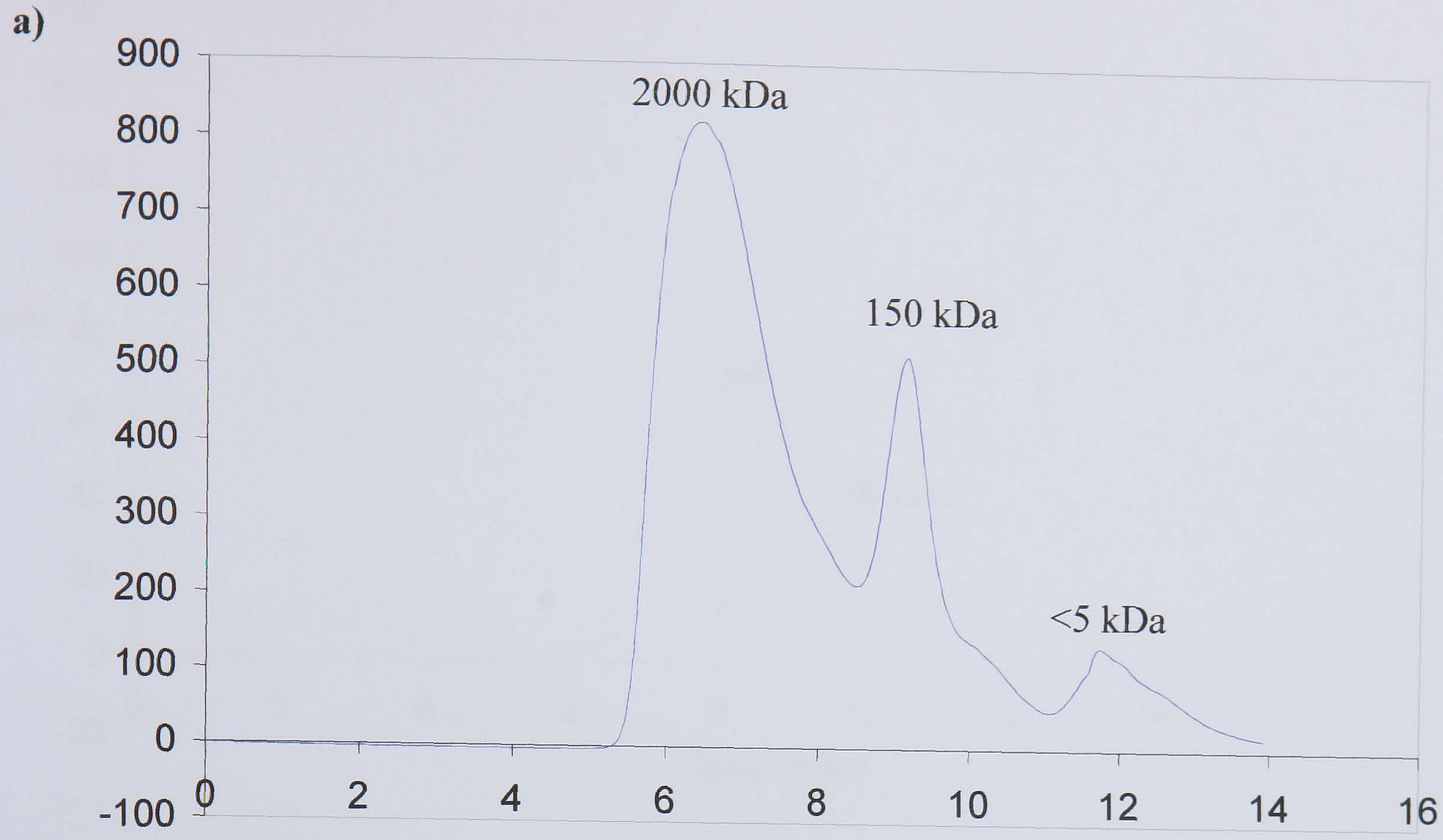

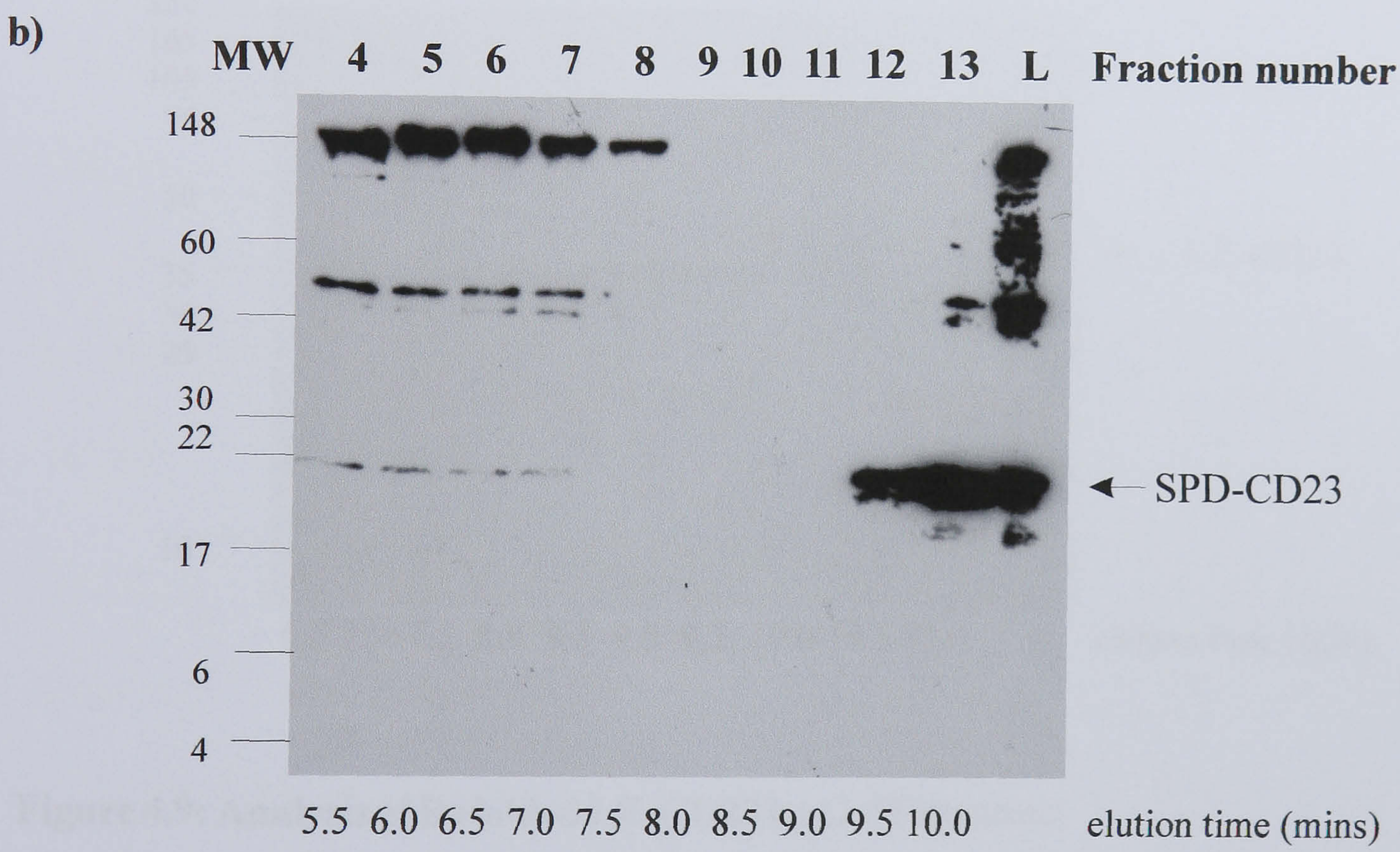

Figure 4.8: Analysis of Refolded SPD-CD23 by Gel Filtration

a) Elution profile (A_{280}) of refolded SPD-CD23 on a calibrated Biosep 3000 column run at 0.75 ml/min in 0.5 M Tris-Cl pH 7.2, 0.25 M NaCl, 0.05% NaN_3. Fractions were collected in 0.5 minute intervals between 5 and 15 minutes. The two major peaks represent aggregated (2 MDa) and a species estimated to be 150 kDa. **b)** Fractions and the protein loaded (L) were analysed under non-reducing conditions by Western Blot with MHM6. Fractions 4-8 contained aggregated SPD-CD23 and represents the majority of the preparation. Fractions 12 and 13 contain non-covalently associated SPD-CD23.

a)

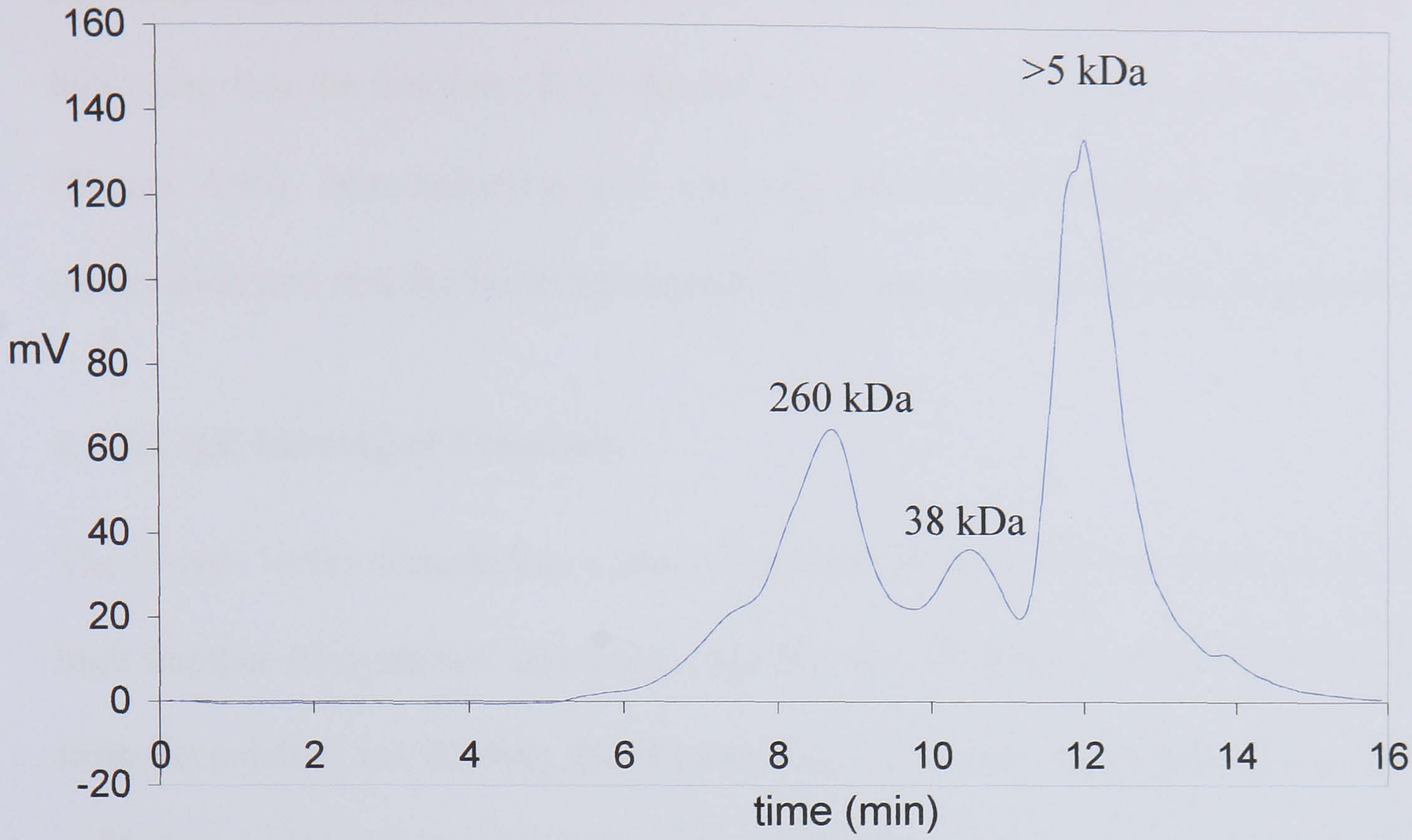

b)

Figure 4.9: Analysis of Refolded LZ-CD23 by Gel Filtration

a) Elution profile of refolded LZ-CD23 on a calibrated Biosep 3000 column. Fractions were taken every 0.5 minutes from 5 minutes. Several species of different molecular weight were observed of estimated weights 260 kDa and 38 kDa presumably representing oligomer and monomer, respectively. **b)** The fractions and refolded protein loaded onto the column (L) were analysed under non reducing conditions by Western blot with MHM6. No aggregation of LZ-CD23 was detected in this preparation but LZ-CD23 appeared to be present in the oligomeric fraction only.

LZ-CD23 fractions that contained CD23 ran at the correct molecular weight (38 kDa), indicating that the fractions 8-12 appeared to be correctly folded and free of aggregate (Figure 4.9b). Non-reducing and reducing SDS-PAGE analysis agreed with this observation and that the fractions contained few contaminants (results not shown).

4.4.4.2 IgE binding of Fractions

The C-type lectin domain has a low proportion of secondary structure and a relatively high number of cysteines that bring together non contiguous parts of the backbone to form the calcium ion binding site (Figure 1.2). Therefore, incorrectly folded species are unlikely to retain the ligand binding site conformation. A ligand binding assay was used as a method to identify correctly folded protein. A CD23-IgE ELISA (Methods 2.5.8.4) was performed with the fractions obtained from gel filtration. The optimisation of this assay is described in Chapter 5. Briefly, the CD23 samples were coated onto a micro-titre plate in TBS-Ca, a biotinylated version of anti NIP-IgE or IgE-Fc was added and the interaction was detected by Streptavidin-horse radish peroxidase conjugate enzyme reaction.

SPD-CD23 fractions (Figure 4.10a) showed low IgE binding activity akin to that of monomeric lectin domain (e.g. Der-CD23). No interactions were detected with biotinylated IgE, only the IgE-Fc mutant would bind in this assay. The lower molecular weight fractions (fractions 13-15) had the greatest relative binding capacity in this assay. The higher molecular weight fractions (fractions 3-9) did not bind IgE-Fc because they contained aggregated and mis-folded CD23 oligomers.

The IgE binding activity of the LZ-CD23 fractions was more promising with relative activities comparable to the full length CD23 construct (Figure 4.10b). Thus, fractions 12-15 of SPD-CD23 and fraction 8-11 of LZ-CD23 were pooled as correctly folded,

a) SPD-CD23 – IgE Fc ELISA

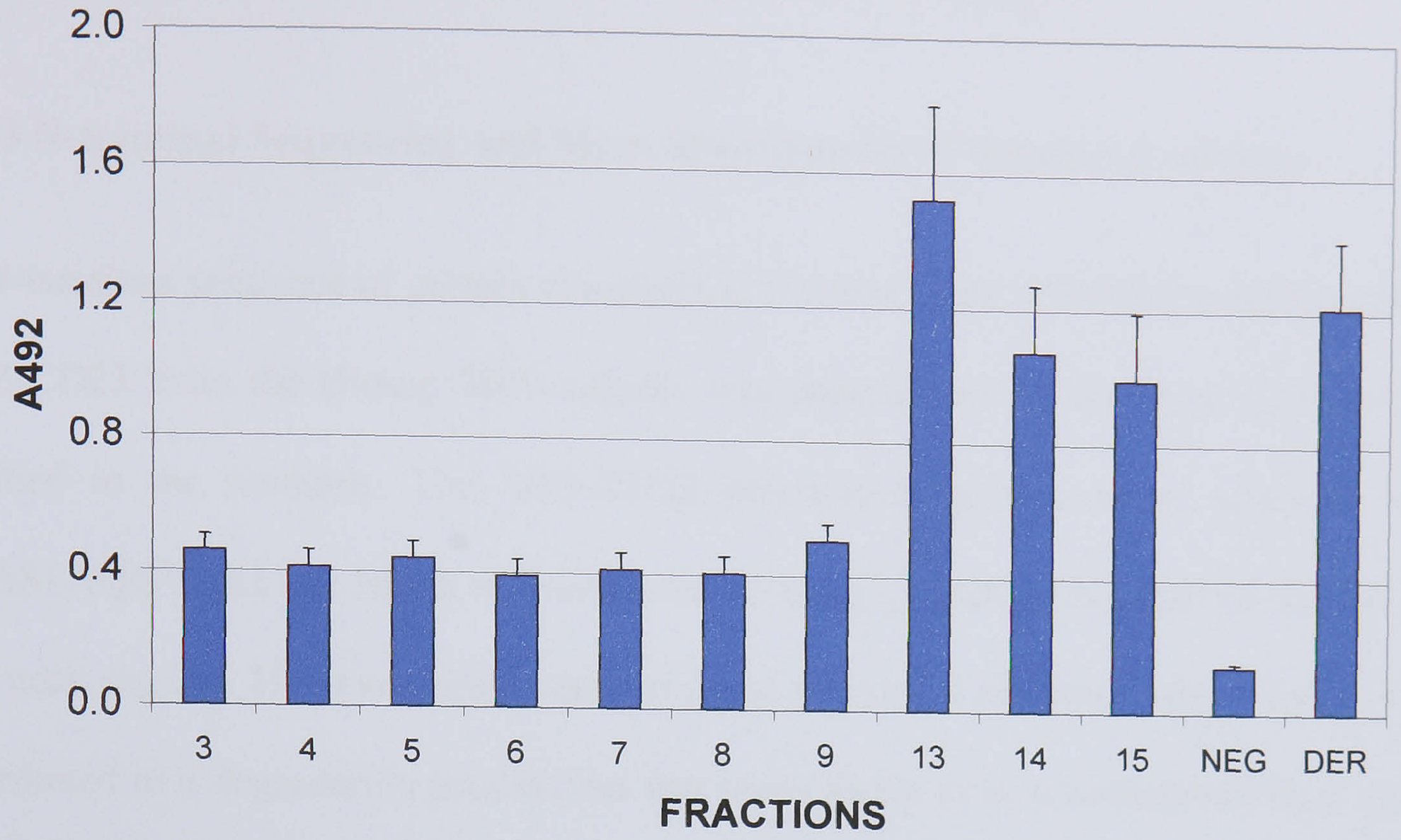

b) LZ-CD23 - IgE ELISA

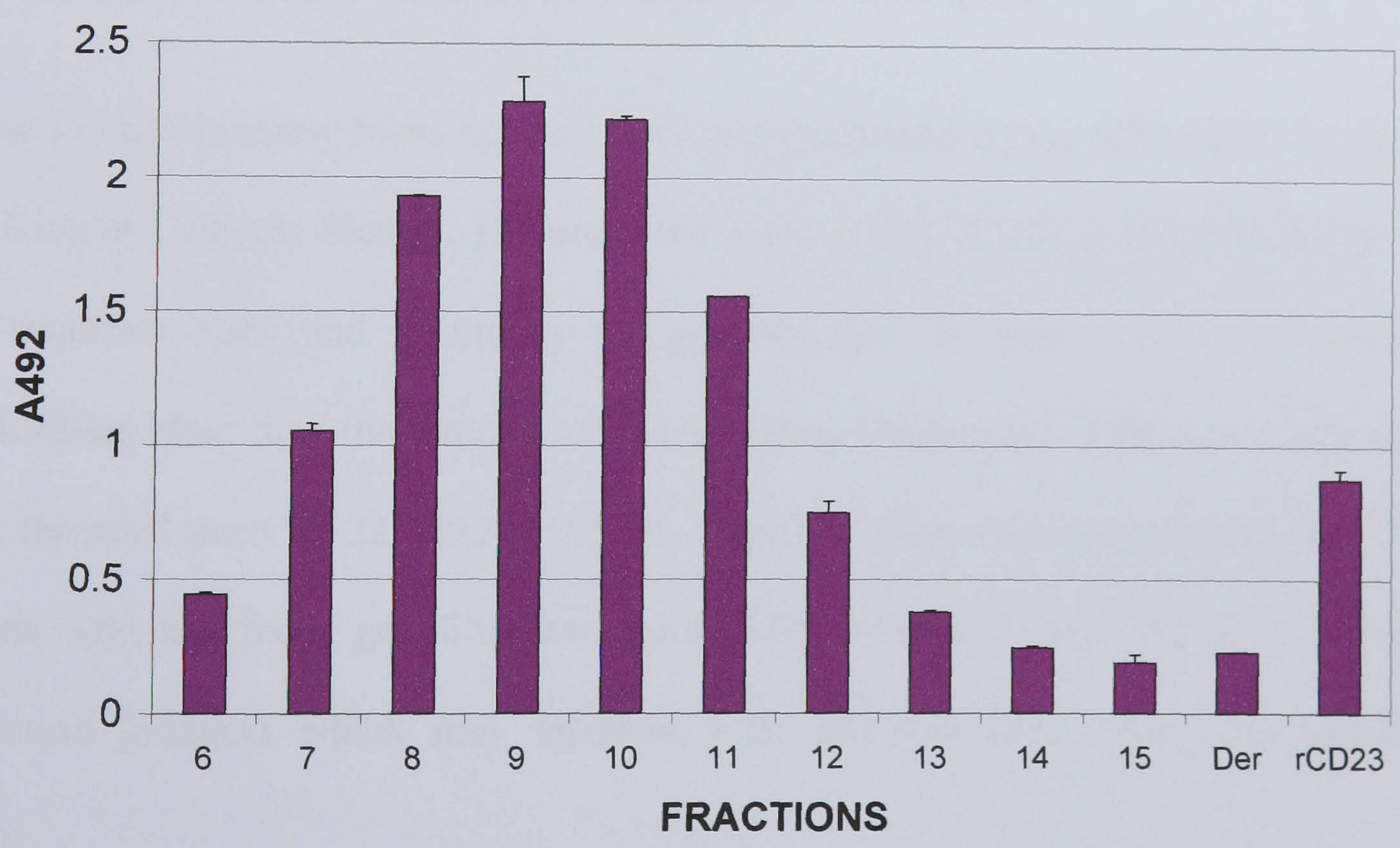

Figure 4.10: IgE Binding Activity of Chimeric CD23 Fractions.

a) 55 nM of each SPD-CD23 fraction was coated in triplicate alongside 55 nM Der-CD23 positive control and a negative control (BSA). 1 μg/ml biotinylated IgE-Fc was added and revealed by streptavidin-HRP **b)** 100 fold dilutions of LZ-CD23 fractions in TBS-Ca were coated in triplicate. 1 μg/ml biotinylated anti-NIP IgE was added and revealed by streptavidin-HRP (assays described in Chapter 5).

active protein for further analysis. Further activity assessments and kinetic constants of ligand binding activity of trimeric CD23 are described in Chapter 5.

4.4.4.3 N-terminal Sequencing and Mass Spectrometry of Selected Fractions

The N-terminus sequence of protein contained in fraction 13 of SPD-CD23 and Fraction 10 LZ-CD23 from the Biosep 3000 column was analysed by B. Smith at Celltech as described in the methods. The SPD-CD23 preparation gave a major sequence of PDVASLRQQVEALQG which represents the correctly processed N-terminal sequence (SPD neck region). However, there was a trace of additional sequence which could not be attributed to a degradation product but was more likely to be a contaminating *E.coli* protein. N-terminal sequence of LZ-CD23 gave a 15 amino acids representing the T7 tag (Met processed) derived from the expression vector, pET24a: ASMTGGQQMGRGSEF. No additional sequences were detected.

Positive Ion Electrospray Mass Spectrometry was performed on the SPD-CD23 fraction by L. King at Celltech, Slough. The predicted mass of SPD-CD23 is 22,325 calculated from sequence data and assuming no glycosylation or other post translational modifications other than the removal of the initiation Methionine. This was confirmed by the recorded mass of 22,320.34 +/-5.59. Together, these data demonstrate that the fractions selected from gel filtration were fully processed and did not contain degradation products which may interfere with oligomerisation and consequently activity.

4.5 Assessing the Oligomerisation State of Chimeric CD23

Having established the contrasting IgE binding abilities of SPD-CD23 and LZ-CD23, it was necessary to determine their oligomerisation state. It was unclear as to whether the low affinity interaction of IgE-Fc with SPD-CD23 was due to the chimera being monomeric or for other structural factors. Chemical crosslinking and analytical size exclusion chromatography using a 'physiological' buffer were used to define the oligomeric state of the chimeric CD23.

4.5.1 Chemical Cross-Linking

1-Ethyl-3-(3-dimethylaminopropyl)carbodiimide Hydrochloride (EDAC or EDC) was utilised in a chemical cross-linking experiment to assess whether a SPD-CD23 and LZ-CD23 was forming oligomers in solution. This method, described in Methods (2.5.5.1) has previously been used to show the stalk region of CD23 fragment forms trimers (Beavil *et al.*, 1995).

A western blot (reduced conditions) in Figure 4.11 shows the products of cross linking SPD-CD23 and LZ-CD23 with a series of EDC concentrations. The reduced monomeric SPD-CD23 species decreases on addition of EDC, and a major trimeric species becomes visible especially with 25 mM EDC. On a longer exposure, small amounts of other oligomers are seen. These are approximate to the molecular mass of a hexamer and nonamer, suggesting SPD-CD23 forms stable trimers.

The EDC crosslinking results of LZ-CD23 again show the reduction in monomeric species (37.5 kDa) and the appearance of a major band around 75 kDa, corresponding to a dimer. A small amount of trimeric LZ-CD23 (114 kDa) may be present, but could be

indistinguishable from a tetramer (150 kDa). At higher EDC concentrations LZ-CD23 was aggregating and did not enter the separating gel.

To confirm the presence of dimeric or trimeric LZ-CD23 species, di-fuoro di-nitrobenzene (DFDNB) was also used. This crosslinker also has a short 'spacer arm' of 0.3 nm and cross links primary amines ($R\text{-}NH_2$) i.e. lysine residues. DFDNB has been used to demonstrate the oligomeric species of other animal C-type lectins e.g. rat asialoglycoprotein receptor (Halberg *et al.,* 1997). A series of DFDNB concentration (0.1 mM, 1 mM and 10 mM) were used with 1 μg/ml LZ-CD23 in carbonate-bicarbonate buffer pH 10 for 2 hours at room temperature. Despite the smeared appearance of the resulting western blot, two major bands (at <75 kDa and ~105 kDa markers) replaced the monomeric species on addition of 1 mM DFDNB. These probably represent LZ-CD23 dimers and trimers. Again, excess crosslinker results in aggregation and consequently no detection of CD23 in the separating gel.

a) SPD-CD23 + EDC (mM)

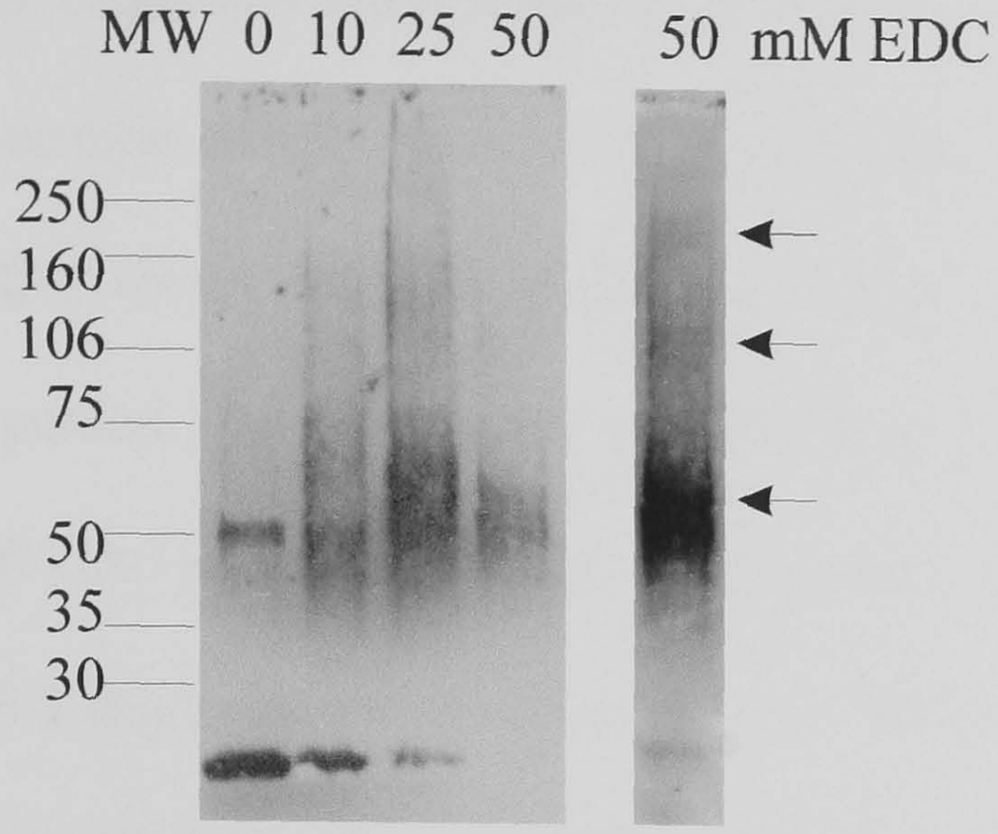

b) LZ-CD23 + EDC (mM)

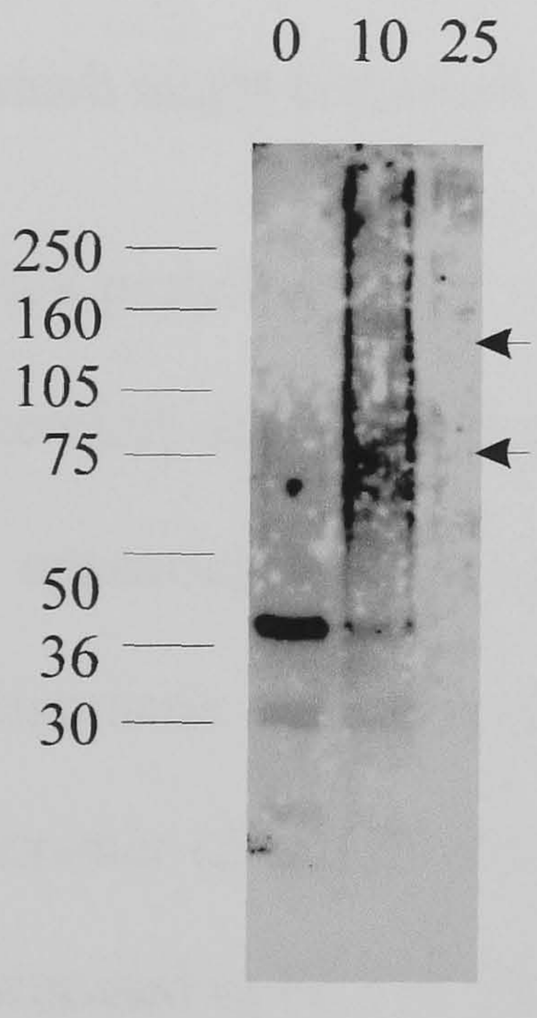

c) LZ-CD23 + DFDNB (M)

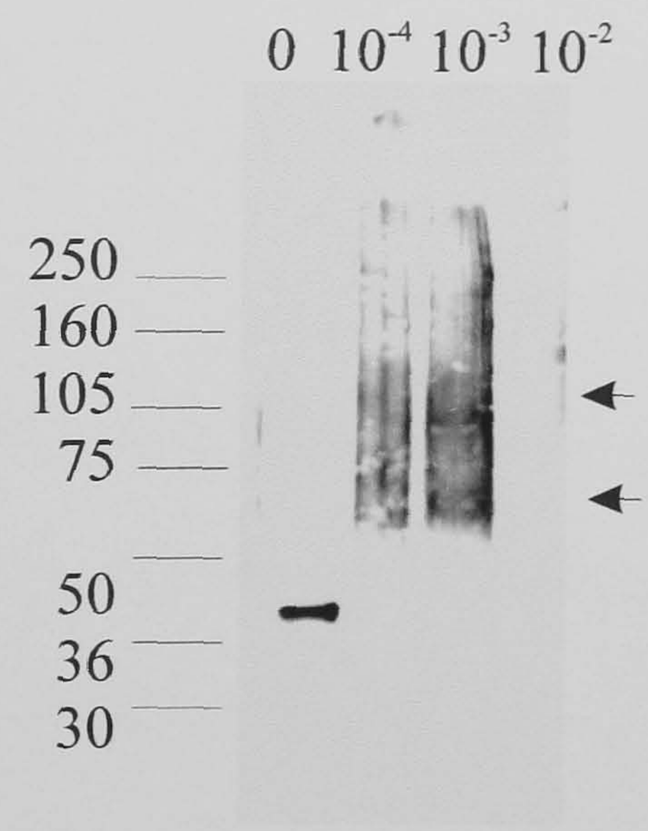

Figure 4.11: Chemical Cross-linking of CD23 Chimeras.

a) 1 μg/ml SPD-CD23 was cross-linked with a range of EDC concentration 10-100 mM in 25 mM acetate buffer pH 5.0 for 15 minutes. The reaction was stopped on addition of reducing SDS loading buffer. Western blot analysis using rb55 (polyclonal anti-CD23) showed the monomeric species decrease and the appearance of a major trimeric species (66 kDa) and possibly further trimeric multimers indicated by arrows. **b)** Using identical conditions LZ-CD23 was also shown to cross link with EDC. Approximate dimeric species (~75 kDa) and a small amount of trimer (~110 kDa) were forming. **c)** This observation was confirmed using DFDNB at 1 mM, pH 10, for 2 hours.

4.5.2 Analytical Gel Filtration HPLC

The oligomerisation state of a protein can be determined simply by measuring its molecular weight in solution. Analytical gel filtration was performed using a running buffer closer to physiological conditions than previously employed for purification. Superdex 200 can resolve proteins over a wide range of molecular weights (20 kDa – 500 kDa) and could identify larger oligomeric forms. Purified SPD-CD23 and LZ-CD23 (~0.3 mg/ml) were dialysed against HBS-Ca and 20 µl was loaded onto a calibrated Superdex 200 column at 0.75 ml/min.

The resulting profile (Figure 4.12) indicates that more than one species was being eluted from each purified protein. Two maxima were estimated to be 95 kDa and 37 kDa, which might corresponded to trimeric (66 kDa) and monomeric (22 kDa) SPD-CD23.

This protein did not behave like the standard proteins, eluting earlier than expected, therefore appearing larger. A non-globular shape due to the SPD stalk could account for it appearing larger. Another maxima approximately 6 times the observed monomeric oligomeric weight may have represented a small fraction of the sample was forming a hexamer (2 sets of trimers). The LZ-CD23 preparation appeared to be largely trimeric, estimated to be 134 kDa (actual trimer size is 113 kDa). Here too, the long stalk of the molecule would cause the LZ-CD23 to behave like a larger protein. The was also evidence of a range of lower molecular weight species in the LZ-CD23 preparation, but wasn't resolved to dimer or monomer positions.

a) SPD-CD23

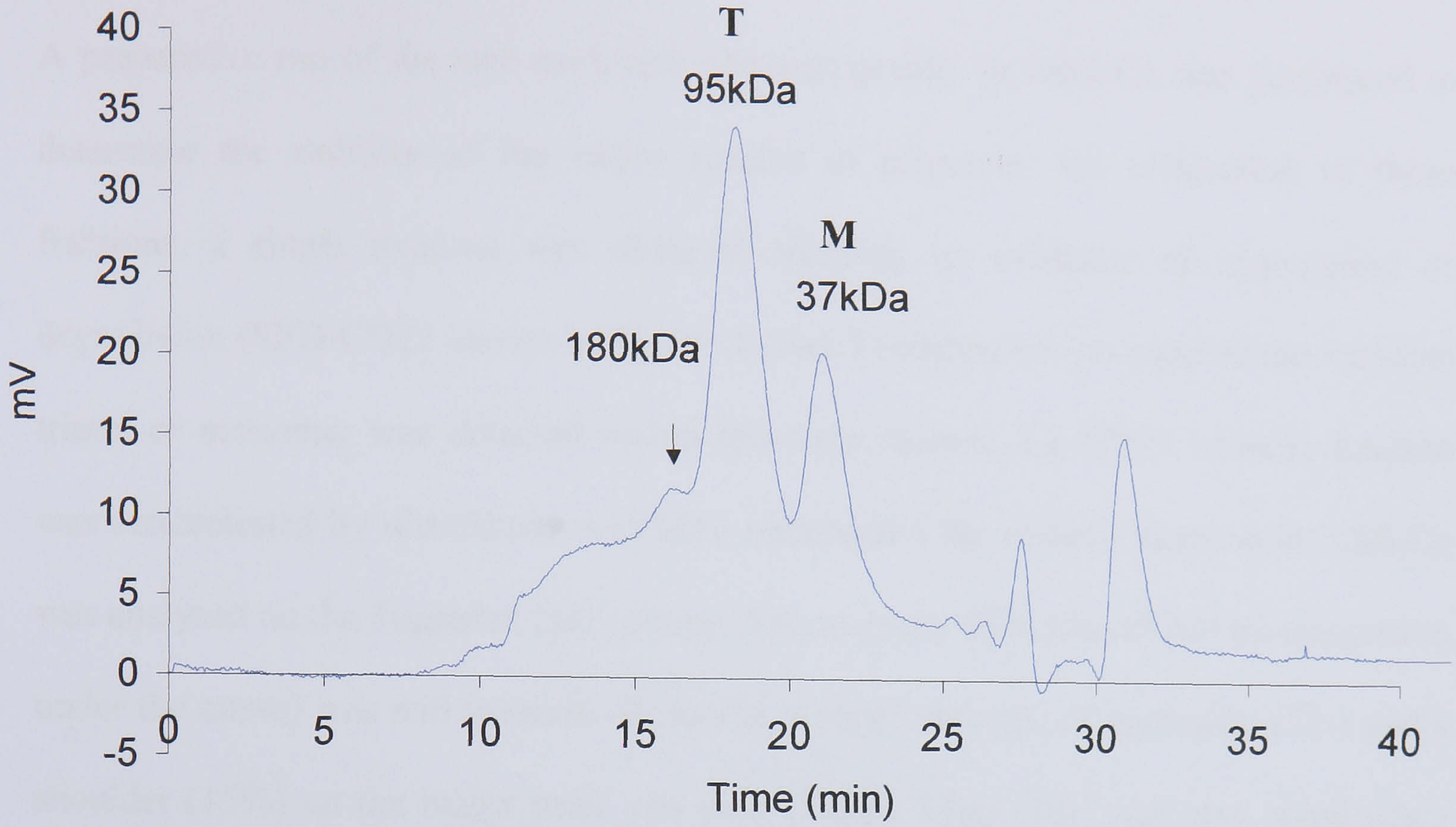

b) LZ-CD23

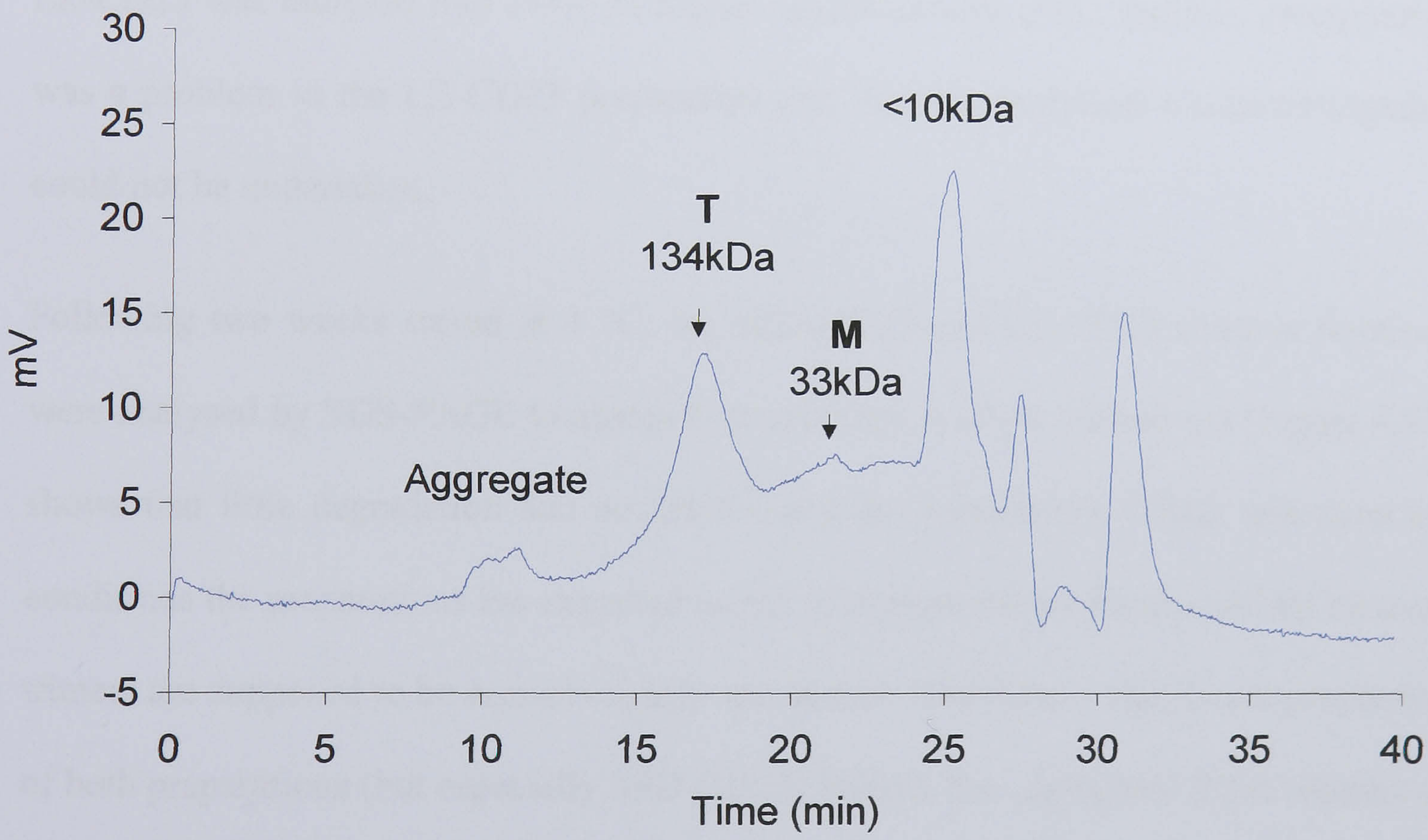

Figure 4.12: Analytical Size Exclusion Chromatography of Purified Chimeras

The fractions selected in the previous section were analysed on a Superdex 200 size exclusion column. Samples were dialysed into HBS-Ca which was also used as a running buffer at 0.75 ml/min. 20 µl of 0.4 mg/ml SPD-CD23 **(a)** and LZ-CD23 **(b)** were loaded. The column had previously been calibrated by protein molecular weight markers (also run in HBS-Ca). The extrapolated molecular weights corresponded only loosely to the predicted mass of the monomers (**M**) and trimers (**T**).

4.5.3 Stability of SPD-CD23 and LZ-CD23 Oligomers in Physiological Buffer

A preparative run of the size exclusion chromatography in HBS-Ca was performed to determine the stability of the major species of oligomer. On reinjection of these fractions, a single maxima was obtained showing no evidence of aggregation or degradation (SPD-CD23 shown in Figure 4.13a). Furthermore, no equilibrium between trimer or monomer was detected within this time (hours). LZ-CD23 trimeric fraction was concentrated by ultrafiltration (YM10 membrane) the trimeric fraction in HBS-Ca was analysed on the Superdex 200 column. The majority 80% (calculated by integration under the curve) was still trimeric. However, a small amount, of aggregate (5%) and a shoulder (15%) on the major peak was seen (Figure 13.a). This was also noted when LZ-CD23 was dialysed into PBS. At higher concentrations (>0.3 mg/ml), precipitation was a problem in the LZ-CD23 preparation and planned analytical ultracentrifugation could not be undertaken.

Following two weeks stored at 4 °C, the SPD-CD23 and LZ-CD23 trimeric fractions were analysed by SDS-PAGE to assess their stability. A silver stained gel (Figure 4.13) shows that little degradation had occurred (reducing conditions). Under non-reducing conditions the preparations are expected to run at monomeric molecular weight because trimers are supposed to be non-covalently associated. However, a significant proportion of both preparations (but especially SPD-CD23) behave like disulphide linked dimers or trimers.

In summary, this section shows LZ-CD23 is forming dimers or trimers and SPD-CD23 was mostly trimeric. However, in physiological buffer both chimeras have a propensity to aggregate and appear mis-folded. Using this method of refolding and purification, these recombinant proteins should be used immediately following buffer exchange.

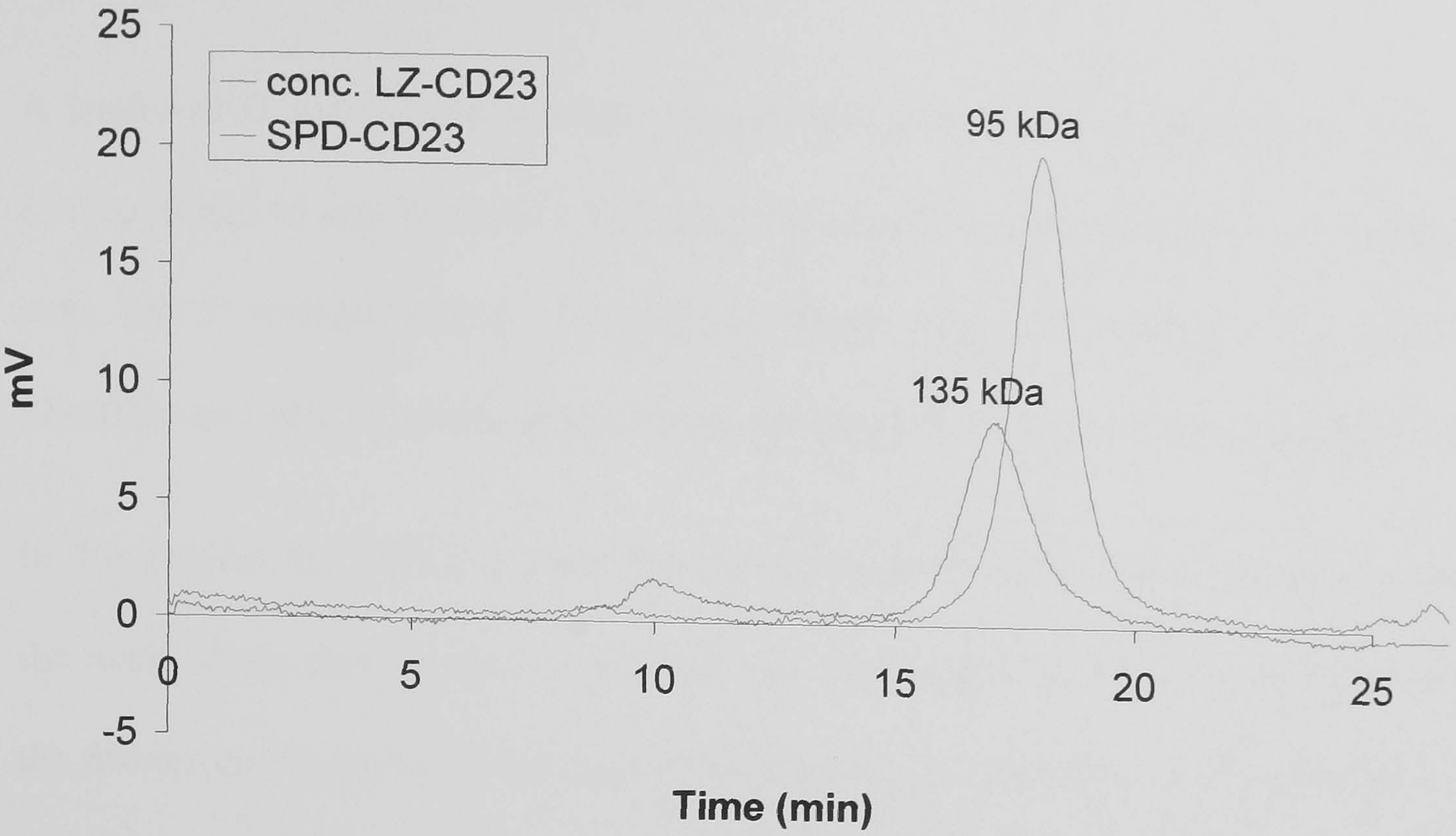

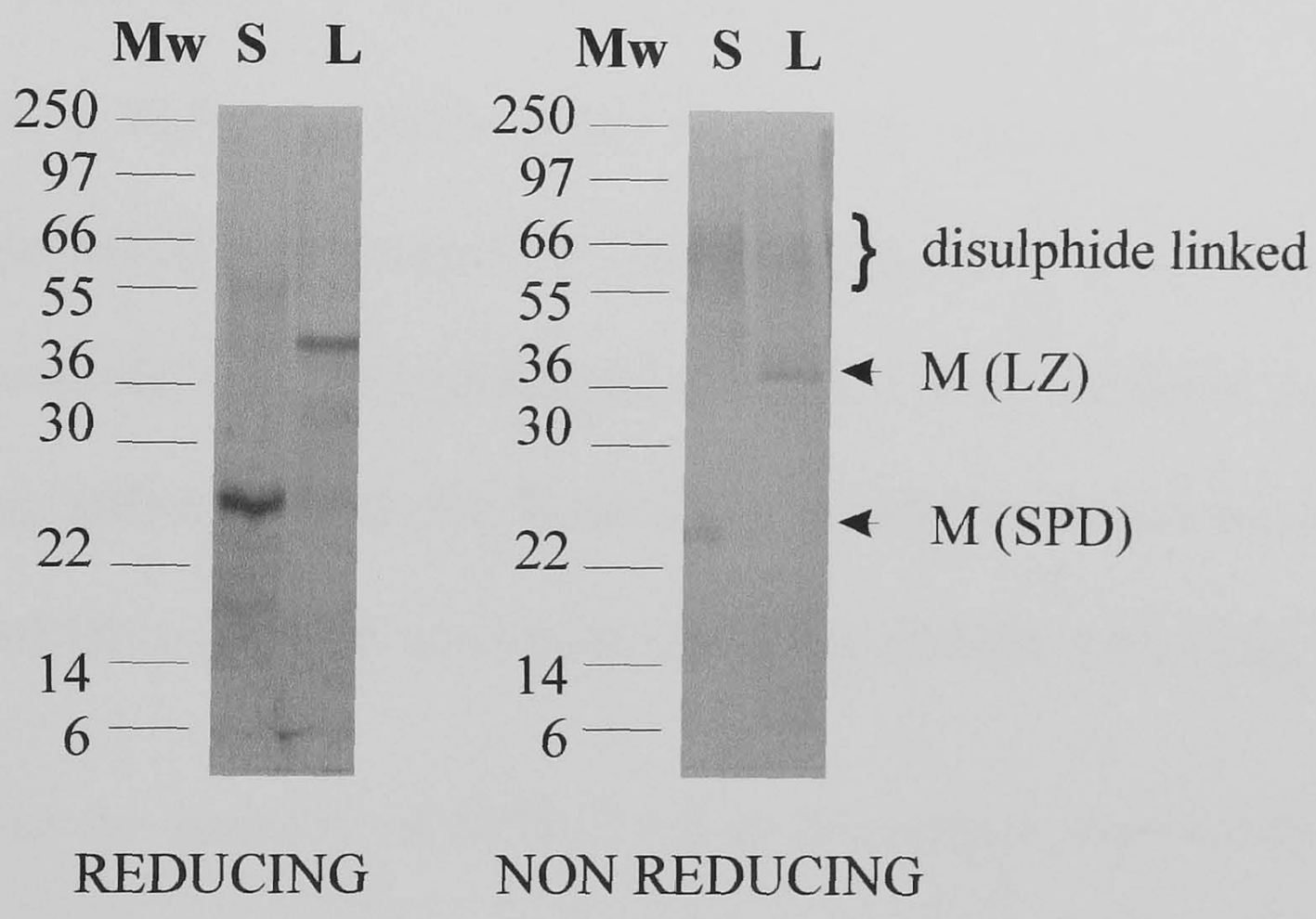

Figure 4.13: Analysis of Purified Trimeric Species.

a) The oligomeric species (SPD-CD23 and LZ-CD23) identified by analytical HPLC (Section 4.52, Figure 4.12) were re-injected onto Superdex 200 in HBS-Ca. No monomer/dimeric/trimer equilibrium was observed. **b)** Purified SPD-CD23 (S) LZ-CD23 (L) stored for 2 weeks was analysed by SDS-PAGE under reducing and non-reducing conditions to assess their stability. Little degradation was observed but the a proportion of the samples ran as intermolecularly bonded oligomers under non-reducing conditions. This suggests the samples are mis-folding with time.

4.6 Summary and Conclusions

A leader-SPD sequence was made from overlapping oligonucleotides by PCR, which can be joined to any point of CD23 (or other target protein) sequence in a single PCR step. The 5' restriction sites (BamHI and XmaI) allow the chimera to be inserted into pFastBac and pEE12 expression vectors and secreted by insect and mammalian cells.

In this project the SPD sequence was fused to the '25 kDa' CD23 fragment including the neck, lectin domain and C-terminal tail. This region of CD23 supposedly contains the minimum requirements of ligand binding and the omission of the principal sites of proteolysis. Expression in insect cells resulted in the secretion of SPD-CD23 into the culture supernatant (10 mg/l). Although enough material could be expressed by 5 l fermentation, purification by affinity chromatography using anti-CD23 antibodies led to the isolation of a high proportion of mis-folded and degraded products. Antibodies to the SPD region would be an attractive alternative especially if they recognise SPD as a coiled coil. However, no such monoclonal antibodies were available. For future chimera purification an affinity tag at the N-terminus would be advisable, for instance, the commonly used His tag which would not interfere with ligand binding.

Of concern was the inability of SPD-CD23 in the culture supernatant to bind an IgE coupled affinity column and its low affinity interaction with IgE-Fc in an ELISA. SPD-CD23 was transferred to a bacterial expression system to investigate this observation further. Large amounts were extracted (100 mg/l) to moderate purity and this was compared to another human chimera, LZ-CD23, also previously uncharacterised, but the human equivalent to a murine chimera which was demonstrated to inhibit high affinity receptor binding to IgE.

A sizeable proportion of the refolded SPD-CD23 and LZ-CD23 was aggregating and precipitating noticeably during concentration. Some effort could be made to reduce the intermolecular bonds forming during concentration by blocking free cysteines (with iodoacetate) or oxidising them (with copper phenanthroline). Initial attempts made little difference and complicated the further analysis (results not shown).

Gel filtration was successful in separating mis-folded aggregate from the remaining preparation. IgE binding assays confirmed that the highest activities were in the non-aggregated fractions. Nevertheless, SPD-CD23 still showed a low affinity to IgE-Fc similar to that of lectin domain alone. Conversely, LZ-CD23 interacted with IgE to an extent similar to recombinant extracellular CD23, as expected (Chapter 5). N-terminal sequencing and mass spectrometry of the selected fractions demonstrated that both SPD-CD23 and LZ-CD23 were intact and correctly processed.

The oligomerisation state was investigated by chemical crosslinking and analytical HPLC. Using EDC, cross-linked SPD-CD23 trimers were detected, and analytical HPLC confirmed the majority of purified SPD-CD23 was trimeric with evidence of multimers of trimers. On closer inspection the trimeric fraction had a tendency to form intermolecular disulphide bonds during concentration and dialysis into a lower ionic strength solution. Crosslinking LZ-CD23 with EDC and DFDNB resulted in dimers and trimers. The estimation of molecular mass of the oligomeric species by analytical HPLC was difficult due to the non-globular shape of the LZ-CD23 molecule which did not behave like the standard proteins of the calibration curve. With time, LZ-CD23 also formed intramolecularly bonded multimers (notably dimers), and tended to aggregate at high concentrations.

The refolding of the cysteine rich lectin domain was complicated by the trimeric association because this may have encouraged aberrant disulphide bonds forming

between domains. It is possible that the SPD motif forced the lectin domains into an orientation that brought cysteine residues on neighbouring domains closer together than the native arrangement. This is supported by crystallography evidence of trimeric SPD (Hakansson *et al.*, 1999). The SPD lectin domains are asymmetrically arranged because of the packing of a tyrosine side-chain in the coiled coil. Altered orientation or 'pitch' of the CD23 lectin domains may also account for the poor affinity of SPD-CD23 for IgE-Fc. Although the SPD motif was effective at forming trimers, SPD-CD23 was unsuitable for use in the intended biological and biophysical studies because of its poor ligand binding ability.

Perhaps LZ-CD23 benefited from having the CD23 stalk region to orient and stabilise the lectin domains. Dimer/trimer stability may have contributed to effective IgE binding of LZ-CD23 and possibly a reduction in proteolysis along the stalk. Enough of the final LZ-CD23 was prepared to quantify its affinity for IgE and investigate its effect in a biological assays (Chapter 5).

CHAPTER 5: FUNCTIONAL CHARACTERISATION OF RECOMBINANT 16 kDa AND OLIGOMERIC CD23

5.1 Introduction

Soluble CD23 was identified as the IgE binding factor from B-cell cultures responsible for the enhancement of IgE production (Sarfati and Delespesse, 1988). Since then, CD21 was discovered as the counter structure for sCD23 which is postulated to up-regulate IgE synthesis (Aubry *et al.,* 1992). There are several possibilities to explain how sCD23 fragments >25 kDa mediate up-regulation of IgE. In addition to a stimulatory signal upon ligation of CD21, the production of sCD23 causes a loss in cell surface CD23, thereby diminishing negative signals mediated by membrane CD23-IgE complexes (Sherr *et al.,* 1989). Also, negative feedback may be abrogated by competition between sCD23 and membrane CD23 for binding soluble IgE. It is still unclear whether up regulation of IgE synthesis by CD23 is a result of B-cell proliferation, a directed switching event or B-cell differentiation to plasma cells.

To investigate these possibilities, an *in vitro* system using stable CD23 was developed. LZ-CD23 produced in Chapter 4 was intended for this purpose. Less is known about the mechanism of IgE suppression mediated by smaller CD23 fragments, i.e. 16 kDa (Sarfati *et al.,* 1992). Der-CD23 characterised in Chapter 1 should be a useful molecular tool to study IgE suppression *in vitro*.

This Chapter compares the ligand binding properties and kinetic binding data of oligomeric sCD23 (LZ-CD23) and CD23 lectin domain (Der-CD23) with IgE Fc in an attempt to rationalise the opposing regulatory properties of native 29-37 kDa and 16 kDa sCD23. ELISA and surface plasmon resonance (SPR) studies were carried out using the recombinant components listed in Table 5.1 and shown in Figure 5.1.

Table 5.1: List of Recombinant Proteins Included in Functional Assays.

Recombinant Protein	Structure	Expression System	MW
Anti-NIP IgE	Soluble IgE	NS0	185 kDa
Der-CD23	Lectin domain	*E.coli*	16 kDa
IgE-Fc (bIIgII)	IgE Fc double glycosylation mutant	NS0	42 kDa (dimer = 84 kDa)
LZ-CD23	Extracellular chimeric trimer	*E.coli*	37.5 kDa (trimer = 113 kDa)
rCD23	Extracellular	*E.coli*	31 kDa (trimer = 93 kDa)
sCD21	Extracellular CD21	Baculovirus	120 kDa

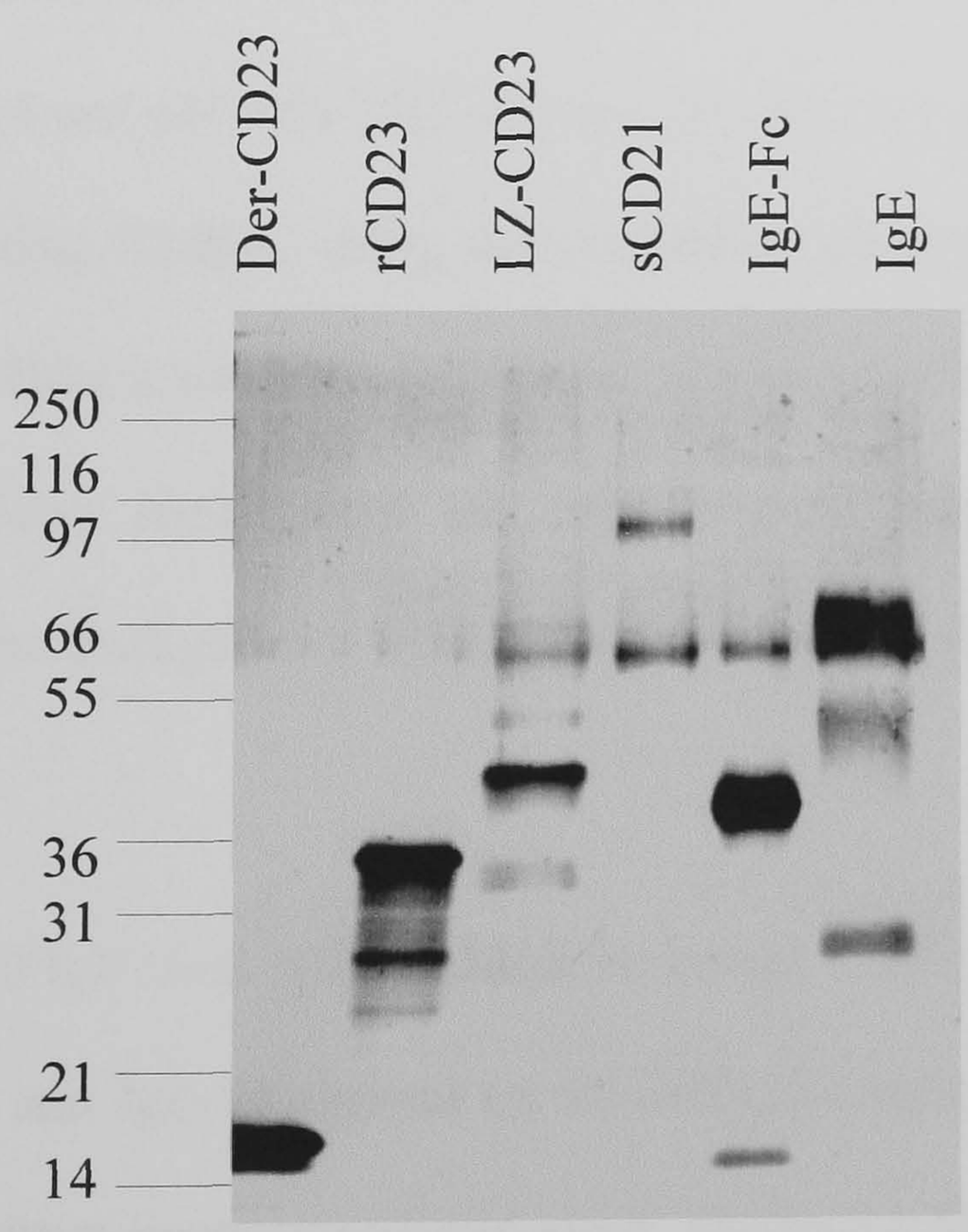

Figure 5.1: Silver Stained SDS-PAGE of Recombinant Proteins.

250 ng of each recombinant protein was analysed by SDS-PAGE under reducing conditions. A small proportion of degradation product was observed in rCD23 and LZ-CD23 samples. BSA and baculovirus gp64 are the likely contaminant in IgE-Fc and sCD21, respectively.

5.2 CD23-Ligand Binding by Enzyme-Linked Immunosorbent Assay.

5.2.1 CD23-IgE Interaction

A rapid and reproducible ELISA was required for simple assessment of CD23 activity. An assay using recombinant extracellular CD23 coated on a microtitre plate followed by the addition of anti-NIP-IgE and anti IgE-HRP conjugate had previously been described by J. Shi (1997). Variations of this assay were investigated using biotinylated IgE fragments in order to improve sensitivity. Optimisation of the steps were also carried out.

From a screen of five buffers (50 mM glycine, 50 mM glycinate, pH 6.0; PBS pH 7.2; TBS, 2 mM $CaCl_2$, pH 7.5; 100 mM sodium carbonate, 100 mM sodium hydrogen carbonate, pH 8.4 and pH 9.0) TBS-Ca was selected as the most efficient coating buffer for the IgE binding ELISA, using the conditions described in section 2.5.8.4 (Figure 5.2a). BSA in TBS-Ca was selected for the blocking buffer and assay buffer because it produced a greater signal than the milk protein mixture (Figure 5.2b) and still maintained a low background signal. Chicken egg Ovalbumin (46 kDa) was also an improvement.

Both biotinylated IgE (anti-NIP) and IgE Fc bound CD23 in the functional assay. Figure 5.2c shows IgE and IgE-Fc titrated on 80 nM (250 ng/ml) rCD23. IgE-Fc produced a greater signal, either because reduced steric hindrance allows more IgE-Fc to bind, or perhaps, because IgE-Fc was more efficiently labelled with biotin. This IgE concentration range was used to compare the relative binding abilities of the soluble CD23 fragments: LZ-CD23 and Der-CD23 (section 5.2.3).

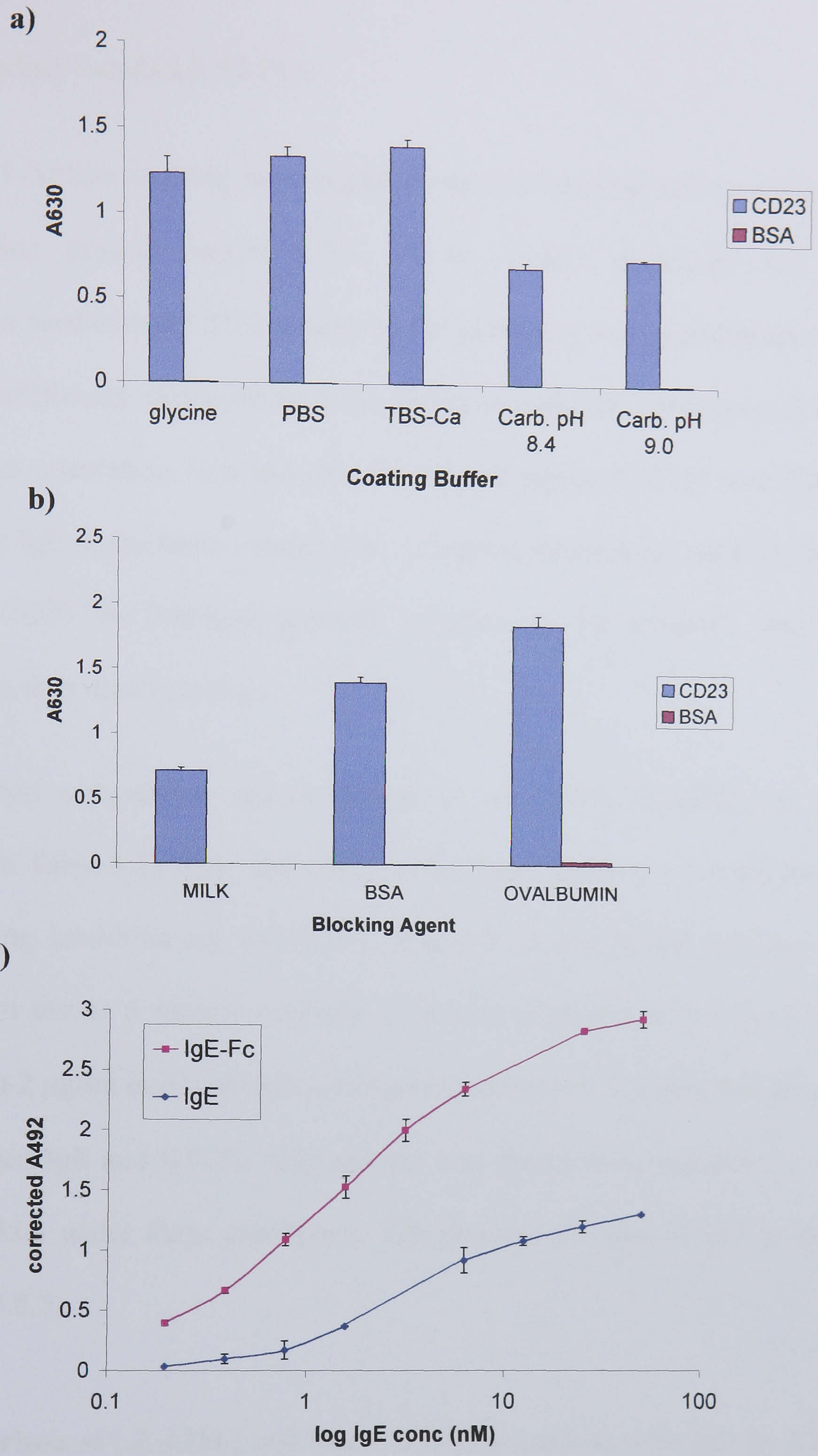

Figure 5.2: Optimisation of an IgE Binding Assay by ELISA (CD23 coated directly onto plate).

a) rCD23 was coated directly onto a microtitre plate using buffers of varying ionic strength and pH. TBS-Ca (pH 7.5, 125 mM NaCl) was selected. **b)** Different blocking agents were tested in the assay. BSA and chicken egg ovalbumin were preferable to the milk protein mixture. **c)** Biotinylated IgE and IgE-Fc were serially diluted to select a concentration range to test relative binding abilities of CD23 in future assays.

5.2.2 IgE binding Sandwich ELISA

An anti-CD23 capture antibody was sought to improve the presentation of CD23 to IgE. The adsorption process causes CD23 to be largely denatured and the high concentrations used to coat CD23 directly to the plate may mimic multimeric molecules and result in artificially strong interactions. Using an anti-CD23 monoclonal antibody it was hoped that orientation, fold and concentration of captured CD23 would be constant and hence the IgE interactions comparable. A capture monoclonal antibody also allows activity of CD23 in non-homogeneous samples to be assessed and at lower concentrations than direct coating.

From published competition assays (Wakai *et al.,* 1995; Bonnefoy *et al.,* 1997; summarised in Table 5.2) some anti-CD23 monoclonal antibodies have a low capacity for IgE binding inhibition e.g. EBVCS-1, 2 and 5. It was hoped that one would be appropriate for use as a capture antibody. A screen of several antibodies (Figure 5.3) were coated at 2 μg/ml in Bicarbonate-carbonate buffer pH 9.8. Using full length rCD23 and biotinylated IgE and IgE-Fc, only mAb25 was found to be suitable for use in the sandwich ELISA under these conditions. The protocol for this ELISA is outlined in Chapter 2 (2.5.8.5).

5.2.3 Comparison of LZ-CD23 and Der-CD23 Interactions with IgE by ELISA

Recombinant CD23 constructs (listed in Table 5.1) were included in both optimised ELISAs added to the wells in equal molar quantities. Serially diluted biotinylated IgE and streptavidin-HRP was added as before. The resulting curves in Figure 5.4 show that biotinylated IgE bound LZ-CD23 and rCD23 but was unable to interact with Der-CD23 significantly above the negative control (BSA). The inability to detect Der-CD23-IgE

Table 5.2: Inhibition of IgE binding By Anti-CD23 Monoclonal Antibodies

Monoclonal Antibody	Inhibition of IgE binding	% Inhibition	Isotype	Reference
B6	Partial	n/d	IgG2b	Bonnefoy *et al.*, 1987
BU38	Yes	n/d	IgG1	Bonnefoy *et al.*, 1987
EBV-CS1	No	0	IgG1	Wakai *et al.*, 1993
EBV-CS2	Partial	16	IgG1	Wakai *et al.*, 1993
EBV-CS4	n/d	n/d	IgM	
EBV-CS5	Partial	17	IgG1	Wakai *et al.*, 1993
IOB8	n/d	n/d	IgG1	
mAb 25	Partial	20-50	IgG1	Wakai *et al.*, 1993
MHM6	Yes	90	IgG1	Wakai *et al.*, 1993

Where n/d = not determined,

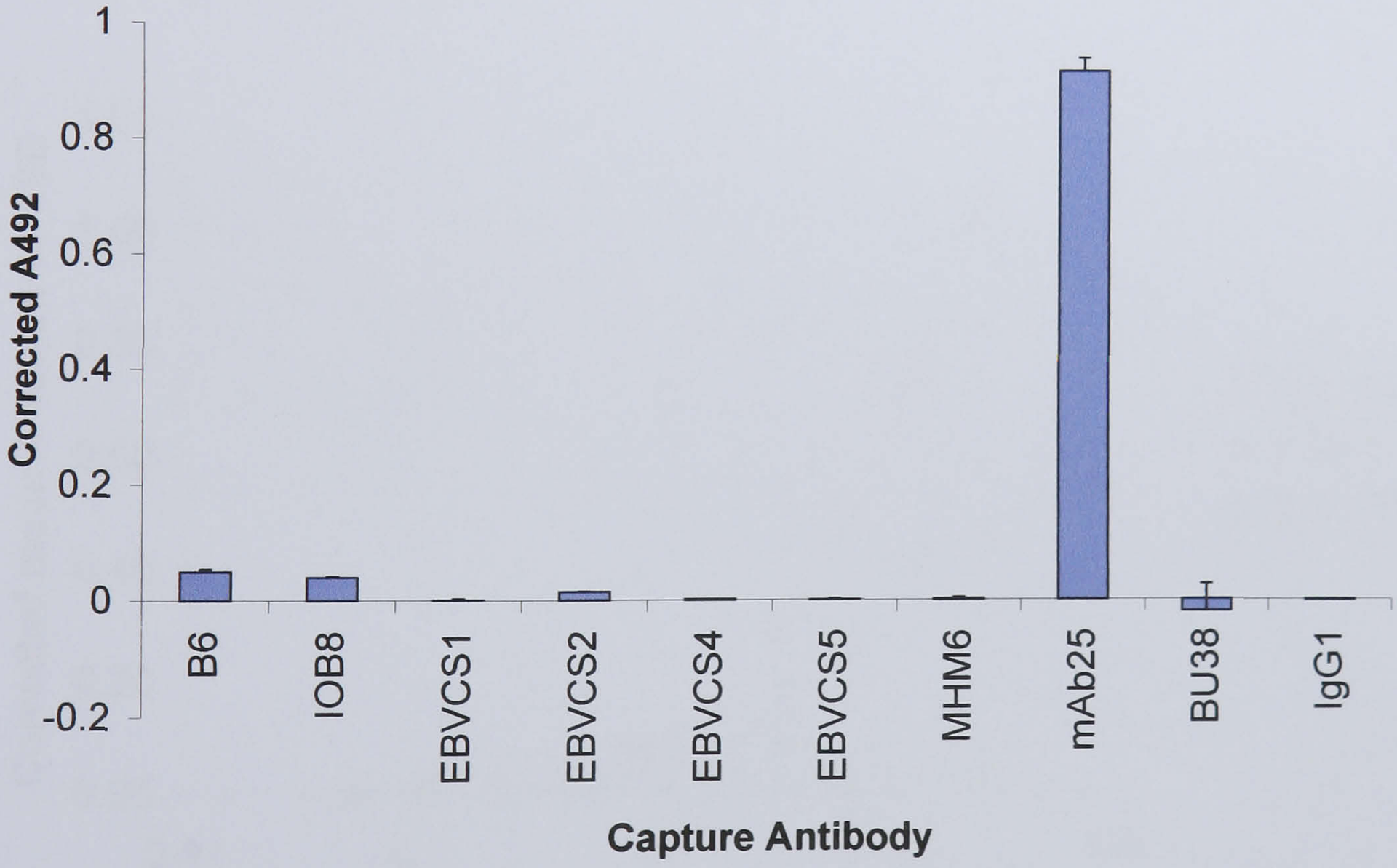

Figure 5.3: Selection of a Capture Antibody for IgE binding Assay

2 μg/ml of each anti-CD23 monoclonal antibody was coated onto a microtitre plate (incubated overnight at 4 ˚C). After standard blocking and wash procedures (Materials and Methods 2.5.8.5) 1 μg/ml rCD23 (positive control protein) and blank samples (no CD23) were incubated at room temperature for 2 hours. 1 μg/ml biotinylated IgE was added and the assay continued as normal. Results are blank subtracted averages of the triplicate samples (+ 1 standard deviation error bar).

a) CD23 Coated Microtitre Plate

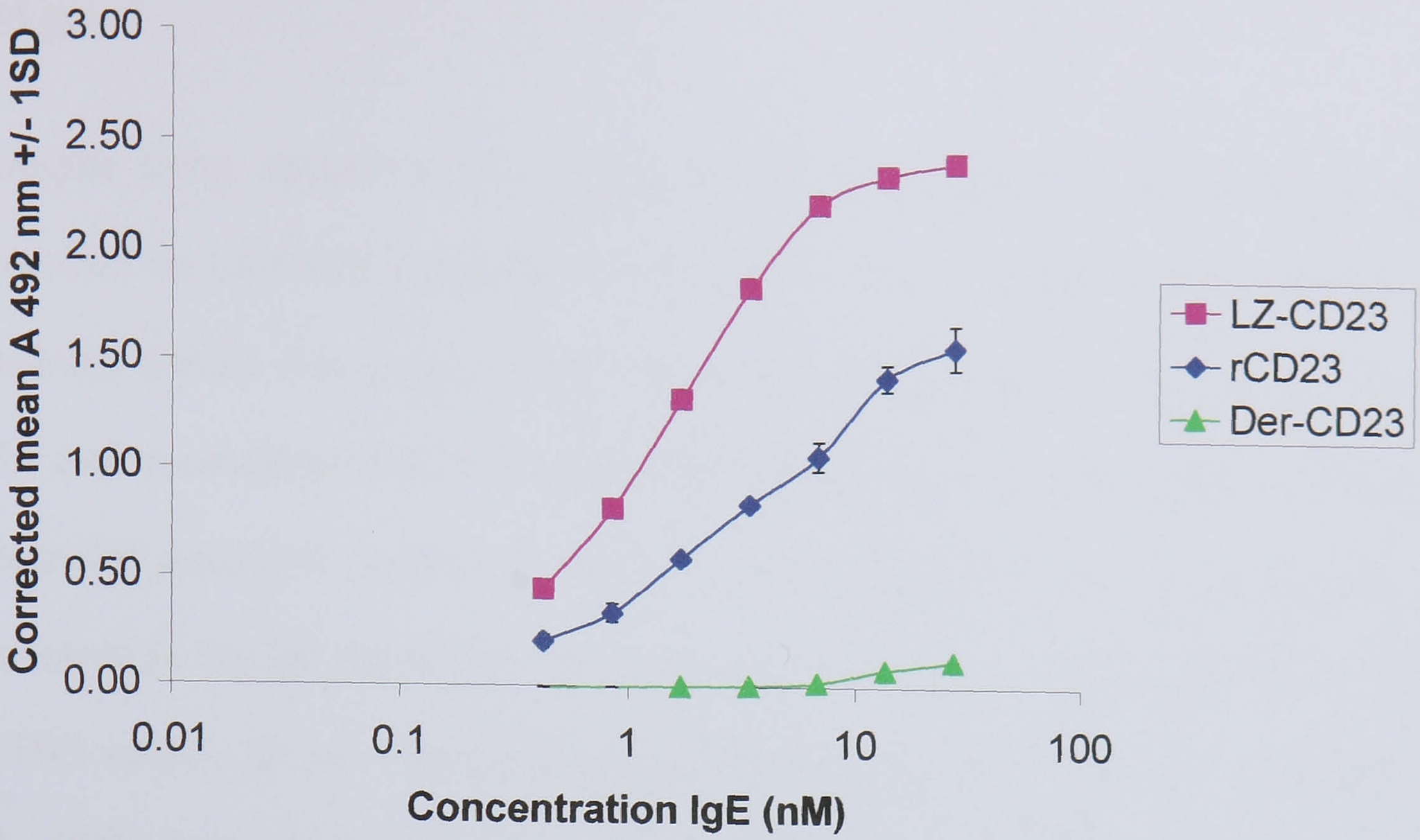

b) anti-CD23 Captured CD23

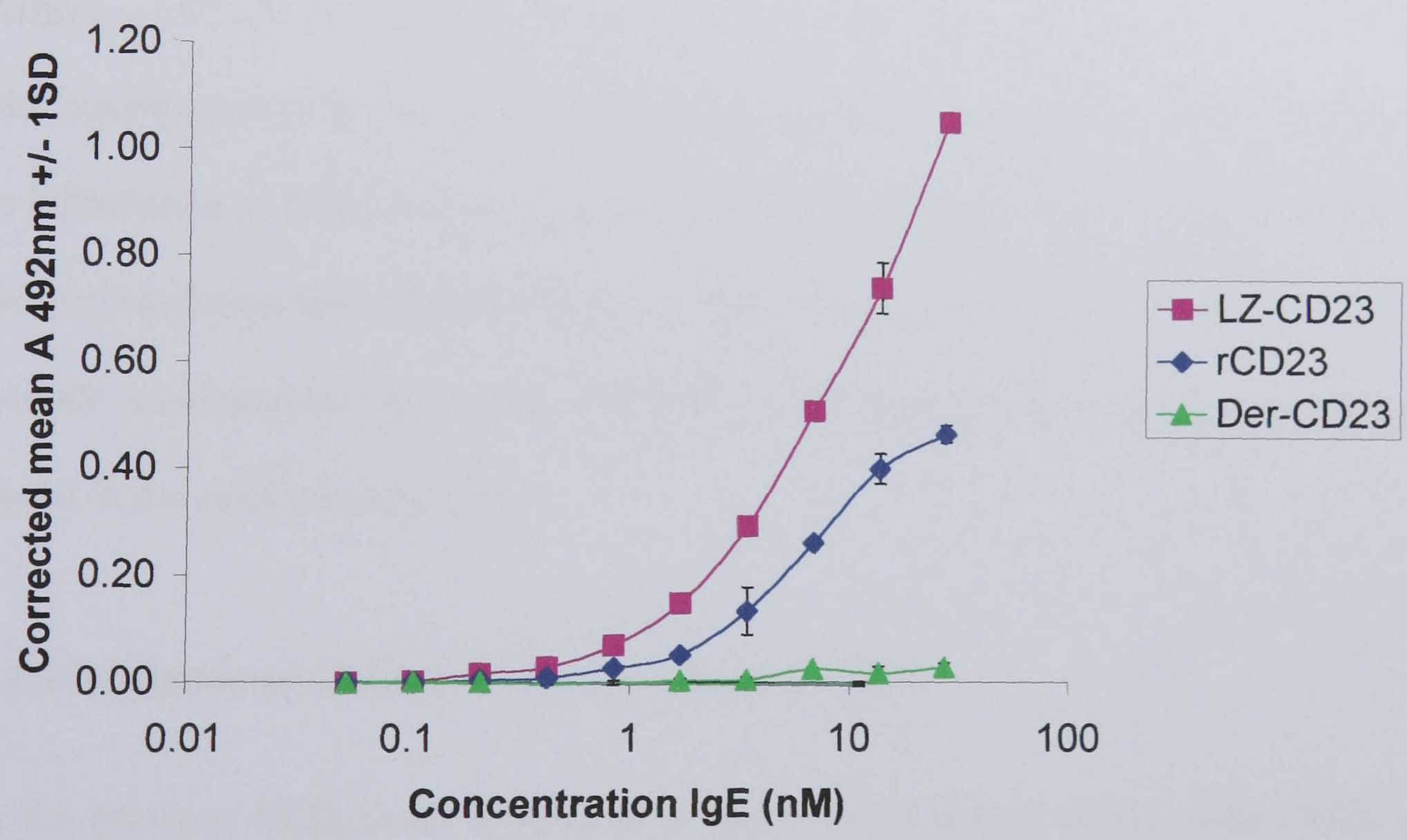

Figure 5.4: Comparison IgE binding to Recombinant CD23 fragments.

Biotinylated IgE was titrated over 80 nM of CD23 fragments **a)** directly coated in TBS-Ca or **b)** captured by 2 μg/ml mAb25. IgE-CD23 interaction was revealed by streptavidin–HRP and the enzyme reaction developed with OPD. Der-CD23 did not bind significantly above background levels (negative control, BSA) whereas the trimeric LZ-CD23 appeared to have a greater binding ability than the full length recombinant CD23.

binding may be due to the disruption of the weak interaction during washing steps of the ELISA.

Despite being applied to the wells in equal molar quantities, the maximum signal obtained for LZ-CD23 and rCD23 were different. This is not necessarily a reflection on affinity, instead, this suggests that the concentration of active molecules was different for each recombinant CD23. Possibly the rCD23 sample contains more mis-folded or degraded molecules (evident in Figure 5.1). Alternatively, as two lectin domains are involved in the IgE interaction, the greater the proportion of oligomeric species in the CD23 sample, the more IgE binding sites are available. Thus, the increased stability of the CD23 trimer by the LZ fusion could be responsible for the greater number of IgE binding sites.

Affinity constants can be derived from ELISA data, either directly through Scatchard plot construction (r/[L] *v*s. r) or by an indirect method (Friguet *et al.,* 1985), but are not as informative as SPR, which would also be able to determine the binding constants for the weaker interaction of Der-CD23 and IgE (section 5.3). However, the ELISAs can provide a comparison of binding ability of CD23 in fractions or batches, particularly useful in the purification of CD23.

5.2.4 Inhibition of CD23-IgE binding with Der-CD23

In the previous ELISAs no specific interaction was detected between Der-CD23 and biotinylated IgE. Der-CD23 will bind biotinylated IgE-Fc in an ELISA (as used in Figure 4.10). The interaction occurs when Der-CD23 is coated at high concentration (>1 μg/ml) which may mimic an oligomeric situation as the interaction can not be demonstrated when Der-CD23 is captured by mAb25. As an alternative, an indirect method for detecting Der-CD23 IgE interactions was tested.

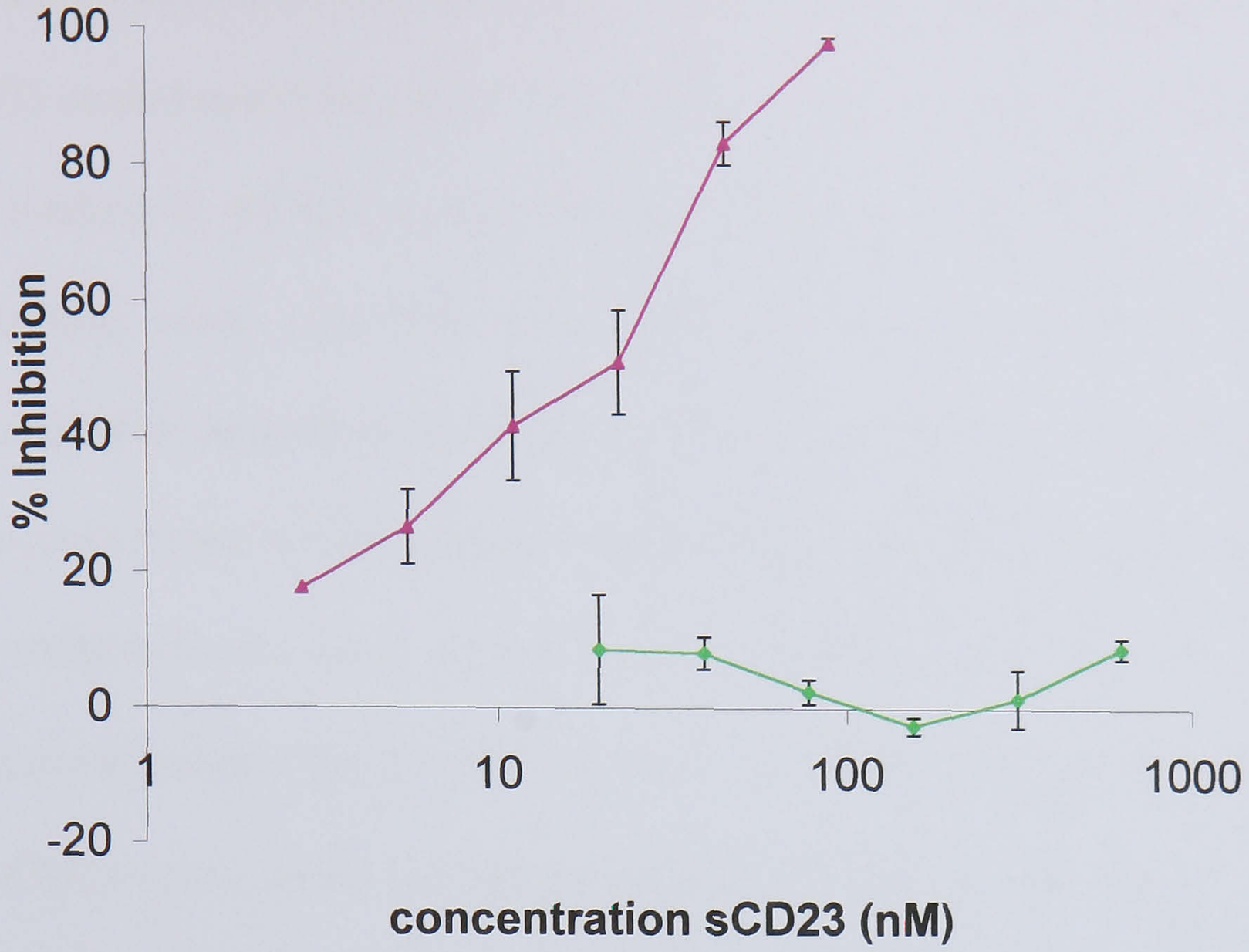

Figure 5.5: Competitive Inhibition of the CD23-IgE Interaction

Serial dilutions (starting from 10 μg/ml) of the CD23 and IgE constructs were made in assay buffer containing 2 μg/ml biotinylated IgE. These mixtures were added to 3 μg/ml rCD23 coated plates and assay completed as previously described. Absorbance values were corrected for IgE and CD23 blanks. Percentage inhibition was calculated from the % Inhibition = (Ao – Ai/)Ao x 100 where Ao is the absorbance at 492 nm with no inhibitor and Ai with inhibitor (averages of triplicate readings).

Der-CD23 at several concentrations was incubated with biotinylated IgE and added to rCD23 coated mitrotitre plates. Der-CD23 IgE interactions should reduce the amount of IgE binding to rCD23. Figure 5.5 shows the percentage inhibition of the rCD23-IgE interaction with LZ-CD23 and Der-CD23. As predicted, LZ-CD23 showed a concentration dependent inhibition maximal at ~250 nM. However, Der-CD23 even at high concentrations (600 nM) did not show any significant competition for IgE binding. The controls for the assay included an irrelevant IgG1 (negative control, no inhibition at all concentrations), IgE-Fc (90% at 10 μg/ml), EDTA (80% at 10 mM) and mAb25 (an anti-CD23 mAb) which partially inhibited IgE binding (60% at 10 μg/ml), confirming the observations from sandwich ELISA optimisation (Figure 5.3).

5.2.5 CD23-CD21 Interaction

A CD21 binding assay has been described by Fremeaux-Bacchi *et al.,* 1996. Their protocol was adapted for use with the recombinant proteins and monoclonal antibodies available in the laboratory. In the following experiment, sCD21, expressed by insect cells and purified by affinity chromatography (HB5 coupled Affi-prep 10) was added to CD23 coated plates. Anti-CD21 monoclonal antibody HB5 (also IF8 or BU32) could be used to reveal the interaction, followed by an anti-mouse Fc-HRP conjugate. Molar equivalents (300 nM) of rCD23, Der-CD23, BSA (negative control) and iC3b (positive control) were coated directly onto microtitre plates. sCD21 was titrated from 10 μg/ml to 0.125 μg/ml. Figure 5.6 shows that the full length extracellular CD23 was the most effective CD23 structure to bind sCD21, albeit much at less extent than iC3b. Binding of sCD21 to Der-CD23 was barely detected above the negative control.

These results may be a reflection of the oligomeric state of the recombinant CD23. Full length extracellular CD23 can form dimers and trimers (R. Reljic, 1996) and may have

an increased affinity due to multivalent interactions. Unfortunately, no LZ-CD23 was available at this time to support this observation. Experiments are ongoing in this laboratory to characterise the LZ-CD23/CD21 interaction. The lectin domain construct would have the molecular requirement to establish the protein-protein interaction between CD23 and the first SCR domain of CD21, but was probably too weak to detect.

The weak CD23-CD21 interaction detected in this assay may also be a result of non-physiological glycosylation of sCD21 by insect cells. Baculovirus expression systems synthesise proteins with N-linked carbohydrate rich in mannose and are unable to process proteins with complex carbohydrate containing sialic acid or galactose. Kijimoto-Ochiai and Uede (1995) demonstrated that CD23 acts as a galactose-binding lectin in the cell aggregation of EBV-transformed human B-cell lines. Mannose and other sugars not found on complex carbohydrate termini did not inhibit the CD21-CD23 interaction (Pochon *et al.,* 1992). It is probable that the baculovirus expressed sCD21 was insufficiently glycoslyated to demonstrate high affinity carbohydrate recognition by the CD23 lectin domain.

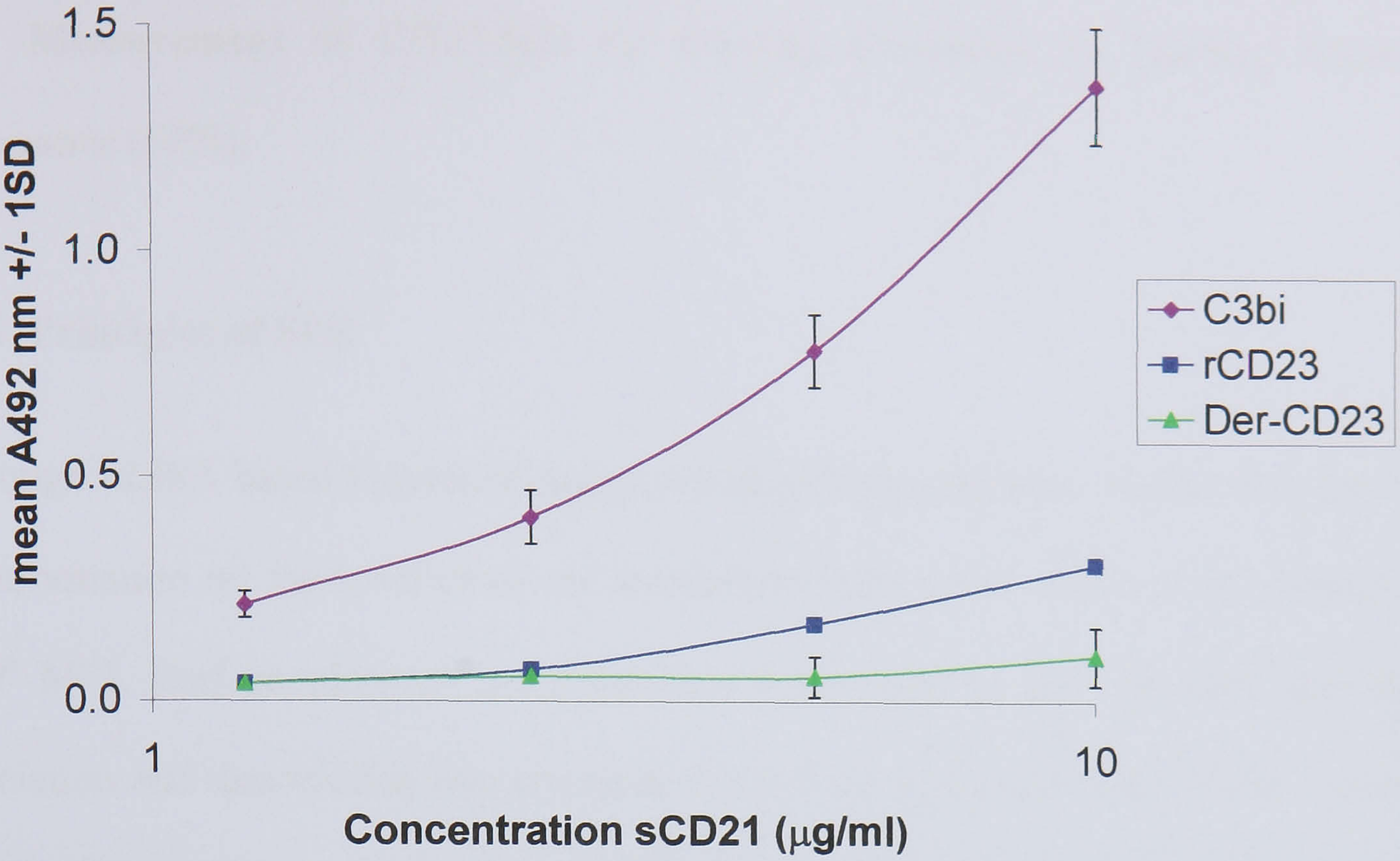

Figure 5.6: Demonstrating the CD23-CD21 Interaction by ELISA

100 nM rCD23 (~10 μg/ml), Der-CD23, C3bi and BSA were coated directly onto a microtitre plate in TBS-Ca. Dilutions of sCD21 were applied and interaction revealed by HB5 and an anti-mouse Fc-HRP conjugate. Triplicate reading were corrected for non-specific binding.

5.3 Measurement of CD23-IgE Fc Binding Constants by Surface Plasmon Resonance (SPR).

5.3.1 Principles of SPR

Although ELISA based functional assays are helpful in qualitative studies, they provide no information on the kinetics of the interaction and cannot detect weak interactions ($<10^6$ M^{-1}). Surface plasmon resonance has been used to provide additional data; association and dissociation rate constants (k_a and k_d) and hence, the affinity constant, K_A. In SPR kinetic experiments, ligands are permanently bound to dextran chains attached to the thin gold surface of up to four flowcells on a sensor chip, either through covalent EDC coupling or, as in this project, very high affinity streptavidin-biotin interactions ($K_A = 10^{-14}$ M^{-1}). Ligand-analyte interactions are detected by a change in refractive index (RI) at the sensor chip surface measured by an optical technique. The binding response is measured in response units (RU) and is particularly sensitive (100 RU is the equivalent of 100 pg mm^{-2}) therefore, little protein is consumed and weak interactions can be detected. Molecular interactions are followed in real time (10 measurements per second) thus, association and dissociation rates can be measured. Evaluation software can be used to fit models of kinetic parameters to the sensorgrams produced.

5.3.2 Flowcell Preparation and Regeneration

In contrast to ELISA, the IgE component (biotinylated IgE-Fc) was bound to the chip surface and soluble CD23 analyte was passed over. This gives a fairer comparison of affinities of the soluble recombinant CD23 fragments. Sparsely biotinylated IgE-Fc was used in preference to IgE because previous attempts at tethering IgE led to poor

responses on CD23 binding. The unusual bent shape of IgE may allow only a limited number of favourable orientations and coupling may be preferred on the convex side (also the Fc receptor binding site). A flowcell containing 447 RU and 900 RU of bound IgE Fc were prepared and a blank flowcell with unbound streptavidin was used as a negative control.

Due to the calcium dependent nature of the CD23-IgE interaction HBS containing 2 mM Ca^{2+} was used as the running buffer at 10 µl/min. The sensorgram in Figure 5.7 shows the binding response following injection of rCD23 and suggests that the bound ligand was not adversely altered by attachment to the chip surface. A series of three regeneration buffers were tested to optimise the removal of bound analyte (CD23) without damaging the ligand (IgE-Fc). Buffers of lowered pH and high salt concentration are often used to disrupt interactions, but 100 mM sodium acetate (pH 5) with and without 0.5 M NaCl, were ineffective for this system even after several injections (Figure 5.7). 10 mM EDTA in HBS was efficient at removing the majority of the remaining analyte. This is a very mild regeneration, able to remove CD23 by disrupting the calcium dependent binding site in the lectin domain. Further optimisation demonstrated 3 two minute injections of 25 mM EDTA were required and maintained identical responses to duplicate injections of CD23 (not shown).

5.3.3 Measurement of Binding Kinetics of Der-CD23 and LZ CD23

The affinity constant of the interaction of IgE-Fc with LZ-CD23 and Der-CD23 was obtained by SPR. Experiments were performed at a flow rate of 10 µl/min in HBS-Ca, collecting association and dissociation phase data for 6 minutes (at 10 Hz). Serial dilutions of analyte protein were injected over the IgE-Fc flowcells and the blank flowcell. Resulting CD23-IgE sensorgrams were corrected for non-specific binding by

Figure 5.7: Regeneration of the IgE-Fc Flowcell

Following a 1 minute injection of 440 nM rCD23, three regeneration buffers (RB1-3) were tested to select the mildest buffer that could remove CD23 bound to IgE Fc. RB1 (100 mM sodium acetate, pH 5) initially removed 22% but did not dislodge on repeat injections. RB2 (100 mM sodium acetate, pH 5, 0.5 M NaCl) was also ineffective (10%). RB3 (HBS, 10 mM EDTA) was the most efficient regeneration buffer able to displace 30% in a single injection.

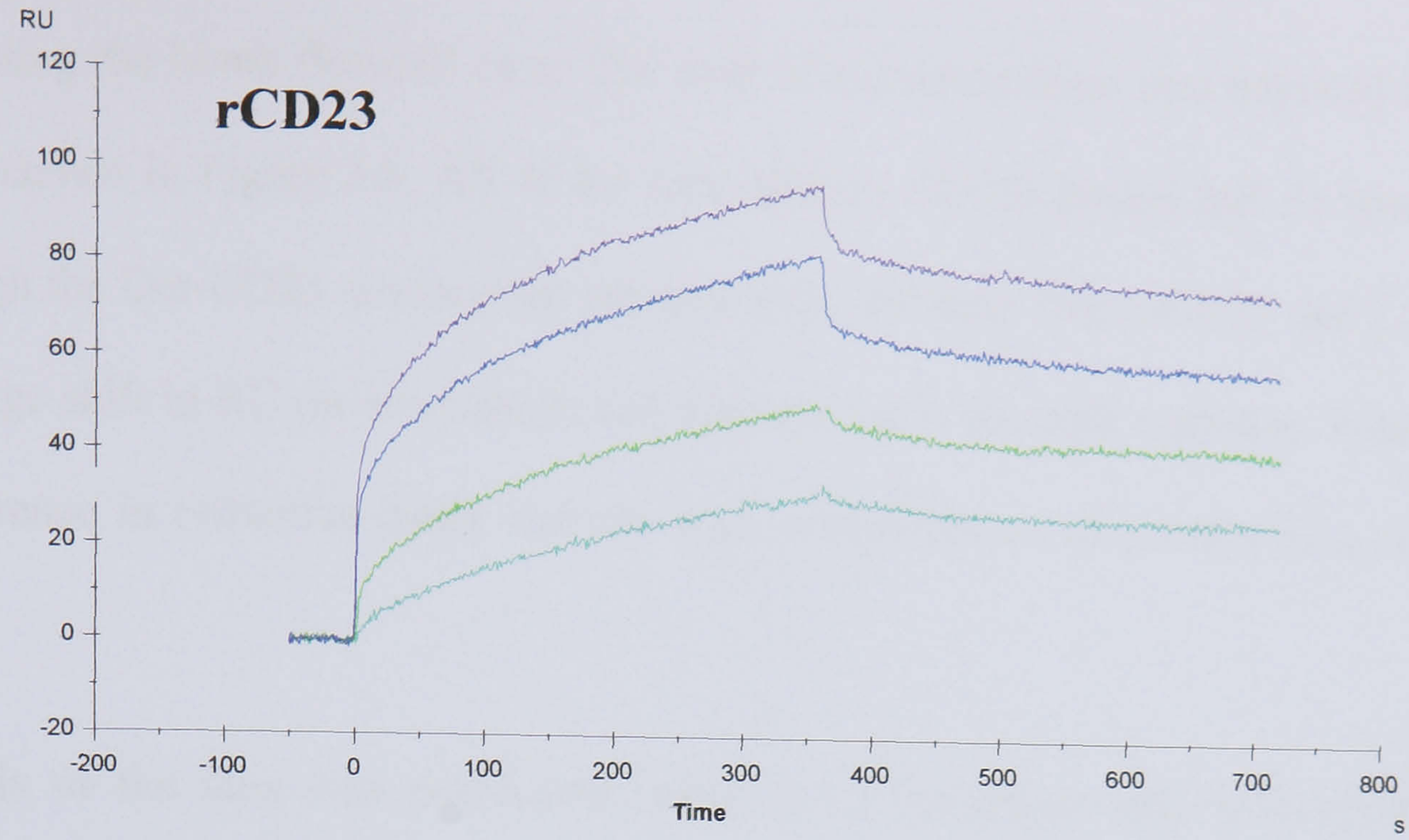

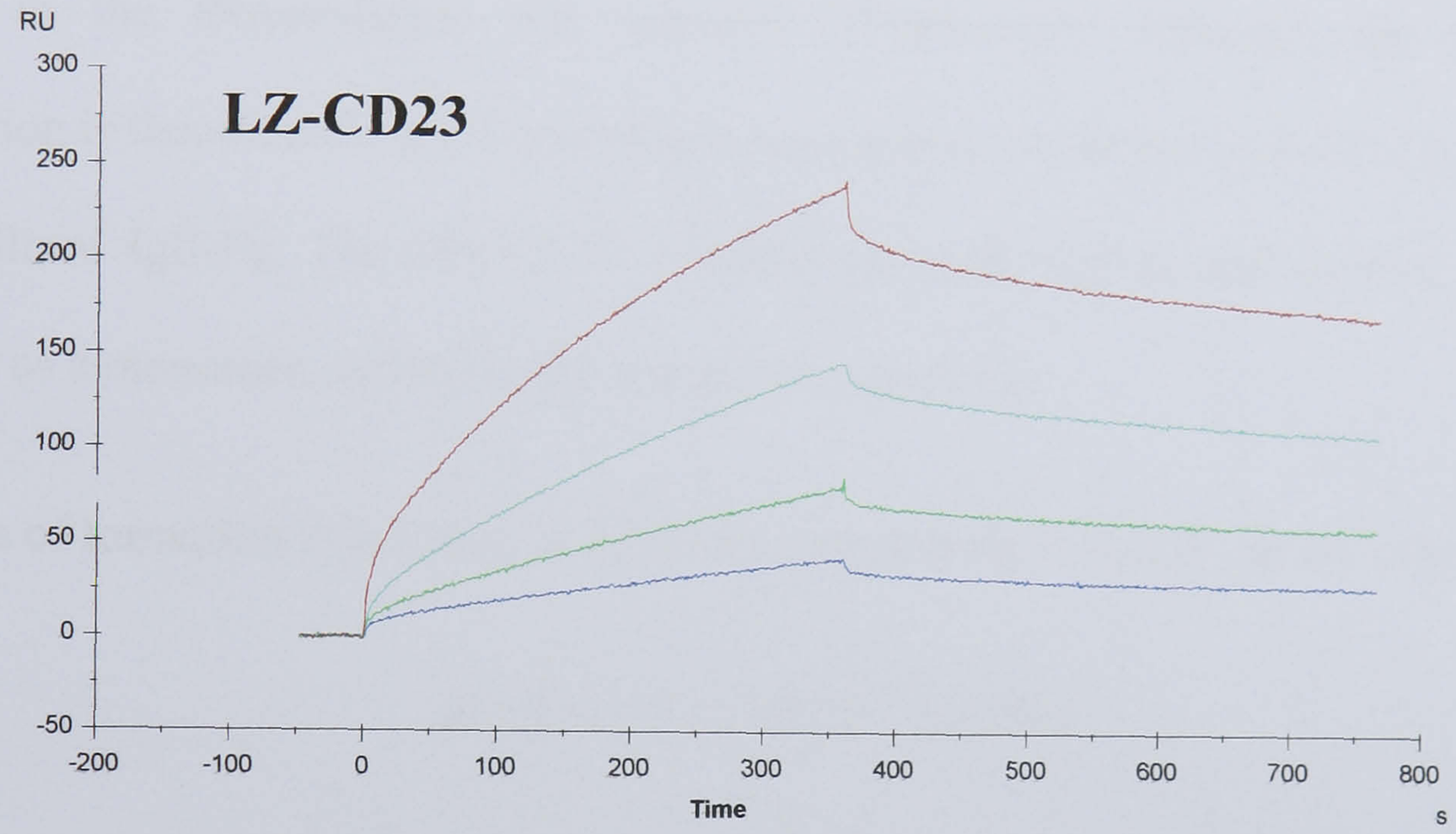

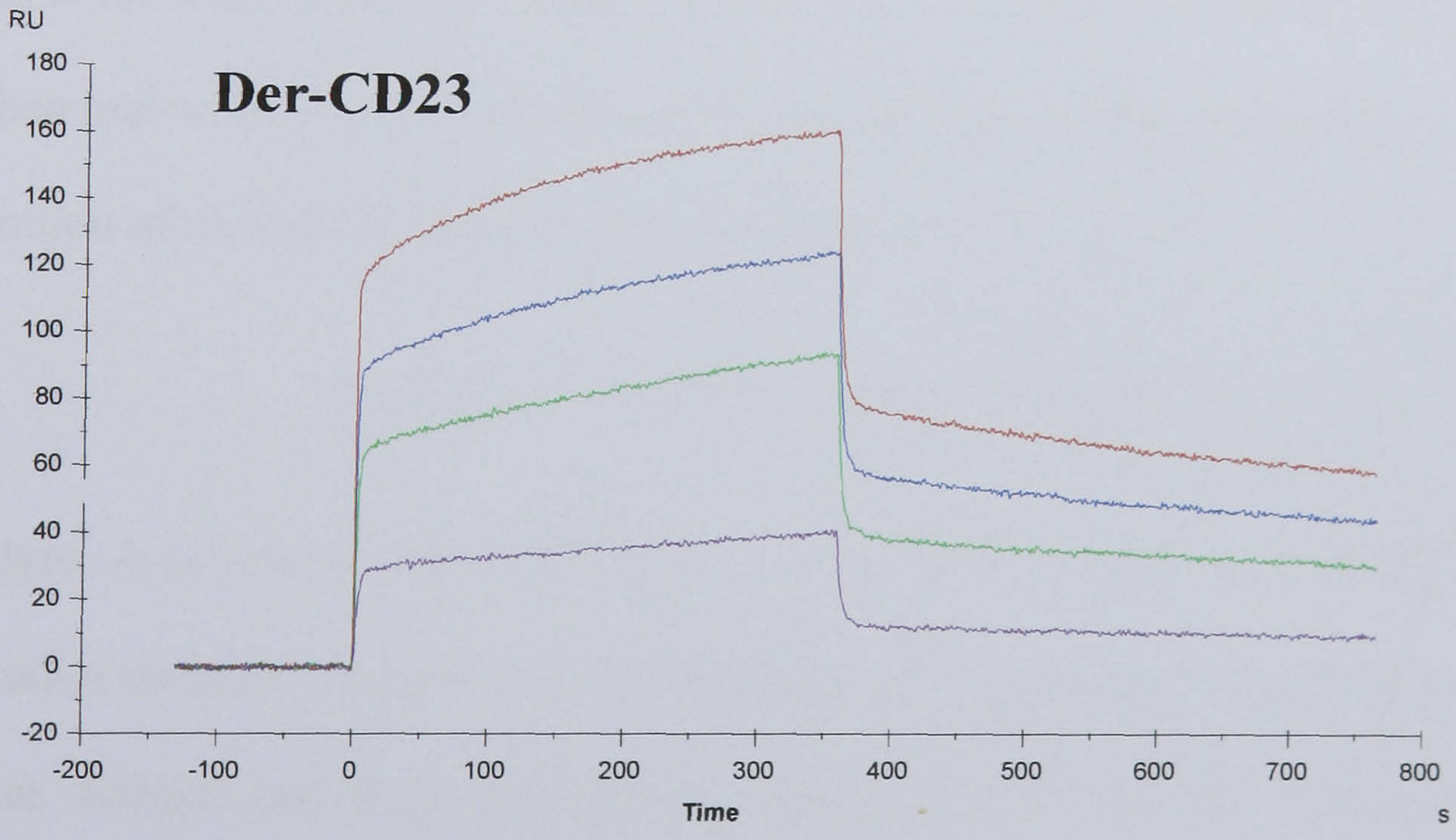

Figure 5.8: BIAcore Sensorgrams of Recombinant CD23 Binding to IgE-Fc

In a single experiment, serial dilutions of rCD23 (- 440, - 220, - 110, - 55 nM); LZ-CD23 (- 166, - 83, - 42, - 21, nM) and Der-CD23 (- 1000, - 500, - 250, - 63 nM) were injected through a flowcell containing 445 RU or 920 RU of bound IgE-Fc at 10 µl/min in HBS-Ca. Association and dissociation phases occurred for 6 minutes. The representative sensorgrams shown here are the result of subtracting the response from the blank flowcell negative control.

subtracting the blank flowcell data. The start of the association was adjusted to 0 RU, t=0 as shown in Figure 5.8. All of the recombinant CD23s bound IgE-Fc specifically, although the Der-CD23 sensorgram appears quite different from rCD23 and LZ-CD23. The large shift in RU on association and dissociation is the bulk response, indicative of a difference in refractive index due the high concentration of protein or a change in buffer.

Analysis of the data was performed using a 1:1 Langmuir association/dissociation model in the BIAevalution 3.0 software (Pharmacia). Although the CD23-IgE interaction is theoretically a 2:1 interaction, we assume one trimer (LZ-CD23) binds one immobilised IgE-Fc. The Der-CD23 contains no stalk region and should, therefore, interact as a monomer, satisfying the Langmuir equations.

The rate of formation of a complex AB from components A and B can be written as:

$$d[AB]/dt = k_a [A][B] - k_d [AB]$$

Where k_a is the association rate constant ($M^{-1}s^{-1}$) and k_d is the dissociation rate constant (s^{-1}). When one of the reactants [B] is substituted for $[B]_0 - [AB]$, where $[B]_0$ is the total concentration of reactant B, the equation is written as

$$d[AB]/dt = k_a [A]([B]_0 - [AB]) - k_d [AB]$$

The analyte, A is continuously replenished in the flowcell, therefore the free analyte concentration remains constant, C. The response, R, corresponds to the amount of AB complexes formed and R_{max} will be proportional to the surface concentration of immobilised ligand $[B]_0$. Therefore:

$$dR/dt = k_a C(R_{max} - R) - k_d R$$

Rearranging the rate equation:

$$dR/dt = k_a\,CRmax - (k_aC + k_d)\,R$$

Plots of dR/dt v R for a range of concentrations of free analyte will have a gradients of $-(k_aC+k_d)$. When these values are plotted versus concentration a line is obtained whose slope is equal to k_a and y intercept corresponding to $-k_d$.

After the association phase the concentration of free analyte drops to zero therefore:

$$dR/dt = -k_dR$$

or

$$\ln(R_0/R_n) = k_d(t_n - t_0)$$

where R_n is the response at time t_n. The dissociation rate is calculated from the slope of the plot $\ln(R_0/R_n)$ versus $(t_n - t_0)$.

In these analyses the dissociation constants were derived from the data first using at least 200 s of the 360 s dissociation time, then these values were used to derive the k_a constant for each concentration.. The software calculates, or fits, the k_a and R_{max} locally (i.e. for each concentration) for at least 200 s of the association phase (selected manually). This calculation is fitted to the observed response curves, whose accuracy is assessed by a residual plot (Appendix IV). Values were accepted whose residuals (deviation of experimental data from the proposed curve) were less than 2.5 and distributed evenly. The results are displayed in Table 5.3, the Chi^2 values give a statistical indication of closeness of fit, values below 2 are considered acceptable.

$$Chi^2 = \Sigma(r_f-r_x)^2/n$$

Where r_f is the fitted value, r_x is experimental value and n is the number of data points.

Table 5.3: Summary of CD23 – IgE Fc Kinetic Data from SPR

CD23 construct	k_d ($x\ 10^{-4}\ s^{-1}$)	k_a ($x\ 10^{3}\ M^{-1}s^{-1}$)	K_A ($x\ 10^{6}\ M^{-1}$)	Chi^2	Number of experiments
Trimeric LZ-CD23	4.3 ± 0.8*	23.2 ± 11.3*	52.8 ± 19.9*	0.317	3
Trimeric rCD23	2.6 ± 0.6‡	14.1 ± 4.2‡	57.0 ± 18.9‡	0.315	1
Monomeric Der-CD23	10.1 ± 3.0*	9.1 ± 4.4*	9.0 ± 2.6*	0.333	3

* The mean of the kinetic constants derived from 10 concentrations ± 1 standard deviation. ‡ The mean of the kinetic constants derived from 4 concentrations ± 1 standard deviation.

The 1:1 Langmuir model fitted well to each recombinant CD23 data, shown by small, well distributed residuals (Appendix IV) and low Chi^2 values (< 0.4). The association constants rates of trimeric CD23 ($k_a = 1.4 – 2.3 \times 10^4\ M^{-1}s^{-1}$) appeared to be higher than the monomeric CD23 ($k_a = 9.1 \times 10^3\ M^{-1}s^{-1}$) however, the standard deviations were large. The dissociation rate, of Der-CD23 ($k_d \sim 10^{-3}\ s^{-1}$) was more than double that of rCD23 and LZ-CD23 (2.6 and $4.0 \times 10^{-4}\ s^{-1}$, respectively). These k_a and k_d differences were reflected in the affinity constant K_A,

$$K_A = k_a/k_d$$

which would suggest that the affinity of rCD23 and LZ-CD23 (5.7 and $5.3 \times 10^7\ M^{-1}$, respectively) approximately six times greater than Der-CD23 ($K_A = 9.0 \times 10^6\ M^{-1}$). When taking into account the deviations for the affinity constants (K_A) the affinities of

monomeric and trimeric CD23 remain distinct (0.7 - 1.2 M^{-1} and 3.3 – 7.6 x 10^7 M^{-1}, respectively). These experiments also show that LZ-CD23 does not appear to differ in affinity from the rCD23 construct, assuming both interact as trimers.

Large standard deviations would be due to errors in concentration estimation, particularly if there is a proportion of the sample that is not active. The dissociation constants, which are not a function of concentration, are considered to be a good comparative indicator of affinity between similar molecules. Focussing on dissociation rates, the Der-CD23 lectin domain has an affinity for IgE three-fold lower than full length CD23.

5.3.4 The Effect of Flow Rate on the Der-CD23-IgE Fc Dissociation Rate Constant.

ELISA data described earlier suggests that Der-CD23 weakly interacts with IgE. Binding was improved when using IgE-Fc and SPR data would suggests the affinity of this interaction was actually fairly high ($K_A = 10^7$ M^{-1}). It is possible that SPR was over-estimating the apparent affinity. The high concentration used in kinetic experiments may encourage rebinding during dissociation and would cause the k_d to be under-estimated. This potential problem was assessed with a faster flow rate (30 µl/min).

A concentration series of Der-CD23 (from 1000 nM) was applied to the flowcells at 30 µl/ml for 6 minute association and dissociation period. The measured k_d displayed in Table 5.4 were calculated as before and represent the mean k_d from a number of experiments. The standard deviations were quite high but no significant difference in k_d was found at 30 µl/min. Therefore, no mass transfer effects were occurring at 10 µl/min and the dissociation rate of 1 x 10^{-3} s^{-1} was a reliable estimation.

Table 5.4: Effect of Experimental Flow Rate on Dissociation Rate Constant for the Der-CD23 IgE-Fc Interaction.

Flow Rate (µl/min)	k_d (x 10^{-3} s^{-1})*	*n*	Chi^2
10	1.0 ± 0.3	16	0.341
30	0.9 ± 0.3	7	0.339

* mean k_d ± 1 SD calculated from *n* number of analyses.

It is likely that the ELISAs are at the limits CD23-ligand affinity detection, with the 3-6 fold greater affinity of the trimeric constructs being sufficient to form stable interactions. The shorter 'lifetime' of Der-CD23-IgE complexes inferred by faster dissociation rates (k_d) may be the crucial factor that results in the lack of detection by ELISA techniques.

5.4 Preliminary IL-4 stimulated IgE Synthesis Assay

The CD23 lectin domain (Der-CD23; Chapter 3) and oligomeric CD23 (LZ-CD23; Chapter 4) were included in an *in vitro* IgE synthesis assay (Zhang *et al.,* 1991) to test whether they had the predicted inhibitory and stimulatory effects, respectively (Sarfati *et al.,* 1992). Peripheral blood mononuclear cells (PBMC) from uncharacterised, non-symptomatic donors, were purified on a Ficoll gradient and cultured in the presence of IL-4 and an anti-CD40 antibody which induces IgE synthesis (kindly performed by N. McCloskey and D. Fear; section 2.5.9). In order to assess the effect of the recombinant CD23 without interference from endogenous sCD23 which can be as high as 200 ng/ml in IL-4 anti-CD40 stimulated tonsillar B cell cultures (N. McCloskey, unpublished data) the following conditions were investigated:

1) an excess of purified recombinant CD23 was included in the assays (sections 5.4.1 and 5.4.2)

2) Batimastat, the metalloprotease inhibitor which prevents the 37 kDa and 33 kDa sCD23 being released from the cell surface (Marolewski *et al.,* 1998) was also employed to eliminate any stimulatory effect of these endogenous products (section 5.4.3).

Each condition was performed in triplicate (Der-CD23) or duplicate (LZ-CD23). After 12-13 days in culture IgE in cell supernatants were quantified by ELISA, also in duplicate or triplicate.

5.4 .1 IgE Production Suppression by Der-CD23

The presence of IL-4 and anti-CD40 stimulated PBMC to synthesise approximately 25 ng/ml IgE (Figure 5.9). Low IgE levels (<4 ng/ml) were detected in controls not containing IL-4 and anti-CD40. The addition of 1 μg/ml Der-CD23 inhibited IgE synthesis by approximately 40% to 15 ng/ml. Adding a greater excess (10 μg/ml) did not inhibit IgE synthesis further.

Previous studies by Sarfati *et al.* (1992) demonstrated the suppressive activity of 16 kDa CD23 using PBMC from atopic donors (~30%). Data presented here showed higher IgE levels (more than tenfold) were obtained from uncharacterised donor PMBC, and observed similar suppression of IgE production, albeit at much greater concentrations of Der-CD23 (50 and 500-fold). It will be necessary to determine whether Der-CD23 was toxic at high concentrations. Cell viability can be measured by trypan blue staining of dead cells. Examination under a light microscope indicated that cultures including Der-CD23 were similar to controls not containing Der-CD23.

Further titration of Der-CD23 in stimulated PBMC cultures will be analysed in future experiments (on-going in this laboratory) to investigate the concentration dependence and obtain an inhibitory constant (IC50) for Der-CD23. Ideally, assays will be carried out in tonsillar B-cell cultures so the cellular mechanism of suppression can be readily elucidated. This has not been possible here because of recent changes to tonsillectomies following detection of prions in tonsils and on sterilised operating equipment. Disposal surgical instrumentation has allowed procedures to be resumed (June 2001).

5.4.2 The Effect on IgE Production by LZ-CD23

In this experiment, PBMC from a different blood donor produced almost tenfold more IgE (255 ng/ml) than the previous donor, on stimulation with IL-4/anti-CD40. Unstimulated PBMC had similar low IgE levels (less than 3 ng/ml). Although the donor was non-symptomatic, the B cells may have been activated *in vivo*. On addition of an excess amount of LZ-CD23 at 800 ng/ml, stimulated cells produced approximately 110 ng/ml IgE, a 56% reduction. Adding further LZ-CD23 (8 μg/ml) produced an even greater inhibition of IgE production of 82% (45ng/ml), more potent than Der-CD23. This was not expected; from several studies fragments >25 kDa CD23, recombinant and native have been shown to enhance IgE synthesis (summarised in Chapter 1; Table 1.1).

It was possible that the LZ-CD23 preparation had been degraded during culture to suppressive fragments less than 25 kDa. Potent inhibition of IgE synthesis was observed by Sarfati *et al.* (1992) with a 1:1 (w/w) mixture of 29 kDa and 16 kDa CD23. The possibility was investigated by Western blot. Figure 5.11 shows that no breakdown product was apparent in culture supernatants at day 13 using a polyclonal antibody. Undetectable amounts of degradation product at optimal concentration for suppression (~25 ng/ml) may still account for the observed suppression. Under non-reducing

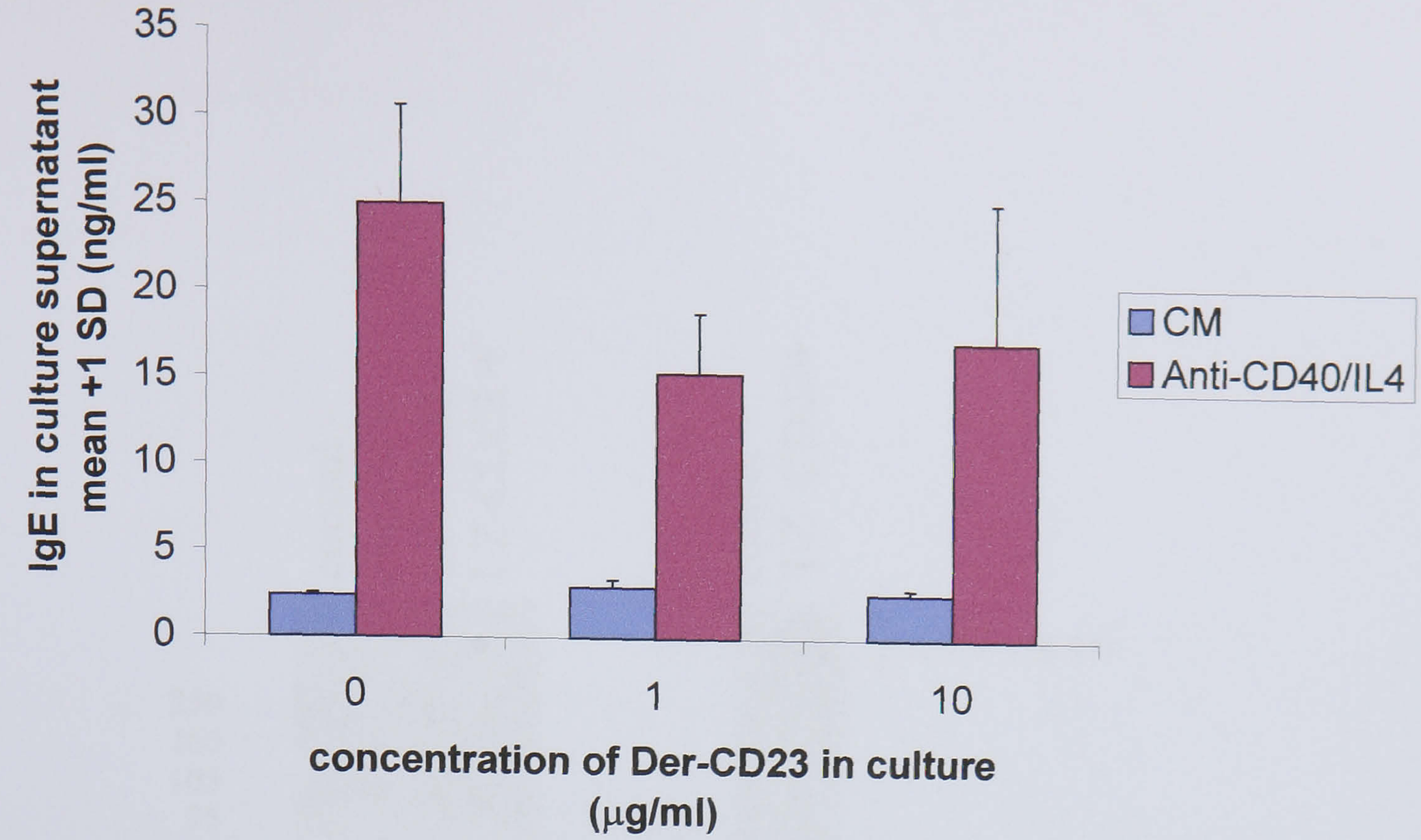

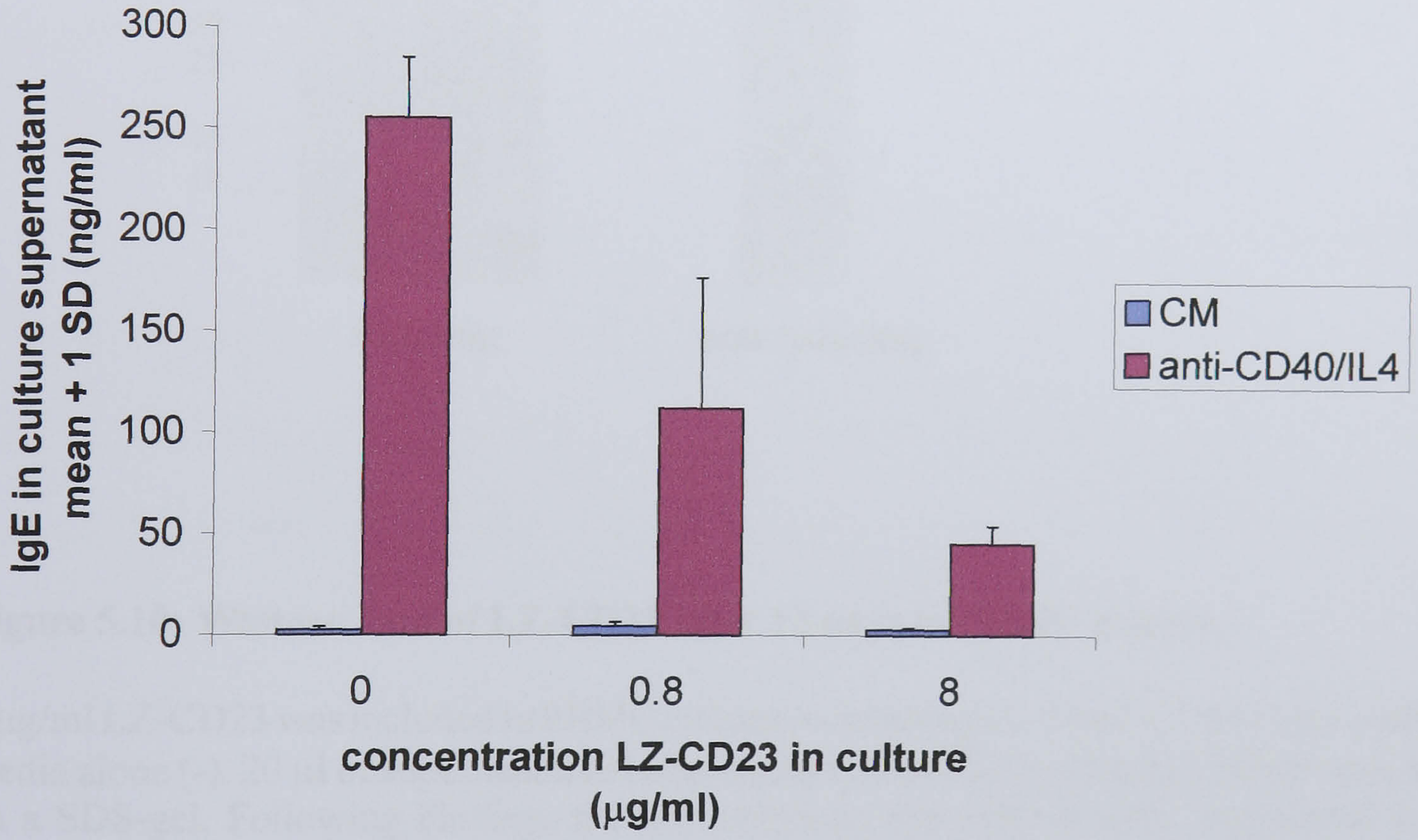

Figure 5.9: Effects of Recombinant sCD23 on IgE Production by IL-4 induced PBMC

Excess amounts of recombinant CD23 were added to purified peripheral blood mononucleic cells (PBMC) stimulated by IL-4 (200 IU/ml) and anti-CD40 (1 μg/ml) or PBMC in culture media (CM) alone. After 12 days of culture, cell supernatants were analysed for secreted IgE by ELISA. Both Der-CD23 and LZ-CD23 were effective inhibitors of IL-4/anti-CD40 induced IgE production under these conditions.

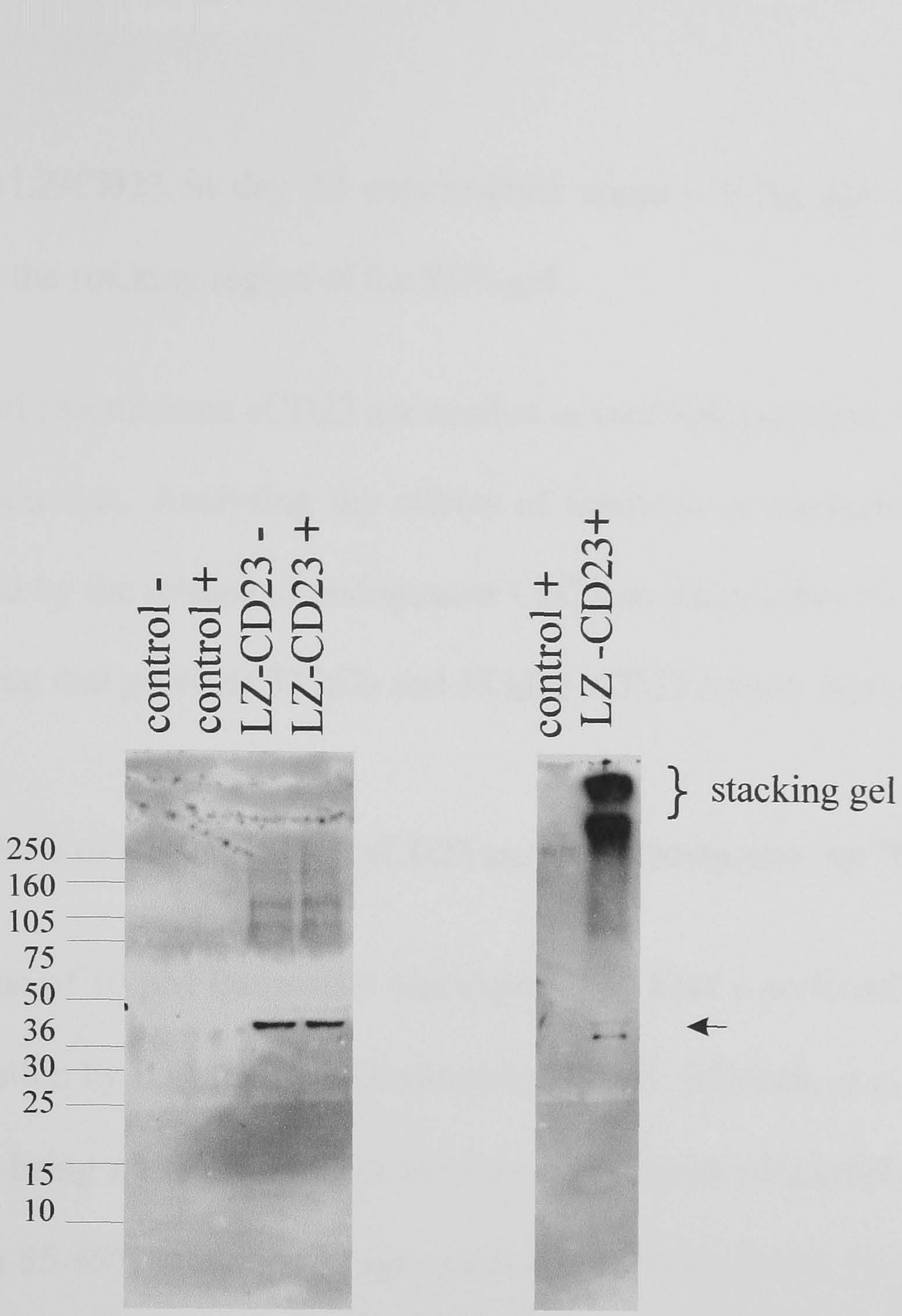

Figure 5.10: Western Blot of LZ-CD23 after 13 days in PBMC culture.

8 μg/ml LZ-CD23 was included in PBMC cultures containing IL-4/anti-CD40 (+) or culture media alone (-). 20 μl of supernatant in reducing and non-reducing loading buffer were run on a SDS-gel. Following blotting, the nitrocellulose was probed with polyclonal anti-CD23, rb55. No breakdown product was detected and LZ-CD23 appeared to remain the correct MW (~38 kDa). Aggregation was evident under non-reducing conditions.

conditions LZ-CD23 in day 13 supernatants appears to be aggregating as it can be detected in the stacking region of the SDS-gel.

Titrations of recombinant sCD23 are needed to establish any dose dependent regulation of IgE production. Analysing the effects of titrations of recombinant sCD23 will be complicated by the release of endogenous CD23 on stimulation. For this reason the use of Batimastat that prevents 37 kDa and 33 kDa sCD23 release was investigated.

5.4.3 Effects of Batimastat on sCD23 and IgE Production by PBMC

The addition of 10 μM Batimastat was expected to have a profound inhibitory effect on IgE production by IL-4/anti-CD40 stimulated PBMC (Christie *et al.*, 1997). Despite the IgE levels being quite different in the two experiments performed, 10 μM Batimastat produced a 55-65% inhibition of IgE production (Figure 5.11). The inhibition observed was not as pronounced as reported by Christie and co-workers with 10 μM Batimastat (~90%). Differences in IgE synthesis inhibition may be attributed to slightly differing culture conditions and different solvent used to make Batimastat stock solutions (ethanol c.f. DMSO).

As Batimastat will be used to evaluate the effects of recombinant CD23 it was necessary to show that the inhibition observed was due to a decrease in sCD23 levels. Analysis of sCD23 in the culture supernatants showed the expected induction of sCD23 with the presence of IL-4/anti-CD40 to approximately 20-40 ng/ml. The effect of 10 μM Batimastat on sCD23 detected were inconsistent (<5% and 35% inhibition) in the 2 experiments performed (Table 5.5 and Figure 5.11). Although generation of 37 kDa and 33 kDa fragments may be inhibited by Batimastat (Marolewski *et al.*, 1998), the 25 kDa fragment is produced by a different proteolytic mechanism and can be cleaved directly

from the cell surface (Moulder *et al.,* 1993). Due to the indiscriminate nature of the sCD23 ELISA, the size of sCD23 detected could not be determined and detection of 25 kDa sCD23 may account for no apparent difference in sCD23 levels. It is possible to quantify 29-37 kDa CD23 by ELISA (Katira and Gordon, 1995) and analyse the size of CD23 by immunoprecipitaton and Western blot. These methods will be used in future studies.

It is expected that addition of LZ-CD23 to Batimastat treated (stimulated) PBMC should restore or enhance IgE synthesis by providing B-cells with an alternative source of sCD23 to trigger the stimulatory signal through binding CD21 (as depicted in Figure 1.4, Chapter 1).

Table 5.5: Effects of Batimastat on IgE and sCD23 Production in IL-4/anti-CD40 Stimulated PBMC Cultures.

	IgE in culture supernatant (ng/ml)		sCD23 in culture supernatant (ng/ml)	
Culture Conditions	**DONOR 1**	**DONOR 2**	**DONOR 1**	**DONOR 2**
Unstimulated	2.4 ± 0.1	2.6 ± 1.5	2.9 ± 0.0	3.1 ± 0.2
IL-4 + anti-CD40	25.0 ± 5.6	255.7 ± 30.0	22.3 ± 4.8	38.5 ± 1.9
Unstimulated +10μM Batimastat	1.8 ± 0.1	1.6 ± 0.8	3.0 ± 0.1	2.8 ± 0.0
IL-4 + anti-CD40 + 10μM Batimastat	10.9 ± 1.6	85.2 ± 22.9	21.9 ± 4.2	24.9 ± 5.8

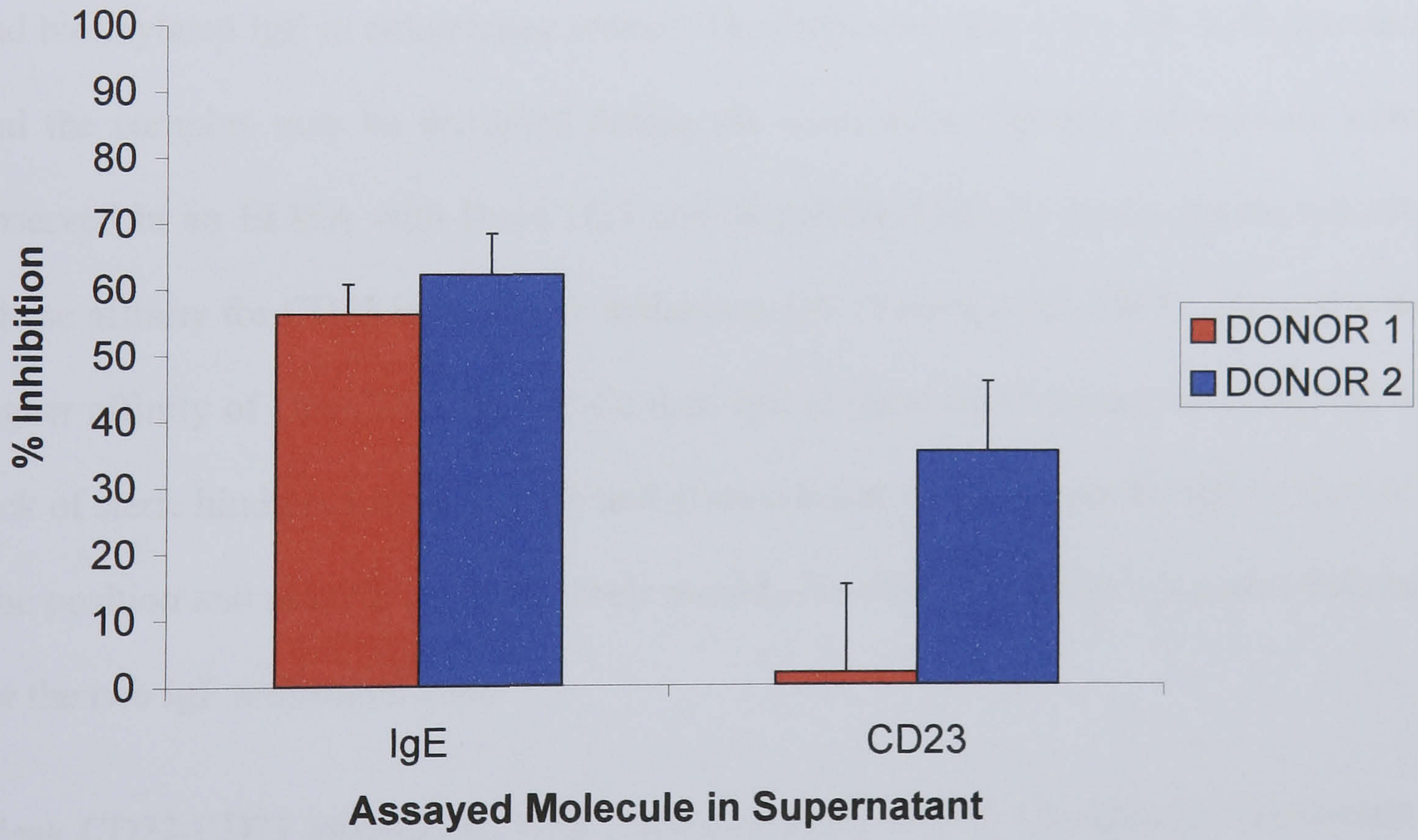

Figure 5.11: Effects of 10μM Batimastat on IgE and sCD23 in PBMC cultures

10 μM Batimastat was added to *in vitro* PBMC cultures (from 2 different donors) stimulated with IL4 and anti-CD40. The resulting IgE and sCD23 concentrations in Day 12-13 cultures were measured by ELISA. Percentage inhibitions were calculated using IgE and CD23 concentrations (Table 5.5) compared to stimulated culture containing no Batimastat.

5.5 Discussion

This chapter characterises the ligand binding properties of the recombinant CD23 molecules expressed and purified in Chapters 3 and 4 and their effect on IgE production. Der-CD23, a 16 kDa recombinant CD23 lectin domain protein, was compared to LZ-CD23, an extracellular CD23 containing an LZ motif to encourage trimer stabilisation (Kelly *et al.,* 1998, Harbury *et al.,* 1994).

IgE binding to LZ-CD23 was demonstrated by two optimised ELISAs; with CD23 coated directly to the solid phase and when captured by a monoclonal antibody mAb25, which only partially inhibits IgE interactions (Wakai *et al.,* 1993, Bettler *et al.,* 1989 and Bonnefoy *et al.,* 1987). No specific interaction was detected between Der-CD23 and biotinylated IgE in either assay format. The interaction was too weak to be detected and the complex may be disrupted during the wash steps. Specific interactions were observed in an ELISA with Der-CD23 and biotinylated IgE-Fc glycosylation mutant, whose affinity for CD23 is similar to melanoma IgE (Young *et al.,* 1995). The apparent higher affinity of Der-CD23 for IgE-Fc than IgE in these ELISAs may be attributed to lack of steric hindrance from the Fab and glycosylation structures on the IgE Fc mutant. The position and number of biotin labels would also effect the relative signals obtained for the two IgE molecules used.

Weak CD23-CD21 interactions were also detected by ELISA (described by Fremeaux-Bacchi *et al.,* 1996). Again, only the full length extracellular CD23 fragment (rCD23) was able to bind above background levels, possibly enhanced by avidity effects from being dimeric or trimeric, or from possessing additional interaction sites not present in Der-CD23. No LZ-CD23 was available at this time to confirm this observation. It is difficult to envisage how monomeric Der-CD23 could physically interact with 2 distant

sites (SCR1-2) and (SCR 5-8) of the CD21 molecule (Aubry *et al.,* 1994). Therefore, only a single weak interaction may have been detected. The signal obtained with the CD21 ELISA was unsatisfactory. There was concern that if CD23 behaves like a galactose specific C-type lectin as demonstrated by Kijimoto-Ochiai and Uede (1995) then the recombinant sCD21 expressed by baculovirus would not be appropriately glycosylated. Native or sCD21 expressed by mammalian cells would be needed to resolve this problem. The CD21/CD23 interaction is likely to be pivotal in regulation of IgE production so an improvement in ELISA and SPR kinetic data will be advantageous.

BIAcore experiments using IgE-Fc tethered to the sensorchip, were able to determine kinetic binding constants for the recombinant CD23s. By fitting a 1:1 Langmuir association/dissociation model to resulting sensorgrams the following affinity constants, K_A were obtained: LZ-CD23 (5.3×10^7 M^{-1}) and Der-CD23 (0.9×10^7 M^{-1}). This suggests that the affinity of trimeric LZ-CD23 for IgE is approximately 6 fold greater than monomeric Der-CD23. The possibility that the Der-CD23-IgE-Fc affinity was over-estimated of due to mass transfer effect was assessed by increasing experimental flow rate to 30 μl/min, but no increase in dissociation rate was observed (from 1.0×10^3 s^{-1} to 0.9×10^3 s^{-1}). The affinity of Der-CD23 for IgE Fc (Cε2-Cε4) is considerably higher than the K_A of the lectin domain interaction to a different IgE Fc construct (Cε3-Cε4) which was estimated to be 10^{-5} M^{-1} by analytical ultracentifugation (Shi *et al.*, 1997). Barlett *et al.,* (1995) also estimated the affinity of the murine monomeric sCD23-IgE interaction to be to between $10^5 - 10^6$ M^{-1}. The IgE-Fc mutant used in these BIAcore experiments has a 10 fold higher affinity than wild type IgE-Fc attributed to the removal of two N glycans (Young *et al.,* 1995) which may explain the discrepancy between these monomeric affinities. Alternatively, the high concentrations of Der-CD23

used (as high as 90 μg/ml) may promote trimerisation and the Der-CD23-IgE complex may be stabilised by additional head-head interactions. Although, Der-CD23 contains no stalk region, cross-linking evidence (section 3.5.7; Beavil *et al.,* 1995) suggests oligomers may occur.

This BIAcore data for the LZ-CD23 and IgE-Fc interaction (K_A = 5.3 x 10^7 M^{-1}) corresponds well to cell binding assays data with membrane bound CD23 on B-cell lines (i.e. trimeric) and this IgE Fc glycosylation mutant (3.2 x 10^7 M^{-1}, Young *et al.*, 1995). The LZ-CD23 affinity constant compares well to wild type IgE and CD23: 4.2 x 10^7 M^{-1} (Anderson and Spiegelberg, 1981), 7 x 10^7 M^{-1} (Bettler *et al.,* 1992) and 5.3 x 10^7 M^{-1} (Sato *et al.,* 1997). The LZ fusion with mouse CD23 (also containing mutated proteolysis sites) inhibited IgE binding to the high affinity receptor (FcεRI) implying that chimeric CD23 has the potential to possess even higher affinities (Kelly *et al.,* 1998). Any inactive or mis-folded LZ-CD23 in the sample is difficult to detect which could lead to an underestimation the affinity constant. Thus, the K_A for the LZ-CD23 IgE Fc interaction may be greater than estimated by BIAcore. Perhaps a higher affinity constant of the human chimera could be obtained with improvements to refolding and purification techniques (as discussed in Chapter 4).

The *in vitro* IgE synthesis assays were carried out with human PBMC cultures stimulated with IL-4 and anti-CD40, which mimic B cell activation signals by cognate T cells (reviewed by Gordon and Pound, 2000). The suppressive effect of Der-CD23 on IgE synthesis appeared to agree with the results obtained by Sarfati *et al.,* 1992 and 1984. LZ-CD23 suppressed IgE production to an even greater extent (84% with 8 μg/ml). Excess amounts of recombinant CD23 were included to prevent interference with endogenous sCD23, which were quantified in these experiments to be 20-40 ng/ml

in stimulated cultures. It is possible that the mechanism of IgE enhancement occurs over a narrow range of sCD23 concentrations. This hypothesis is supported by Chretien *et al.,* 1990 who obtained enhancement of IgE synthesis in IL-4 stimulated human peripheral blood lymphocytes using 10-1000 pg/ml recombinant 33 kDa sCD23, above less pronounced enhancement of IgE occurred. Furthermore, soluble CD23 may only enhance IgE synthesis in sub-optimal IL-4 conditions (10-20 IU/ml) as used in previous studies (Pene *et al.,* 1988, Chretien *et al.,* 1990). These conditions would have resulted in lower endogenous sCD23.

Many variables to this *in vitro* assay need to be assessed; not only concentration dependence of sCD23 and the IL-4/anti-CD40 stimulus but also the alternative strategy to eliminate endogenous sCD23 with matrix metalloproteinase inhibitors. Preliminary studies with Batimastat, which prevents the release of 37 kDa and 33 kDa sCD23 from the cell surface (Marolewski *et al.,* 1998), suppressed IgE synthesis in accordance with Christie *et al.,* 1997. It is expected that the addition of LZ-CD23 to Batimastat treated B-cells will overcome IgE suppression. This strategy may be preferable to adding excess concentrations of recombinant CD23 as it is likely that high concentrations of LZ-CD23 were affecting other cells and cellular mechanisms, e.g. cell proliferation and differentiation. Work is continuing in our laboratory to investigate the mechanisms underlying IgE regulation by CD23 using purified B-cells from tonsils.

CHAPTER 6: EXPRESSION OF RECOMBINANT, SOLUBLE INTEGRIN, CD11b/CD18.

6.1 Introduction

The interaction of CD23 with the β_2 integrins CD11b/CD18 and CD11c/CD18 has been partially characterised on the cell surface of monocytes and transfected CHO cells (Lecoanet-Henchoz *et al.,* 1995). Further characterisation of the receptor-ligand interaction will require binding assays to be carried out with the receptors in a homogeneous environment. Ideally, a soluble form of the integrin is needed to be included in biophysical studies to elucidate binding kinetics and stoichiometry of the CD23 binding. Furthermore, purification of soluble heterodimer leads to the possibility of attaining a high resolution structure of the integrin. Therefore, the feasibility of expressing CD11b/CD18 (αMβ2, CR3, Mac-1) as a soluble heterodimer was explored.

Soluble receptor can be attained through recombinant DNA technology in preference to the use of detergents or proteolytic release from the membrane. Dana *et al.,* 1991, demonstrated that recombinant αMβ2 lacking the transmembrane and cytoplasmic domains was secreted by COS cells as a heterodimer and still retained specific ligand binding. Other integrins have also been expressed as active soluble heterodimers in this system, (Table 6.1). However, the yields were generally too low for purification and further studies.

To improve yields an alternative expression system could be investigated. The choice of expression system for recombinant soluble integrin is limited to cells which will fold, process and secrete heterodimers. These criteria rule out bacterial systems because the

Table 6.1: Review of Expression Systems and Designs for Recombinant Soluble Integrin

Integrin	Expression system	Integrin Design	Results, Activity and Yield	1st author, year
αMβ2	COS co-transfection		Active, 20 ng/ml	Dana, 1991
αIIbβ3	COS Single and co-tranfections		αIIbβ3 secreted αIIb retained β3 secreted	Bennett, 1993
αIIbβ3	COS Co-transfection and dual vector		Active, processed and glycosylated	Gulino, 1995
αIIbβ3	Baculovirus Co-infection	Interspecies chimeras	200 ng/ml	McKay, 1996
αIIbβ3	Baculovirus Dual vector	No αIIb light chain	Active but low yields	Wippler, 1997
αIIbβ3	Baculovirus Dual vector		Active conformation, 1000 ng/ml	Peterson, 1998
αvβ3	Baculovirus Co-infection		Cation regulated activity, 850ng/ml	Mehta, 1998
α3β1	Drosophila Co-transfection	Jun/Fos fusion	Regulated activity, 200 ng/ml	Eble, 1998
α8β1	COS co-transfection	α8-His-c-myc, β1-AP tags	Active, 1000ng/ml heterodimer	Denda, 1998
αLβ2	CHO co-transfection		Active, 1000ng/ml	Tominaga, 1998
αvβ3	*E.coli*	Maltose binding protein fusion	Insoluble, Inactive	Schroeckh, 2000
α4β1	Baculovirus Hi5 coinfection	α4-BB2 epitope tag	Active, Purified 100-850 ng/ml	Clark, 2000
α4β1	CHO and COS co-transfection	IgG1Fc fusion	Cation regulated activity	Stephens, 2000

large complex integrin subunits would be unglycosylated, potentially insoluble and difficult to renature, as experienced by Schroeckh *et al.,* 2000.

Some success has been attained with the baculovirus expression system (Table 6.1). There are several benefits of this method over mammalian cell cultures particularly the faster and simpler selection of recombinant clones than co-transfection of mammalian cells. Furthermore, insect cells minimise contamination with endogenous integrins and the cultures use serum free media without the need for enriched carbon dioxide atmosphere. Potential pitfalls of the baculovirus system are that O-linked glycosylation can not be processed in insect cells and high mannose type N-linked carbohydrate replaces any complex glycosylation. Although integrins are highly glycosylated (25 N-linked sites on αMβ2) it is unclear whether complex carbohydrate is essential for CD23 binding. The removal of sialic acid by neuraminadase did not have any effect on CD23 binding to CD11b or CD11c transfected CHO cells (Lecoanet-Henchoz *et al.,* 1995).

This chapter describes the cloning and expression of a truncated recombinant αMβ2 using the baculovirus expression system and preliminary ligand binding studies with recombinant soluble integrin expressed in mammalian cell cultures (Stephens *et al.,* 2000).

6.2 Production of Recombinant CD11b/CD18 Baculovirus

The DNA sequence used for cloning of the soluble integrin subunits included the whole of the extracellular domain up to the transmembrane sequence N700 (CD18, numbering by Kishimoto *et al.,* 1987) and N1104 (CD11b, Arnaout *et al.,* 1988). Truncation of the subunits was achieved through sub-cloning fragments from the cDNA using PCR techniques.

To assist the detection of expressed product, the alpha subunit was cloned with a aspartate rich octapeptide FLAG epitope (DYKDDDDK) placed at the C-terminus. In addition, an accessible, non-interfering epitope could be used as a tag for purification and immunoprecipitation studies to assess heterodimerisation of the subunit chains.

Cloning of each subunit was achieved by PCR in several steps as outlined in Figures 6.1 and 6.2 and Table 6.2. By constructing each subunit sequence in parts, the future addition of alternative leader sequences and optional epitope tags can be added by PCR without having to re-sequence the whole construct. This will be particularly useful for these large constructs of 3.3 kb (αM, CD11b) and 2.1 kb (β2, CD18).

6.2.1 Constructing Extracellular CD11b

The first fragment was produced by PCR using the primers and conditions outlined in Table 6.2. The fragment denoted αN1 (the first alpha subunit fragment including its native leader sequence) was ligated into the HindIII and EcoRV sites of pBluescript. One positive clone (pBS-αN1) was identified and sequenced with primers listed in Appendix I (sequence data of the selected clone are detailed in Appendix II).

The second fragment α2 was more problematic to clone. It was a larger fragment ~1.7 kb with one blunt end restriction site and a high content of repeat sequences. Low yields of PCR product were obtained and attempts at cloning directly into pBS-αN1 were unsuccessful using standard methods. Therefore, a new primer with a HindIII site 5' to EcoRV was used to produce fragment α2, which was ligated into pBluescript vector used for amplification of the insert and sequencing. Several clones obtained from PCR with *Taq* polymerase contained several substitutions leading to coding mismatches. The PCR was subsequently performed using High Fidelity/proof-reading polymerase (*Pwo*).

When a pBS-α2 clone of correct sequence was identified (Appendix II), it was excised using EcoRV and XbaI and ligated into pBS-αN1. An improved transformation efficiency was observed and several clones (denoted pBSαN2) were identified, all presumed to have correct sequence as no further PCR was involved.

The third fragment (α3E) with a FLAG epitope sequence was also cloned into the BamHI and SacI sites of the pBluescript shuttle vector. Sequence analysis of pBS-α3E identified no errors. The final fragment was excised by NdeI and SacI and ligated into the same sites of pBS-αN2.

Finally, the completed CD11b construct in pBS-αN3E was excised with HindIII and ligated into pFastBac and named pFB-CD11bNE (Figure 6.1). Insert identification and correct orientation in selected clones were checked with a series of restriction digests NcoI and HindIII (released 0.7, 2.7 and 4.7 kb fragments) and NotI and NdeI (released a 3 kb fragment).

Table 6.2: PCR conditions for CD11b and CD18 Fragments

PCR fragment	Size (kb)	Primers Appendix I	Annealing temp. °C	DNA Polymerase	Polymerase time (min)	Mg^{2+} conc. mM
αN1	1290	αNF αNR	50	*Taq*	1.5	3
α2	1681	α2F' α2R	50	*Pwo*	1.5	1
α3E	421	α3F α3ER	50	*Pwo*	1	3
βN1	900	βNF βNR	50	*Taq*	1.5	2
β2	1200	β2F β2R	52	*Taq*	1.5	2

a)

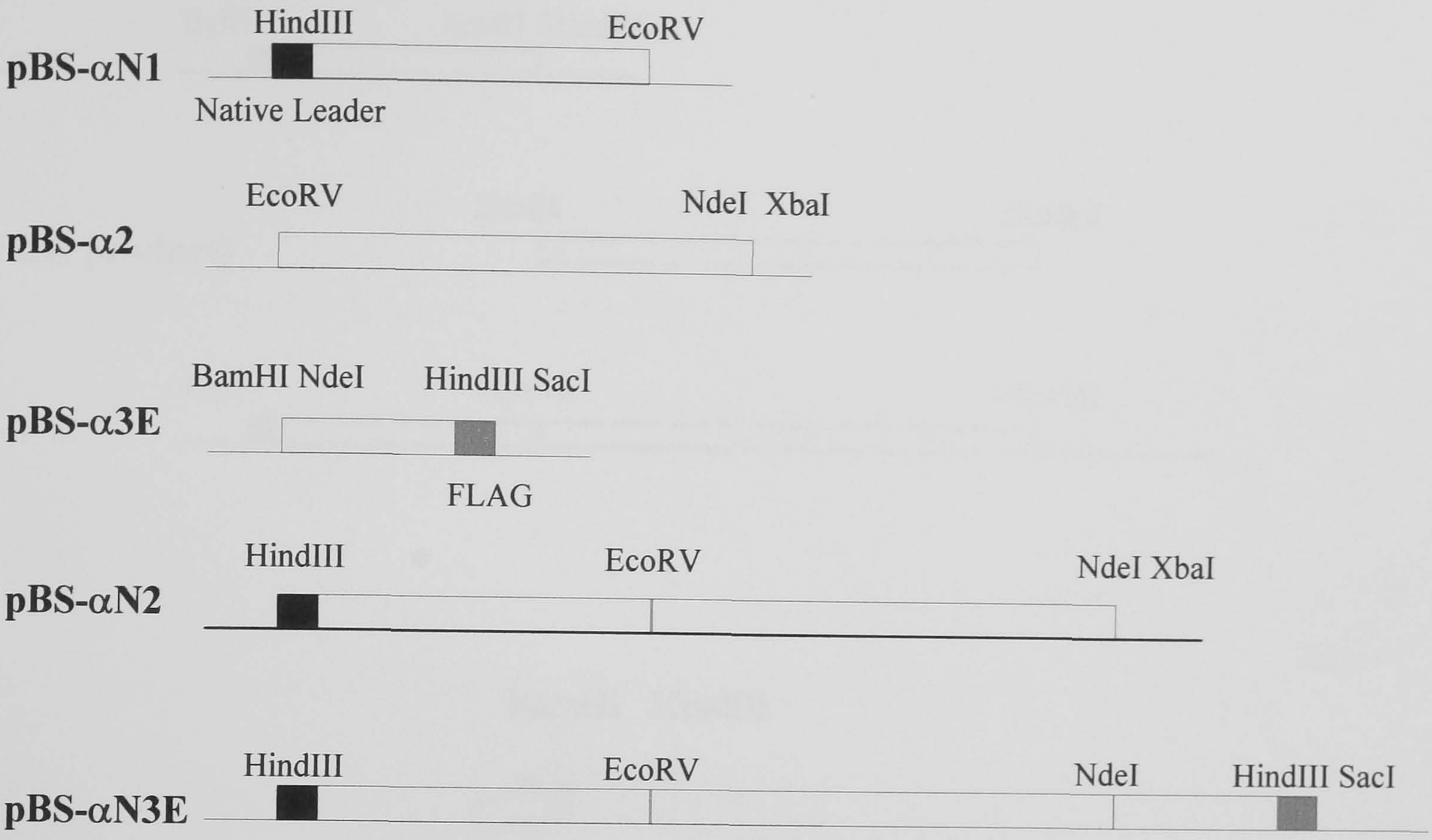

b)

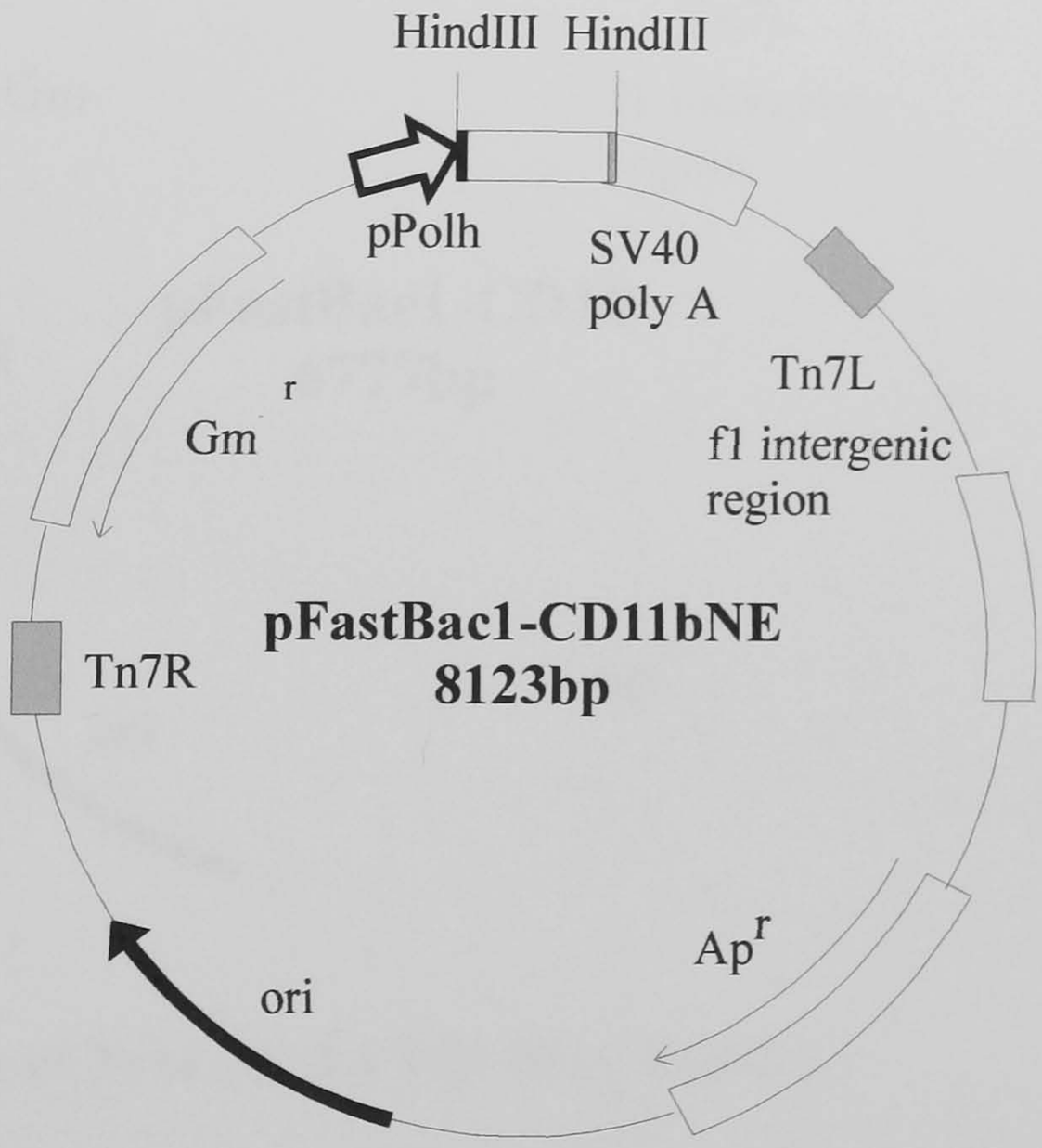

Figure 6.1: Construction of Truncated CD11b DNA Sequence.

a) Sequence coding for the truncated CD11b (M1-N1104) contained native leader sequence and an epitope tag. It was constructed from the sequential ligation of three cloned fragments in pBluescript. **b)** The final construct was excised using HindIII and ligated into the site in the baculovirus expression vector, pFastBac1.

a)

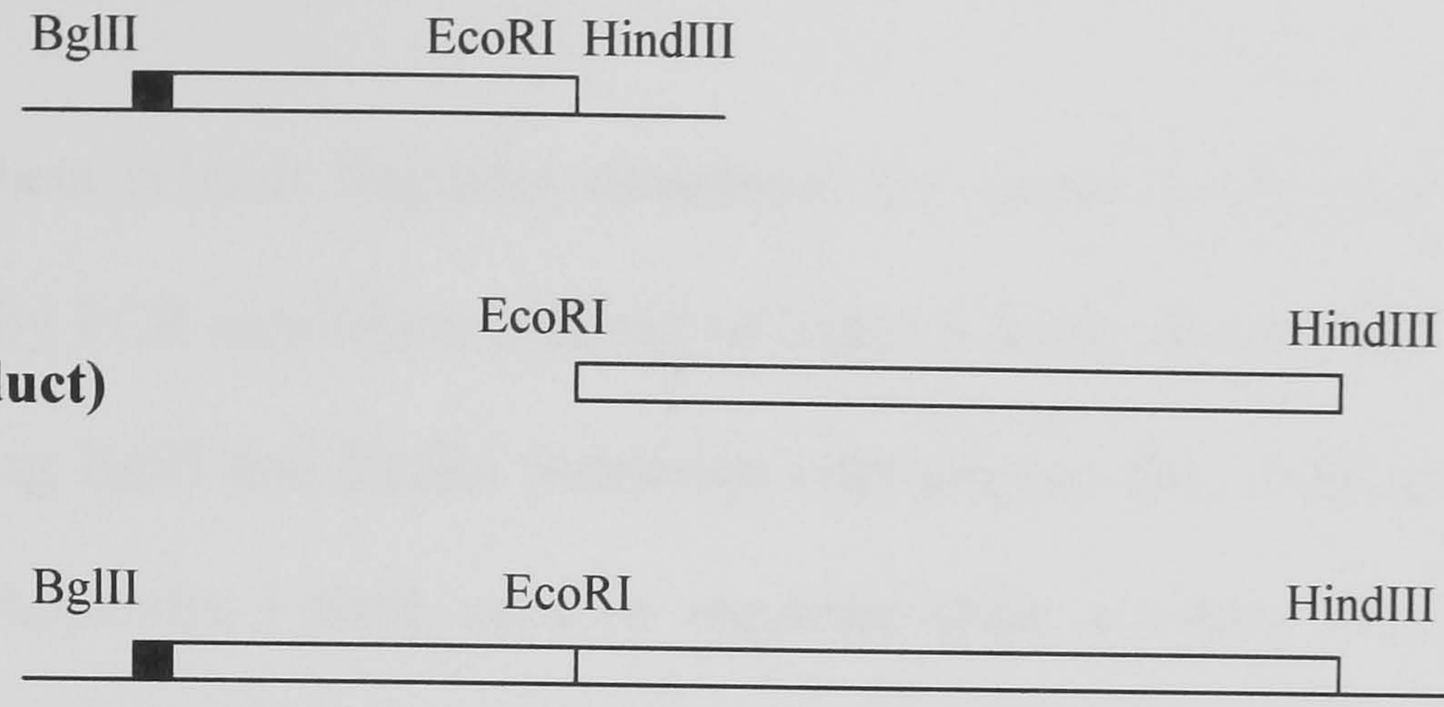

b)

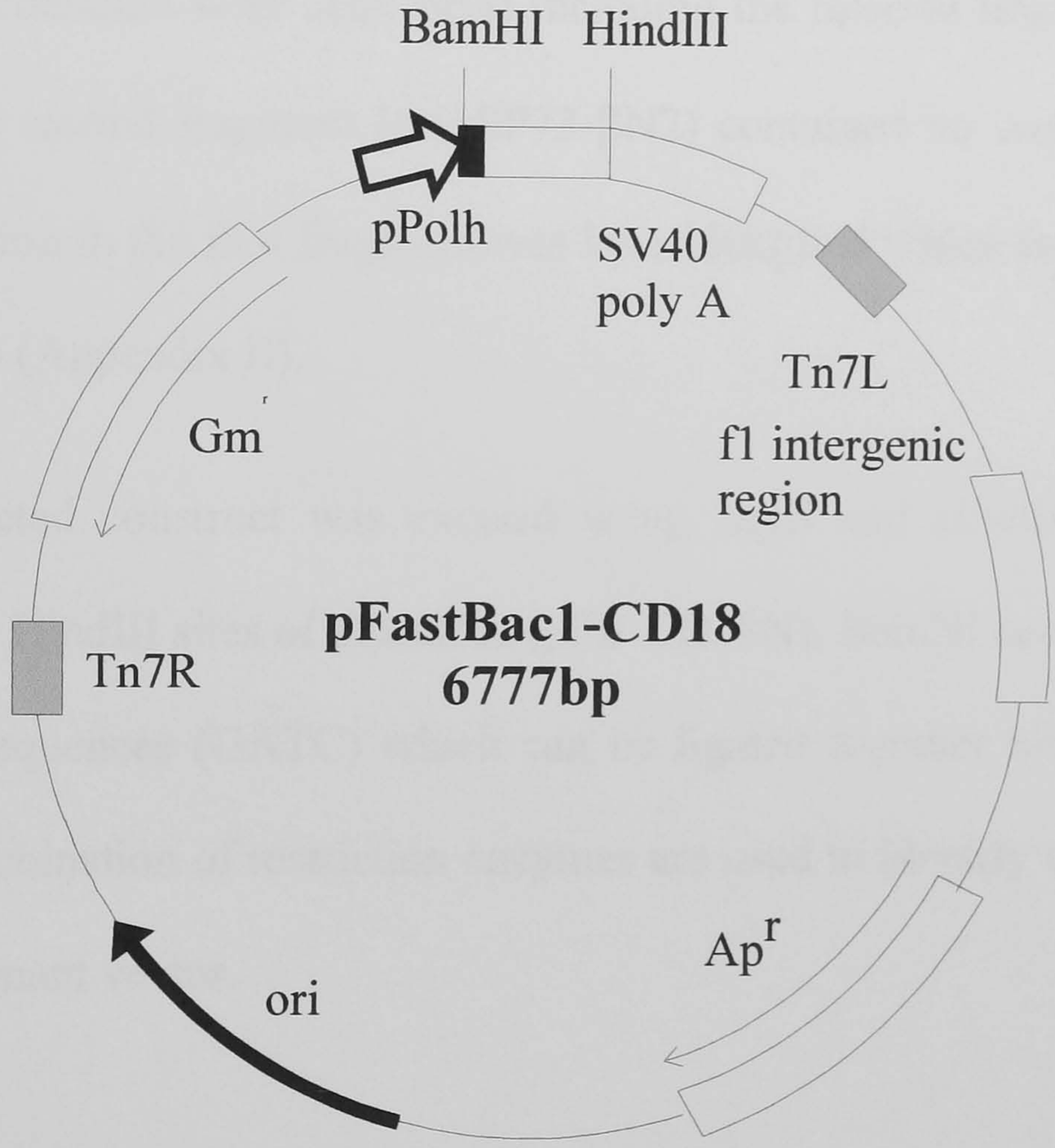

Figure 6.2: Construction of Truncated CD18 DNA Sequence

a) The sequence coding for extracellular CD18, including the native leader sequences and truncated at the transmembrane domain (M1-N700) was constructed in pSP73 from two PCR fragments. **b)** The completed construct was excised by BglII and HindIII and ligated into the BamHI, HindIII sites of pFastBac1.

6.2.2 Extracellular CD18

The first beta subunit fragment containing the native leader sequence (βN1, 0.9kb) produced by PCR conditions outlined in Table 6.2 was inserted into the pSP73 shuttle vector using BglII and EcoRI restriction sites (Figure 6.2). Sequencing using Primers listed in Appendix I were used to sequence three colonies identified by analytical restriction digest. The second PCR product of the β subunit (β2) was then inserted into the EcoRI and HindIII sites of one of the clones (pSP73-βN1). Positive clones of the completed construct were sequenced including the internal fragment joint. Sequencing showed the second fragment in (pSP73-βN2) contained no coding errors but a single point mutation in the first fragment was later identified which lead to a K194 –R amino acid change (Appendix II).

The completed construct was excised using BglII and HindIII and ligated into the BamHI and HindIII sites of pFastBac (pFB-CD18N). BamHI and BglII have compatible overhang sequences (GATC) which can be ligated together but both sites are lost so another combination of restriction enzymes are used to identify the inserted fragment in the recombinant vector.

6.2.3 Dual Vector Construct.

In order to engineer a recombinant bacmid capable of inducing dual expression of the truncated subunits, further cloning steps were necessary but no PCR. CD18N was able to be transferred into the BamHI and HindIII as in the single promoter vector (Figure 6.3). Due to the size of the CD18 and CD11b constructs, many of the unique restriction sites of the multiple cloning sites of vector were unsuitable. Consequently, the CD11b HindIII fragment had to be inserted into a new pBluescript vector (in the orientation

shown in Figure 6.3). Once excised with XbaI and SalI, the fragment could be ligated into the NheI and XhoI sites of the second cloning site by virtue of the complementary overhang sequences of these digested ends. This final step proved problematic, possibly due to the increasing size of the vector (10.6 kb) and difficulties in separating cut vector from fragment after excision. Only 4 out of 96 colonies proved positive in a PCR screen and of these, only 2 gave the correct restriction digest pattern. No PCR was involved in the creation of the dual vector, therefore, it was assumed the sequence would remain unchanged (see 5.3).

6.2.4 Virus Amplification

Recombinant CD18N and CD11bNE bacmids were produced from the pFastBac expression vector as described in the methods. The titre of the recombinant baculovirus (rbv) was low for rbvCD18N and rbvCD11bNE (detailed in Table 6.4). Only the dual expression baculovirus stock was sufficient for standard infections for protein expression studies. Despite several rounds of infection to increase viral titre, these plaque forming unit estimates were never improved upon. Although it is difficult to assess why, it is possible that the integrin subunits were interfering with the baculovirus infection cycle.

Table 6.3: Recombinant Baculovirus Titres as Estimated by Plaque Assay.

Recombinant Baculovirus	Stock Viral Titre (pfu/ml)	Vol. Required for 2 x 10^6 cell infection, MOI=5 (ml)
rbvCD11bNE	6 x 10^6	1.7
rbvCD18N	2 x 10^5	50.0
rbvCD11bNE/CD18N dual	5 x 10^7	0.2

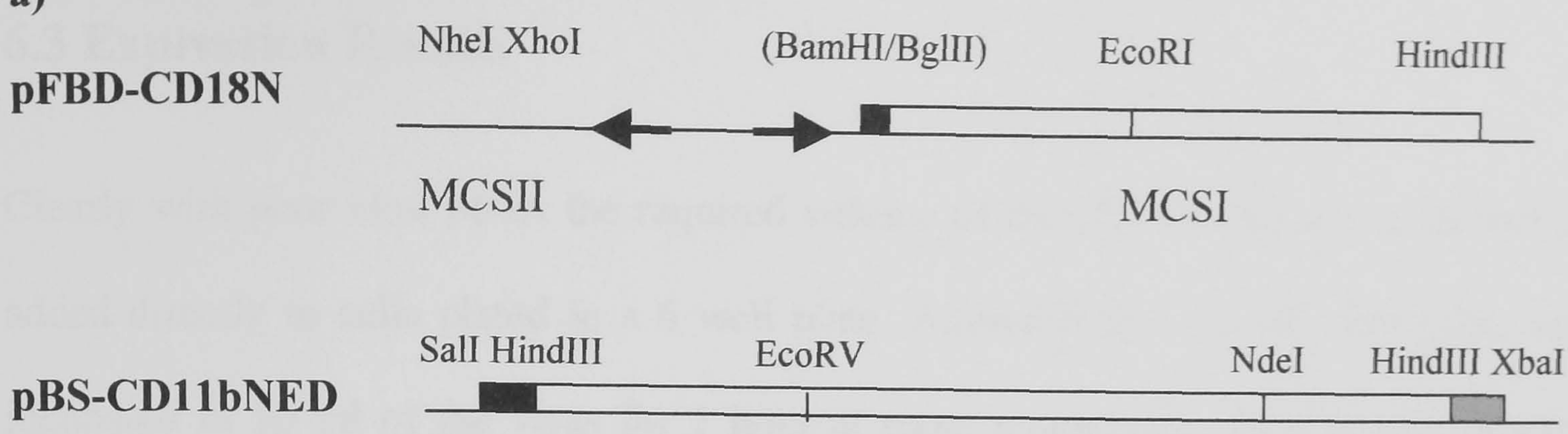

Figure 6.3: Construction the CD11b/CD18 Baculovirus Co-expression Vector

a) The extracellular CD18 coding sequence (pSP-βN2 in figure 6.2) was excised with BglII/HindIII and ligated into the BamHI/HindIII site of the first multi-cloning site (MCSI) of pFastBacDual. The HindIII extracellular CD11b fragment was cloned into pBluescriptKS in the orientation shown. The fragment was excised with XbaI and SalI and ligated to NheI and XhoI sites of second multi-cloning site (MCSII) by virtue of complementary overhang sequences. **b)** The completed recombinant dual vector had CD11b under the control of a strong early p10 promoter whereas CD18 was upstream of the polyhedron promoter.

6.3 Expression Results

Clearly with poor viral titres, the required volume of rbvCD18N (50 ml) could not be added directly to cells plated in a 6 well plate. Alternatively, 2 x 10^6 Sf9 cells were incubated in 50 ml of the virus for 1 hour at room temperature on a slowly rotating wheel. In this time it was envisaged that the virus would be adsorbed onto the cell surface. The cells were pelleted upon gentle centrifugation, resuspended in 2 ml fresh media and plated.

The viral stocks were produced from 5 day culture supernatants, by which time essential nutrients are depleted and toxic cell by-products and debris from infected cells increase to a level which makes it unsuitable for further cell culture. Therefore, due to the high volumes of rbvCD11bNE needed, the virus was allowed to adsorb onto plated cells for 1 hour, then carefully removed and replaced by 2 ml fresh media. All infections were allowed to proceed for 3 days and the cultures were harvested for analysis.

6.3.1 Single infections

Infected cell cultures were harvested, and the supernatant and cellular proteins were analysed by immunoblot techniques. Recombinant CD11b protein of the correct approximate molecular weight was detected in the cell extract of rbvCD11bNE infected cells by using an anti-FLAG mAb in a western blot (Figure 6.4a) CD11bNE was not detected in the culture supernatant. This result is similar to the observations by Bennett *et al.,* 1993, where the αIIb subunit was expressed without the β3 subunit was found retained within the COS cells. This also appears to be the case for αMβ2 expression in leukocytes but, Berman *et al.,* (1993) established that heterodimer formation was not

required for the export of CD11b in human kidney cell line (293) or from COS cells (Dana *et al.,* 1991). This was not the finding in the baculovirus expression system.

Cells infected with the CD18N baculovirus showed secretion of the recombinant protein of the correct size in the supernatant using a 'wet' transferred western blot with anti-CD18 mAb, KIM89 (Figure 6.4b). Several attempts were made to demonstrate CD18 within the cell by western blotting with an array of anti-CD18 monoclonal antibodies, but no specific binding could be detected. A dot-blot technique did show the presence of CD18 in cell extracts (section 5.3.2). The antibodies were apparently sensitive to the native fold of the protein and the solubilisation and denaturation of total cell protein during SDS-PAGE may have prevented the epitope being recognised.

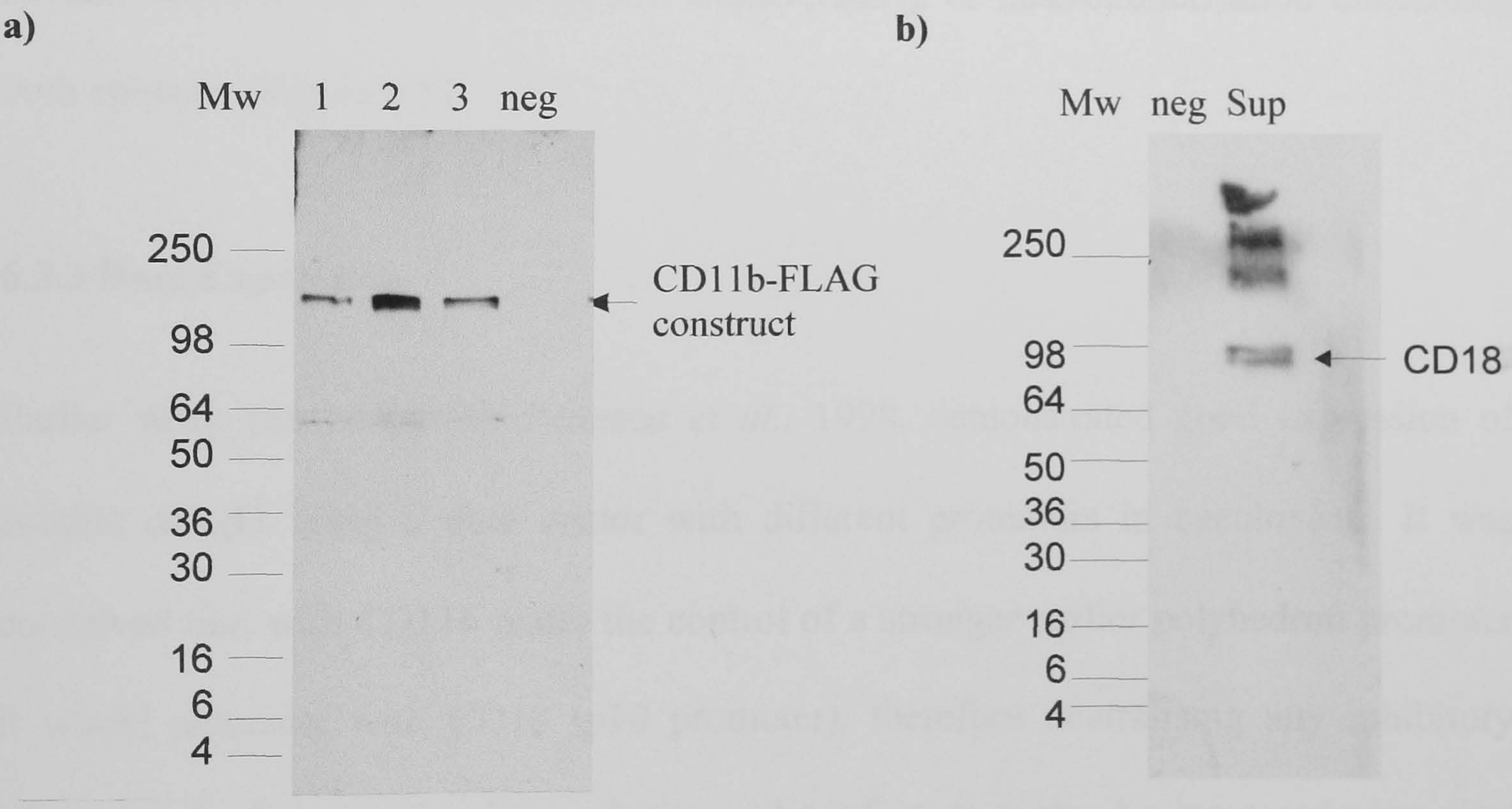

Figure 6.4: Western Blot Analysis of Expression of Single Subunits in Insect Cells

a) The cellular fraction of four 2 ml Sf9 cell infections with three CD11bNE baculoviral clones (and one negative control infection) were suspended in 2 ml PBS and 5 µl was loaded onto a 4-20% SDS gel in non-reducing buffer. Protein was transferred to Imobilon-P by the 'wet' method, detailed in Chapter 2 and probed with M2 anti-FLAG monoclonal antibody. **b)** A four fold concentrated sample of CD18 infected cell culture supernatant was run on a 4-20% SDS gel under non-reducing conditions alongside a negative control supernatant. Following wet transfer, the CD18 was detected by anti-CD18 monoclonal antibody (KIM89).

6.3.2 Co-infections

A dot blot immuno-technique was used to analyse the results of co-infections of the recombinant integrin subunits because of the difficulty of detecting CD18 within the cell fraction by western blot. The cell extract was applied directly to nitrocellulose. Although this technique does not give any information on the size of the protein detected, it was shown with negative controls (SPD-CD23 and CD11b infected cells) to be a stringent detection method. When CD18N was co-infected with CD11bNE, a reduction in the amount of CD18 in the supernatant was detected. No CD11b was detected through the FLAG epitope in the co-infection culture supernatants, even at tenfold concentrations of the supernatants. This would be indicative of either the alpha subunit sequestering the beta subunit intracellularly or heterodimerisation concealing both epitopes (Figure 6.5).

6.3.3 Dual Expression

Earlier work carried out by Peterson *et al.,* 1998, demonstrated good expression of soluble αIIbβ3 using a dual vector with different promoters in baculovirus. It was conceived that with CD11b under the control of a stronger earlier polyhedron promoter it would associate with CD18 (p10 promoter), therefore neutralising any inhibitory effect the single beta subunit may have on the infection cycle. An increased virus titre would improve co-infection experiments, increasing the likelihood of heterodimer formation and transport out of the cell.

Unfortunately, expression of heterodimer was not detected. The beta subunit expressed similarly to the single construct baculovirus, in that it was detected by anti-CD18 mAb in the media and within the cell. However, no CD11b was detected using dot blot

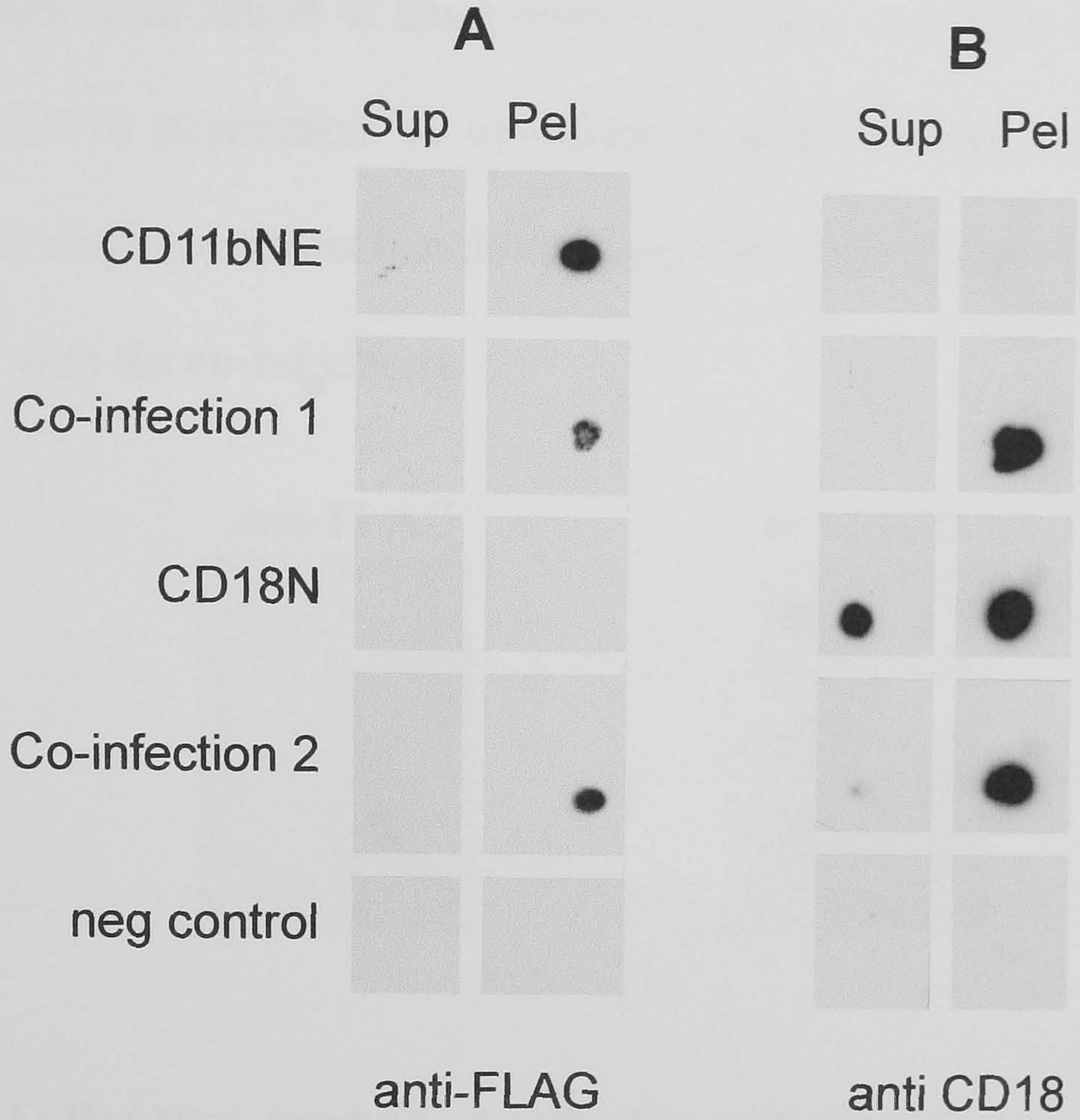

Figure 6.5: Dot Blot Analysis of CD11bNE/CD18N Co-infections in Sf9 cells

2×10^6 Sf9 cells were infected with recombinant baculovirus at a MOI of 5. Following 3 days culture, 1 µl of culture supernatant (Sup) and cell extract (Pel, cells suspended in 1 ml PBS) were transferred directly to nitrocellulose. Recombinant CD11b and CD18 protein were detected by M2 anti-FLAG and KIM89 anti-CD18. Co-infections were performed in duplicate alongside single transfections and a negative control (SPD-CD23).

analysis of the infected cells and supernatant with an anti-FLAG monoclonal antibody (Figure 6.6).

On sequencing the dual expression vector used in the transfection it was discovered that these clones were found to have several deletions and mismatches which explains the lack of CD11b expression. A co-infection with the dual expressing baculovirus and CD11bNE single construct baculovirus gave the same intracellular expression pattern as observed with the co-infections.

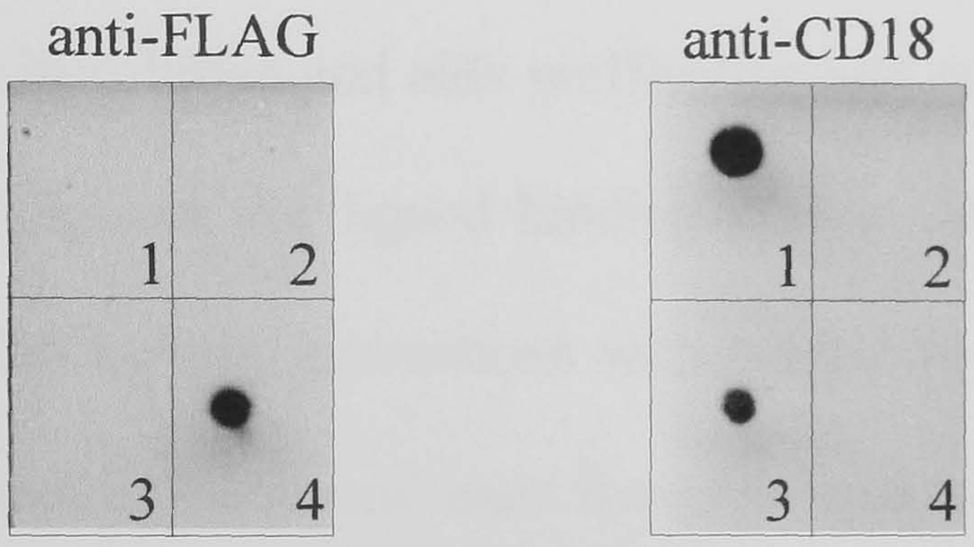

Figure 6.6: Dot Blot Analysis of Infection with Dual Expression Baculovirus

1 μl of Sf9 culture supernatants infected (MOI = 5) with recombinant baculovirus were directly blotted onto nitrocellulose and probed with anti-FLAG to detect CD11b expression and KIM89 to detect CD18. The following infections were analysed: (1) ten fold concentration of rbvCD11bNE/CD18N; (2) ten fold concentration of negative control supernatant (SPD-CD23); (3) CD18N positive control supernatant (4) CD11bNE positive control cell extract. CD18 was detected in the supernatant of the dual expression infection but not CD11b.

Table 6.4: Summary of Expression of Integrin subunits.

Baculovirus	Location	Size
CD18N	Secreted into media	~80kDa, some oligomerisation
CD11bNE	Cellular	~120kDa
CD11bNE/CD18N Co-infection	CD11b and CD18 in cellular fraction	Not determined
CD11bNE/CD18N Dual Expression	CD18 in media No CD11b detected	Not determined (CD11b DNA rearrangements)

6.4 Integrin binding Assays by ELISA

Expression of recombinant soluble αMβ2 using the baculovirus expression system was unproductive. Therefore, an alternative source of recombinant integrin was used for initial CD23 interaction studies. Soluble recombinant integrins (truncated at the transmembrane domain) have been successfully expressed in mammalian cells (CHO and COS cells) at Celltech (Stephens *et al.*, 2000). The alpha and beta subunits are secreted into the culture medium with a mouse-IgG Fc (mFc) or human IgG-Fc (hFc) fusion on the carboxy terminal end of the extracellular subunit. Fc promotes heterodimerisation in solution and aids purification and quantification, as well as being a useful additional epitope for ligand binding assays. Although the expression levels were fairly low (200 ng/ml), interactions with control proteins have been detected by ELISA. Table 6.5 details the recombinant integrins used and control ligands.

Table 6.5: Soluble recombinant integrins used in the following assays.

Integrin	Expression System	Control Ligand
αMβ2-mFc	CHO	iC3b
αvβ1-mFc	COS	Fibronectin
αvβ3-hFc	COS	Fibronectin RGD peptide
αvβ5-mFc	COS	Vitronectin RGD peptide

6.4.1 alpha m beta 2 (CD11b/CD18, Mac-1, CR3)

A ligand binding assay for αMβ2 interactions was established with iC3b by B. Sweeney, Celltech (described in Materials and Methods 2.5.8.7). Microtitre plates were coated overnight at 4 °C with 5 μg/ml Der-CD23 (Chapter 1), 5 μg/ml control ligand

iC3b and a BSA negative control. The culture supernatant and supernatant from mock transfected CHO cell was serially diluted and added to the wells. After three hours incubation at room temperature, the binding of the recombinant integrin was detected by an anti mouse Fc –HRP conjugate. Der-CD23 appeared to bind to the recombinant soluble αMβ2, above background levels, but was a much weaker interaction than the positive control (Figure 6.7a). A_{630} measurements greater than 1.0 could be obtained for the Der-CD23-integrin interaction by developing the enzyme reaction for longer (15 minutes).

To test the validity of the interaction, a serial dilution of anti- αMβ2 antibodies was incubated with a 1 in 5 dilution of αMβ2 supernatant for 1 hour and added to Der-CD23 coated wells. Any inhibition of binding would confirm that the interaction was occurring specifically via the integrin. Ab44 (anti αM) was reported to partially inhibit CD23 (in liposomes) binding to activated blood monocytes (Lecoanet-Henchoz *et al.*, 1995). This was also observed in these experiments (Figure 6.7b). KIM170, (recognising the heterodimeric receptor) and 6.5E (recognising the β_2 subunit) appeared to completely block binding at 1 μg/ml (antibodies mapped by Stephens et al., 1995). The blocking of CD23 interactions with anti-β2 antibodies demonstrates the requirement of the β subunit for ligand binding in the alpha subunit.

6.4.2 alpha v beta 3 (Vitronectin Receptor)

Another reported integrin to bind CD23 is αvβ3/CD47 complex on monocytes (Hermann *et al.*, 1999). A similar ELISA (materials and methods) was used to investigate whether CD23 was able to interact with the αvβ3 human IgG Fc fusion

a)

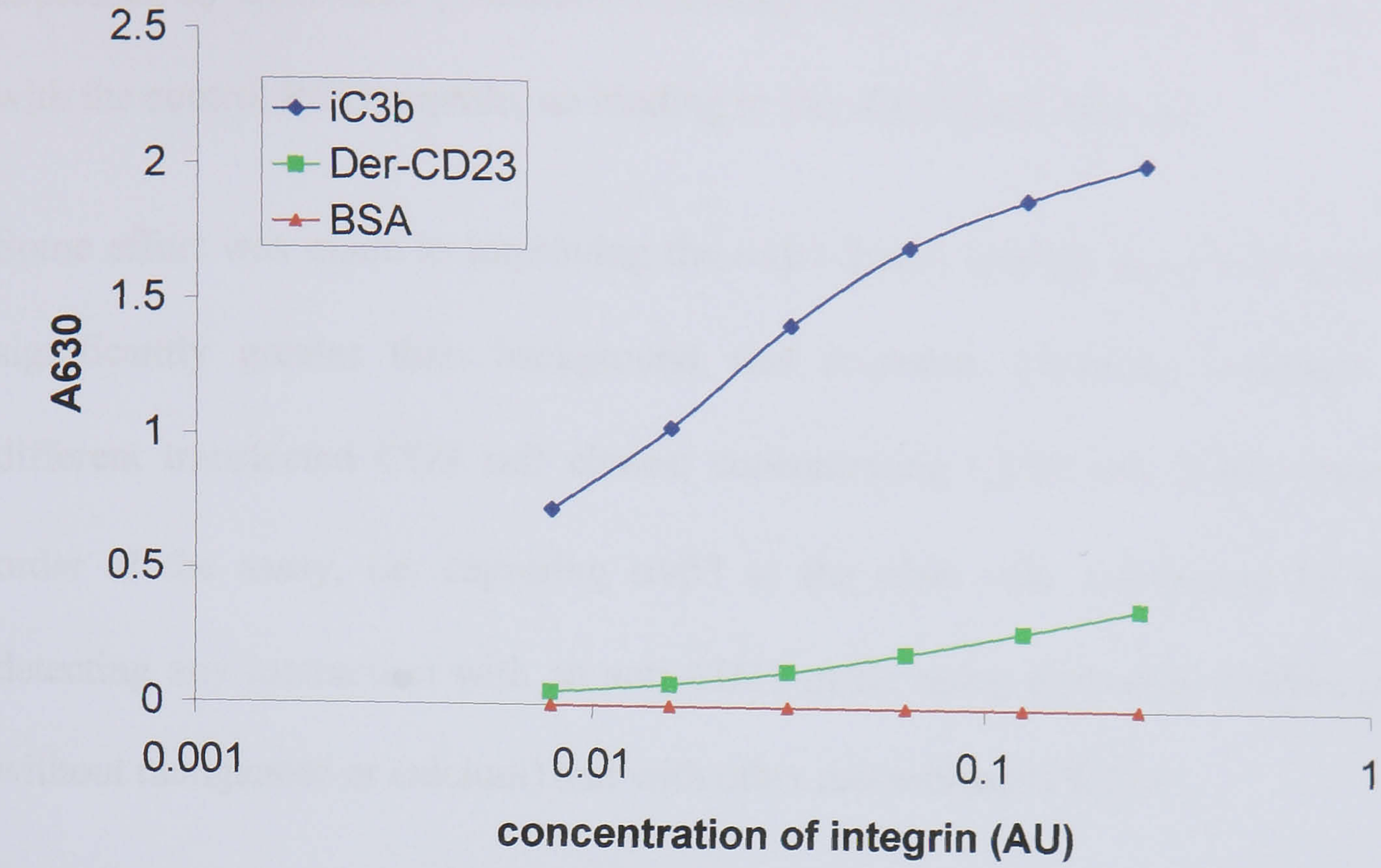

b)

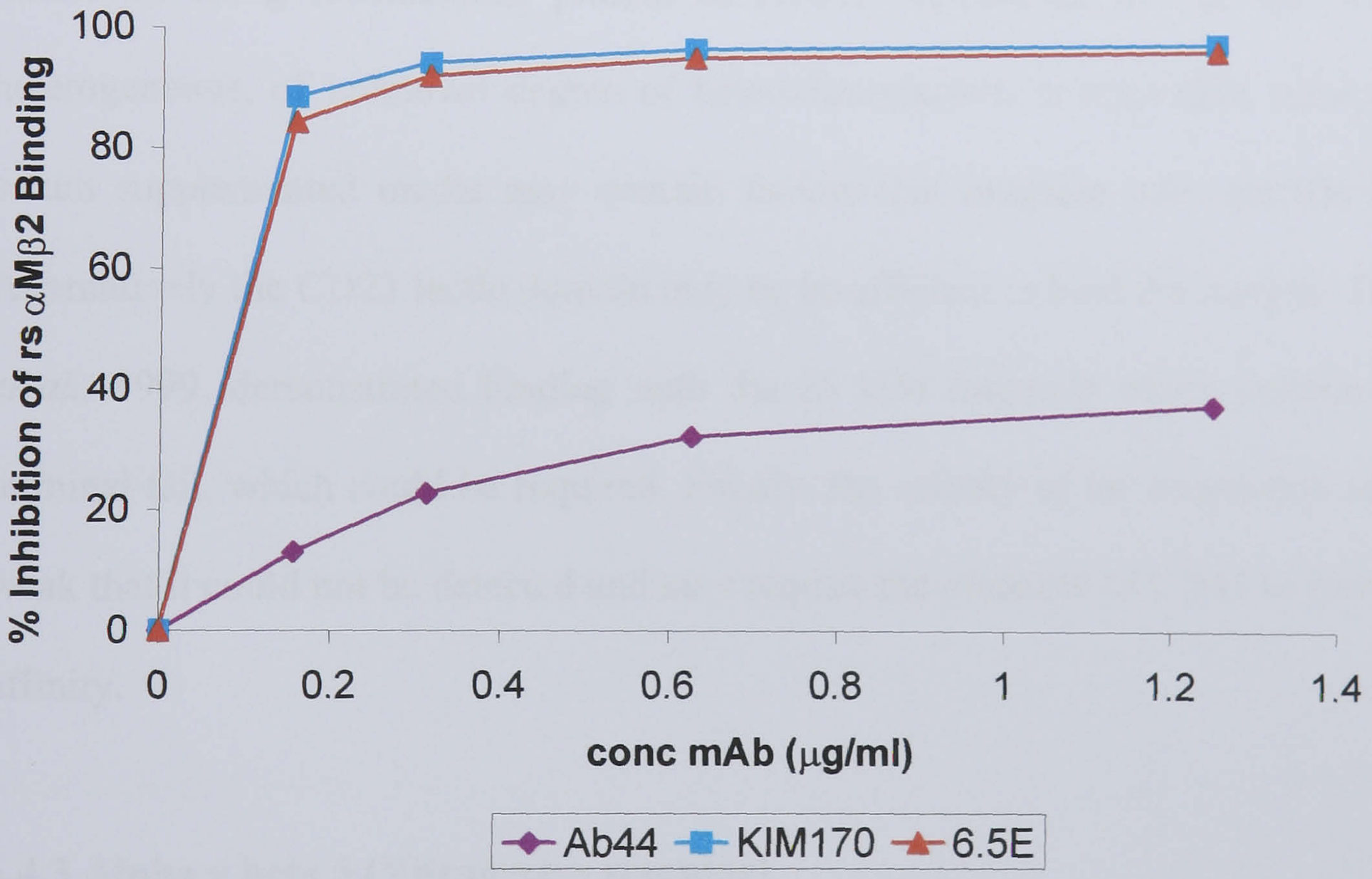

Figure 6.7: Recombinant Soluble αMβ2 Interaction with CD23

a) 5 μg/ml of ligand iC3b, Der-CD23 and BSA were coated on a microtitre plate. Serial dilutions of CD11b/CD18 CHO cell supernatants (and mock-transfected supernatant) were applied. Interactions were detected by an anti-mouse IgG-Fc HRP conjugate. No background signal was detected for either BSA or mock-transfected CHO culture supernatant. **b)** Dose dependent inhibition of the CD23-CD11b/CD18 interaction was seen with by incubation of supernatants with anti-CD11b/CD18 antibodies.

expressed by COS cells (Celltech). Although the recombinant αvβ3 integrin interacted with the control RGD peptide, no binding to Der-CD23 was detected.

Some effort was made to improving the αvβ3 ligand binding assay but no interaction significantly greater than background was recorded. Measures included: using a different transfected COS cell clones; concentrating CD23 and αvβ3; reversing the order of the assay, i.e. capturing αvβ3 to the plate with anti-human Fc mAb and detecting any interaction with an anti-CD23 mAb; using alternative buffers (with and without manganese or calcium) and with other recombinant CD23s.

There are many reasons why this interaction might not have been demonstrated. The hazard of using recombinant protein in culture supernatant is that the integrin is heterogeneous, of unknown degree of heterodimerisation or activation state and also serum supplemented media may contain factors that interfere with specific binding. Alternatively the CD23 lectin domain may be insufficient to bind the integrin. Hermann *et al.,* 1999, demonstrated binding with the 25 kDa fragment which contains the C-terminal tail, which could be required. Finally, the affinity of the interaction maybe so weak that it could not be detected and may require the presence of CD47 to increase the affinity.

6.4.3 Alpha v beta 5 (Vitronectin receptor)

Hermann *et al.,* 1999, mapped the CD23 interaction to the alpha subunit, and they also demonstrated binding to purified αv. This lead to an investigation of CD23 interactions with other αv integrins, in particular the closely related vitronectin receptor αvβ5. Matheson *et al.,* 1999, identified αvβ5 as a CD23 binding structure expressed on pre-B cells. In an attempt to support this evidence, CD23 was included in an αvβ1 αvβ5 ligand binding assay previously established at Celltech.

As before, 5 μg/ml CD23 was coated onto the plate, dilutions of recombinant integrin supernatants added and binding detected by anti-mouse IgG Fc HRP conjugate. All control proteins showed the integrins were active but specific binding to Der-CD23 was detected only with the recombinant αvβ5 (Figure 6.8). In order to establish optimum component concentrations for further experiments, Der-CD23 and αvβ5 supernatant were titrated against each other. Der-CD23 concentrations greater than 1.25 μg/ml were required to obtain A_{630} >1.0 with 4 fold dilutions of αvβ5 supernatant in TBS-Ca-Mn (results not shown).

To test whether the CD23 interaction was specific to αvβ5 in the culture supernatant, three anti-αvβ5 monoclonal antibodies were used to inhibit the soluble integrin binding to a CD23 coated plate. A serial dilution of the antibodies were made in a 4 fold dilution of αvβ5 supernatant (in TBS-Ca-Mn) and incubated at room temperature for 1 hour. The samples were added to CD23 coated plates (1.25 μg/ml Der-CD23) and interactions detected by an anti- mouse IgG Fc-HRP. Figure 6.9 shows that each antibody to some degree inhibited the interaction by blocking the ligand binding site in the alpha subunit or causing an unfavourable ligand-binding conformation. Furthermore, 2 mM EDTA was effective at inhibiting Der-CD23 αvβ5 binding. Divalent ions chelated by EDTA must be important for the ligand binding sites of CD23 or the integrin, or both.

Although the recombinant integrin supernatant may have been a heterogeneous, non purified mixture of subunits, the inhibition studies suggest that the interactions detected was not due to non-specific binding.

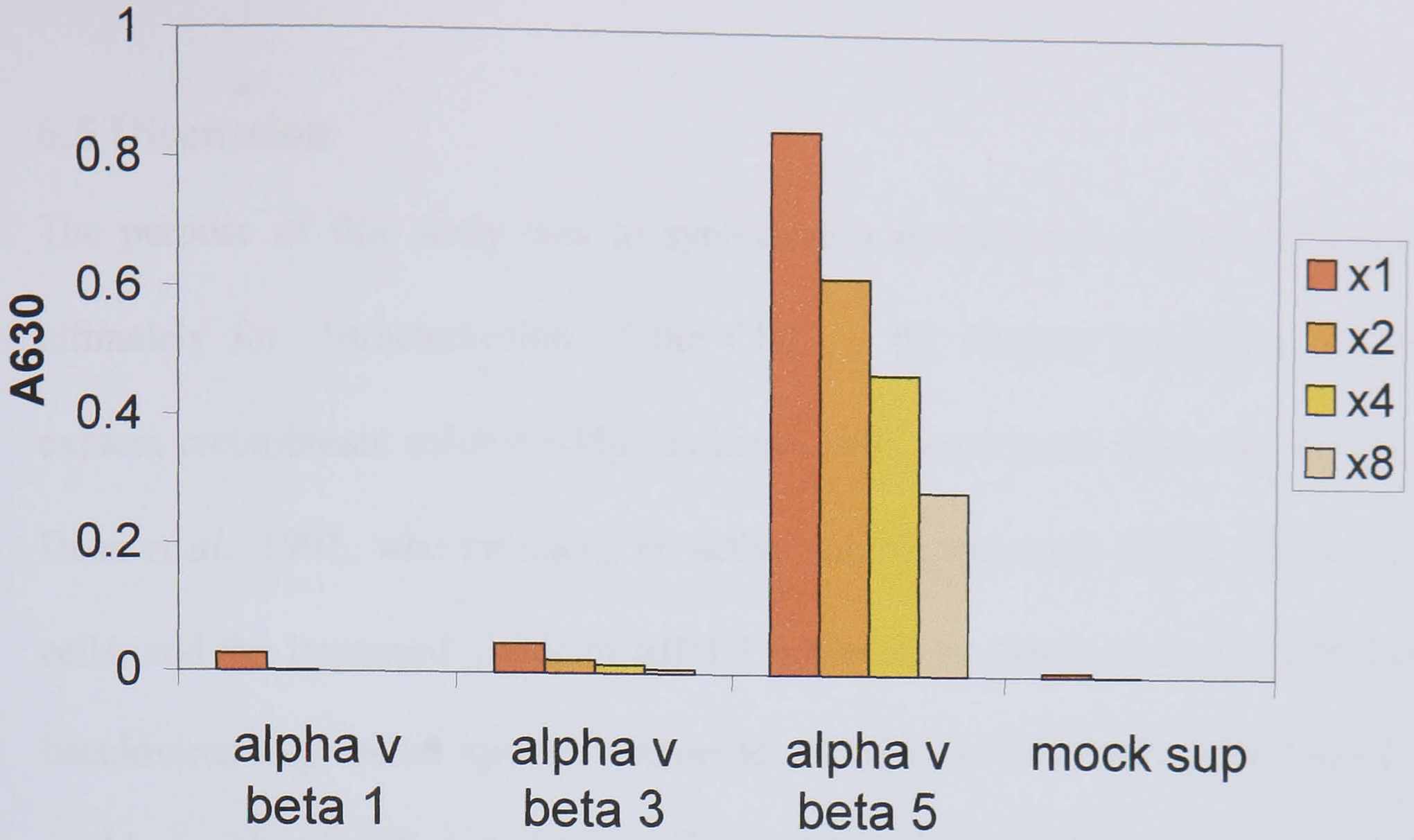

Figure 6.8: Interaction of Der-CD23 with Recombinant αv Integrin Supernatants

Serial dilutions of recombinant soluble αv integrins with IgG-Fc fusion (x1, x2, x4, x8) were added to Der-CD23 coated wells (5 μg/ml). Following a three hour incubation, interactions were detected by an anti-IgG Fc-HRP conjugate developed by TNB for 5 minutes. Each recombinant integrin bound their control ligand but only the αvβ5-Der-CD23 interactions was detected.

Figure 6.9: Inhibition of the CD23-αvβ5 Interaction.

5 μg/ml anti-αvβ5 monoclonal antibodies (Ab1961, Ab1980 and L230) were incubated in a 4-fold dilution of recombinant αvβ5-mouse IgG-Fc cell culture supernatant and blank supernatant (diluted into TBS-Ca-Mn). After 1 hour incubation, the samples were added to wells coated with 1 μg/ml Der-CD23. 5 mM EDTA was also effective at inhibiting the CD23-αvβ5 interaction.

6.5 Discussion

The purpose of this study was to synthesise a recombinant soluble β2 heterodimer ultimately for characterisation of the CD23 – β2 integrin interaction. Attempts to express recombinant soluble αMβ2 in insect cells were made following the success of Dana *et al.,* 1991, who produced an active soluble truncated αMβ2 secreted by COS cells, and the improved yields of αIIbβ3 achieved by Peterson *et al.,* 1998, using the baculovirus expression system. Fermenter cultures at this expression yield (1 mg/l) could provide enough material to purify and included in informative experiments such as surface plasmon resonance.

Using PCR techniques truncated CD11b and CD18 with their native leader sequences (N) were constructed in fragments, in doing so, an alternative leader and optional epitope tag (E) could be added. The assembled subunits termed CD18N and CD11bNE were cloned into pFastBac and recombinant baculovirus (rbv) containing each subunit were produced.

Analysis of transfected Sf9 cells by western blot show secretion of CD18 in the culture supernatant. The CD11b construct was present only in the cellular protein fraction. These findings were similar to those observed by Bennett *et al.,* 1993, where the presence of the β subunit of platelet αIIbβ3 was essential for the transport of the heterodimer to the membrane. Both CD18N and CD11bNE were the correct approximate molecular weight.

Unfortunately, co-infection of rbvCD18N and rbvCD11bNE resulted in neither construct being detected in the culture supernatants. This observation may be consistent with the heterodimer forming complexes within the cell that are insoluble or unable to be exported. There is a possibility that the optimal co-infection conditions were not

achieved, factors include: multiplicity of infection (MOI), infection time, temperature, media and host cell. The optimal MOI for CD11b fragments in one study was as low as 0.1 (Xia *et al.*, 1999) although the standard range is between 1-10. It was difficult to assess optimum conditions because of the low titre of rbvCD18N (1×10^5 pfu/ml) and large volumes required. The reason for low titre was not apparent but likely that the β2 subunit was interfering with the infection cycle of the baculovirus.

A dual expression baculovirus was used to overcome low titres and co-infection difficulties. By having the alpha subunit under the control of an earlier promoter, it was envisaged that less beta subunit would be free to able to interfere with subsequent rounds of infection. Indeed, a higher virus titre was achieved with dual expression baculovirus (5×10^7 pfu/ml). CD18 was secreted into the media, as before. However, the difficulties experienced in cloning the alpha subunit into the dual vector were reflected in the discovery of a rearrangement event that lead to the production of frameshifts and deletions in the CD11b DNA. This accounted for the lack of detection of the C-terminal FLAG epitope.

The baculovirus expression system using these subunit constructs failed to produce recombinant soluble αMβ2. The extracellular regions of the subunits are relatively complex for recombinant expression, with several domains of unknown structure or function, different activation conformations and many glycosylation sites. For our purposes the recombinant integrin can not be simplified. The CD23 binding site was mapped to the alpha subunit (Lecoanet-Henchoz *et al.*, 1995). Expressing alpha subunit alone has resulted in a recombinant subunit unable to bind ligand or was retained within the cell, as demonstrated with αIIb (O'Toole *et al.*, 1989; Bennett *et al.*, 1993 and also observed with these results). Simplifying the integrin further, for instance, expression of the αM I domain (Fairbanks *et al.*, 1995) was also not an option because it is unclear

whether the CD23 binding site is wholly encompassed in this region. Factor X has been shown to be the most effective inhibitor of CD23 binding to CD11b/c CD18 transfected COS cells of the β2 ligands tested by Lecoanet-Henchoz *et al.,* 1995. Although most CD11b/CD18 ligands map to the I domain, Factor X appeared to be only partially recognised by the I domain (Zhou *et al.,* 1994). This evidence could imply that other structural features (e.g. β subunit or the putative β propeller) are required for Factor X and, by extension, CD23 binding.

In collaboration with Celltech (Slough, UK) recombinant, soluble integrins expressed by mammalian cells were available for use in preliminary ligand binding assays with soluble CD23. These integrins contain an IgG Fc fusion to enhance heterodimerisation, aid purification and serve as a useful epitope in ligand binding assays (Stephens *et al.,* 2000). Interactions were detected Der-CD23 (CD23 lectin domain) and recombinant αMβ2 and αvβ5 culture supernatants. The interactions were shown to be integrin dependent because binding was inhibited by three integrin specific monoclonal antibodies. The interaction between Der-CD23 and αvβ5 was also metal ion dependant established by its inhibition with EDTA. Furthermore, these results stress that neither the stalk region nor the C-terminal tail (containing a reverse RGD sequence) of CD23 are essential for αMβ2 or αvβ5 binding. These studies support the findings of Lecoanet-Hencoz and Matheson *et al.,* 1999 and provide a basis for future detailed mapping and binding properties once the recombinant integrins are purified and characterised.

CHAPTER 7: GENERAL DISCUSSION

The work presented in thesis was intended to elucidate the structure of the CD23 C-type lectin domain and provide recombinant CD23 molecules to study the functions of human soluble CD23 fragments. To achieve these aims two novel recombinant proteins were expressed and characterised. Chapter 3 described the production of large yields of correctly folded CD23 lectin domain in *E.coli*. By using a different approach to purification, replacing size exclusion chromatography with hydrophobic interaction chromatography, pure folded CD23 was attained in a single step and losses were reduced. This domain was shown to bind an IgE Fc glycosylation mutant with an appreciable affinity ($K_A = 0.9 \times 10^7\ M^{-1}$) and had a low affinity for sCD21. Labelled preparations of Der-CD23 were made (^{15}N and $^{15}N/^{13}C$) and the assignment of residues in 2D and 3D NMR spectrometry is currently being carried out by J. McDonnell at the University of Oxford.

If successful, CD23 will be the first animal C-type lectin whose structure has been determined by NMR techniques. Using this data, the identification of the ligand binding sites can be also be elucidated without the delays generally encountered with co-crystallisation. The homology model based on mannose binding protein A (Weis *et al.*, 1991) shows large areas of charged residues and hydrophobicity (Figure 7.1). These are potentially important for forming ligand binding and additional trimer/dimer stabilisation to the stalk region. CD23 is a particularly interesting subject for ligand binding site analysis with respect to its many ligands and its ability to form protein-carbohydrate and protein-protein interactions.

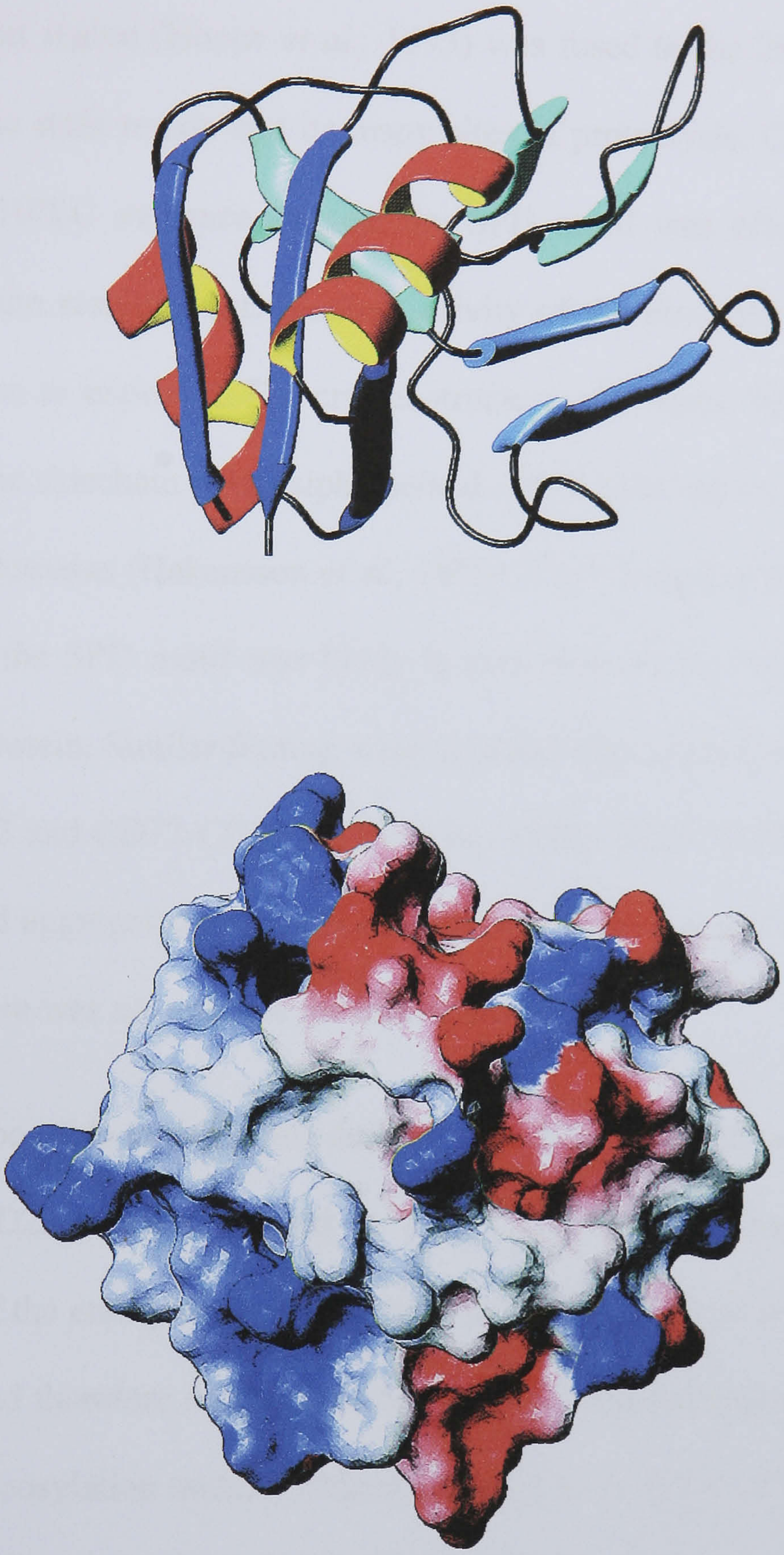

Figure 7.1: Models of CD23 C-type Lectin Domain

Top, shows a ribbon diagram of the secondary structure elements. The space filling model (by J. McDonnell), below, shows regions of hydrophobicity (blue) and charged residues (red).

Chapter 4 described the production of two designs for chimeric CD23 to provide a stable trimeric CD23 for molecular and biological studies. A surfactant protein-D trimerisation region (Hoppe *et al.,* 1993) was fused to the 25kDa CD23 fragment thus omitting the stalk region and its many sites of proteolysis. Chemical cross-linking and analytical HPLC evidence suggest the SPD motif was effective at forming trimers. However, the resulting IgE binding activity of the molecule was not enhanced by its trimerisation as expected. The crystal structure of trimeric SPD shows that the packing of a tyrosine sidechain in the alpha helical coiled coils causes asymmetric orientation of the lectin domains (Hakansson *et al.,* 1999). The wrong orientation of the CD23 lectins caused by the SPD motif was likely to contribute to the weak IgE interaction of this chimeric protein. Similar finding were obtained with other C-type animal lectin fusions: MBP-CD23 and CD72-CD23 (Kelly *et al.,* 1998). SPD-CD23 also readily degraded to 16 kDa and aggregated on purification from baculovirus and *E.coli* expression systems and therefore was not suitable for further studies.

It was not possible to determine definitively whether the LZ motif resulted in dimeric or trimeric CD23 when expressed in *E.coli* and refolded from inclusion bodies. The presence of the endogenous stalk region may have benefited the orientation of the lectin domains and therefore its IgE binding activity. BIAcore data estimates the LZ-CD23 – IgE Fc (glycosylation mutant) affinity constant to be $5.3 \times 10^7\ M^{-1}$ which was similar to the cell binding data with membrane bound CD23 and this Fc mutant ($K_A = 3.2 \times 10^7\ M^{-1}$, Young *et al.,* 1995). This recombinant chimera appeared to be stable in culture conditions for two weeks without any evidence of detectable breakdown product. This made LZ-CD23 a suitable molecular tool for functional assays.

Many anti-CD23 antibodies have been shown to inhibit IL-4/CD40L induced IgE production (Wakai *et al.,* 1993, Bonnefoy *et al.,* 1987, Bettler *et al.,* 1987) yet the mechanism of CD23's role in IgE regulation is not fully understood. The inclusion of Der-CD23 and LZ-CD23 in an *in vitro* IgE synthesis assay was hoped to demonstrate the reported suppression and enhancement of IgE synthesis of the 16kDa and >25kDa sCD23, respectively (Sarfati *et al.,* 1992 and Chretien *et al.,* 1990). Using excess amounts of each recombinant protein resulted in the inhibition of IgE production, particularly LZ-CD23. It is likely that LZ-CD23 in high concentrations was effecting other cellular mechanisms and possibly on cells other than B cells in the PBMC preparation e.g. monocytes. Work is ongoing in our laboratory to optimise the concentrations of the components in the *in vitro* system with human PBMC and tonsillar B cells.

The molecular details of the activity of sCD23 on monocytes was explored using recombinant integrins in cell free binding assays. The integrins αMβ2, αXβ2, (i.e. CD11b and CD11b integrins, Lecoanet-Henchoz *et al.,* 1995) and αvβ3 (Hermann *et al.,* 1999) have been identified as sCD23 binding receptors on monocytes, and αvβ5 on a pre B cell like cell line (Matheson *et al.,* 1999). In Chapter 6 work was presented on the construction of a recombinant soluble integrin (αMβ2) using the baculovirus expression system. Expression of both subunits was detected but no heterodimer was secreted. Considering the complexity and uncharacterised nature of the integrin subunits recombinant expression remains an ambitious task.

Alternatively, binding assays were carried out in a using recombinant soluble integrin successfully expressed in mammalian cells (in collaboration with Celltech, Slough). Interactions between Der-CD23 and αMβ2 and αvβ5 were detected. Inhibition of these interactions with an array of anti- αMβ2 and anti- αvβ5 antibodies and EDTA suggest

these experiments are first evidence of CD23-integrin binding without the presence of other membrane proteins. Interactions with the lectin domain protein (Der-CD23) show that the inverse RGD integrin binding motif in the C-terminal tail is not required for binding. To date no RGD peptides or anti RGD monoclonal antibodies have been demonstrated to inhibit CD23 ligand binding. The ELISAs described are a good basis for future characterisation and inhibition of interactions using purified recombinant soluble integrin.

The ability of the 16 kDa fragment to bind certain integrins may provide an explanation to how these sCD23 fragments are able to suppress IgE synthesis *in vitro* PBMC cultures. Monomeric CD23 triggers the release of pro-inflammatory cytokines by monocytes through CD11b/CD18, CD11c/CD18 and αvβ3 (Armant *et al.*, 1994; Lecoanet-Henchoz *et al.*, 1995; Hermann *et al.*, 1999; Aubry *et al.*, 1997; Rezzonico *et al.*, 2000). In particular, the inflammatory cytokine IFN-γ has an antagonistic effect on IL-4 stimulated IgE production (Chretien *et al.*, 1990). The bias toward of T_H1 immunity through the hypothetical binding of Der-CD23 to β2 or αv integrins could be investigated further using PBMC cultures.

High sCD23 serum levels are found in IgE independent chronic inflammatory diseases. The importance of CD23 in inflammatory mechanisms was demonstrated by the alleviation of symptoms in the collagen induced mouse model of rheumatoid arthritis with anti-CD23 monoclonal antibodies (Plater-Zyberg and Bonnefoy, 1995). Ultimately, the structural details of the CD23 lectin domain and well characterised interactions with its ligands will aid the understanding of the biological role of CD23 and benefit the development of potential therapies for allergic, certain B cell lymphomas and inflammatory diseases.

REFERENCES

Anderson CL, Spiegelberg HL. Macrophage receptors for IgE: binding of IgE to specific IgE Fc receptors on a human macrophage cell line, U937. J Immunol. 1981 Jun;126(6):2470-3.

Armant M, Ishihara H, Rubio M, Delespesse G, Sarfati M. Regulation of cytokine production by soluble CD23: costimulation of interferon gamma secretion and triggering of tumor necrosis factor alpha release. J Exp Med. 1994 Sep 1;180(3):1005-11.

Armant M, Rubio M, Delespesse G, Sarfati M. Soluble CD23 directly activates monocytes to contribute to the antigen-independent stimulation of resting T cells. J Immunol. 1995 Nov 15;155(10):4868-75.

Arnaout,M.A., Gupta,S.K., Pierce,M.W. and Tenen,D.G. Amino acid sequence of the alpha subunit of human leukocyte adhesion receptor Mo1 (complement receptor type 3) J. Cell Biol. 106 (6), 2153-2158 (1988)

Arock M, Michel L, Dalloul AH, Guillosson JJ, Debre P, Mossalayi MD. Soluble CD23 increases IL-3 induction of histamine synthesis by human bone marrow cells. Int Arch Allergy Appl Immunol. 1991;96(2):190-2.

Aubry JP, Dugas N, Lecoanet-Henchoz S, Ouaaz F, Zhao H, Delfraissy JF, Graber P, Kolb JP, Dugas B, Bonnefoy JY. The 25-kDa soluble CD23 activates type III constitutive nitric oxide-synthase activity via CD11b and CD11c expressed by human monocytes. J Immunol. 1997 Jul 15;159(2):614-22.

Aubry JP, Pochon S, Gauchat JF, Nueda-Marin A, Holers VM, Graber P, Siegfried C, Bonnefoy JY. CD23 interacts with a new functional extracytoplasmic domain involving N-linked oligosaccharides on CD21. J Immunol. 1994 Jun 15;152(12):5806-13.

Aubry JP, Pochon S, Graber P, Jansen KU, Bonnefoy JY. CD21 is a ligand for CD23 and regulates IgE production. Nature. 1992 Aug 6;358(6386):505-7.

Bajorath J, Aruffo A. Structure-based modeling of the ligand binding domain of the human cell surface receptor CD23 and comparison of two independently derived molecular models. Protein Sci 1996 Feb;5(2):240-7

Bartlett WC, Kelly AE, Johnson CM, Conrad DH. Analysis of murine soluble Fc epsilon RII sites of cleavage and requirements for dual-affinity interaction with IgE. J Immunol. 1995 May 1;154(9):4240-6.

Beavil AJ, Edmeades RL, Gould HJ, Sutton BJ. Alpha-helical coiled-coil stalks in the low-affinity receptor for IgE (Fc epsilon RII/CD23) and related C-type lectins. Proc Natl Acad Sci U S A. 1992 Jan 15;89(2):753-7.

Beavil AJ, Young RJ, Sutton BJ, Perkins SJ. Bent domain structure of recombinant human IgE-Fc in solution by X-ray and neutron scattering in conjunction with an automated curve fitting procedure. Biochemistry. 1995 Nov 7;34(44):14449-61.

Beavil RL, Graber P, Aubonney N, Bonnefoy JY, Gould HJ. CD23/Fc epsilon RII and its soluble fragments can form oligomers on the cell surface and in solution. Immunology. 1995 Feb;84(2):202-6.

Ben-Bassat A. Purification and analysis of Recombinant proteins. Ed Seetharam and Sharma 1990 Chapter 6 148-159

Bennett JS, Kolodziej MA, Vilaire G, Poncz M. Determinants of the intracellular fate of truncated forms of the platelet glycoproteins IIb and IIIa. J Biol Chem. 1993 Feb 15;268(5):3580-5.

Berman PW, Nakamura GR, Riddle L, Chiu H, Fisher K, Champe M, Gray AM, Ward P, Fong S. Biosynthesis and function of membrane bound and secreted forms of recombinant CD11b/CD18 (Mac-1). J Cell Biochem. 1993 Jun;52(2):183-95.

Bertho JM, Fourcade C, Dalloul AH, Debre P, Mossalayi MD. Synergistic effect of interleukin 1 and soluble CD23 on the growth of human CD4+ bone marrow-derived T cells. Eur J Immunol. 1991 Apr;21(4):1073-6.

Bettler B, Texido G, Raggini S, Ruegg D, Hofstetter H. Immunoglobulin E-binding site in Fc epsilon receptor (Fc epsilon RII/CD23) identified by homolog-scanning mutagenesis. J Biol Chem. 1992 Jan 5;267(1):185-91.

Billaud M, Busson P, Huang D, Mueller-Lantzch N, Rousselet G, Pavlish O, Wakasugi H, Seigneurin JM, Tursz T, Lenoir GM. Epstein-Barr virus (EBV)-containing nasopharyngeal carcinoma cells express the B-cell activation antigen blast2/CD23 and low levels of the EBV receptor CR2. J Virol. 1989 Oct;63(10):4121-8.

Birnboim HC. A rapid alkaline extraction method for the isolation of plasmid DNA. Methods Enzymol. 1983;100:243-55.
Bohmann D, Tjian R. Biochemical analysis of transcriptional activation by Jun: differential activity of c- and v-Jun. Cell. 1989 Nov 17;59(4):709-17.

Bonnefoy JY, Aubry JP, Peronne C, Wijdenes J, Banchereau J. Production and characterization of a monoclonal antibody specific for the human lymphocyte low affinity receptor for IgE: CD 23 is a low affinity receptor for IgE. J Immunol. 1987 May 1;138(9):2970-8.

Bonnefoy JY, Guillot O, Spits H, Blanchard D, Ishizaka K, Banchereau J. The low-affinity receptor for IgE (CD23) on B lymphocytes is spatially associated with HLA-DR antigens. J Exp Med. 1988 Jan 1;167(1):57-72.

Cairns JA, Gordon J. Intact, 45-kDa (membrane) form of CD23 is consistently mitogenic for normal and transformed B lymphoblasts. Eur J Immunol. 1990 Mar;20(3):539-43.

Chen JR, Gu BJ, Dao LP, Bradley CJ, Mulligan SP, Wiley JS. Transendothelial migration of lymphocytes in chronic lymphocytic leukaemia is impaired and involved down-regulation of both L-selectin and CD23. Br J Haematol. 1999 Apr;105(1):181-9.

Chretien I, Pene J, Briere F, De Waal Malefijt R, Rousset F, De Vries JE. Regulation of human IgE synthesis. I. Human IgE synthesis in vitro is determined by the reciprocal antagonistic effects of interleukin 4 and interferon-gamma. Eur J Immunol. 1990 Feb;20(2):243-51.

Christie G, Barton A, Bolognese B, Buckle DR, Cook RM, Hansbury MJ, Harper GP, Marshall LA, McCord ME, Moulder K, Murdock PR, Seal SM, Spackman VM, Weston BJ, Mayer RJ. IgE secretion is attenuated by an inhibitor of proteolytic processing of CD23 (Fc epsilonRII). Eur J Immunol. 1997 Dec;27(12):3228-35.

Clark K, Newham P, Burrows L, Askari JA, Humphries MJ. Production of recombinant soluble human integrin alpha4beta1. FEBS Lett. 2000 Apr 14;471(2-3):182-6.

Dana N, Fathallah DM, Arnaout MA. Expression of a soluble and functional form of the human beta 2 integrin CD11b/CD18. Proc Natl Acad Sci U S A. 1991 Apr 15;88(8):3106-10.

Delespesse G, Sarfati M, Hofstetter H. Human IgE-binding factors. Immunol Today. 1989 May;10(5):159-64.

Delespesse G, Suter U, Mossalayi D, Bettler B, Sarfati M, Hofstetter H, Kilcherr E, Debre P, Dalloul A. Expression, structure, and function of the CD23 antigen. Adv Immunol. 1991;49:149-91.

Denda S, Reichardt LF, Muller U. Identification of osteopontin as a novel ligand for the integrin alpha8 beta1 and potential roles for this integrin-ligand interaction in kidney morphogenesis. Mol Biol Cell. 1998 Jun;9(6):1425-35.

Eble JA, Wucherpfennig KW, Gauthier L, Dersch P, Krukonis E, Isberg RR, Hemler ME. Recombinant soluble human alpha 3 beta 1 integrin: purification, processing, regulation, and specific binding to laminin-5 and invasin in a mutually exclusive manner. Biochemistry. 1998 Aug 4;37(31):10945-55.

Fairbanks MB, Pollock JR, Prairie MD, Scahill TA, Baczynskyj L, Heinrikson RL, Stockman BJ. Purification and structural characterization of the CD11b/CD18 integrin alpha subunit I domain reveals a folded conformation in solution. FEBS Lett. 1995 Aug 7;369(2-3):197-201.

Fearon DT, Carroll MC. Regulation of B lymphocyte responses to foreign and self-antigens by the CD19/CD21 complex. Annu Rev Immunol. 2000;18:393-422.

Flores-Romo L, Cairns JA, Millsum MJ, Gordon J. Soluble fragments of the low-affinity IgE receptor (CD23) inhibit the spontaneous migration of U937 monocytic cells: neutralization of MIF-activity by a CD23 antibody. Immunology. 1989 Aug;67(4):547-9.

Flores-Romo L, Johnson GD, Ghaderi AA, Stanworth DR, Veronesi A, Gordon J. Functional implication for the topographical relationship between MHC class II and the low-affinity IgE receptor: occupancy of CD23 prevents B lymphocytes from stimulating allogeneic mixed lymphocyte responses. Eur J Immunol. 1990 Nov;20(11):2465-9.

Fremeaux-Bacchi V, Aubry JP, Bonnefoy JY, Kazatchkine MD, Kolb JP, Fischer EM. Soluble CD21 induces activation and differentiation of human monocytes through binding to membrane CD23. Eur J Immunol. 1998 Dec;28(12):4268-74.

Fremeaux-Bacchi V, Bernard I, Maillet F, Mani JC, Fontaine M, Bonnefoy JY, Kazatchkine MD, Fischer E. Human lymphocytes shed a soluble form of CD21 (the C3dg/Epstein-Barr virus receptor, CR2) that binds iC3b and CD23. Eur J Immunol. 1996 Jul;26(7):1497-503.

Garman SC, Wurzburg BA, Tarchevskaya SS, Kinet JP, Jardetzky TS. Structure of the Fc fragment of human IgE bound to its high-affinity receptor Fc epsilonRI alpha. Nature. 2000 Jul 20;406(6793):259-66.

Gordon J, Pound JD. Fortifying B cells with CD154: an engaging tale of many hues. Immunology. 2000 Jul;100(3):269-80.

Graber P, Jansen K, Pochon S, Shields J, Aubonney N, Turcatti G, Bonnefoy JY. Purification and characterization of biologically active human recombinant 37 kDa soluble CD23 (sFc epsilon RII) expressed in insect cells. J Immunol Methods. 1992 May 18;149(2):215-26.

Graves BJ, Crowther RL, Chandran C, Rumberger JM, Li S, Huang KS, Presky DH, Familletti PC, Wolitzky BA, Burns DK. Insight into E-selectin/ligand interaction from the crystal structure and mutagenesis of the lec/EGF domains. Nature. 1994 Feb 10;367(6463):532-8.

Grosjean I, Lachaux A, Bella C, Aubry JP, Bonnefoy JY, Kaiserlian D. CD23/CD21 interaction is required for presentation of soluble protein antigen by lymphoblastoid B cell lines to specific CD4+ T cell clones. Eur J Immunol. 1994 Dec;24(12):2982-6.

Grzesiek S, Bax A. Amino acid type determination in the sequential assignment procedure of uniformly 13C/15N-enriched proteins. J Biomol NMR 1993 Mar;3(2):185-204

Gu B, Bendall LJ, Wiley JS. Adenosine triphosphate-induced shedding of CD23 and L-selectin (CD62L) from lymphocytes is mediated by the same receptor but different metalloproteases. Blood. 1998 Aug 1;92(3):946-51.

Gulino D, Martinez P, Delachanal E, Concord E, Duperray A, Alemany M, Marguerie G. Expression and purification of a soluble functional form of the platelet alpha IIb beta 3 integrin. Eur J Biochem. 1995 Jan 15;227(1-2):108-15.

Hakansson K, Lim NK, Hoppe HJ, Reid KB. Crystal structure of the trimeric alpha-helical coiled-coil and the three lectin domains of human lung surfactant protein D. Structure Fold Des. 1999 Mar 15;7(3):255-64.

Hakansson K, Reid KB. Collectin structure: a review. Protein Sci. 2000 Sep;9(9):1607-17.

Halberg DF, Wager RE, Farrell DC, Hildreth J 4th, Quesenberry MS, Loeb JA, Holland EC, Drickamer K. Major and minor forms of the rat liver asialoglycoprotein receptor are independent galactose-binding proteins. Primary structure and glycosylation heterogeneity of minor receptor forms. J Biol Chem. 1987 Jul 15;262(20):9828-38.

Hasbold J, Lyons AB, Kehry MR, Hodgkin PD. Cell division number regulates IgG1 and IgE switching of B cells following stimulation by CD40 ligand and IL-4. Eur J Immunol. 1998 Mar;28(3):1040-51.

Henchoz S, Gauchat JF, Aubry JP, Graber P, Pochon S, Bonnefoy JY. Stimulation of human IgE production by a subset of anti-CD21 monoclonal antibodies: requirement of a co-signal to modulate epsilon transcripts. Immunology. 1994 Feb;81(2):285-90.

Henchoz-Lecoanet S, Jeannin P, Aubry JP, Graber P, Bradshaw CG, Pochon S, Bonnefoy JY. The Epstein-Barr virus-binding site on CD21 is involved in CD23 binding and interleukin-4-induced IgE and IgG4 production by human B cells. Immunology. 1996 May;88(1):35-9.

Hermann P, Armant M, Brown E, Rubio M, Ishihara H, Ulrich D, Caspary RG, Lindberg FP, Armitage R, Maliszewski C, Delespesse G, Sarfati M. The vitronectin receptor and its associated CD47 molecule mediates proinflammatory cytokine synthesis in human monocytes by interaction with soluble CD23. J Cell Biol. 1999 Feb 22;144(4):767-75.

Heyman B, Tianmin L, Gustavsson S. In vivo enhancement of the specific antibody response via the low-affinity receptor for IgE. Eur J Immunol. 1993 Jul;23(7):1739-42.

Heyman B. Regulation of antibody responses via antibodies, complement, and Fc receptors. Annu Rev Immunol. 2000;18:709-37.

Holmskov U, Laursen SB, Malhotra R, Wiedemann H, Timpl R, Stuart GR, Tornoe I, Madsen PS, Reid KB, Jensenius JC. Comparative study of the structural and functional properties of a bovine plasma C-type lectin, collectin-43, with other collectins. Biochem J. 1995 Feb 1;305 (Pt 3):889-96.

Hoppe HJ, Barlow PN, Reid KB. A parallel three stranded alpha-helical bundle at the nucleation site of collagen triple-helix formation. FEBS Lett. 1994 May 16;344(2-3):191-5.

Huissoon AP, Emery P, Bacon PA, Gordon J, Salmon M. Increased expression of CD23 in rheumatoid synovitis. Scand J Rheumatol. 2000;29(3):154-9.

Ikuta K, Takami M, Kim CW, Honjo T, Miyoshi T, Tagaya Y, Kawabe T, Yodoi J. Human lymphocyte Fc receptor for IgE: sequence homology of its cloned cDNA with animal lectins. Proc Natl Acad Sci U S A. 1987 Feb;84(3):819-23.

Jeannin P, Lecoanet-Henchoz S, Delneste Y, Gauchat JF, Bonnefoy JY. Alpha-1 antitrypsin up-regulates human B cell differentiation selectively into IgE- and IgG4- secreting cells. Eur J Immunol. 1998 Jun;28(6):1815-22.

Joshi L, Davis TR, Mattu TS, Rudd PM, Dwek RA, Shuler ML, Wood HA. Influence of baculovirus-host cell interactions on complex N-linked glycosylation of a recombinant human protein. Biotechnol Prog. 2000 Jul-Aug;16(4):650-6.

Katira A, Gordon J. An enzyme-linked immunosorbent assay specific for transient (29-37-kDa) fragments of soluble CD23/IgE-binding factors. Allergy. 1995 Aug;50(8):689-92.

Kelly AE, Chen BH, Woodward EC, Conrad DH. Production of a chimeric form of CD23 that is oligomeric and blocks IgE binding to the Fc epsilonRI. J Immunol. 1998 Dec 15;161(12):6696-704.

Kijimoto-Ochiai S, Horimoto E, Uede T. Demonstration of the interaction between the CD23 molecule and the galactose residue of glycoproteins. Immunol Lett. 1994 Apr;40(1):49-53.

Kijimoto-Ochiai S, Noguchi A. Two peptides from CD23, including the inverse RGD sequence and its related peptide, interact with the MHC class II molecule. Biochem Biophys Res Commun. 2000 Jan 27;267(3):686-91.

Kijimoto-Ochiai S, Uede T. CD23 molecule acts as a galactose-binding lectin in the cell aggregation of EBV-transformed human B-cell lines. Glycobiology. 1995 Jun;5(4):443-8.

Kikutani H, Inui S, Sato R, Barsumian EL, Owaki H, Yamasaki K, Kaisho T, Uchibayashi N. Hardy RR, Hirano T, et al. Molecular structure of human lymphocyte receptor for immunoglobulin E. Cell. 1986 Dec 5;47(5):657-65.

Kishimoto,T.K., O'Connor,K., Lee,A., Roberts,T.M. and Springer,T.A. Cloning of the beta subunit of the leukocyte adhesion proteins: homology to an extracellular matrix receptor defines a novel supergene family Cell 48 (4), 681-690 (1987)

Kondo H, Ichikawa Y, Nakamura K, Tsuchiya S. Cloning of cDNAs for new subtypes of murine low-affinity Fc receptor for IgE (Fc epsilon RII/CD23). Int Arch Allergy Immunol. 1994 Sep;105(1):38-48.

Kyhse-Andersen J. Electroblotting of multiple gels: a simple apparatus without buffer tank for rapid transfer of proteins from polyacrylamide to nitrocellulose.
J Biochem Biophys Methods. 1984 Dec;10(3-4):203-9.

Laemmli UK. Cleavage of structural proteins during the assembly of the head of bacteriophage T4. Nature. 1970 Aug 15;227(259):680-5.

Lantero S, Alessandri G, Spallarossa D, Scarso L, Rossi GA. Stimulation of eosinophil IgE low-affinity receptor leads to increased adhesion molecule expression and cell migration. Eur Respir J. 2000 Nov;16(5):940-6.

Lecoanet-Henchoz S, Plater-Zyberk C, Graber P, Gretener D, Aubry JP, Conrad DH, Bonnefoy JY. Mouse CD23 regulates monocyte activation through an interaction with the adhesion molecule CD11b/CD18. Eur J Immunol. 1997 Sep;27(9):2290-4.

Lee JO, Rieu P, Arnaout MA, Liddington R. Crystal structure of the A domain from the alpha subunit of integrin CR3 (CD11b/CD18). Cell. 1995 Feb 24;80(4):631-8.

Letellier M, Nakajima T, Delespesse G. IgE receptor on human lymphocytes. IV. Further analysis of its structure and of the role of N-linked carbohydrates. J Immunol. 1988 Oct 1;141(7):2374-81.

Letellier M, Nakajima T, Pulido-Cejudo G, Hofstetter H, Delespesse G. Mechanism of formation of human IgE-binding factors (soluble CD23): III. Evidence for a receptor (Fc epsilon RII)-associated proteolytic activity. J Exp Med. 1990 Sep 1;172(3):693-700.

Letellier M, Sarfati M, Delespesse G. Mechanisms of formation of IgE-binding factors (soluble CD23)--I. Fc epsilon R II bearing B cells generate IgE-binding factors of different molecular weights. Mol Immunol. 1989 Dec;26(12):1105-12.

Liu YJ, Mason DY, Johnson GD, Abbot S, Gregory CD, Hardie DL, Gordon J, MacLennan IC. Germinal center cells express bcl-2 protein after activation by signals which prevent their entry into apoptosis. Eur J Immunol. 1991 Aug;21(8):1905-10.

Lopez-Matas M, Rodriguez-Justo M, Morilla R, Catovsky D, Matutes E. Quantitative expression of CD23 and its ligand CD21 in chronic lymphocytic leukemia. Haematologica. 2000 Nov;85(11):1140-5.

Ludin C, Hofstetter H, Sarfati M, Levy CA, Suter U, Alaimo D, Kilchherr E, Frost H, Delespesse G. Cloning and expression of the cDNA coding for a human lymphocyte IgE receptor. EMBO J. 1987 Jan;6(1):109-14.

Marolewski AE, Buckle DR, Christie G, Earnshaw DL, Flamberg PL, Marshall LA, Smith DG, Mayer RJ. CD23 (FcepsilonRII) release from cell membranes is mediated by a membrane-bound metalloprotease. Biochem J. 1998 Aug 1;333 (Pt 3):573-9.

Marshall LA, Hansbury MJ, Bolognese BJ, Gum RJ, Young PR, Mayer RJ. Inhibitors of the p38 mitogen-activated kinase modulate IL-4 induction of low affinity IgE receptor (CD23) in human monocytes. J Immunol. 1998 Dec 1;161(11):6005-13.

Matheson J, White L, Ozanne B, Cushley W. The alpha v beta 5 vitronectin receptor binds CD23 in human B-cell precursor cell lines. Immunology 1999; 98 (supplement 1):58

Mayer RJ, Bolognese BJ, Al-Mahdi N, Cook RM, Flamberg PL, Hansbury MJ, Khandekar S, Appelbaum E, Faller A, Marshall LA. Inhibition of CD23 processing correlates with inhibition of IL-4-stimulated IgE production in human PBL and hu-PBL-reconstituted SCID mice. Clin Exp Allergy. 2000 May;30(5):719-27.

McDonnell JM, Calvert R, Beavil RL, Beavil AJ, Henry AJ, Sutton BJ, Gould HJ, Cowburn D. The structure of the IgE Cepsilon2 domain and its role in stabilizing the complex with its high-affinity receptor FcepsilonRIalpha. Nat Struct Biol. 2001 May;8(5):437-41.

McKay BS, Annis DS, Honda S, Christie D, Kunicki TJ. Molecular requirements for assembly and function of a minimized human integrin alphaIIbbeta3. J Biol Chem. 1996 Nov 29;271(48):30544-7.

Mehta RJ, Diefenbach B, Brown A, Cullen E, Jonczyk A, Gussow D, Luckenbach GA, Goodman SL. Transmembrane-truncated alphavbeta3 integrin retains high affinity for ligand binding: evidence for an 'inside-out' suppressor? Biochem J. 1998 Mar 1;330 (Pt 2):861-9.

Morris AE, Remmele RL Jr, Klinke R, Macduff BM, Fanslow WC, Armitage RJ. Incorporation of an isoleucine zipper motif enhances the biological activity of soluble CD40L (CD154). J Biol Chem. 1999 Jan 1;274(1):418-23.

Mossalayi MD, Paul-Eugene N, Ouaaz F, Arock M, Kolb JP, Kilchherr E, Debre P, Dugas B. Involvement of Fc epsilon RII/CD23 and L-arginine-dependent pathway in IgE-mediated stimulation of human monocyte functions. Int Immunol. 1994 Jul;6(7):931-4.

Moulder K, Barton A, Weston B. CD23-mediated homotypic cell adhesion: the role of proteolysis. Eur J Immunol. 1993 Sep;23(9):2066-71.

Moulder K. The role of RGD in CD23-mediated cell adhesion. Immunol Today. 1996 Apr;17(4):198-9.

Munoz O, Brignone C, Grenier-Brossette N, Bonnefoy JY, Cousin JL. Binding of anti-CD23 monoclonal antibody to the leucine zipper motif of FcepsilonRII/CD23 on B cell membrane promotes its proteolytic cleavage. Evidence for an effect on the oligomer/monomer equilibrium. J Biol Chem. 1998 Nov 27;273(48):31795-800.

Nakamura T, Kloetzer WS, Brams P, Hariharan K, Chamat S, Cao X, LaBarre MJ, Chinn PC, Morena RA, Shestowsky WS, Li YP, Chen A, Reff ME. In vitro IgE inhibition in B cells by anti-CD23 monoclonal antibodies is functionally dependent on the immunoglobulin Fc domain. Int J Immunopharmacol. 2000 Feb;22(2):131-41.

Neuhoff V, Arold N, Taube D, Ehrhardt W. Improved staining of proteins in polyacrylamide gels including isoelectric focusing gels with clear background at nanogram sensitivity using Coomassie Brilliant Blue G-250 and R-250. Electrophoresis. 1988 Jun;9(6):255-62.

O'Toole TE, Loftus JC, Plow EF, Glass AA, Harper JR, Ginsberg MH. Efficient surface expression of platelet GPIIb-IIIa requires both subunits. Blood. 1989 Jul;74(1):14-8.

Padlan EA, Helm BA. Modeling of the lectin-homology domains of the human and murine low-affinity Fc epsilon receptor (Fc epsilon RII/CD23). Receptor. 1993 Winter;3(4):325-41.

Paul-Eugene N, Mossalayi D, Sarfati M, Yamaoka K, Aubry JP, Bonnefoy JY, Dugas B, Kolb JP. Evidence for a role of Fc epsilon RII/CD23 in the IL-4-induced nitric oxide production by normal human mononuclear phagocytes. Cell Immunol. 1995 Jul;163(2):314-8.

Peterson JA, Visentin GP, Newman PJ, Aster RH. A recombinant soluble form of the integrin alpha IIb beta 3 (GPIIb-IIIa) assumes an active, ligand-binding conformation and is recognized by GPIIb-IIIa-specific monoclonal, allo-, auto-, and drug-dependent platelet antibodies. Blood. 1998 Sep 15;92(6):2053-63.

Plater-Zyberk C, Bonnefoy JY. Marked amelioration of established collagen-induced arthritis by treatment with antibodies to CD23 in vivo. Nat Med. 1995 Aug;1(8):781-5.

Pochon S, Graber P, Yeager M, Jansen K, Bernard AR, Aubry JP, Bonnefoy JY. Demonstration of a second ligand for the low affinity receptor for immunoglobulin E (CD23) using recombinant CD23 reconstituted into fluorescent liposomes. J Exp Med. 1992 Aug 1;176(2):389-97.

Reljic R, Cosentino G, Gould HJ. Function of CD23 in the response of human B cells to antigen. Eur J Immunol. 1997 Feb;27(2):572-5.

Reljic R. PhD Thesis, University of London, 1996

Rezzonico R, Chicheportiche R, Imbert V, Dayer JM. Engagement of CD11b and CD11c beta2 integrin by antibodies or soluble CD23 induces IL-1beta production on primary human monocytes through mitogen-activated protein kinase-dependent pathways. Blood. 2000 Jun 15;95(12):3868-77.

Rezzonico R, Imbert V, Chicheportiche R, Dayer J. Ligation of CD11b and CD11c beta(2) integrins by antibodies or soluble CD23 induces macrophage inflammatory protein 1alpha (MIP-1alpha) and MIP-1beta production in primary human monocytes through a pathway dependent on nuclear factor-kappaB. Blood. 2001 May 15;97(10):2932-40.

Richards ML, Katz DH. The binding of IgE to murine Fc epsilon RII is calcium-dependent but not inhibited by carbohydrate. J Immunol. 1990 Apr 1;144(7):2638-46.

Riffo-Vasquez Y, Pitchford S, Spina D. Murine models of inflammation: role of CD23. Allergy. 2000;55 Suppl 61:21-6.

Rose K, Turcatti G, Graber P, Pochon S, Regamey PO, Jansen KU, Magnenat E, Aubonney N, Bonnefoy JY. Partial characterization of natural and recombinant human soluble CD23. Biochem J. 1992 Sep 15;286 (Pt 3):819-24.

Rust,K., Grosso,L., Zhang,V., Chang,D., Persson,A., Longmore,W., Cai,G.Z. and Crouch,E. Human surfactant protein D: SP-D contains a C-type lectin carbohydrate recognition domain Arch. Biochem. Biophys. 290 (1), 116-126 (1991)

Sambrook, Fritsch, Maniatis. Molecular Cloning a laboratory Manual (2nd edition) Cold Spring Harbour Laboratory Press 1989.

Sarfati M, Bettler B, Letellier M, Fournier S, Rubio-Trujillo M, Hofstetter H, Delespesse G. Native and recombinant soluble CD23 fragments with IgE suppressive activity. Immunology. 1992 Aug;76(4):662-7.

Sarfati M, Rector E, Rubio-Trujillo M, Wong K, Sehon AH, Delespesse G. In vitro synthesis of IgE by human lymphocytes. III. IgE-potentiating activity of culture supernatants from Epstein-Barr virus (EBV) transformed B cells. Immunology. 1984 Oct;53(2):207-14.

Sarfati M, Rector E, Wong K, Rubio-Trujillo M, Sehon AH, Delespesse G. In vitro synthesis of IgE by human lymphocytes. II. Enhancement of the spontaneous IgE synthesis by IgE-binding factors secreted by RPMI 8866 lymphoblastoid B cells. Immunology. 1984 Oct;53(2):197-205.

Sarfati M, Rector E, Sehon AH, Delespesse G. In vitro synthesis of IgE by human lymphocytes. IV. Suppression of the spontaneous IgE synthesis by IgE-binding factors secreted by tunicamycin-treated RPMI 8866 cells. Immunology. 1984 Dec;53(4):783-90.

Sato T, Konishi A, Yasuno S, Arai J, Kamei M, Bitoh M, Yamaguchi T. A new method for studying the binding of human IgE to CD23 and the inhibition of this binding. J Immunol Methods. 1997 Nov 10;209(1):59-66.

Saxon A, Ke Z, Bahati L, Stevens RH. Soluble CD23 containing B cell supernatants induce IgE from peripheral blood B-lymphocytes and costimulate with interleukin-4 in induction of IgE. J Allergy Clin Immunol. 1990 Sep;86(3 Pt 1):333-44.

Schroeckh V, Hortschansky P, Fricke S, Luckenbach GA, Riesenberg D. Expression of soluble, recombinant alphavbeta3 integrin fragments in Escherichia coli. Microbiol Res. 2000 Sep;155(3):165-77.

Schulz O, Laing P, Sewell HF, Shakib F. Der p I, a major allergen of the house dust mite, proteolytically cleaves the low-affinity receptor for human IgE (CD23). Eur J Immunol. 1995 Nov;25(11):3191-4.

Schulz O, Sewell HF, Shakib F. Proteolytic cleavage of CD25, the alpha subunit of the human T cell interleukin 2 receptor, by Der p 1, a major mite allergen with cysteine protease activity. J Exp Med. 1998 Jan 19;187(2):271-5.

Schulz O, Sutton BJ, Beavil RL, Shi J, Sewell HF, Gould HJ, Laing P, Shakib F. Cleavage of the low-affinity receptor for human IgE (CD23) by a mite cysteine protease: nature of the cleaved fragment in relation to the structure and function of CD23. Eur J Immunol. 1997 Mar;27(3):584-8.

Shakib F, Schulz O, Sewell H. A mite subversive: cleavage of CD23 and CD25 by Der p 1 enhances allergenicity. Immunol Today. 1998 Jul;19(7):313-6.

Sherr E, Macy E, Kimata H, Gilly M, Saxon A. Binding the low affinity Fc epsilon R on B cells suppresses ongoing human IgE synthesis. J Immunol. 1989 Jan 15;142(2):481-9.

Shi J, Ghirlando R, Beavil RL, Beavil AJ, Keown MB, Young RJ, Owens RJ, Sutton BJ, Gould HJ. Interaction of the low-affinity receptor CD23/Fc epsilonRII lectin domain with the Fc epsilon3-4 fragment of human immunoglobulin E. Biochemistry. 1997 Feb 25;36(8):2112-22.
Shi J. PhD Thesis, University of London, 1998

Smith JW, Cheresh DA. Integrin (alpha v beta 3)-ligand interaction. Identification of a heterodimeric RGD binding site on the vitronectin receptor. J Biol Chem. 1990 Feb 5;265(4):2168-72.

Soilleux EJ, Barten R, Trowsdale J. DC-SIGN; a related gene, DC-SIGNR; and CD23 form a cluster on 19p13. J Immunol. 2000 Sep 15;165(6):2937-42.

Springer TA. Folding of the N-terminal, ligand-binding region of integrin alpha-subunits into a beta-propeller domain. Proc Natl Acad Sci U S A. 1997 Jan 7;94(1):65-72.

Stephens PE, Ortlepp S, Perkins VC, Robinson MK, Kirby H. Expression of a soluble functional form of the integrin alpha4beta1 in mammalian cells. Cell Adhes Commun. 2000 May;7(5):377-90.

Suggs SV, Wallace RB, Hirose T, Kawashima EH, Itakura K. Use of synthetic oligonucleotides as hybridization probes: isolation of cloned cDNA sequences for human beta 2-microglobulin. Proc Natl Acad Sci U S A 1981 Nov;78(11):6613-7

Sutton BJ, Beavil RL, Beavil AJ. Inhibition of IgE-receptor interactions. Br Med Bull. 2000;56(4):1004-18.

Sutton BJ, Gould HJ. The human IgE network. Nature. 1993 Dec 2;366(6454):421-8.

Taylor MA, Pratt KA, Revell DF, Baker KC, Sumner IG, Goodenough PW. Active papain renatured and processed from insoluble recombinant propapain expressed in Escherichia coli. Protein Eng. 1992 Jul;5(5):455-9.

Ten RM, McKinstry MJ, Trushin SA, Asin S, Paya CV. The signal transduction pathway of CD23 (Fc epsilon RIIb) targets I kappa B kinase. J Immunol. 1999 Oct 1;163(7):3851-7.

Timens W, Boes A, Vos H, Poppema S. Tissue distribution of the C3d/EBV-receptor: CD21 monoclonal antibodies reactive with a variety of epithelial cells, medullary thymocytes, and peripheral T-cells. Histochemistry. 1991;95(6):605-11.

Tominaga Y, Kita Y, Uchiyama T, Sato K, Sato K, Takashi T, Horiuchi T. Expression of a soluble form of LFA-1 and demonstration of its binding activity with ICAM-1. J Immunol Methods. 1998 Mar 1;212(1):61-8.

Trask B, Fertitta A, Christensen M, Youngblom J, Bergmann A, Copeland A, de Jong P, Mohrenweiser H, Olsen A, Carrano A and et al. Fluorescence in situ hybridization mapping of human chromosome 19: cytogenetic band location of 540 cosmids and 70 genes or DNA markers.Genomics 1993; 15 (1), 133-145

Wakai M, Pasley P, Sthoeger ZM, Posnett DN, Brooks R, Hashimoto S, Chiorazzi N. Anti-CD23 monoclonal antibodies: comparisons of epitope specificities and modulating capacities for IgE binding and production. Hybridoma. 1993 Feb;12(1):25-43.

Watson JL, Jackson KA, King DP, Stott JL. Molecular cloning and sequencing of the low-affinity IgE receptor (CD23) for horse and cattle. Vet Immunol Immunopathol. 2000 Mar 15;73(3-4):323-9.

Weis WI, Kahn R, Fourme R, Drickamer K, Hendrickson WA. Structure of the calcium-dependent lectin domain from a rat mannose-binding protein determined by MAD phasing. Science. 1991 Dec 13;254(5038):1608-15.

Wheeler DJ, Parveen S, Pollock K, Williams RJ. Inhibition of sCD23 and immunoglobulin E release from human B cells by a metalloproteinase inhibitor, GI 129471. Immunology. 1998 Sep;95(1):105-10.

White LJ, Ozanne BW, Graber P, Aubry JP, Bonnefoy JY, Cushley W. Inhibition of apoptosis in a human pre-B-cell line by CD23 is mediated via a novel receptor. Blood. 1997 Jul 1;90(1):234-43.

Whittle N, Adair J, Lloyd C, Jenkins L, Devine J, Schlom J, Raubitschek A, Colcher D, Bodmer M. Expression in COS cells of a mouse-human chimaeric B72.3 antibody. Protein Eng. 1987 Dec;1(6):499-505.

Wippler J, Kouns WC, Schlaeger EJ, Kuhn H, Hadvary P, Steiner B. The integrin alpha IIb-beta 3, platelet glycoprotein IIb-IIIa, can form a functionally active heterodimer complex without the cysteine-rich repeats of the beta 3 subunit. J Biol Chem. 1994 Mar 25;269(12):8754-61.

Wolff MW, Murhammer DW, Jarvis DL, Linhardt RJ. Electrophoretic analysis of glycoprotein glycans produced by lepidopteran insect cells infected with an immediate early recombinant baculovirus encoding mammalian beta1,4-galactosyltransferase. Glycoconj J. 1999 Dec;16(12):753-6.

Wray W, Boulikas T, Wray VP, Hancock R. Silver staining of proteins in polyacrylamide gels. Anal Biochem. 1981 Nov 15;118(1):197-203.

Wurzburg BA, Garman SC, Jardetzky TS. Structure of the human IgE-Fc C epsilon 3-C epsilon 4 reveals conformational flexibility in the antibody effector domains. Immunity. 2000 Sep;13(3):375-85.

Wuthrich K. Protein structure determination in solution by NMR. Science 1989 243 45-50

Xia Y, Ross GD. Generation of recombinant fragments of CD11b expressing the functional beta-glucan-binding lectin site of CR3 (CD11b/CD18). J Immunol. 1999 Jun 15;162(12):7285-93.

Yokota A, Yukawa K, Yamamoto A, Sugiyama K, Suemura M, Tashiro Y, Kishimoto T, Kikutani H. Two forms of the low-affinity Fc receptor for IgE differentially mediate endocytosis and phagocytosis: identification of the critical cytoplasmic domains. Proc Natl Acad Sci U S A. 1992 Jun 1;89(11):5030-4.

Young RJ, Owens RJ, Mackay GA, Chan CM, Shi J, Hide M, Francis DM, Henry AJ, Sutton BJ, Gould HJ. Secretion of recombinant human IgE-Fc by mammalian cells and biological activity of glycosylation site mutants. Protein Eng. 1995 Feb;8(2):193-9.

Yu P, Kosco-Vilbois M, Richards M, Kohler G, Lamers MC. Negative feedback regulation of IgE synthesis by murine CD23. Nature. 1994 Jun 30;369(6483):753-6.

Zhang K, Clark EA, Saxon A. CD40 stimulation provides an IFN-gamma-independent and IL-4-dependent differentiation signal directly to human B cells for IgE production. J Immunol. 1991 Mar 15;146(6):1836-42.

Zheng Y, Shopes B, Holowka D, Baird B. Conformations of IgE bound to its receptor Fc epsilon RI and in solution. Biochemistry. 1991 Sep 24;30(38):9125-32.

Zhou L, Lee DH, Plescia J, Lau CY, Altieri DC. Differential ligand binding specificities of recombinant CD11b/CD18 integrin I-domain. J Biol Chem. 1994 Jun 24;269(25):17075-9.

APPENDIX I: LIST OF OLIGONUCLEOTIDES

Primers for the Construction of H-CD23

HF TAG TAG AAG CTT CAT ATG GAG TTG CAG GTG TCC AG
HR TAG TAG GGA TCC TTA TCA TCA GCA TGT GGC GAC CCG G

Primers for the Construction of Der-CD23

DF TAC TAC AAG CTT CAT ATG AGC GGC TTT GTG TGC AAC AC
DR TAC TAC GGA TCC TTA TCA TCA CTC CGC GGA ACC TTC GCT

Primers for the Construction of SPD-CD23

O1 TAG TAG GGA TCC CCC GGG ATG AGT GTG CCC ACT CAG GTC CTG GGG TTG CTG CTG CTG TG

O2 GAA GCA ACA TCT GGG ATG TCA CAT CTG GCA TCT GTA AGC CAC AGC AGC AGC AAC CCC AG

O3 GAC ATC CCA GAT GTT GCT TCT CTG AGG CAG CAG GTT GAG GCC TTA CAG GGA CAA GTA CAG C

O4 CTG CTG CTC GAG CTT ATA CTG AGA GAA AGC AGC CTG GAG GTG CTG TAC TTG TCC CTG TAA GG

PF1 TAG TAG GGA TCC CCC GGG AT
PR1 CTG CTG CTC GAG CTT ATA CTG
CD23FF TCT CAG TAT AAG ATG GAG TTG CAG GTG TCC AG
SPDFR CTG CAA CTC CAT CTT ATA CTG AGA GAA AGC AG
PF2 ACT AGT GGA TCC CCC GG
PR2 TAG TAG GAA TTC TTA TCA TCA AGA GTG GAG AGG GGC AGA
PF3 *(E.coli)* CTA CTA AAG CTT CAT ATG CCA GAT GAT GTT GCT TCT CTG AG
PR3 *(E.coli)* TCG TCG GGA TCC GAA TTC TTA TCA TCA AGA GTC

Primers for the Construction of CD11b

αNF ATG TAG AAG CTT ATG GCT CTC AGA GTC CTT C
αNR TGTGCT GAT ATC GAG GTG CC
α2F' CAC CTC GAT ATC AGC ACA T
α2R TAG TAG TCT AGA CAT ATG ACA GTC TGG TTC AG
α3F GAC TGT CAT ATG GGA CCG CC
α3R TAG TAG GAG CTC AAG CTT TTA TCA TCA CTT GTC ATC GTC GTC CTT GTA GTC GTT GGG GAC CTC GAA CG

CD11b sequencing primers

CD11b-F478	CAG AAG TTC CCA GAG GCC CT
CD11b-R478	AGG GCC TCT GGG AAC TTC TG
CD11b-F977	ATA CCA TCG CAT CCA AGC CG
CD11b-R977	CGG CTT GGA TGC GAT GGT AT
CD11b -F1235	GCA CCT TCA TCA ACA TGA CC
CD11b-F1515	CCA TTA CTA CGA GCA GAC CC
CD11b-R1593	CCG TAG AGA ACA GCA TCA CA
CD11b-F1822	TTT GGT CAG TCA CTG AGT GG
CD11b-R1919	CTT GAC TCT CAG TAC TGG CT
CD11b-F2139	CGC CGT CTT CAA TGA GAC AA
CD11b-R2200	TTC AGG GTC TCA CAA GTC TG
CD11b-F2428	AGT TTC ATG AGC CTG GAC TG
CD11b-R2505	TGT CCT GTA GGA GTC CTC CA
CD11b-F2727	TGT AGA CTC TAA GGC TTC CC

Primers for the Construction of CD18

βNF	TAG TAG AGA TCT ATG CTG GGC CTG CGC C
βNR	GTA GTC GAA TTC GTT GCT C
β2F	AGC AAC GAA TTC GAC TAC CC
β2R	TAG TAG AAG CTT TTA TCA TCA GTT GGG GCC TGC CAC AC

Sequencing Primers for CD18

CD18-F491	TTG ATG ACC TCA GGA ATG TC
CD18-R491	GAC ATT CCT GAG GTC ATC AA
CD18-F860	CTG ATG ACG GCT TCC ATT TC
CD18-1152	CAA TAA ACT CTC CTC CAG GG
CD18-1234	TTC CTG TGC GTC ACT CCA TT
CD18-1476	CAT CTG CAG GTG TGA CAC TG
CD18-1576	CCT GAG CAG ATG ATG GAG TT
CD18-1832	GTG TTG AGT GTA GTG GTC GT
CD18-1930	ATG TAC TTG CCA CAG GGT GA

Sequencing Primers (Vector Specific)

pBluescript KS	**T7**	GTA ATA CGA CTC ACT ATA GGG C
	T3	AAT TAA CCC TCA CTA AAG GG
pET5a	**RpET5a**	CCG AAA AGT GCC ACC TGA CG
pSP73:	**FpSP73**	CAC CAT ATG GAC ATA TTG TCG

APPENDIX II: SEQUENCE DATA OF RECOMBINANT PROTEINS

H-CD23 *(E.coli)*

```
  1  MELQVSSGFV CNTCPEKWIN FQRKCYYFGK GTKQWVHARY ACDDMEGQLV
 51  SIHSPEEQDF LTKHASHTGS WIGLRNLDLK GEFIWVDGSH VDYSNWAPGE
101  PTSRSQGEDC VMMRGSGRWN DAFCDRKLGA WVCDRLATC
```

Der-CD23 *(E.coli)*

```
  1  SGFVCNTCPE KWINFQRKCY YFGKGTKQWV HARYACDDME GQLVSIHSPE
 51  EQDFLTKHAS HTGSWIGLRN LDLKGEFIWV DGSHVDYSNW APGEPTSRSQ
101  GEDCVMMRGS GRWNDAFCDR KLGAWVCDRL ATCTPPASEG SAE
```

SPD-CD23 (baculovirus)

```
  1  MSVPTQVLGL LLLWLTDARC DIPDVASLRQ QVEALQGQVQ HLQAAFSQYK
 51  MELQVSSGFV CNTCPEKWIN FQRKCYYFGK GTKQWVHARY ACDDMEGQLV
101  SIHSPEEQDF LTKHASHTGS WIGLRNLDLK GEFIWVDGSH VDYSNWAPGE
151  PTSRSQGEDC VMMRGSGRWN DAFCDRKLGA WVCDRLATCT PPASEGSAES
201  MGPDSRPDPD GRLPTPSAPL HS
```

SPD-CD23 *(E.coli)*

```
  1 (M)PDVASLRQQV EALQGQVQHL QAAFSQYKME LQVSSGFVCN TCPEKWINFQ
 51  RKCYYFGKGT KQWVHARYAC DDMEGQLVSI HSPEEQDFLT KHASHTGSWI
101  GLRNLDLKGE FIWVDGSHVD YSNWAPGEPT SRSQGEDCVM MRGSGRWNDA
151  FCDRKLGAWV CDRLATCTPP ASEGSAESMG PDSRPDPDGR LPTPSAPLHS
```

CD11b- Translated αN1 Fragment Sequence Data

```
CD11b           MALRVLLLTALTLCHGFNLDTENAMTFQENARGFGQSVVQLQGSRVVVGAPQEIVAANQR 60
seqdata         MALRVLLLTALTLCHGFNLDTENAMTFQENARGFGQSVVQLQGSRVVVGAPQEIVAANQR 60
                ************************************************************

CD11b           GSLYQCDYSTGSCEPIRLQVPVEAVNMSLGLSLAATTSPPQLLACGPTVHQTCSENTYVK 120
seqdata         GSLYQCDYSTGSCEPIRLQVPVEAVNMSLGLSLAATTSPPQLLACGPTVHQTCSENTYVK 120
                ************************************************************

CD11b           GLCFLFGSNLRQQPQKFPEALRGCPQEDSDIAFLIDGSGSIIPHDFRRMKEFVSTVMEQL 180
seqdata         GLCFLFGSNLRQQPQKFPEALRGCPQEDSDIAFLIDGSGSIIPHDFRRMKEFVSTVMEQL 180
                ************************************************************

CD11b           KKSKTLFSLMQYSEEFRIHFTFKEFQNNPNPRSLVKPITQLLGRTHTATGIRKVVRELFN 240
seqdata         KKSKTLFSLMQYSEEFRIHFTFKEFQNNPNPRSLVKPITQLLGRTHTATGIRKVVRELFN 240
                ************************************************************

CD11b           ITNGARKNAFKILVVITDGEKFGDPLGYEDVIPEADREGVIRYVIGVGDAFRSEKSRQEL 300
seqdata         ITNGARKNAFKILVVITDGEKFGDPLGYEDVIPEADREGVIRYVIGVGDAFRSEKSRQEL 300
                ************************************************************

CD11b           NTIASKPPRDHVFQVNNFEALKTIQNQLREKIFAIEGTQTGSSSSFEHEMSQEGFSAAIT 360
seqdata         NTIASKPPRDHVFQVNNFEALKTIQNQLREKIFAIEGTQTGSSSSFEHEMSQEGFSAAIT 360
                ************************************************************

CD11b           SNGPLLSTVGSYDWAGGVFLYTSKEKSTFINMTRVDSDMNDAYLGYAAAIILRNRVQSLV 420
seqdata         SNGPLLSTVGSYDWAGGVFLYTSKEKSTFINMTRVDSDMNDAYLGYAAAIILRNRVQSLV 420
                ************************************************************

CD11b           LGAPRY 426
seqdata         LGAPRY 426
                ******
One DNA point mutation, but no coding error
```

CD11b- Translated α2 Fragment

```
CD11b           YQHIGLVAMFRQNTGMWESNANVKGTQIGAYFGASLCSVDVDSNGSTDLVLIGAPHYYEQ 60
alpha2          YQHIGLVAMFRQNTGMWESNANVKGTQIGAYFGASLCSVDVDSNGSTDLVLIGAPHYYEQ 60
                ************************************************************

CD11b           TRGGQVSVCPLPRGRARWQCDAVLYGEQGQPWGRFGAALTVLGDVNGDKLTDVAIGAPGE 120
alpha2          TRGGQVSVCPLPRGRARWQCDAVLYGEQGQPWGRFGAALTVLGDVNGDKLTDVAIGAPGE 120
                ************************************************************

CD11b           EDNRGAVYLFHGTSGSGISPSHSQRIAGSKLSPRLQYFGQSLSGGQDLTMDGLVDLTVGA 180
alpha2          EDNRGAVYLFHGTSGSGISPSHSQRIAGSKLSPRLQYFGQSLSGGQDLTMDGLVDLTVGA 180
                ************************************************************

CD11b           QGHVLLLRSQPVLRVKAIMEFNPREVARNVFECNDQVVKGKEAGEVRVCLHVQKSTRDRL 240
alpha2          QGHVLLLRSQPVLRVKAIMEFNPREVARNVFECNDQVVKGKEAGEVRVCLHVQKSTRDRL 240
                ************************************************************

CD11b           REGQIQSVVTYDLALDSGRPHSRAVFNETKNSTRRQTQVLGLTQTCETLKLQLPNCIEDP 300
alpha2          REGQIQSVVTYDLALDSGRPHSRAVFNETKNSTRRQTQVLGLTQTCETLKLQLPNCIEDP 299
                ************************************************************

CD11b           VSPIVLRLNFSLVGTPLSAFGNLRPVLAEDAQRLFTALFPFEKNCGNDNICQDDLSITFS 360
alpha2          VSPIVLRLNFSLVGTPLSAFGNLRPVLAEDAQRLFTALFPFEKNCGNDNICQDDLSITFS 360
                ************************************************************

CD11b           FMSLDCLVVGGPREFNVTVTVRNDGEDSYRTQVTFFFPLDLSYRKVSTLQNQRSQRSWRL 420
alpha2          FMSLDCLVVGGPREFNVTVTVRNDGEDSYRTQVTFFFPLDLSYRKVSTLQNQRSQRSWRL 420
                ************************************************************

CD11b           ACESASSTEVSGALKSTSCSINHPIFPENSEVTFNITFDVDSKASLGNKLLLKANVTSEN 480
alpha2          ACESASSTEVSGALKSTSCSINHPIFPENSEVTFNITFDVDSKASLGNKLLLKANVTSEN 479
                ************************************************************

CD11b           NMPRTNKTEFQLELPVKYAVYMVVTSHGVSTKYLNFTASENTSRVMQHQYQVSNLGQRSP 540
alpha2          NMPRTNKTEFQLELPVKYAVYMVVTSHGVSTKYLNFTASENTSRVMQHQYQVSNLGQRSP 540
                ************************************************************

CD11b           PISLVFLVPVRLNQTVI 557
alpha2          PISLVFLVPVRLNQTVI 557
                *****************
```

CD11bNE- Translated α3E Fragment Sequence Data

```
alpha3E         IWDRPQVTFSENLSSTCHTKERLPSHSDFLAELRKAPVVNCSIAVCQRIQCDIPFFGIQE 60
Cd11bNE         IWDRPQVTFSENLSSTCHTKERLPSHSDFLAELRKAPVVNCSIAVCQRIQCDIPFFGIQE 60
                ************************************************************

alpha3E         EFNATLKGNLSFDWYIKTSHNHLLIVSTAEILFNDSVFTLLPGQGAFVRSQTETKVEPFE 120
Cd11bNE         EFNATLKGNLSFDWYIKTSHNHLLIVSTAEILFNDSVFTLLPGQGAFVRSQTETKVEPFE 120
                ************************************************************

alpha3E         VPNDYKDDDDKKLEL 135
Cd11bNE         VPNDYKDDDDKKLEL 135
                ***************
```

CD18N- Translated Construct

```
seqdata         MLGLRPPLLALVGLLSLGCVLSQECTKFKVSSCRECIESGPGCTWCQKLNFTGPGDPDSI 60
CD18            MLGLRPPLLALVGLLSLGCVLSQECTKFKVSSCRECIESGPGCTWCQKLNFTGPGDPDSI 60
                ************************************************************

seqdata         RCDTRPQLLMRGCAADDIMDPTSLAETQEDHNGGQKQLSPQKVTLYLRPGQAAAFNVTFR 120
CD18            RCDTRPQLLMRGCAADDIMDPTSLAETQEDHNGGQKQLSPQKVTLYLRPGQAAAFNVTFR 120
                ************************************************************

seqdata         RAKGYPIDLYYLMDLSYSMLDDLRNVKKLGGDLLRALNEITESGRIGFGSFVDKTVLPFV 180
CD18            RAKGYPIDLYYLMDLSYSMLDDLRNVKKLGGDLLRALNEITESGRIGFGSFVDKTVLPFV 180
                ************************************************************

seqdata         NTHPDKLRNPCPNREKECQPPFAFRHVLKLTNNSNQFQTEVGKQLISGNLDAPEGGLDAM 240
CD18            NTHPDKLRNPCPNKEKECQPPFAFRHVLKLTNNSNQFQTEVGKQLISGNLDAPEGGLDAM 240
                ************:***********************************************

seqdata         MQVAACPEEIGWRNVTRLLVFATDDGFHFAGDGKLGAILTPNDGRCHLEDNLYKRSNEFD 300
CD18            MQVAACPEEIGWRNVTRLLVFATDDGFHFAGDGKLGAILTPNDGRCHLEDNLYKRSNEFD 300
                ************************************************************

seqdata         YPSVGQLAHKLAENNIQPIFAVTSRMVKTYEKLTEIIPKSAVGELSEDSSNVVHLIKNAY 360
CD18            YPSVGQLAHKLAENNIQPIFAVTSRMVKTYEKLTEIIPKSAVGELSEDSSNVVHLIKNAY 360
                ************************************************************

seqdata         NKLSSRVFLDHNALPDTLKVTYDSFCSNGVTHRNQPRGDCDGVQINVPITFQVKVTATEC 420
CD18            NKLSSRVFLDHNALPDTLKVTYDSFCSNGVTHRNQPRGDCDGVQINVPITFQVKVTATEC 420
                ************************************************************

seqdata         IQEQSFVIRALGFTDIVTVQVLPQCECRCRDQSRDRSLCHGKGFLECGICRCDTGYIGKN 480
CD18            IQEQSFVIRALGFTDIVTVQVLPQCECRCRDQSRDRSLCHGKGFLECGICRCDTGYIGKN 480
                ************************************************************

seqdata         CECQTQGRSSQELEGSCRKDNNSIICSGLGDCVCGQCLCHTSDVPGKLIYGQYCECDTIN 540
CD18            CECQTQGRSSQELEGSCRKDNNSIICSGLGDCVCGQCLCHTSDVPGKLIYGQYCECDTIN 540
                ************************************************************

seqdata         CERYNGQVCGGPGRGLCFCGKCRCHPGFEGSACQCERTTEGCLNPRRVECSGRGRCRCNV 600
CD18            CERYNGQVCGGPGRGLCFCGKCRCHPGFEGSACQCERTTEGCLNPRRVECSGRGRCRCNV 600
                ************************************************************

seqdata         CECHSGYQLPLCQECPGCPSPCGKYISCAECLKFEKGPFGKNCSAACPGLQLSNNPVKGR 660
CD18            CECHSGYQLPLCQECPGCPSPCGKYISCAECLKFEKGPFGKNCSAACPGLQLSNNPVKGR 660
                ************************************************************

seqdata         TCKERDSEGCWVAYTLEQQDGMDRYLIYVDESRECVAGPN 700
CD18            TCKERDSEGCWVAYTLEQQDGMDRYLIYVDESRECVAGPN 700
                ****************************************
```

Contained three DNA mutations, one leading to CAA (Lysine) to CAG (Arginine) aminoacid change

APPENDIX III: CALIBRATION OF SIZE EXCLUSION COLUMNS

a) Superdex 75.

0.75 ml/min in 0.25 M Tris-Cl, pH 7.2, 0.125 M NaCl, 2 mM $CaCl_2$, 0.05% NaN_3

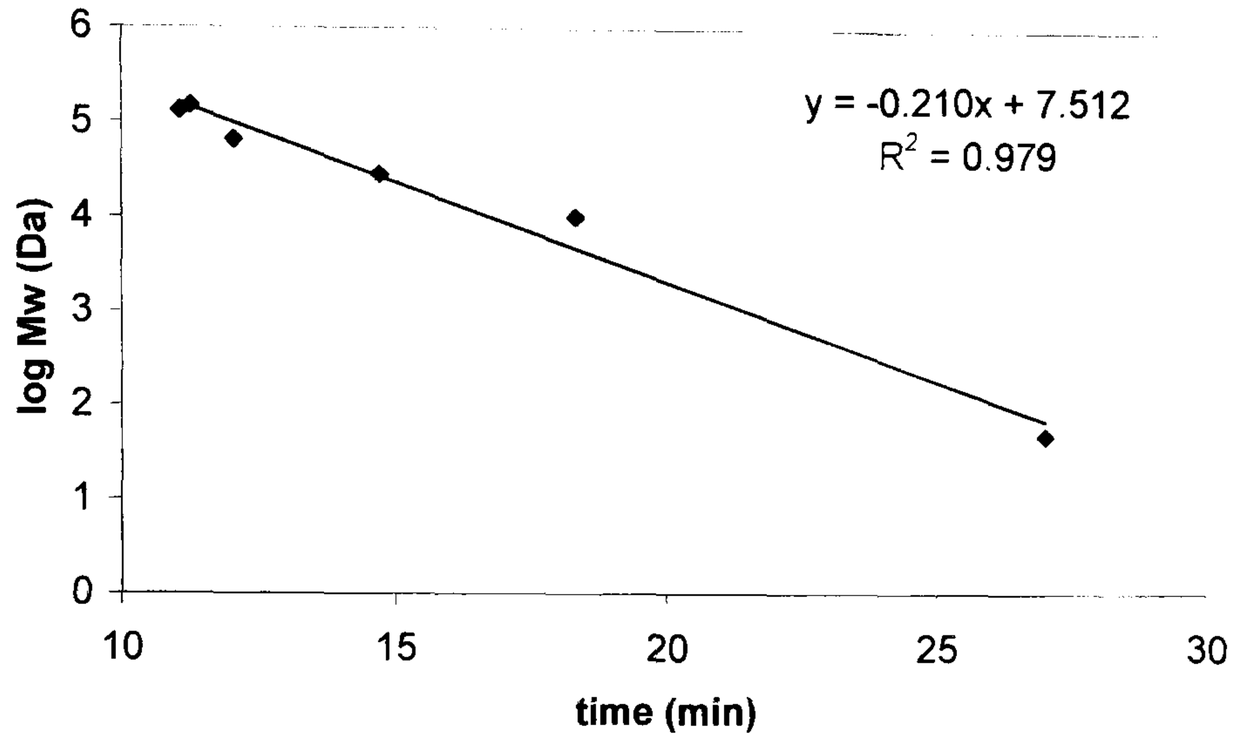

Standards	Mw (Da)	log Mw	time (min)
acetone	50	1.70	27.00
cyctochrome c	10500	4.02	18.29
carbonic anhydrase	29000	4.46	14.70
BSA	66000	4.82	12.03
BSA dimer	132000	5.12	11.25
alcohol dehydrogenase	150000	5.18	11.05
Blue dextran	2000000	6.30	10.80

b) Biosep 3000.

0.75 ml/min, 0.5 M Tris-Cl pH 7.2, 0.25 M NaCl, 2 mM $CaCl_2$, 0.05% NaN_3

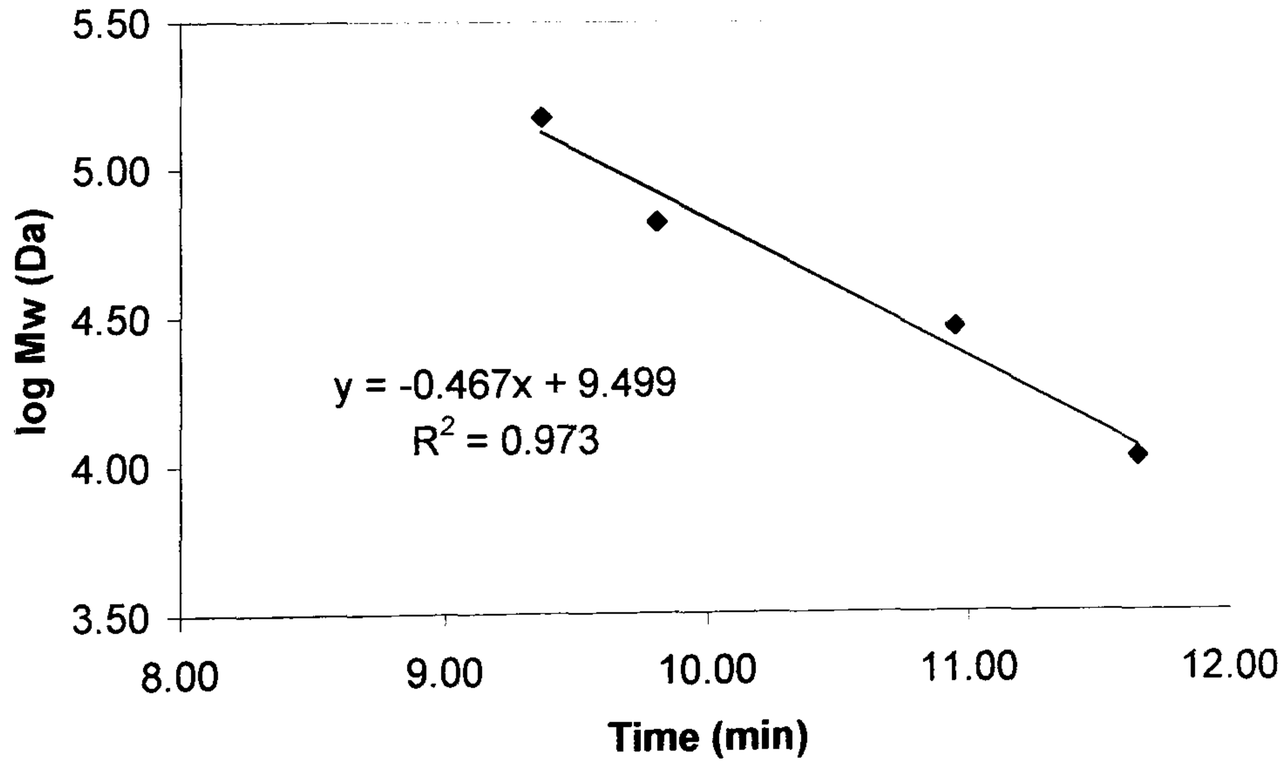

Standards	MW	log MW	time (min)
cytochrome c	10500	4.02	11.65
carbonic anhydrase	29000	4.46	10.95
BSA	66000	4.82	9.81
alcohol dehydronase	150000	5.18	9.37

c) Superdex 200

0.75 ml/min (0.5 M Tris-Cl, pH 7.2, 0.25 M NaCl, 2 mM $CaCl_2$, 0.05% NaN_3)

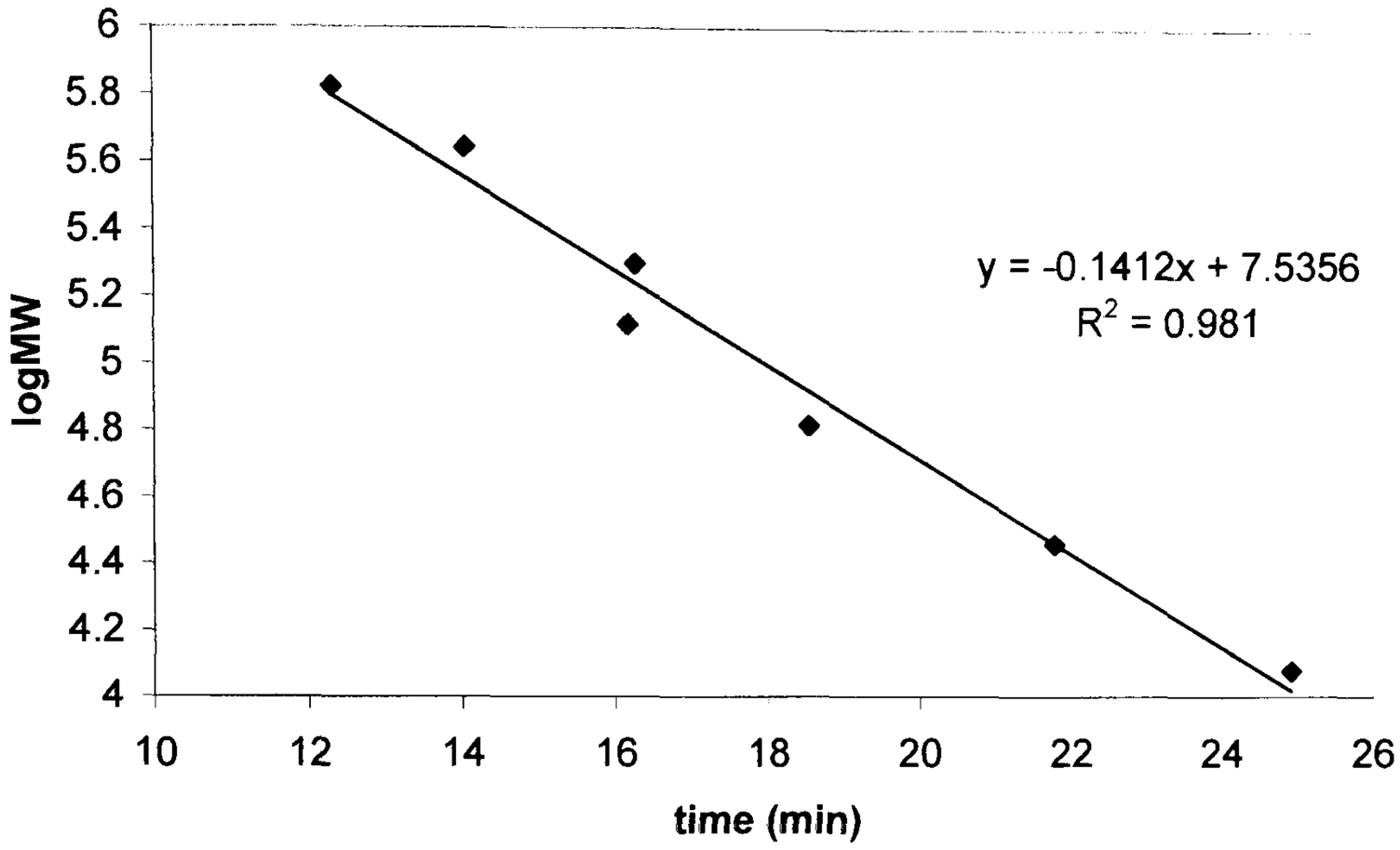

Standards	MW	log MW	time (min)
cytochrome c	12000	4.08	24.92
carbonic anhydrase	29000	4.46	21.77
bovine serum albumin	66000	4.82	18.52
BSA (dimer)	132000	5.12	16.15
amylase	200000	5.30	16.24
apoferritin	443000	5.65	14.03
thyroglobulin	669000	5.83	12.31

d) Superdex 200 (0.75 ml/min in HBS-Ca)

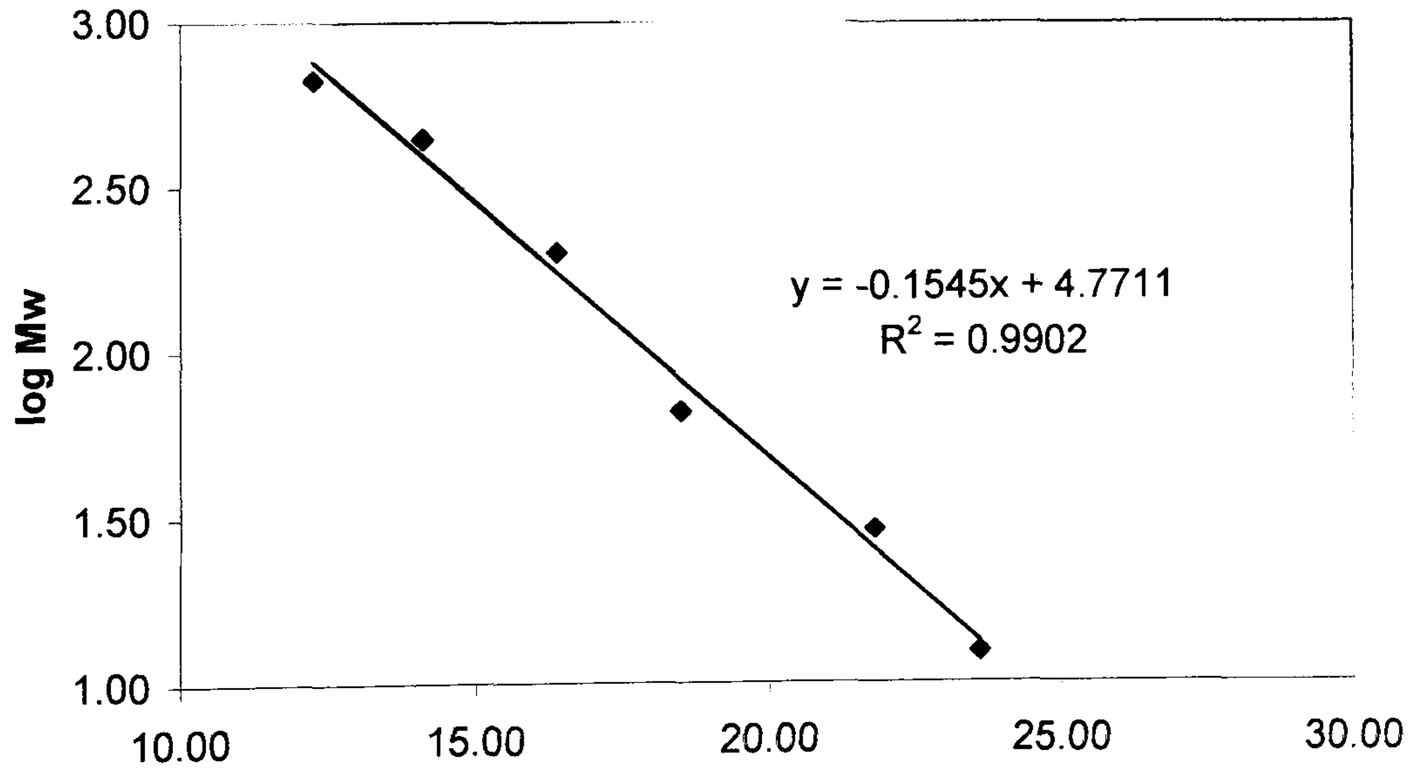

Standard Protein	MW	log10 MW	time (min)
cytochrome c	12.40	1.09	23.60
carbonic anhydrase	29.00	1.46	21.80
BSA	66.00	1.82	18.50
b-amylase	200.00	2.30	16.39
apoferritin	443.00	2.65	14.10
thyroglobulin	669.00	2.83	12.25

APPENDIX IV: EXAMPLES OF BIACORE KINETIC EVALUATION

Der-CD23 BIAcore 1: 1 Langmuir Association, Dissociation Fits

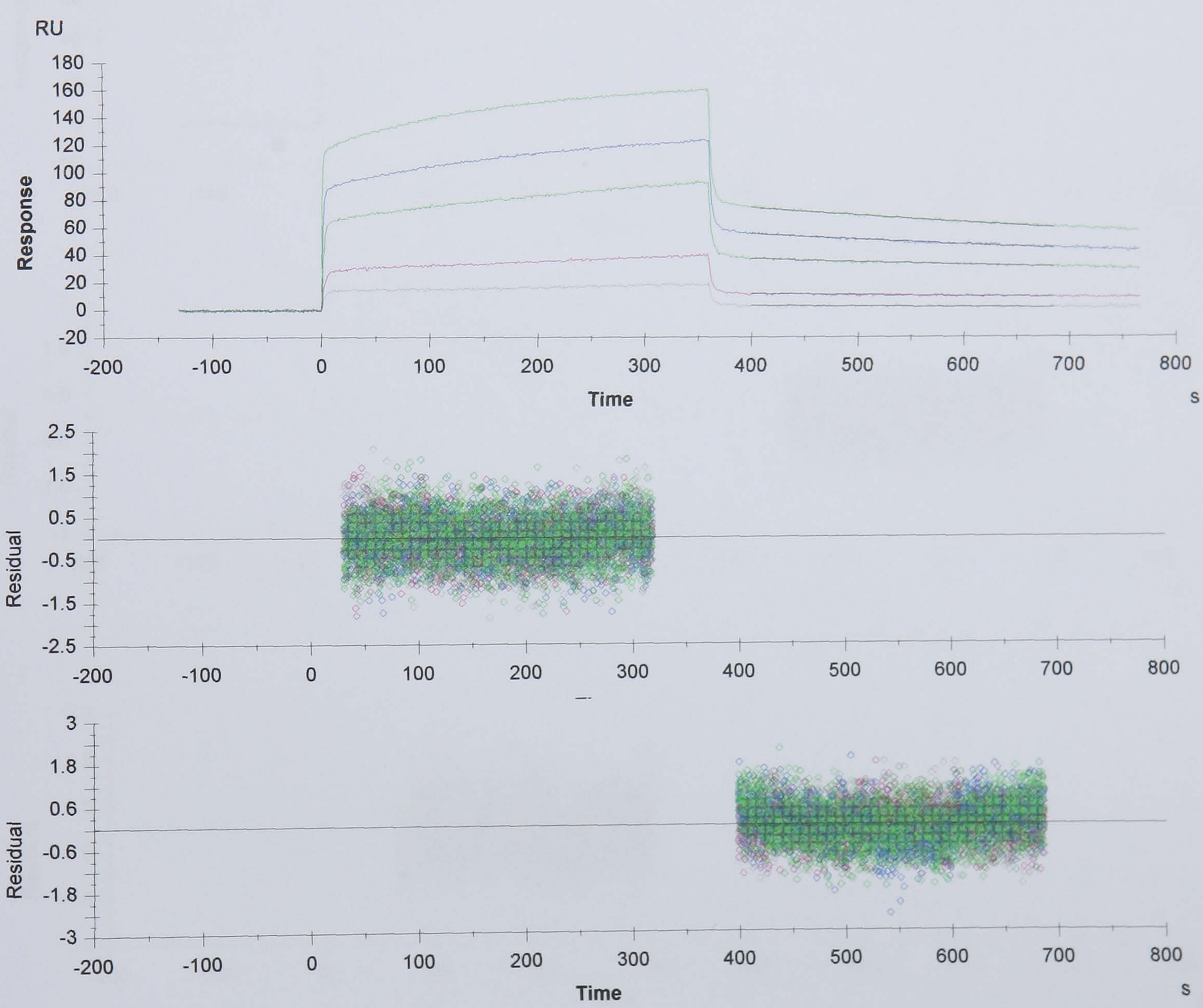

rCD23 BIAcore 1: 1 Langmuir Association, Dissociation Fits

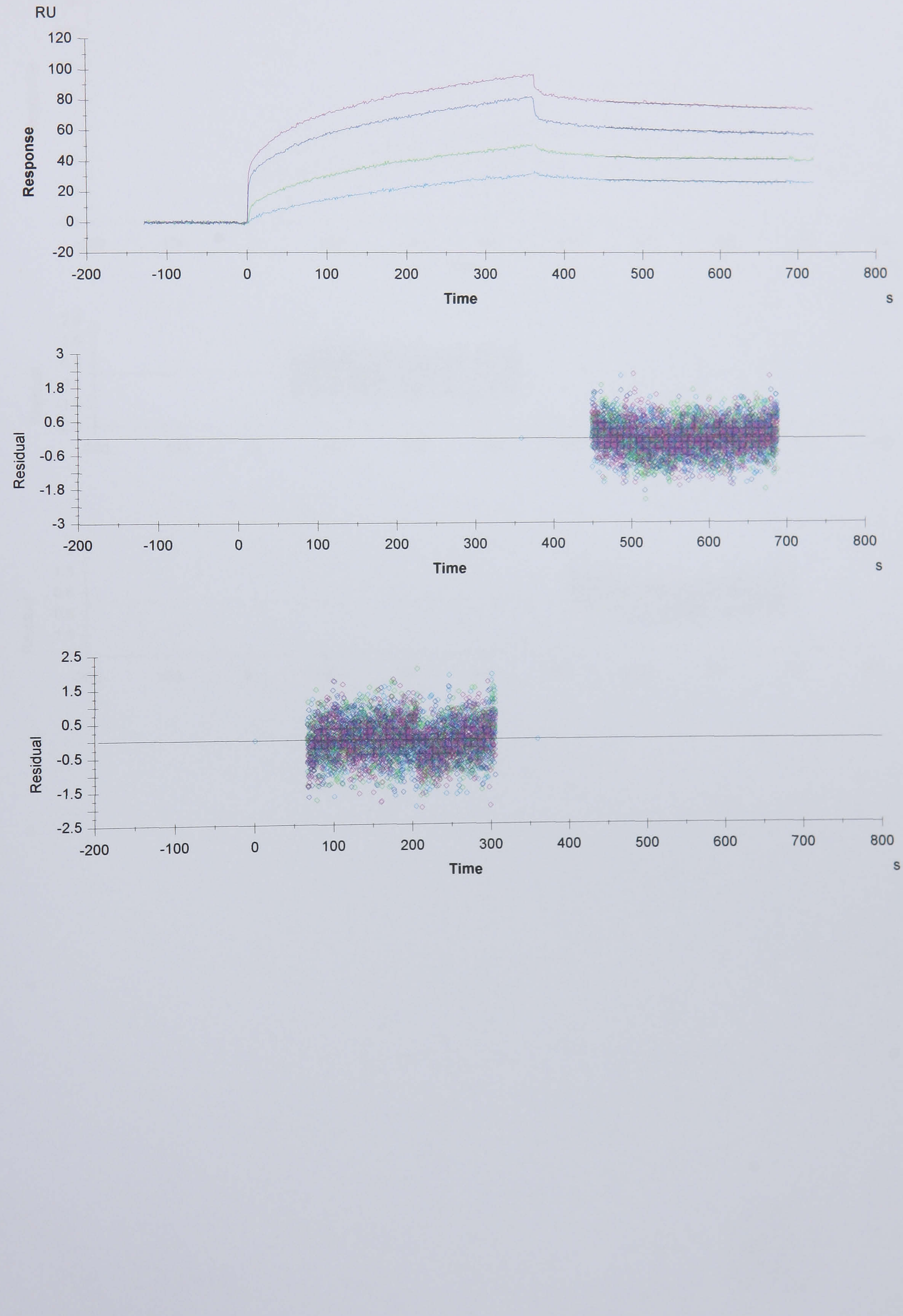

LZ-CD23 BIAcore 1:1 Langmuir Association, Dissociation Fits